

การศึกษาลักษณะเฉพาะของอัญมณีบางชนิดโดยเอฟที-ไออาร์สเปกโทรสโกปี



นางสาวพิมพ์ทอง ทองนพคุณ

สถาบันวิทยบริการ

วิทยานิพนธ์นี้เป็นส่วนหนึ่งของการศึกษาตามหลักสูตรปริญญาวิทยาศาสตรดุษฎีบัณฑิต

สาขาวิชาเคมี ภาควิชาเคมี

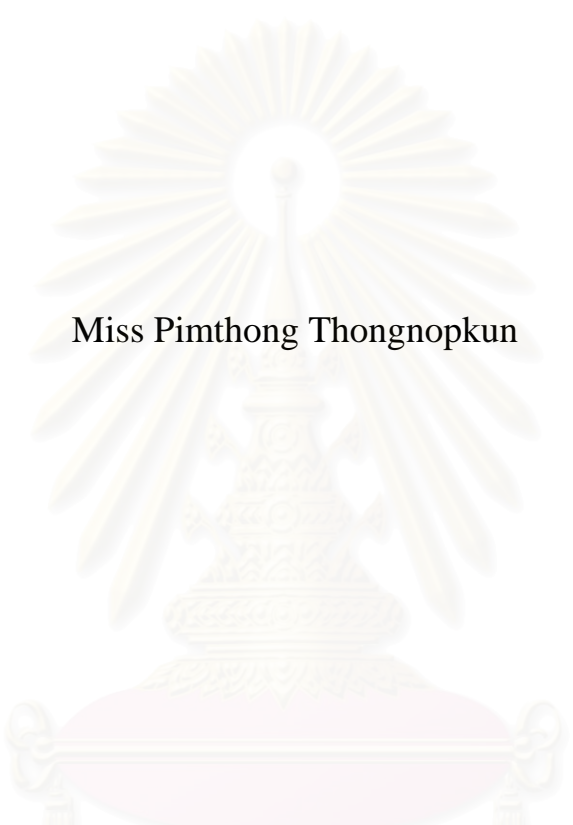
คณะวิทยาศาสตร์ จุฬาลงกรณ์มหาวิทยาลัย

ปีการศึกษา 2548

ISBN 974-53-2463-9

ลิขสิทธิ์ของจุฬาลงกรณ์มหาวิทยาลัย

CHARACTERIZATION OF SOME VARIETIES OF GEMSTONES  
BY FT-IR SPECTROSCOPY



Miss Pimthong Thongnopkun

A Dissertation Submitted in Partial Fulfillment of the Requirements  
for the Degree of Doctor of Philosophy Program in Chemistry

Department of Chemistry

Faculty of Science

Chulalongkorn University


Academic Year 2005

ISBN 974-53-2463-9

Thesis Title           Characterization of Some Varieties of Gemstones by FT-IR Spectroscopy  
By                       Miss Pimthong Thongnopkun  
Field of Study        Chemistry  
Thesis Advisor       Associate Professor Sanong Ekgasit, Ph.D.  
Thesis Co-advisor   Mrs. Wilawan Atichat


---

Accepted by the Faculty of Science, Chulalongkorn University in Partial Fulfillment of the Requirements for the Doctor's Degree

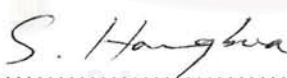
  
.....Dean of the Faculty of Science  
(Professor Piamsak Menasveta, Ph.D.)

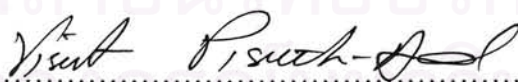
THESIS COMMITTEE


  
.....Chairman  
(Associate Professor Sirirat Kokpol, Ph.D.)

  
.....Thesis Advisor  
(Associate Professor Sanong Ekgasit, Ph.D.)

  
.....Thesis Co-advisor  
(Mrs. Wilawan Atichat)



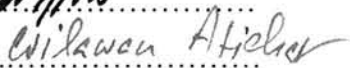
  
.....Member  
(Professor Supot Hannongbua, Ph.D.)

  
.....Member  
(Associate Professor Visut Pisutha-Armond, Ph.D.)

  
.....Member  
(Assistant Professor Pornsawat Wathanakul, Dr. rer. nat.)

พิมพ์ทอง ทองนพคุณ: การพิสูจน์เอกลักษณ์ของอัญมณีบางชนิดโดยเอฟที-ไออาร์สเปกโทรสโกปี (CHARACTERIZATION OF SOME VARIETIES OF GEMSTONES BY FT-IR SPECTROSCOPY) อ. ที่ปรึกษา: รศ. ดร. สนอง เอกสิทธิ์, อ. ที่ปรึกษาร่วม: นาง วิลาวัลย์ อติชาติ, 173 หน้า. ISBN 974-53-2463-9

เทคนิคทรานสเฟลกแดนซ์เป็นเทคนิคการวิเคราะห์ใหม่ซึ่งใช้ร่วมกับกล้องจุลทรรศน์อินฟราเรด เพื่อนำมาประยุกต์ใช้ในการวิเคราะห์อัญมณีที่เจียรไนแล้วและอัญมณีบนเครื่องประดับ เทคนิคนี้พัฒนามาจากปรากฏการณ์การสะท้อนกลับหมดของแสงภายในอัญมณีที่เจียรไนแล้ว โดยแสงอินฟราเรดจากกล้องจุลทรรศน์อินฟราเรดจะตกกระทบสู่หน้าตัดบนของอัญมณี และแสงทรานสเฟลกแดนซ์ที่สะท้อนจากภายในตัวอัญมณีจะถูกส่งไปยังตัวตรวจรับด้วยเลนส์กลาสสิกเรเนียนที่มีกำลังขยาย 15 เท่า การวิเคราะห์ทำได้สะดวกรวดเร็วด้วยอุปกรณ์เสริมที่ประดิษฐ์ขึ้นสำหรับใช้ร่วมกับกล้องจุลทรรศน์อินฟราเรด อุปกรณ์นี้สามารถปรับระนาบสะท้อนแสงของอัญมณีได้ ทำให้เทคนิคนี้เป็นการวิเคราะห์ที่ไม่ทำลายตัวอย่าง ไม่ต้องเตรียมตัวอย่างในการวิเคราะห์ และใช้เวลาในการวิเคราะห์สั้น อินฟราเรดสเปกตรัมของอัญมณีแท้ อัญมณีสังเคราะห์ และอัญมณีเลียนแบบ ที่วิเคราะห์ด้วยเทคนิคดิฟฟิวรีเฟลกแดนซ์ เทคนิคการสะท้อนแบบสเปกูลารีเฟลกชัน และเทคนิคทรานสเฟลกแดนซ์จะถูกนำมาเปรียบเทียบ สเปกตรัมจากการวิเคราะห์ด้วยเทคนิคทรานสเฟลกแดนซ์มีคุณภาพดีเทียบเท่า หรือดีกว่าเทคนิคดิฟฟิวรีเฟลกแดนซ์ที่เป็นที่ยอมรับโดยทั่วไป นอกจากนี้ทรานสเฟลกแดนซ์สเปกตรัมที่วิเคราะห์ได้แต่ละครั้งจะให้ผลเหมือนกัน เนื่องจากสเปกตรัมที่ได้จะไม่ขึ้นอยู่กับการวางตัวอย่างในการวิเคราะห์ เทคนิคที่พัฒนาขึ้นสามารถใช้ในการวิเคราะห์อัญมณีที่เจียรไนแล้วและอัญมณีบนเครื่องประดับได้โดยไม่ต้องถอดออกมาจากตัวเรือนเครื่องประดับ สามารถวิเคราะห์อัญมณีแต่ละเม็ดที่อยู่บนตัวเรือนเครื่องประดับที่ซับซ้อนได้อย่างมีประสิทธิภาพ จากลักษณะเฉพาะของแถบการดูดกลืนแสงอินฟราเรดที่มีความสัมพันธ์โดยตรงกับโครงสร้างและองค์ประกอบทางเคมี ข้อมูลที่ได้สามารถแสดงถึงโครงสร้าง ความบกพร่องของโครงสร้าง และสิ่งเจือปนในอัญมณี ทำให้สามารถประยุกต์ใช้เทคนิคอินฟราเรดในการจำแนกอัญมณีสังเคราะห์ และอัญมณีเลียนแบบ ออกจากอัญมณีธรรมชาติ และบ่งบอกการปรับปรุงคุณภาพของอัญมณีได้อย่างมีประสิทธิภาพ

ภาควิชา.....เคมี.....ลายมือชื่อนิสิต.....  
 สาขาวิชา.....เคมี.....ลายมือชื่ออาจารย์ที่ปรึกษา.....  
 ปีการศึกษา.....2548.....ลายมือชื่ออาจารย์ที่ปรึกษาร่วม.....

## 4373860823 : MAJOR CHEMISTRY

KEY WORDS: FT-IR SPECTROSCOPY / TRANSFLECTANCE / DIFFUSE REFLECTANCE / SPECULAR REFLECTION / KRAMER KRONIG TRANSFORMATION / FACETED GEMSTONE / DIAMOND / EMERALD / RUBY / SAPPHIRE / TURQUOISE

PIMTHONG THONGNOPKUN: CHARACTERIZATION OF SOME VARIETIES OF GEMSTONES BY FT-IR SPECTROSCOPY: ASSOC. PROF. SANONG EKGASIT, PH.D., THESIS CO-ADVISOR: MRS. WILAWAN ATICHAT. 173 pp. ISBN

A novel transreflectance technique using an infrared microscope was introduced for spectral acquisition of loose and mounted faceted gemstones. The transreflectance technique exploited total internal reflection phenomenon within the faceted gemstone for the spectral acquisition. The incident radiation is coupled to the gemstone via the table facet while the transreflectance radiation is collected by the built-in 15X Cassegrain objective. A novel accessory for adjusting the reflection plane of the faceted gemstone was constructed and was utilized with the infrared microscope. The technique is nondestructive, requires no sample preparation, and has short analysis time. FTIR spectra of faceted gemstones, synthetic gemstones and gemstone simulants collected by diffuse reflectance, specular reflection, and transreflectance techniques were compared. The same spectra features with better spectral quality as those from the well-accepted diffuse reflectance technique are observed by the transreflectance technique. Unlike the diffuse reflectance spectrum, the transreflectance spectrum was not affected by the diamond arrangements. The technique can be employed for direct spectra acquisition of mounted gemstone without taking the gemstone out of the jewelry setting. Moreover, an individual gemstone on the complex jewelry setting can be selectively measured. Infrared absorption bands unique to the chemical compositions, impurities, and treatment processes of the gemstone were discussed. The observed transreflectance spectra can be exploited for gems classification.

Department.....Chemistry.....Student's signature.....

Field of study.....Chemistry.....Advisor's signature.....

Academic year.....2005.....Co-advisor's signature.....

*Wm*  
*Sanong Ekgasit*  
*Wilawan Atichat*

## ACKNOWLEDGEMENTS

The fellowship and financial support via the University Development Committee (UDC) through the Chanthaburi IT Campus of Burapha University to Pimthong Thongnopkun is gratefully acknowledged.

I would like to express my sincere gratitude to Associate Professor Dr. Sirirat Kokpol, Associate Professor Dr. Supot Hannongbua, Associate Professor Dr. Visut Pisutha-Arnond, and Assistant Professor Dr. Pornsawat Wathanakul, for the insightful suggestions and contribution as thesis committee.

Gratefully thanks to my thesis co-advisor, Mrs. Wilawan Atichat, for the suggestions on gemological background and gemstone samples. The gemstone material supports from Associate Professor Dr. Arunee Terdtheppitak at the Gems College of Burapha University are truly appreciated. I am also thankful to Mr. Taweesak Janduang for his substantial assistance in the fabrication of novel accessory.

In essence, the research would never be successfully completed without the excellent advice and pioneering spirit from my thesis advisor, Associate Professor Dr. Sanong Ekgasit, whose trust and scientific excitement inspire me in the most important moments of making right decisions. I learned so much from him and accumulated hands-on experiences and skills critical to my future. I have greatly enjoyed the innovative and challenging atmosphere in his laboratory. His translation of cares into action, guidance, and understanding are deeply thankful.

Warmest thanks to my friends and colleagues at the Sensor Research Unit for the everlasting friendship and spiritual supports throughout the time of study. I wish to express my appreciation for sharing good times, surviving hard times together.

Above all, I am profoundly grateful to my wonderful parents and the endearing family for their patient love, perpetual encouragement, and overwhelming support.

## CONTENTS

	Pages
ABSTRACT IN THAI.....	iv
ABSTRACT IN ENGLISH.....	v
ACKNOWLEDGEMENTS.....	vi
LIST OF FIGURES.....	xi
LIST OF TABLES.....	xviii
LIST OF ABBREVIATIONS.....	xix
LIST OF SYMBOLS.....	xx
 CHAPTER I INTRODUCTION.....	 1
1.1 What is a Gemstone.....	1
1.2 Gem Identification.....	5
1.2.1 Identification via Physical Properties.....	5
1.2.2 Identification via Chemical Information.....	6
1.3 Disclosure Requirements and Ongoing Challenges for Gems Identification...	10
1.4 FT-IR Spectroscopy for Gem Characterization.....	13
1.5 Scope of the Research.....	14
1.6 Objectives of the Research.....	15
 CHAPTER II THEORETICAL BACKGROUND.....	 16
2.1 Fundamentals of Light Propagation.....	16
2.1.1 Interaction of Light and Matters.....	16
2.1.2 Snell's Law: A Principle of Light Reflection and Refraction.....	18
2.2 Practical Sampling Techniques of Infrared Spectroscopy for Gem Analysis...	19
2.2.1 Transmission Technique.....	19
2.2.2 Specular Reflection Technique.....	21
2.2.3 Diffuse Reflection Technique.....	23

2.3 Infrared Microscopy.....	25
2.4 Transflectance: Novel Technique for Characterization of Faceted Gemstone.	27
2.4.1 Principle of light that entering the gemstone .....	27
2.4.2 Principle of Gems Cutting.....	29
2.4.3 Transflectance Phenomena .....	33
<b>CHAPTER III EXPERIMENTAL SECTION.....</b>	<b>35</b>
3.1 Materials and Equipments.....	36
3.1.1 Gemstone Samples.....	36
3.1.2 Instruments.....	38
3.1.3 Default Spectral Acquisition Parameters.....	38
3.2 The novel accessory.....	39
3.2.1 The Optical Design and Fabrication Procedure.....	39
3.2.2 Setting of the Novel Accessory with IR Microscope.....	44
3.3 Experimental Procedures.....	45
3.3.1 Transmission Technique .....	45
3.3.2 Diffuse Reflectance Technique.....	45
3.3.3 Specular Reflection Technique.....	46
3.3.4 Transflectance Technique.....	47
3.4 Influence of Sample Arrangement .....	48
3.5 Influence of the Varying Aperture Size in Transflectance Technique.....	49
3.6 Unique Identification of Gemstone.....	51
3.6.1 Sample of Interest.....	51
3.6.2 Instruments for Data Acquisition .....	51
3.6.3 Default Instrumental Parameters.....	51
3.6.4 Experimental Procedure.....	52



CHAPTER IV RESULTS AND DISCUSSION.....	53
4.1 Comparison of FT-IR Sampling Techniques.....	53
4.2 Diffuse Reflectance Technique for Gem Characterization.....	56
4.2.1 Diamond Characterization .....	56
4.2.2 Emerald Characterization.....	62
4.2.3 Ruby and Sapphire Characterization.....	70
4.2.4 Turquoise Characterization.....	75
4.3 Specular Reflection Technique for Gem Characterization.....	82
4.3.1 Diamond Characterization .....	82
4.3.2 Emerald Characterization.....	85
4.3.3 Ruby and Sapphire Characterization.....	91
4.3.4 Turquoise Characterization.....	93
4.4 Transflectance Technique for Gem Characterization.....	102
4.4.1 Parameter Affecting Transflectance Spectrum .....	102
4.4.1.1 Effect of Cut shape .....	102
4.4.1.2 Effect of Defect in Gemstone.....	105
4.4.1.3 Effect of Transparency.....	107
4.4.1.4 Effect of Sample Arrangement.....	108
4.4.1.5 Effect of Aperture Size.....	114
4.4.2 Identification of Gemstones.....	117
4.4.2.1 Diamond Characterization.....	117
4.4.2.2 Emerald Characterization.....	121
4.4.2.3 Ruby and Sapphire Characterization.....	122
4.4.3 Other Applications of Transflectance Technique.....	128
4.4.3.1 Unique Identification of diamonds.....	128
4.4.3.2 Jewelry Analysis.....	137

CHAPTER V CONCLUSIONS.....	141
REFERENCES.....	143
APPENDICES.....	149
Appendix A Publication I.....	150
Appendix B Publication II.....	159
Appendix C Publication III.....	166
CURRICULUM VITAE.....	173



สถาบันวิทยบริการ  
จุฬาลงกรณ์มหาวิทยาลัย

## LIST OF FIGURES

	Pages
1.1 Synthetic gemstone.....	2
1.2 Raw gemstones and faceted gemstones.....	6
1.3 Various cut shapes of gemstone .....	12
1.4 Complex gems setting on jewelries.....	12
2.1 Propagation of a linearly polarized electromagnetic wave in the direction of propagation.....	16
2.2 Interactions of light with matter.....	17
2.3 Reflection and refraction of a plane wave at a dielectric interface based on Snell's Law.....	19
2.4 Simplified schematic of the transmission measurement.....	20
2.5 Simplified schematic of the transmission measurement which coupled infrared radiation passes through the girdle.....	21
2.6 Schematic showing specular reflection measurement of faceted gemstone.....	22
2.7 Infrared spectra of polymethyl methacrylate (Lucite); (a) The infrared reflection spectrum, (b) the spectrum A after Kramers-Kronig Transformation, and (c) the transmission spectrum.....	23
2.8 Schematic showing diffuse reflectance measurement of faceted gemstone.....	24
2.9 Optical diagram of an infrared microscope used for infrared microscopy.....	26
2.10 Schematic of angle of incidence, refraction and reflection in faceted gemstone. The angle of incidence equals angle of reflection at the air/gemstone interface.	28
2.11 Schematic of refraction in relation to the direction normal. ( $n_{\text{gemstone}} > n_{\text{air}}$ ).....	29
2.12 Light rays are reflected back from a gemstone's facet at angle to the direction normal (N) is greater than the critical angle. The radiation refracts out of the gemstone at an angle less than the critical angle.....	31

2.13 (A) the total internal reflection of ray 1, which meets the pavilion facets of diamond at angles greater than the critical angle, and the refraction of ray 2 out of the pavilion when it meets it at an angle less than the critical angle. (B) the pavilion has been made deeper to maintain the total internal reflection or ray 1 in quartz, which has a much larger critical angle than diamond.....	33
2.14 A schematic drawing of a round brilliant cut diamond (A). Ray tracing of different radiations inside a round brilliant cut diamond (B). A summary of angles at diamond/air interface are shown.....	35
3.1 Composition of a novel accessory for nondestructive characterization of faceted gemstone using infrared microscope.....	40
3.2 Arrangement of the novel accessory for nondestructive characterization of faceted gemstone (A), and jewelry (B).....	42
3.3 Example of experimental procedures for spectral acquisition of gems on jewelries: a necklace (A), and a ring (B). The jewelry is placed on the sample holder of novel accessory without removing the gemstones from the jewelry setting.....	43
3.4 Actual experimental setup for gem characterization using novel accessory with an infrared microscope .....	44
4.1 FTIR spectra of a 0.1050 ct round brilliant cut type IaB natural diamond acquired by (A) diffuse reflectance, (B) transreflectance, and (C) specular reflection techniques.....	54
4.2 FTIR spectra of a 0.1075 ct round brilliant cut type IaA natural diamond acquired by (A) diffuse reflectance, (B) transreflectance, and (C) specular reflection techniques.....	55
4.3 Diffuse reflectance spectra of faceted diamonds: 0.11 ct green diamond (A), 0.08 ct red diamond (B), 0.07 ct pink diamond (C), 0.10 ct yellow diamond (D), and 0.13 ct black diamond (E).....	58

4.4	Normalized diffuse reflectance spectra of the diamond in Figure 4.2 under different arrangements. The diamond was rotated: 0° (A), 45° (B), 90° (C), 135° (D), 180° (E), 225° (F), 270° (G), and 315° (H) with respect to a reference position. Due to a significant variation of absorption magnitudes, the observed spectra were normalized by the absorption at 2493 cm <sup>-1</sup> . The inset of absorptions in the one-phonon region was added for clarity.....	59
4.5	FTIR spectra of round brilliant cut diamond simulants acquired by diffuse reflectance technique.....	61
4.6	FTIR spectra of emerald acquired by (A) transmission (KBr pellet method) and (B) diffuse reflectance techniques of a 0.730 ct oval cut natural emerald...	63
4.7	FTIR spectra of faceted natural emerald acquired by diffuse reflectance technique; 0.6800 ct (A), 0.6105 ct (B), 0.2535 ct (C), and 0.2315 ct (D). The absorption of CO <sub>2</sub> in the ambient air was eliminated by purging the spectrometer with a dry nitrogen gas.....	66
4.8	FTIR spectra of natural and synthetic emeralds acquired by diffuse reflectance technique.....	67
4.9	Normalized diffuse reflectance spectra of 0.4960 ct hydrothermal emerald (princess cut) under different arrangement. The emerald was rotated: 0° (A), 45° (B), 90° (C), 135° (D), 180° (E), 225° (F), 270° (G), and 315° (H) with respect to a reference position.....	69
4.10	FTIR spectra of natural and synthetic rubies acquired by diffuse reflectance technique.....	72
4.11	FTIR spectra of rubies and sapphire from different country of origin acquired by diffuse reflectance technique.....	73
4.12	Diffuse reflectance spectra of 1.1510 ct hydrothermal ruby (oval cut) under different arrangement. The ruby was rotated: 0° (A), 45° (B), 90° (C), 135° (D), 180° (E), 225° (F), 270° (G), and 315° (H) with respect to a reference position.....	74
4.13	FTIR spectra of natural turquoise acquired by (A) transmission (KBr pellet method) and (B) diffuse reflectance techniques.....	76

4.14 Diffuse reflectance spectra of 6.3805 ct natural turquoise (rough stone) under different arrangement. The turquoise was rotated: 0° (A), 45° (B), 90° (C), 135° (D), 180° (E), 225° (F), 270° (G), and 315° (H) with respect to a reference position.....	78
4.15 FTIR spectra of natural, impregnated and imitation turquoises acquired by diffuse reflectance technique.....	79
4.16 FTIR spectra of round brilliant cut diamonds acquired by specular reflectance technique.....	83
4.17 FTIR spectra of round brilliant cut diamond simulants acquired specular reflection technique.....	84
4.18 Specular reflection spectra of the 0.7520 ct hydrothermal emerald under different arrangements. The diamond was rotated: 0° (A), 45° (B), 90° (C), 135° (D), 180° (E), 225° (F), 270° (G), and 315° (H) with respect to a reference position. The inset of absorptions in the fundamental region was added for clarity.....	86
4.19 FTIR spectra of natural emeralds acquired by specular reflection technique.....	87
4.20 Specular reflectance spectra of hydrothermal emeralds acquired by specular reflection technique.....	88
4.21 FTIR spectra of flux emeralds acquired by specular reflection technique.....	89
4.22 FTIR spectra of the same specimens in Figure 4.19 - 4.21. The spectra are Kramer-Kronig transformations.....	90
4.23 FTIR spectra of natural and synthetic ruby acquired by specular reflection technique.....	91
4.24 FTIR spectra of ruby and sapphires from different mine acquired by specular reflectance technique.....	92
4.25 FTIR spectra of natural turquoise (cabochon) acquired by (A) transmission (KBr pellet method), (B) specular reflection, and (C) KK transformation of spectrum (B).....	93

4.26 FTIR spectra of imitation turquoise (Gibbsite) acquired by (A) transmission (KBr pellet method), (B) specular reflection, and (C) KK transformation of spectrum (B).....	95
4.27 FTIR spectra of natural, impregnated and imitation turquoises acquired by specular reflection technique.....	96
4.28 FTIR spectra of the same natural, impregnated and imitation turquoises in Figure 28 acquired by specular reflection technique and then corrected by KK transformation.....	97
4.29 FTIR spectra of 6.3805 ct natural turquoise at different sampling areas acquired by specular reflection technique. The observed spectra are KK-transformed.....	99
4.30 FTIR spectra of a treated turquoise at different sampling areas acquired by specular reflection technique. The shown spectra are KK-transformed.....	100
4.31 FT-IR spectra of faceted emerald with various cutting styles and shapes. <u>Note.</u> (A) and (B) are well-cut proportion emeralds, (C) and (D) are poor-cut proportion emeralds.....	103
4.32 FTIR spectra of emeralds with different number of defects acquired by transfectance techniques. <u>Note:</u> Number of defect $D > C > B > A$ .....	106
4.33 Transflectance spectra of various gemstones with different diaphaneity: (A) diamond: transparency, (B) natural ruby: translucency, and (C) hydrothermal emerald: semi-transparency.....	107
4.34 Transflectance spectra of a 0.1075 ct round brilliant cut diamond under different arrangement. The diamond was rotated: $0^\circ$ (A), $45^\circ$ (B), $90^\circ$ (C), $135^\circ$ (D), $180^\circ$ (E), $225^\circ$ (F), $270^\circ$ (G), and $315^\circ$ (H) with respect to a reference position. The inset of absorptions in the one-phonon region was added for clarity.....	109

4.35	Transflectance spectra of the 1.0595 ct moissanite under different arrangement. The diamond was rotated: 0° (A), 45° (B), 90° (C), 135° (D), 180° (E), 225° (F), 270° (G), and 315° (H) with respect to a reference position. The inset of absorptions in the one-phonon region was added for clarity.....	110
4.36	Transflectance spectra of the 0.4960 ct hydrothermal emerald (princess cut) under different arrangement. The emerald was rotated: 0° (A), 45° (B), 90° (C), 135° (D), 180° (E), 225° (F), 270° (G), and 315° (H) with respect to a reference position.....	112
4.37	Transflectance spectra of the 1.1510 ct hydrothermal ruby (oval cut) under different arrangement. The ruby was rotated: 0° (A), 45° (B), 90° (C), 135° (D), 180° (E), 225° (F), 270° (G), and 315° (H) with respect to a reference position.....	113
4.38	Transflectance spectra of the 0.105 ct Type IaB diamond under different aperture size setting. The aperture of infrared microscope was 20 (A), 30 (B), 40 (C), 50 (D), 60 (E), 70 (F), 80 (G), 90 (H) and 100 (I).....	115
4.39	Transflectance spectra of the 0.752 ct hydrothermal emerald under different aperture size setting. The aperture of infrared microscope was 20 (A), 30 (B), 40 (C), 50 (D), 60 (E), 70 (F), 80 (G), 90 (H) and 100 (I).....	116
4.40	Transflectance spectra of colored and treated diamonds: 0.2845 ct type IaA brown diamond (A), 0.4440 ct type IaB brown diamond (B), 0.0750 ct HPHT type Ib diamond (C), and 0.1440 ct irradiated and annealed diamond (D).....	118
4.41	FTIR spectra of round brilliant cut diamond simulants acquired transflectance techniques.....	120
4.42	FTIR spectra of natural and synthetic emeralds acquired by transflectance technique.....	122
4.43	FTIR spectra of natural and synthetic rubies acquired by transflectance technique.....	123
4.44	FTIR spectra of fancy color sapphires acquired by transflectance technique....	125



4.45 FT-IR spectra of different types of diamonds acquired by transreflectance technique.....	130
4.46 FT-IR spectra of different types of diamonds acquired via transreflectance technique.....	132
4.47 FTIR spectra of a 0.1075 ct round brilliant cut diamond acquired by transreflectance technique from different spectrometers.....	135
4.48 Normalized spectra of the 0.1075 ct round brilliant cut diamond acquired by transreflectance technique from different spectrometers. The observed spectra were normalized by the absorption in the two-phonon at 2493 cm <sup>-1</sup> . The inset of absorptions in one-phonon region was added for clarity.....	135
4.49 Transreflectance spectra of the 0.1075 ct round brilliant cut diamond under different arrangement. The diamond was rotated: 0° (A), 45° (B), 90° (C), 135° (D), 180° (E), 225° (F), 270° (G), and 315° (H) with respect to a reference position. The inset of absorptions in the one-phonon region was added for clarity.....	136
4.50 Normalized transreflectance spectra of mounted round brilliant cut diamonds on a ring before cleaning (A) and after cleaning (B). The observed spectra were normalized by the absorption in the two-phonon at 2493 cm <sup>-1</sup> . The inset of absorptions in C-H stretching region was added for clarity.....	138
4.51 Transreflectance spectra of faceted sapphire and diamonds on a ring.....	140
4.52 Transreflectance spectra of faceted diamond simulatant on a brooch and natural diamond on a ring.....	140

**LIST OF TABLES**

	Pages
1.1 Instruments for gem identification .....	9
3.1 Physical and optical properties of the measured gemstones.....	37
4.1 Peak assignment of water molecules in emerald.....	64
4.2 Infrared absorption spectra of turquoise.....	76



สถาบันวิทยบริการ  
จุฬาลงกรณ์มหาวิทยาลัย

**LIST OF ABBREVIATIONS**

Al <sub>2</sub> O <sub>3</sub>	: aluminum oxide
C	: carbon
CZ	: cubic zirconia
DRIFT	: diffuse reflectance infrared Fourier transform
DTGS	: deuterated triglycine sulfate
EDXRF	: energy-dispersive X-ray fluorescence
ESR	: electron spin resonance
FT-IR	: Fourier transform infrared
GGG	: gadolinium gallium garnet
HPHT	: high pressure-high temperature
IR	: infrared
KBr	: potassium bromide
KK	: Kramers-Kroing
K-M	: Kubelka-Munk
MCT	: mercury cadmium telluride
MIR	: mid infrared
μm	: micron
RI	: refractive index
S/N	: signal-to-noise
SrTiO <sub>3</sub>	: strontium titanate
TIR	: total internal reflection
YAG	: yttrium aluminium garnet

**LIST OF SYMBOLS**

$A$	: absorbance
$c$	: concentration
$\varepsilon$	: absorption coefficient
$I$	: intensity of incident radiation
$I_A$	: intensity of absorbed radiation
$I_R$	: intensity of reflected radiation
$I_S$	: intensity of scattered radiation
$I_T$	: intensity of transmitted radiation
$k$	: molar absorptivity
$l$	: film thickness
$n$	: refractive index
$R$	: absolute reflectance
$s$	: scattering coefficient
$\theta$	: angle of incidence
$\theta_c$	: critical angle
$\bar{\nu}$	: wavenumber

สถาบันวิทยบริการ  
จุฬาลงกรณ์มหาวิทยาลัย

# CHAPTER I

## INTRODUCTION

Gemstone is currently one of the champion products of Thailand in the world market. Quality control and quality assurances of the gem products have become important issues. There are various problems regarding gem analysis and sample preparation for analysis especially faceted gems and jewelry. In general, the identity of gem is easily performed based on physical and optical properties. However, the characterization techniques encounter limitations and cannot provide vital information particularly when chemical composition and structure related information are required. Therefore more sophisticated techniques are necessary [1-5].

### 1.1 What is a gemstone?

Gemstone is a mineral or rock that when cut or faceted and polished is collectible or can be used in jewelry. Others are organic, such as amber (fossilized tree resin) and jet (a form of coal). The gemstones possessed the desirable attributes of beauty, rarity, durability, portability, as well as the transient appeal of fashion at certain times and places [4]. These attributes have contributed to the popularity of gemstones that has continued since ancient times. Gemstones are described and differentiated by gemmologists with certain technical specifications. First, what is it made of or its chemical composition. Diamonds, for example, are made of carbon (C) while rubies are made of aluminium oxide ( $\text{Al}_2\text{O}_3$ ). Next, many gems are crystals which are classified by crystal system such as cubic or trigonal or monoclinic. Another term is habit or the form of the gem is usually found, for example diamonds which have a cubic crystal system are often found as octahedrons.

In mineralogy there are over 2000 different minerals species. In order to subdivide these into manageable numbers, they are classified initially into a series of

*groups*, each of which contains those mineral species which have similar features or characteristics. In addition, gem minerals are further subdivided into *species*, which have their own individual chemical compositions and characteristics, and *varieties* of species, which differ from each other only in color or general appearance. Gemstones have a certain refractive index, dispersion, specific gravity, hardness, cleavage, fracture and luster. They may exhibit pleochroism, double refraction and have an optic sign. They may have a certain luminescence and a distinctive absorption spectrum associated with chemical compositions and structures [4-5].

### ***Gemstone Synthesis***

A synthetic gem material has the same chemical composition and crystal structure as a natural gemstone. In contrast, a gem simulant or imitation has the appearance of a natural gemstone, but possesses a different chemical composition, physical properties, and crystal structure. Both synthetic and simulant gem materials always possess gemological properties that allow them to be distinguished from the corresponding natural gemstones [2-4].



**Figure 1.1** Synthetic gemstone

There are two general classes of growth technologies that are used to prepare crystalline synthetic gems; 1) crystallization from a fluid of different composition (such as aqueous hydrothermal solution), and 2) crystallization from a melt with roughly the same chemical composition as the crystal being grown (such as flux or

flame fusion techniques) [2-4]. Both are high-temperature processes and each can be divided into a number of subtechniques. The resulting products reflect the direct characteristic of the melt or the crystallographic character of the seed orientation and the impact of specific chromophores or chemical colorants simultaneously dissolved in the crystallization system (see Figure 1.1).

Some gemstones are manufactured to imitate other gemstones. For example, cubic zirconia is a synthetic artificial diamond substitute composed of zirconium oxide. The imitations has the look and color of the real stone but possess neither their chemical nor physical characteristics. However, true synthetic gemstones are not necessarily imitation. For example, diamond, ruby, sapphire and emerald synthesized in laboratories which possess very nearly identical chemical and physical characteristics as the genuine article. Diamond has long been the prime interest of gem and jewelry markets due to its popularity, mystic beliefs, and commercial value. Due to its high commercial value, various types of diamond simulants have been produced. Recently, large gem quality synthetic diamonds are available in jewelry market. As a result, gemologists and jewelry traders are increasingly dependent on chemical-based analytical techniques to defend the integrity of their trade against aggressive tampering. Among colored stones, the most important synthetics are synthetic corundum (sapphire and ruby), emerald, spinel and amethyst. They are produced by both solution and melt crystallization techniques. In the marketplace, flame-fusion and crystal-pulled synthetics (corundum and spinel) are relatively less expensive and therefore are more abundant than the flux and hydrothermal synthetics [2-5].

### ***Gemstone Enhancement***

The term 'enhancement' is a treatment or process other than cutting and polishing that improves the appearance (color/ clarity/ phenomena), durability, value or availability of a gemstone. Today, many gemstones in the gems market have been enhanced by a variety of methods. Such processes may range from simple heating (such as tanzanite) to sophisticated irradiation (such as blue topaz). However, gems

which have not been subject to enhancement are generally worth more than those of the same quality which have been enhanced.

Various gem treatment methods currently performed can be grouped into two general categories – methods to change color, and methods to change clarity. Not all treatment methods are obviously appropriate for every gemstone. The costs of the starting material and the treatment method itself, versus the value of the resulting treated materials, are also significant factors in determining if a particular treatment method will be used. The method to change color, the use of color foil or paper behind a poorly colored or colorless stone, usually in a closed setting, was commonplace in antique jewelry. Another relatively simple way of improving or changing a gem's appearance is to dye or stain it. Some gem materials such as turquoise are legitimately impregnated with colorless paraffin wax (or plastic, which gives a more permanent result) to stabilize them and prevent attack from acidic perspiration. Veins of turquoise that are too irregular or too thin to be made into cabochons are often backed with a metal-loaded epoxy resin. The colorless oils are also used to hide surface cracks, and color oil serves the double purpose of hiding surface flaws and improving the color appearance of emeralds, rubies and sapphires (both polished and rough). In addition, lower-clarity polished diamonds can be treated with special, high-refractive index glasses to fill surface-reaching cracks, making these filled fractures much less visible, and thus improving the apparent clarity of the diamond. The enhanced or treated diamonds are more difficult to detect or to exclude from the natural un-treated counterparts [2-5].

An increasing number of gemstones are subjected to various forms of heat treatment to improve or change their color. Some stones even experience several heat treatments as they are purchased and resold, each owner attempting to improve the stone's appearance and value, with occasionally disastrous results. The mechanism by which irradiation increases or modifies color in gemstone is to do with the production of color centers, which can then be altered by subsequent heat treatment. Unless some residual radioactivity is detected (which has happened when high energy radiation has been used to produce deeper color and the stones released on the



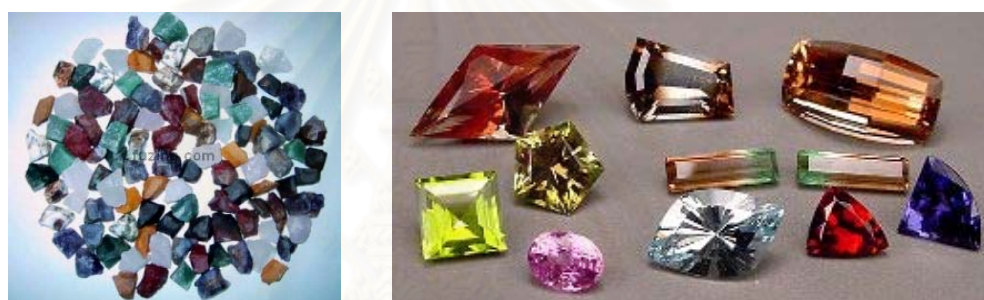
market too soon) there is no simple way of distinguishing between natural blue topaz and the irradiated stone. Pale or colorless corundum can be transformed into the rich colors of ruby or sapphire by first packing the preformed stones (faceted except for the final polish) in a clay mixture containing the appropriate transition element additives. With earlier treatments, the resulting surface-diffused color was only a few thousands of an inch (less than a tenth of a millimeter) deep, but thicker layers of diffusion are now being produced. Because of surfacing pitting caused by the high temperature, final polishing of the faceted stone or the cabochon is carried out after the diffusion process. The thinness of the coating, and the possibility of it being removed if the stone ever needs repolishing, makes surface-induced enhancement an unacceptable treatment [1-5].

## **1.2 Gem identification**

### **1.2.1 Identification via Physical Properties**

In the past, most gemstones can be identified by a variety of standard testing instruments which provided the physical properties and optical characteristics of the stones. These instruments are listed in Table 1, along with the kind of data that each instrument provided [2-3]. In general, an obtained result from a single test cannot be concluded, thus a gemologist often needs to perform several different tests to obtain a positive identification. The most important of these basic gemological instruments is the binocular microscope. The microscope is utilized to examine inclusions, growth features, color zoning and other aspects of appearance that provide important clues regarding an identification of gemstone. Since refractive index (RI) values are distinctive of many gemstones, measurement of RI by means of a refractometer is also very important. The spectroscope is sometimes used to separate natural from synthetic gem materials, as variations in chemical composition can be revealed in the absorption spectrum. Although their absorption spectra by means of spectroscope related to color of gemstone but they are indirectly associated with chemical composition. Thermal and electrical conductometers, as well as reflectometers, are mostly widely used for distinguishing diamond from imitation materials such as

cubic zirconia. Within the past few years, a new material, synthetic moissanite (silicon carbide), has been marketed for jewelry purposes. It has been imposed serious identification problems among jewelers, because it cannot be distinguished from diamond by thermal conductivity test [6]. However, synthetic moissanite displays optical features due to its anisotropic optical character which allow it to be recognized by trained gemologists. Detection of treatment processes and gemstone simulants are major tasks for gemstone testing laboratories, especially those of the faceted gemstone and gemstone on jewelry setting where nondestructive and/or noninvasive characterization is required.



A: Raw gemstones

B: Faceted gemstones

**Figure 1.2** Raw gemstones and faceted gemstones

### 1.2.2 Identification via Chemical Information

In the recent years, various synthetic gemstones with the same chemical composition as the natural gemstones was encountered in the market. In many cases, they cannot be differentiated from their natural counterparts by the conventional characterization techniques such as refractive index, hardness, color, specific gravity, and light dispersion measurements [1-4]. As mentioned earlier, there are various gemstone simulants of different chemical composition with similar appearances to those of the natural gemstones. Moreover, various treatments (i.e., irradiation, heat, and high pressure-high temperature (HPHT) treatments) were normally applied to the low quality gemstones in order to improve their appearances (i.e., eliminate inclusion, enhance color, and improve clarity). Due to their distinct commercial

values, it is important for gemologist to correctly identify synthetic, natural, and treated gemstones.

Some advance equipments for gemstone characterization are listed in Table 1 [3]. Advance analytical techniques providing information associated with chemical structures and compositions such as Fourier transform infrared (FT-IR) spectroscopy [7-13], Raman spectroscopy [14], electron spin resonance (ESR) spectroscopy [15-16], and photoluminescence spectroscopy [17-19] are necessary for gemstone characterization. The advanced analytical instrumentation that may be accessible to well equipped gemological laboratories is listed in Table 1 [2-4]. Since, these analytical techniques normally involve little damage to sample, the materials that suitable for these analyses are rough and raw gemstones (see Figure 1.2).

An energy-dispersive X-ray fluorescence (EDXRF) spectroscopy was employed for analyzing polished gemstones which the characteristic of chemical elements (between sodium and uranium on the periodic chart) in the sample were observed [2-4]. If suitable standards of known chemical composition are available, comparison of analyses of the standards and the unknown sample can provide semiquantitative from chemical composition data of the unknown. The EDXRF method is rapid, and requires no sample preparation other than the requirement for a flat polished surface for analysis. The electron microprobe is a more expensive analytical instrument that offers ability to quantitatively analyze small areas on a sample but the sample itself must possess a polished flat surface, and must usually be carbon coated for the analysis. Radiography is an important tool for obtaining images of the internal structure of pearls, and is used for distinguishing natural from cultured pearls. This method has also been employed for fracture-filled diamonds, since the filler glass is relatively opaque to X-rays in comparison to the diamond. If sufficient material is available for destructive analysis to prepare a powder sample, a diffractometer or powder camera can provide an X-ray diffraction pattern for the identification of colored stones or mineral inclusions. It can also examine any cathodoluminescence when a gemstone is exposed to a beam of electrons in a vacuum chamber [2].

Spectroscopic techniques also widely employed for gem characterization. The techniques include the visible spectroscopy, infrared spectroscopy, luminescence and Raman spectroscopy. For experiment, faceted gemstones must be cut in styles to control the transmission of light to optimize the amount of incident light that exits the gemstone through the upper facets. Therefore, it is sometimes difficult to mount a gemstone (or a gemstone set in a piece of jewelry) in a spectrometer in such a way that a sufficient light intensity can pass through the gemstone to the detector. Moreover, other sensitivity problems can exist for recording spectra of highly colored or highly defective gemstones. The path-length of light traveling through the gemstone cannot be accurately measured, thus the obtained absorption intensities are not directly related to the path-length [2-4]. In the case of Raman technique, observed spectra were normally employed for identify inclusions within gemstones. Raman spectroscopy was employed to identify inclusions within diamond, and to separate naturals from simulants. Photoluminescence is used to differentiate natural and synthetic diamonds and to detect certain color centers. Visible spectra provide information on causes of color and evidences of some treatments. For determining causes of color, it may be important to record oriented spectra using polarizing filters for optically anisotropic gemstones. These spectra can also be used to expect the face-up color appearance of a gemstone. FT-IR spectroscopy gains popularity in gem characterization due to its rich chemical information where direct relationships between spectral features and material characteristics (i.e., chemical composition, structure and additives) are obtained. Various FT-IR sampling techniques and accessory designed for specific applications and sample form are available. Due to the non-destructive nature of the techniques, they are especially useful for cut gem characterization. However, different sampling techniques encounter different difficulties. For example, infrared spectra utilized for the presence of a foreign material in a treated gemstone, such as oil or resins in the open fractures of treated emeralds, and plastic in treated opals. Moreover, infrared spectroscopy was widely employed for characterization of treated diamonds and diamond simulants based on the chemical composition and impurities in the crystal lattice [10-11, 20].

**Table 1** Instruments for gem identification [3].

<b>Instruments</b>	<b>Information</b>
<i>Standard equipment</i>	
Hand lens (or loupe)	10X magnification of visual features
Binocular microscope	10X – 60X magnification of visual features (often used with various illumination, immersion, polarization, photographic and other imaging techniques)
Refractometer	Refractive indices, optic character, birefringence
Spectroscope	Visible spectra (both prism and diffraction grating designs)
Polariscope	Optic character, birefringence
Ultraviolet lamp	Fluorescence, UV transparency
Balance	Weight, specific gravity
Calcite dichroscope	Pleochroic colours
Reflectometer	Surface luster (reflectivity)
Thermal conductometer	Thermal conductivity (thermal inertia)
Electrical conductometer	Electrical conductivity
<i>Advanced equipment</i>	
Spectrophotometer	Ultraviolet, visible and near-infrared spectra (can also be used for color measurement)
FTIR spectrometer	Infrared spectra
Raman microspectrometer	Raman spectra of gems or inclusions
Luminoscope	Cathodoluminescence
X-ray fluorescence	Non-destructive chemical analysis of an area of sample
Electron microprobe	Non-destructive chemical analysis of a small area of a sample

Scanning electron microscope	High magnification images, element distribution mapping, non-destructive chemical analysis of a small area of a sample
Radiograph	X-ray transparency images
Diffractometer	X-ray diffraction patterns (or recorded photographically with a powder camera)

---

### 1.3 Disclosure Requirements and Ongoing Challenges for Gems Identification

Because of the large price differential between synthetic and natural gems, it is important that the gemologist be not only able to identify a stone but also able to determine whether it is a natural or a synthetic material. Furthermore, modern technology is increasing its impact on gemstone trading. Methods for changing color, and consequently the value, of gemstone are becoming more and more advanced and complicated. The treatment processes are difficult to determine via a conventional gemological characterization techniques. The degree of detection difficulty for synthetic gems increases significantly as the growth environment more closely approximates the processes of natural crystal development. As crystallization techniques continue to improve, the technical challenges facing gem testing laboratories will be increased dramatically. Some laboratory-grown gemstone have become so similar to their natural counterparts that there is a confidence crisis both in the marketplace and particularly in gem testing facilities that are required to consistently differentiate synthetic and natural materials. However, regardless of the similarities between natural and laboratory-grown products, the telltale differences between these growth environments can be entrapped in the chemical and physical natures of each material. Whether laboratory-grown or natural, each growth system leaves its indelible fingerprint on the final product. As the technical differences diminish between the natural and laboratory-grown gemstones, the degree of laboratory sophistication necessary to nondestructively distinguish between these materials must increase significantly. Technical superiority is essential to maintain the long-term stability of the gemstone market and the credibility of laboratory testing facilities [1-4].

Advance analytical techniques providing information associated with chemical structures and compositions are necessary for gemstone characterization. However, they are not widely employed in general laboratories because of the instrument themselves are quite expensive. Some analytical techniques must normally involve little damage to sample. The materials that available for these analyses are rough and raw gemstones. Some measurement techniques are not suitable for faceted gemstone due to its destructive nature. Gem characterization becomes a major task for gemstone testing laboratories, especially those of the high commercial value faceted gemstones and gemstones on jewelry where nondestructive and/or noninvasive characterization is required.

Recently, FT-IR spectroscopy is an alternative technique that widely employed for gems characterization. The technique is easy to use while infrared spectrometer is a standard instrument in characterization laboratories around the world. FT-IR spectrum is directly correlated to the chemical structure and chemical composition of the materials. Based on the observed spectral features of gem materials, classification of gemstone, determination of defects, impurities, and treatment process can be performed. Now, various FT-IR accessories designed for specific applications and sample form are available. Various sampling techniques and FT-IR accessory designed for specific applications and sample form are available. Due to the non-destructive nature of the techniques, they are especially useful for cut gem characterization. However, different sampling techniques encounter different difficulties. For faceted gemstone, major disadvantages of FT-IR conventional techniques are its cutting, thickness and complex reflections of the cut and polished surfaces (see Figure 1.3). The characterization becomes a major task for gemstone testing laboratories, especially those of the high commercial value faceted gemstones and gemstones on jewelry where nondestructive and/or noninvasive characterization is required. For gems with complex setting on jewelry, spectrum of an individual gemstone cannot be selectively measured by the conventional FT-IR technique. As shown in Figure 1.4, there are many gemstones on jewelry. According to the jewelry design, different sizes and varieties of faceted gemstones are imbedded in the metal setting. The only observable parts of the gems are the table facet, the star facet and

parts of the upper girdle facet. As a result, their infrared spectra cannot be acquired by diffuse reflectance or transmission classical techniques. In order to solve these problems, it necessary to develop a novel technique enables the collection of FT-IR spectra of all the mounted and loose faceted gemstones.

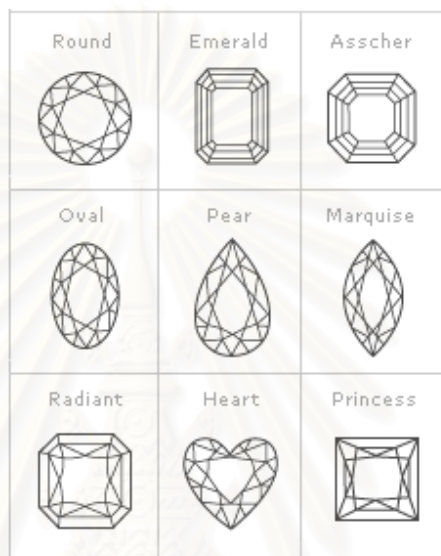


**Figure 1.3** Various cuttings of gemstone.



**Figure 1.4** Complex gems setting on jewelries.



#### 1.4 FT-IR Spectroscopy for Gem Characterization

FT-IR spectroscopy is an established and well-known technique for material characterization [7-8]. The technique is easy to use while infrared spectrometer is a standard instrument in gems testing laboratories around the world. FT-IR spectral fingerprints provide information directly related to chemical structure, chemical compositions, impurities and additive in the analyzed materials. As the results, the technique was employed for gem classification based on the particular species relates to both its chemical composition and its crystal structure. It was also employed for differentiating simulants from natural gemstone as well as determining the treatment processes applied onto the gemstone. However, conventional infrared characterization techniques encountered several problems that make them unsuitable for routine analysis of faceted gemstones and jewelry.

Transmission technique is a widely sampling technique for gem characterization. The technique required the pressing of sample with an alkali halide material as a pellet (most often use a potassium bromide, KBr). It is important that the sample can be ground and be well mixed with the KBr thus the hard gemstones are difficult to perform. Because the technique is destructive, it is not suitable for high commercial value faceted gemstone. Moreover, the disadvantage of this method is high interfering bands from water or moisture absorbed by KBr. Another classical transmission measurement is use a thin slab of specimen which is not suitable for faceted gemstone due to its destructive nature and complex reflections of the cut and polished surfaces (see Figures 1.2 and 1.3). Transmission measurement of a faceted gemstone using beam condenser is complicated by sample arrangement where the coupled infrared radiation must pass through girdle [21-22]. In addition, the semitransparent and opaque gemstone cannot be performed with this technique. As the results, transmission technique is considered to be undesirable because it is tedious and time-consuming, destructive nature, tend to be non-reproducible, and require significant sample modification

Another alternative sampling technique is reflection mode which permits a very rapid and nondestructive determination. It is particularly useful with polished gems. Since most crystals are anisotropic and the reflection spectrum depends on crystal orientation, the measurements of faceted gemstone tend to be non-reproducible. In order to analyze gemstone using specular reflection technique, gemstone is necessary to have a flat polished facet. If the gem facet has a curved or spherical surface (i.e. cabochon or bead), it is very difficult to obtain the high quality reflection spectrum [8-9]. A major disadvantage of the technique is the obtained reflectance spectrum shows strong refractive-index-type features at the absorption frequencies, which is not easily interpreted. Another reflection technique is diffuse reflectance, but the measurement of faceted gemstone tends to be non-reproducible since the spectral intensity depends strongly on the sample orientation within the sample holder [8-10]. Because of the restriction of working area in diffuse reflectance accessory, the technique cannot be employed for the large sample. Moreover, both transmission and diffuse reflectance techniques are not applicable for mounted gemstones on jewelry.

In order to solve the problems associated with characterization of faceted gemstones and gemstone on jewelries, a novel transreflectance technique using infrared microscopy is developed [23-25]. The technique is nondestructive, provides unambiguous results, requires no sample preparation, and has short analysis time. The technique is applicable for both loose and mounted gemstone and suitable for various types of gemstones, jewelries, and/or cutting. The observed transreflectance spectrum will be compared with the corresponding spectra from conventional sampling techniques such as diffuse reflectance or specular reflection.

### **1.5 Scope of the Research**

In this work, we have proposed and developed a novel nondestructive transreflectance technique for characterization of faceted gemstone and jewelry using infrared microscopy. The technique was employed for characterization and identification of faceted natural, synthetic, treated gemstones and gemstone simulants. To obtain high accuracy measurement and high spectral quality, we also

designed and constructed a homemade accessory which facilitates reflecting plane adjustment for spectral acquisitions by means of transreflectance and reflectance techniques.

FT-IR spectroscopy with various classical sampling techniques such as transmission, specular reflection and diffuse reflection were employed for gem characterization. The transreflectance phenomenon of faceted gemstone was studied by representative gemstones from different varieties such as diamond, emerald, ruby and turquoise. The transreflectance spectra were compared to the well accepted spectra from the classical FT-IR sampling techniques. The spectra of natural, synthetic and treated gemstones were compared in order to identify characteristic of functional group. The unique spectral features associated with chemical compositions, impurities, and treatment processes were also discussed.

The research also aims at understanding the factors influencing the quality of spectra recorded in transreflectance techniques. These included the varieties of gemstones, cutting, the comparative transparency of samples, the thickness of samples, pleochroic directions through samples and the defect in the crystal structure. The study of sample arrangement observed for transreflectance technique and those observed for diffuse reflectance technique were also monitored in order to study the influence of crystal structure of gemstone that may affect the observed spectra.

## **1.6 Objectives of the Research**

1. To develop a novel technique for non-destructive characterization of faceted gemstone and jewelry using infrared microscope.
2. To determine characteristic infrared absorption of some varieties of faceted gemstones using various sampling techniques.
3. To differentiate various gems varieties including natural, synthetic, enhanced gemstones and gemstone simulants based on their infrared spectra.

## CHAPTER II

### THEORETICAL BACKGROUND

#### 2.1 Fundamentals of Light Propagation

Light is by nature an electromagnetic wave produced by the vibration of an electric charge. In its simplest monochromatic form, light can be represented as polarized, oscillating electric and magnetic fields that propagate in space, as depicted in Figure 2.1 [26].

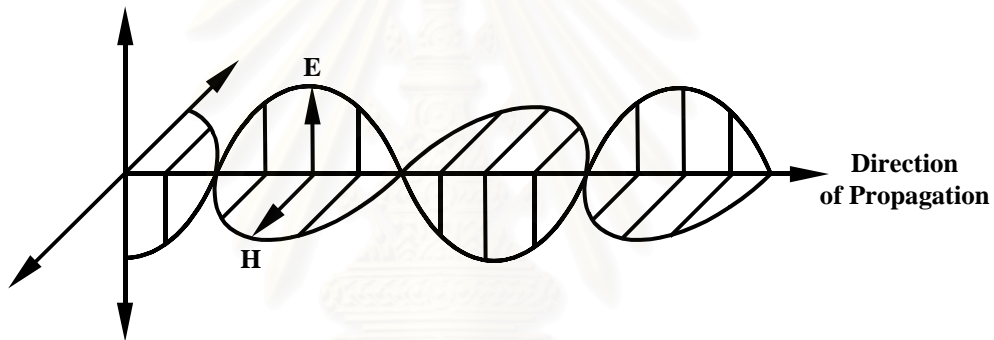


**Figure 2.1** Propagation of a linearly polarized electromagnetic wave in the direction of propagation.

The electric ( $E$ ) and magnetic ( $H$ ) vectorial components are orthogonal to each other and to the direction of propagation. In unpolarized light, the electric component  $E$  is randomly oriented in an infinite number of directions, but remains always perpendicular to the direction of propagation.

##### 2.1.1 Interaction of Light and Matters

Spectroscopy is a scientific discipline concerned with the interactions of electromagnetic radiation with matter. When the electromagnetic radiation impinges on the surface of an object, interactions between the incident beam and the molecules will alter the incident radiation. The incident beam can be reflected, scattered,

transmitted, or absorbed by the matter. Since a spectroscopic experiment allows detection of reflected, scattered, and transmitted light, it needs a source of light or excitation, an object of study, and a suitable detector. Thus, changes in the electromagnetic radiation can be observed. The modification of the electromagnetic radiation by the matter carries information about the molecular characteristic, physical properties and/or chemical properties of matters.

When an electromagnetic radiation impinges on a specimen, rays of the incident beam may be reflected, scattered, transmitted, or absorbed depending on the experimental arrangement. The total amount of incident energy is the sum of reflected, scattered, transmitted, and absorbed light. A schematic illustration for an interaction between light and matter is illustrated in Figure 2.2 [26].

$$I_0 = I_R + I_S + I_T + I_A \quad (2.1)$$

where  $I_0$  is the intensity of the incident radiation and  $I_R$ ,  $I_S$ , and  $I_T$  are the reflected, scattered and transmitted radiation, respectively.  $I_A$  is the radiation absorbed by matter. The intensity of each radiation depends on the intensity and wavelength of the incident radiation, the optical properties of the specimen, and the geometry of the experimental setup.

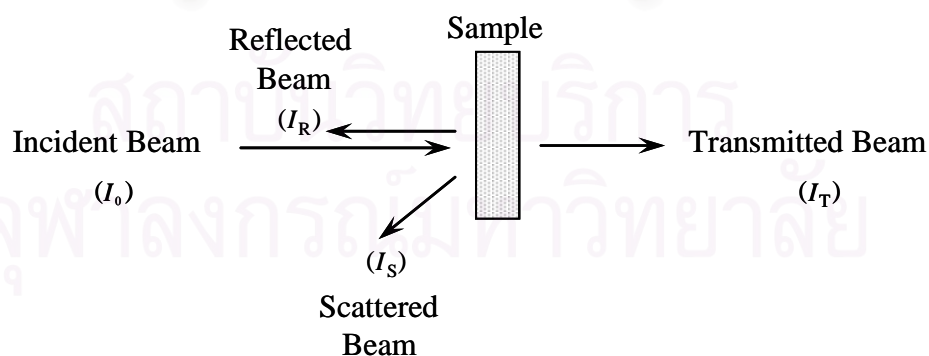


**Figure 2.2** Interactions of light with matter.

Let's consider the electromagnetic radiation when a sample is inserted between a source of light and a detector. The sample absorbs a fraction of the incident radiation. In order to measure the region and amount of light being absorbed by the sample, we need to measure the ratio of the sample attenuated ( $I$ ) and nonattenuated ( $I_0$ ) intensities of the radiation. The ratio is proportional to the transmittance of the sample. This relationship can be quantitatively related to the chemical composition of the sample by the Beer-Lambert law as:

$$I / I_0 = e^{-A(\bar{\nu})} = e^{-c_2 \varepsilon(\bar{\nu}) l} \quad (2.2)$$

where  $A(\bar{\nu})$  is the sample absorbance at a given wavenumber  $\bar{\nu}$ ,  $c_2$  is the concentration of the absorbing functional group,  $\varepsilon(\bar{\nu})$  is the wavenumber-dependent absorption coefficient, and  $l$  is the film thickness for the IR beam at a normal incidence to the sample surface.

### 2.1.2 Snell's Law: A Principle of Light Reflection and Refraction

When an electromagnetic radiation strikes a boundary between two media with different refractive indices (*i.e.*, a dielectric interface), refraction and reflection occurs. The law that governs the reflection process requires that the angle of incidence be equal to the angle of reflection. In this case, reflection is specular. If electromagnetic radiation passes from one medium to another that has a different refractive index, a sudden change of beam direction takes place because of the differences in propagation velocity through two media. If light propagates through an incident medium with refractive index  $n_1$  and enters a medium with refractive index  $n_2$  (see Figure 2.3), the light path will be changed and the extent of refraction is given by the following expression, known as Snell's law [26]:

$$n_1 \sin \alpha_1 = n_2 \sin \alpha_2 \quad (2.3)$$

where  $\alpha_1$  and  $\alpha_2$  are the angles of incidence and refraction, respectively.

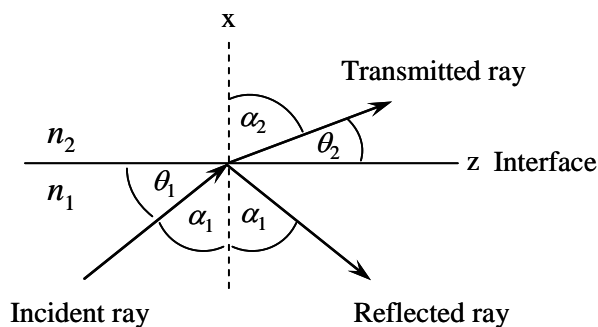


**Figure 2.3** Reflection and refraction of a plane wave at a dielectric interface based on Snell's Law.

## 2.2 Practical Sampling Techniques of Infrared Spectroscopy for Gem Analysis

Infrared spectroscopy is an analytical technique for chemical identification. It is based on the fact that different chemical contain functional groups that absorb infrared light at different wavelengths dependent upon the nature of the particular functional group. Currently, there are several techniques for obtaining infrared spectra of samples. Each has its own unique advantages and disadvantages for optimizing the quality of the observed spectrum. As a result, FT-IR spectroscopy gains popularity in gem characterization due to the direct relationship between spectral features and material characteristics (*i.e.*, chemical composition, structure and additives). There are many sampling techniques in FT-IR spectroscopy for the proper analysis of various fashioning styles of gems such as raw, cut and polished gems. The popular sampling techniques for characterization of gemstone included transmission, specular reflection and diffuse reflection. However, conventional infrared characterization techniques encountered several problems that make them unsuitable for routine analysis of faceted diamond.

### 2.2.1 Transmission Technique

#### *Principle of Transmission Technique*

The transmission technique involves passing the infrared energy through the sample and detecting that portion of the beam that is transmitted, *i.e.*, not absorbed

(see Figure 2.4). The infrared beam passes through the sample and the energy that comes through the sample is measured versus the respective wavelength to generate a spectrum. A widely used technique for the investigation of solid samples in the transmission mode is the pressing of an alkali halide pellet (most often a potassium bromide pellet). The method consists of grinding the sample together with pure, dry spectroscopic grade potassium bromide (KBr) to a fine powder, then transferring the mixture to a compression die [27-28]. The mixture is then placed under high pressure until the mixture forms a pellet that is transparent to infrared light. Today, transmission technique is considered to be undesirable because it is tedious and time-consuming, tend to be non-reproducible, and require significant sample modification.

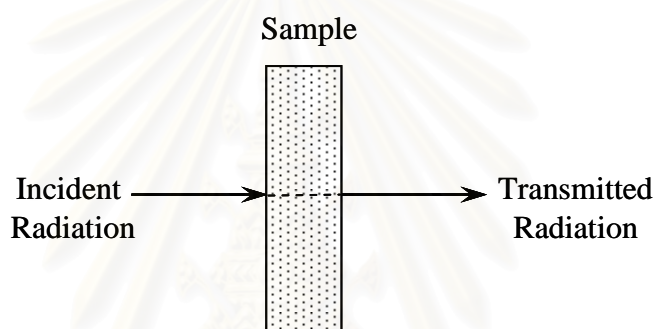


**Figure 2.4** Simplified schematic of the transmission measurement.

### *Transmission Technique for Characterization of Gemstone*

Transmission is the sampling technique generally employed for gem characterization. This mode is not applicable for faceted gemstone because of its destructive nature. Moreover the disadvantage of this method is high interfering bands from absorbed water molecular by the hydroscopic KBr. It is important that the sample be well mixed with the KBr thus the hard gemstones are difficult to ground and press into the pellet. Another widely used technique for the characterization of gemstone in transmission mode is the measurement of thin slab which is also not suitable for faceted gemstone due to its destructive nature and complex reflections of the cut and polished surfaces [10-13].



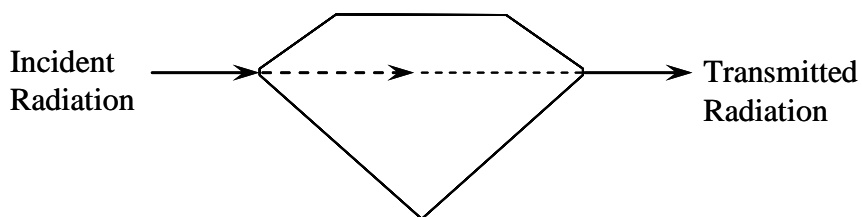


**Figure 2.5** Simplified schematic of the transmission measurement which coupled infrared radiation passes through the girdle.

Recently, beam condenser, the infrared-accessory with high optical throughput providing excellent sensitivity for analysis of a wide range of samples, was adapted for gemstone analysis [21-22]. However, transmission measurement of a faceted gemstone using beam condenser is complicated by sample arrangement where the coupled infrared radiation must pass through girdle or thin facet of gemstone body (see Figure 2.5). This technique can not be employed for thick gemstone, translucent and opaque gemstone and it is impossible to employ for mounted gemstone.

### 2.2.2 Specular Reflection Technique

#### *Principle of Specular Reflection Technique*

Reflection technique is an optically simpler technique (particularly for solids) than transmission technique and involves reflecting the infrared light off the sample. When an infrared radiation is directed onto the surface of solid sample two types of reflected radiations are obtained: specular and diffuse reflection.

Specular reflectance is defined as reflection in which the angle of incidence on the sample is exactly equal to the angle of reflection as shown in Figure 2.6. Near normal angle of incidence are most common. In order to produce a good spectrum, the surface of the sample must be smooth and flat. The reflected intensity also depends upon the index of refraction. Since the refractive index of material goes through an anomalous dispersion in the region of absorption band, the true specular reflectance spectrum qualitatively resembles the dispersion in refractive index. The result is a spectrum that shows strong dispersion features at the absorption

frequencies, which is not easily interpreted, as shown in Figure 2.7(a) [29]. A mathematical process known as the Kramers-Kronig (KK) transformation can convert the specular reflectance spectrum into transmission-like spectrum. This transform can be readily carried out by the computer associated with the FT-IR spectrometer and the suitable software furnished by all FT-IR manufacturers. Figure 2.7(b) shows the result of the transform and compares the spectrum obtained with a normal transmission spectrum (Figure 2.7(c)). The transform works well only if the spectrum is purely specular (no diffuse reflection) and the dispersion is low at both the beginning and the end of the range being transformed [27-29].

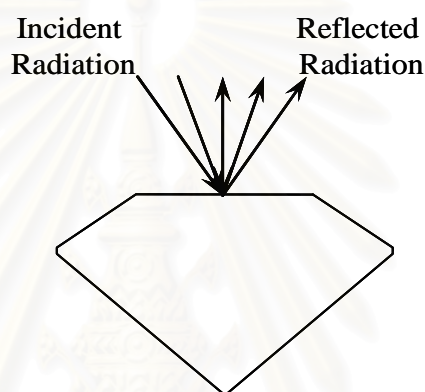


**Figure 2.6** Schematic showing specular reflection measurement of faceted gemstone.

### ***Specular Reflection Technique for Characterization of Gemstone***

Specular reflection infrared spectroscopy permits a very rapid and nondestructive determination of the species of a mineral. It is particularly useful with polished gems. Since most crystals are anisotropic and the reflection spectrum depends on crystal orientation, the measurements of faceted gemstone tend to be non-reproducible [8-9]. In order to analyze gemstone using specular reflection technique, it is necessary to have a flat polished facet of gemstone. If the gem facet has a curved or spherical surface (*i.e.*, cabochon, bead), it is very difficult to obtain the high quality of reflection spectrum. With such information it is important to keep in mind to avoid making a diagnostic mistake. In addition, it is impossible to record reflection spectrum from gems mounted in large items or jewelry because of the limited size of the reflectance accessory.

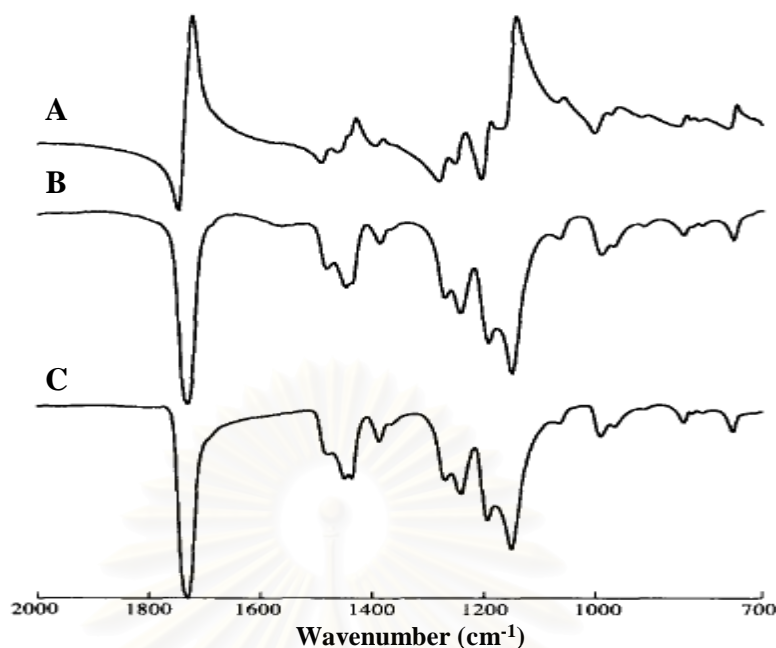


**Figure 2.7** Infrared spectra of polymethyl methacrylate (Lucite); (A) The infrared reflection spectrum, (B) the spectrum (A) after Kramers-Kronig Transformation, and (C) the transmission spectrum.

### 2.2.3 Diffuse Reflection Technique

#### *Principle of Diffuse Reflection Technique*

Recently, the diffuse reflectance infrared Fourier transform spectroscopy (DRIFTS) sampling technique has gained popularity for the study of powders, solids, and species absorbed on solids. The theory related to DRIFTS is based on incident radiation on a sample being scattering in all direction or the process which the angle of reflection is different from the angle of incidence (see Figure 2.8). The scattered radiation by the sample yields the spectrum, as with most other infrared techniques. The diffuse reflectance spectrum looks very similar to the transmission spectrum of the same sample. However, the relative intensities of the absorption bands will be different. The resulting spectrum will be expressed in term of Kubelka-Munk (K-M) unit. The Kubelka-Munk function is defined by the following expression [27-30]:

$$f(R_{\infty}) = \frac{(1-R)^2}{2R_{\infty}} = \frac{k}{s} = \frac{2.03ac}{s} \quad 2.4$$

where  $R$  is the absolute reflectance of the layer,  $s$  is the scattering coefficient,  $c$  is the concentration of the sample, and  $k'$  is related to the particle size and molar absorptivity of the sample by  $k' = s/2.303e$ . The theory predicts a linear relationship between the molar absorption coefficient and the maximum value of  $f(R_{\infty})$  for each peak if the scattering coefficient,  $s$ , is a constant. The scattering coefficient is dependant on the particle size and must be constant in order to obtain quantitative results.

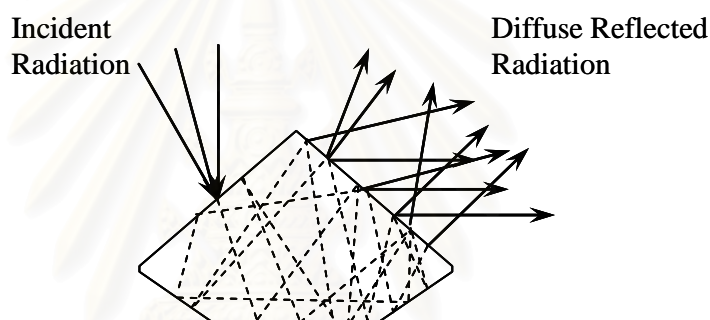


**Figure 2.8** Schematic showing diffuse reflectance measurement of faceted gemstone.

### ***Diffuse Reflection Technique for Characterization of Gemstone***

Although DRIFTS is a powerful non-destructive technique for gemstone analysis, the accessory and its sample holder has restrict working area which cannot perform for a large size gemstone or jewelry. The measurements of faceted gemstone tend to be non-reproducible since the spectral intensity depends strongly on the gems orientation within the sample holder [8,10]. The other drawbacks of the diffuse reflectance technique arise from the specular component of the reflected radiation. The specular component does not penetrate the sample. This becomes a particular problem in spectral regions where there is a highly absorbing species and the surface effects dominate the bulk effect leading to Reststrahlen bands. The Reststrahlen phenomenon can lead to distortion or inversion of the absorption bands. As before, it

is important that result spectrum be obtained at two or three different orientation before any conclusion is drawn as to the origins of a particular sample.

### 2.3 Infrared Microscopy

Infrared microspectroscopy (IR microscopy), the coupling of optical microscopes to infrared spectrometers, has been one of the most important advances for spectroscopic characterizations in materials research over the recent years. This has facilitated the combination of morphological examination (light and electron microscopy) with infrared spectroscopy for chemical identification of microscopic samples or domains. It is, of course, a requirement that the microscope also functions as a visible microscope and that the visible radiation be parfocal and colinear with the infrared radiation. The visible system is used first to locate the sample and focus on the face to be investigated. Then the infrared system is switched in and the spectrum is collected. This is necessary to align the sample of interest in the infrared beam and to ensure, that the infrared radiation reaching the detector will only be that transmitted or reflected by the sample of interest. A simplified diagram of an infrared microscope is given in Figure 2.9 [31].

The two primary modes of IR microscopy are reflection and transmission [28,31]. For transmission mode, the IR energy must be able to pass through the sample to the condenser. Therefore, samples must be very thin or compressible in order to allow the light to pass through. Transmission may require more sample preparation but is extremely versatile and sensitive. In addition, most libraries consist of transmission data, thus searches are easily conducted on a transmission sample with no additional data manipulation. Reflectance mode can be further subdivided into reflection-absorption and specular reflection. In reflection-absorption mode, light must be able to pass through a sample and bounce off a reflective substrate beneath the objective. Typically, samples must be very thin ( $<5\ \mu\text{m}$ ) and are placed on a mirror-surface. In specular reflection mode, light must bounce directly off the sample surface to the objective. A dull or rough surface is not amenable to this type of microscopy. However, an appropriate sample (fairly smooth, shiny) requires

almost no sample preparation. Reflectance spectra are typically somewhat noisier than their transmission counterpart. Since specular reflection mode is a surface characterization technique, the thickness of the sample is irrelevant. This reflected spectrum is quite different from the transmission spectrum since it contains refractive index data as well as absorption data (see Figure 2.7(a)) [29]. This observed spectrum can be converted to a useful spectrum by means of a mathematical procedure, the Kramers-Kronig transformation [31-32].

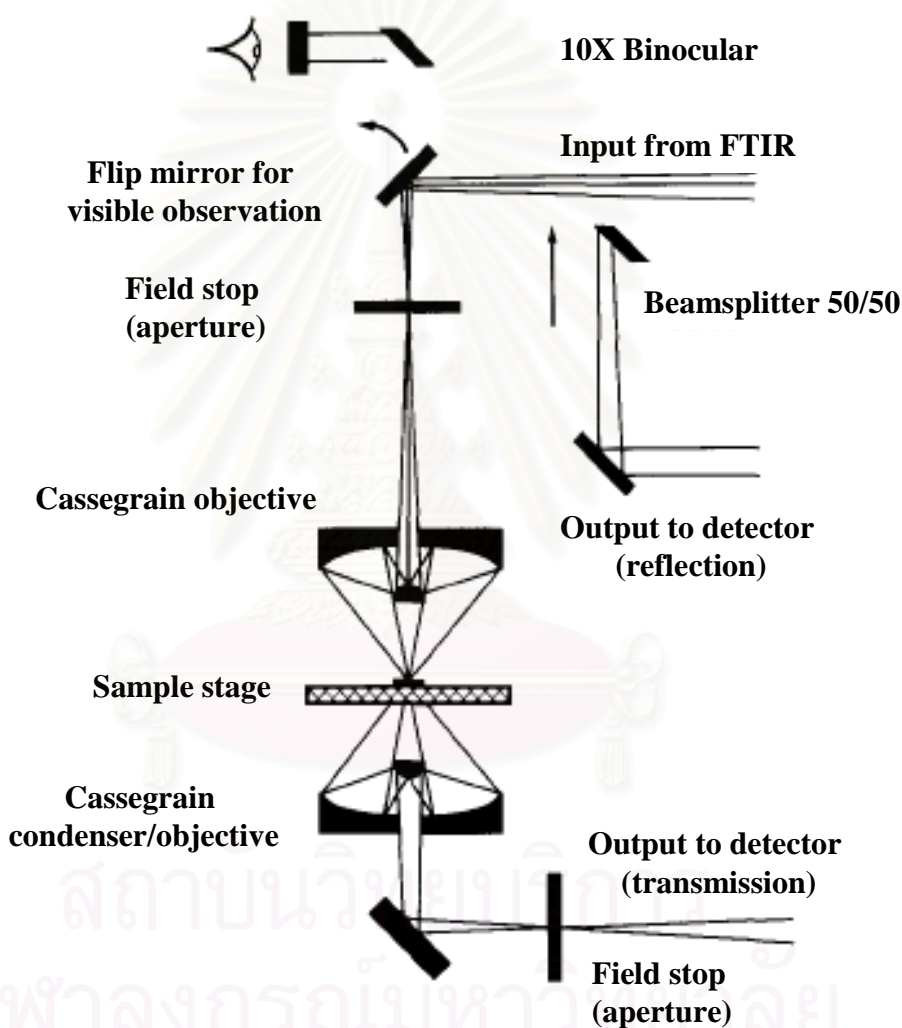


**Figure 2.9** Optical diagram of an infrared microscope used for infrared microscopy [29].

## ***Infrared Microscopy for Characterization of Gemstone***

Infrared spectroscopy is now widely used in gem laboratories to characterize natural, treated and synthetic gemstones. Because of technical limitations in classical infrared sampling technique, the method is not appropriated for all gemstones. Recently, infrared microscope is an alternative instrument widely employed for gem characterization. The obtained spectra were acquired by transmission and specular reflection modes. The original experimental procedure of transmission technique involved measurement of powders or thin slabs of materials which is not suitable for faceted gemstone due to its destructive nature. Reflection mode of microscope enabled gemstone with at least one polished face to be analyzed [33]. The method utilized for uncut or polished gems, loose or mounted in jewelry because it is a non-destructive process. However, the reflectance spectrum depends strongly on the sample orientation because of the directional arrangement of atom in crystal structure of minerals. The main disadvantage of the technique is the obtained spectrum shows strong refractive-index-type features at the absorption frequencies, which is not easily interpreted.

### **2.4 Transflectance: Novel Technique for Characterization of Faceted Gemstone**

#### **2.4.1 Principle of light that entering the gemstone**

To understand the transflectance phenomena in a faceted gemstone, sufficient knowledge about the path of any ray of light passing through the gemstone is required. This knowledge comprises the essential part of optics: reflection, refraction and critical angle. When light strikes the outside surface of a well-polished gemstone, or any other transparent material, some of that incident light is *reflected* (bounced) back from the surface. The remaining incident light is *refracted*, which means that it is transmitted (or enters) through the surface and into the gemstone. This also means that some of the incident light's *energy* is reflected, while the rest of the light's *energy* is transmitted into the gemstone. How much of that light's energy reflects or refracts depends on several factors: the angle at which the light strikes the

surface; the optical properties of the material, the wavelength and the polarization state of the incident radiation [34].

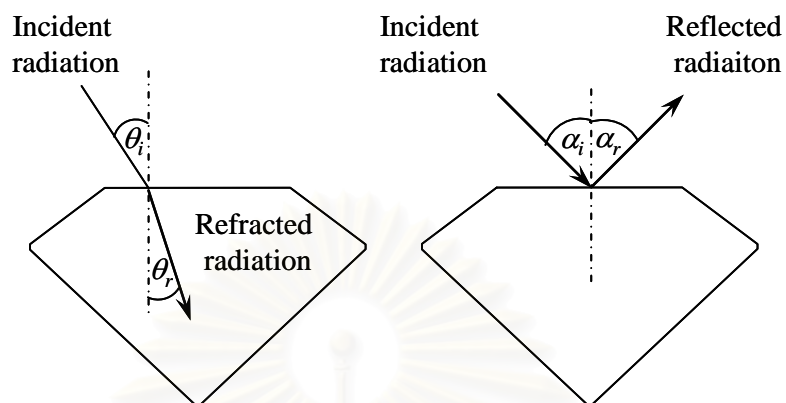


**Figure 2.10** Schematic of angle of incidence, refraction and reflection in faceted gemstone. The angle of incidence equals angle of reflection at the air/gemstone interface.

As shown in Figure 2.10, the angle at which light strikes a surface is called the *angle of incidence* ( $\theta_i$ ). If the angle of incidence is  $0^\circ$  (*i.e.*, the light ray is perpendicular to the surface), the light will slow down but continue to travel in its original direction within the denser medium. However, if the angle of incidence is oblique (more than  $0^\circ$  but less than  $90^\circ$ ), any transmitted light will not only slow down but also bend, or change the direction in which it is traveling. This bending of light is called *refraction*, and the angle at which the ray bends (again, measured from the normal) is called the *angle of refraction* ( $\theta_r$ ). The angle at which the light bounces off is called the *angle of reflection* ( $\alpha_r$ ). Both angles are measured from the normal, an imaginary line perpendicular to the surface at the point where the light strikes. Therefore, a perpendicular ray ( $90^\circ$  to the surface plane) has a  $0^\circ$  angle of incidence (from the normal). The angle of incidence always equals the angle of reflection. The amount of reflection depends on the optical properties of the material.

The direction of the refracted radiation depends on whether that light is traveling into a medium that is of greater or lesser optical density. When light enters a gemstone, which is optically denser than the air, it will bend toward the normal (see Figure 2.11). Its angle of refraction ( $\theta_r$ ) will be less than that of incidence ( $\theta_i$ ), ( $\theta_r <$



$\theta_i$ ). However, when light leaves a gemstone it bends away from the normal. In these cases, its angle of refraction is greater than its angle of incidence ( $\theta_r > \theta_i$ ).

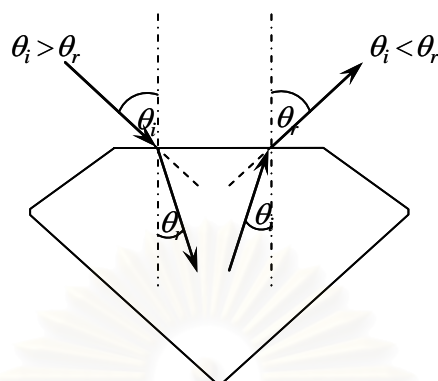


**Figure 2.11** Schematic of refraction in relation to the direction normal. ( $n_{\text{gemstone}} > n_{\text{air}}$ )

Summary:

- The angle at which light reflects from a surface is equal to the angle at which it strikes the surface. Both angles are measured from the direction normal.
- When a light beam passes from a material of lesser optical density (e.g., air) to a material of greater optical density (e.g., diamond), it will be bent from the original direction unless it impinge the optically denser medium at the normal incidence.
- A beam of light will bend toward the normal when entering a gemstone and away from the normal when leaving the gemstone.
- The critical angle (based on a material's refractive index) partially determines when a light beam striking the inner surface of a gemstone will reflect back into, or transmit out of, the gemstone.

#### 2.4.2 Principle of Gems Cutting

As seen in the previous section, the reflection of light plays an important part in the appearance of a gemstone. For identification purposes, the most important single item of information about a gemstone is its refractive index (RI). This is because the RI of most gemstones is a constant which can be measured to two decimal places

(and often estimated to the third decimal place). For this reason, many gems can be distinguished from each other with certainty even when there is very little difference in their RIs (e.g. natural and synthetic spinel; pink topaz and tourmaline) [4].

Non-crystalline substances such as glass and amber, or gemstones belonging to the cubic crystal system, are in this category, and light entering these materials produces a single refracted ray. Such materials are called isotropic or singly refractive. However, crystalline materials, including gemstones, belonging to the tetragonal, trigonal, hexagonal, orthorhombic, monoclinic and triclinic system (*i.e.* all systems other than cubic) have two refractive indices. When a ray of light enters these materials it is split into two polarized rays travel through the crystal at different speeds, and as with light of different wavelengths they are refracted by different amount. Gemstones which produce two polarized rays are called doubly refractive, birefringent or anisotropic.

### ***The fashioning of gemstone***

With a colorless transparent stone, one of the main aims is to achieve a polished gem which has the maximum possible brilliance of appearance. As mentioned earlier, this brilliance is dependent on both the surface reflectivity and luster of the stone (which some stones are evident even in the rough uncut form) and on the total internal reflection of those rays entering the gem's crown facets. If the stone has an appreciable degree of dispersion, the cut must also exploit this to bring out the gem's 'fire'. For this reason, the design of the stone's cut has to strike a balance between fire and brilliance. Incident rays which meet the table facet at right angle (*i.e.* normal) its surface are not refracted as they pass from the air into the stone, and are therefore not dispersed. With color gemstones, a cutting style may be chosen which emphasizes or lightens the depth of color viewed through the crown facets [4,34].

With the possible exception of a few gems, such as pearl and occasionally amber, most of organic and inorganic gem materials have their appearance enhanced by some form of shaping or polishing. With translucent or opaque stones this may be as basic as an abrasive tumbling operation to develop a smooth and lustrous surface

while retaining the baroque profile of the original rough material. Alternatively, stones of this type may be cut in the rounded cabochon to bring out their surface color or banding with malachite and agate. If the stone is translucent but dark, the cabochon can be shallow cut to lighten the color. Although tumble polishing a rough stone improves its appearance, and the cabochon cut is appropriate for opaque and ‘specialty’ stones, most transparent gem minerals are faceted to enhance features such as **body color**, **brilliance** (the surface and total internal reflection of light), **fire** (dispersion) and **scintillation** (the sparkles of reflected light produced when the light source or the gemstone is moved) [4,34].

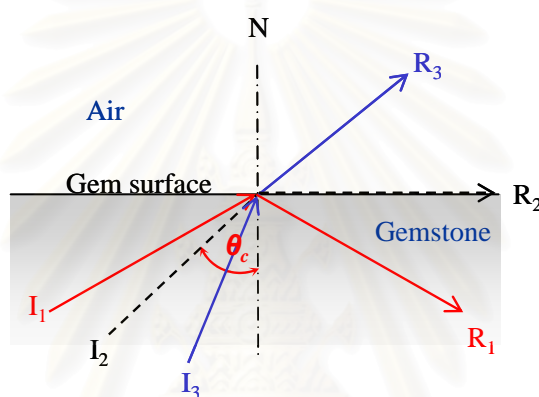


**Figure 2.12** Light rays are reflected back from a gemstone’s facet at angle to the direction normal (N) is greater than the critical angle. The radiation refracts out of the gemstone at an angle less than the critical angle.

The surface component of a gemstone’s brilliance (*i.e.* its luster or reflectivity) is related to its refractive index. However, the proportion of brilliance due to the light reflected from within the stone depends on the style of cutting, which in turn is partly dictated by the **critical angle**.

### **Critical Angle**

If the denser medium is a gemstone and the less dense medium is air, as in Figure. 2.12, the ray  $I_1$  will be reflected back into the gemstone as  $R_1$ . At the critical angle of total reflection, however, ray  $I_2$  will cease to obey the law of reflection, and will be refracted along the surface of the gemstone as  $R_2$ . At angles less than the

critical angle, all rays (such as  $I_3$ ) will be refracted out of the gemstone into the surrounding air ( $R_3$ ) [4,34].

In order to fully exploited the brilliance of a transparent faceted gemstone, it is important that as much as possible the rays entering the gem through its top (crown) facets be reflected back from the lower (pavilion) facets, and re-emerge from the crown of the stone via the total internal reflection. To achieve this, both the lapidary and the gemstone polisher must adjust the angles of the crown and pavilion facets so that the majority of rays entering the crown facets meet the interior faces of the pavilion facets at angles greater than the critical angle. If the angles of the facets are wrong, many of these rays will pass out through the pavilion facets and the stone will appear dark. It is equally important that the rays reflected back from the pavilion facets meet the crown facets at an angle less than the critical angle. If the fail to do this, they will be reflected back into the stone again.

The critical angle of a gemstone is dependent on both the RI of the gemstone and that of the surrounding medium. For example, RI of diamond is 2.417, the critical angle is  $24.43^\circ$ , for quartz with an RI of 1.545, and the critical angle is  $40.33^\circ$ . It can be seen that for maximum brilliance, the pavilion/crown angle for quartz will be significantly different from that for a diamond. In Figure 2.13A, a single ray (1) undergoes total internal reflection in a diamond (in either direction). A second ray (2) enters the diamond's table facet at a shallow angle and being refracted out through the back of the stone. If a quartz gem is cut to the same pavilion/crown angle as the diamond, neither ray would be reflected back from the pavilion facets as they would impinge them at an angle less than  $40.33$  (the critical angle for quartz). However, if the pavilion/ girdle angle of quartz is increased from 40 to 43 (see Figure 2.13), ray 1 is reflected back successfully through the table facet. The schematic diagram in Figure 2.13 is only simple ones intended to illustrate the importance of the critical angle in the design of a gemstone's profile. Ray path diagrams that take into account all of the rays entering the crown facets are much more complicated.

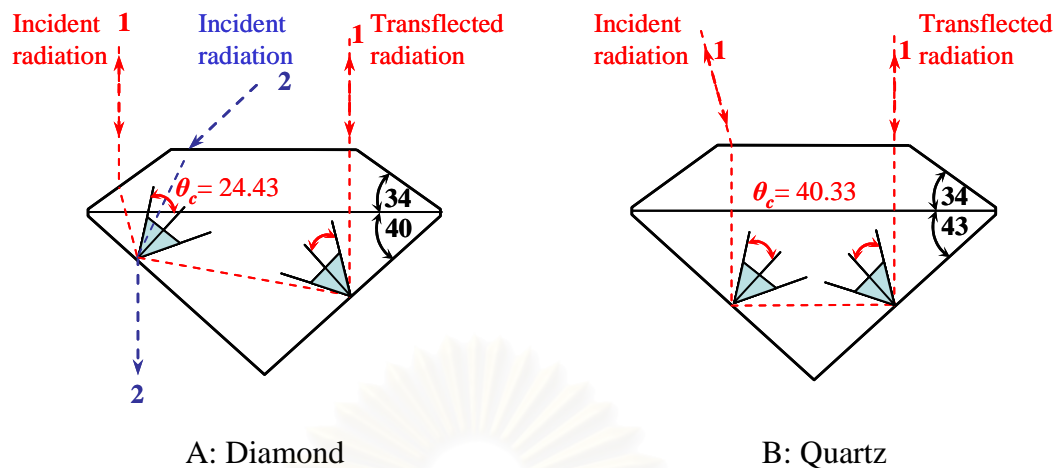


**Figure 2.13** (A) the total internal reflection of ray 1, which meets the pavilion facets of diamond at angles greater than the critical angle, and the refraction of ray 2 out of the pavilion when it meets it at an angle less than the critical angle. (B) the pavilion has been made deeper to maintain the total internal reflection or ray 1 in quartz, which has a much larger critical angle than diamond.

### 2.4.3 Transflectance Phenomena

In principle, a faceted gemstone was cut in such a proportion that total internal reflection within the gemstone is enhanced. To increase the number of total internal reflection, the cutting proportion of the gemstone is carefully design with respect to refractive index, size, shape, and carat weight. The number of total internal reflection depends on the angle and positions that light enter the gemstone. The greater the number of reflection within the gemstone, the better is *fire* and *brilliance* of the faceted gemstone. To obtain the better understand of the phenomenon, the employed cut proportion of diamond introduced how transflectance phenomenon behaves in gemstone, see Fig. 2.14 (A). A modern brilliant cut diamond consists of 57 + 1 facets depending on the presence of the culet. Since the refractive index of diamond ( $n_{\text{diamond}} = 2.417$ ) is greater than that of air ( $n_{\text{air}} = 1.0$ ), total internal reflection at the diamond/air interface is observed when a radiation traveling inside the diamond impinges the interface with an angle greater than the critical angle. The critical angle  $\theta_c$  is given in terms of the refractive indices by  $\theta_c = \sin^{-1}(n_{\text{air}}/n_{\text{diamond}})$  and is equal  $24.44^\circ$  for diamond/air interface [34-36].

In order to collect transreflectance infrared spectra of a faceted gemstone using an infrared microscope, the infrared radiation is coupled into and is collected from the table facet by the built-in 15X Cassegrainian objective [31]. According to the optical design of the objective, the coupled radiation is inherently convergence. For the coupled infrared radiation with a normal incidence to the table facet, the radiation totally reflects at the pavilion facet. Under the employed cut proportion shown in Figure. 2.14(B), (*i.e.*, a set of Tolkowsky's recommended cut proportion with pavilion angle of  $41^\circ$  and crown angle of  $34^\circ$ ), the reflecting angles at the pavilion facet are  $41^\circ$  and  $57^\circ$ , respectively, for the first and second reflections. The radiation reaches the gemstone/air interface at the table facet with  $16^\circ$  angle of incidence and refracts into air with an angles of  $41.77^\circ$ . Due to the complex cut surfaces of the faceted gemstone and the divergence of the coupled radiations, the radiations impinge the table facet with different angles undergoes different reflections before emerging into the air. However, some radiations may not emerge from the table facet but undergo multiple internal reflections before emerging into the air at any facet.

According to the traveling path of the coupled radiation in Figure 2.14(B), the out going radiation from the table facet is defined as the *transflected radiation* [23-24]. Since the gemstone has absorption bands in the mid-infrared region, attenuations of the infrared radiation at gemstone characteristic absorption frequencies are expected. As a result, by collecting the transflected radiation, the absorption spectra of the gemstone can be measured. Since the absorption bands in an infrared spectrum are directly associated with chemical structures and compositions, they can be employed for gemstone classification, characterization, and determination of the impurities and/or inclusions in the gemstone. Moreover, it can be exploited for the determination of the treatment processes applied onto the gemstone [23-25].

As before, a novel nondestructive transreflectance technique based on principle of reflection and refraction within gemstone was developed in order to solve the problems associated with characterization of faceted gemstone and jewelry. The transreflectance technique for FTIR spectral acquisition using an infrared microscope was introduced.

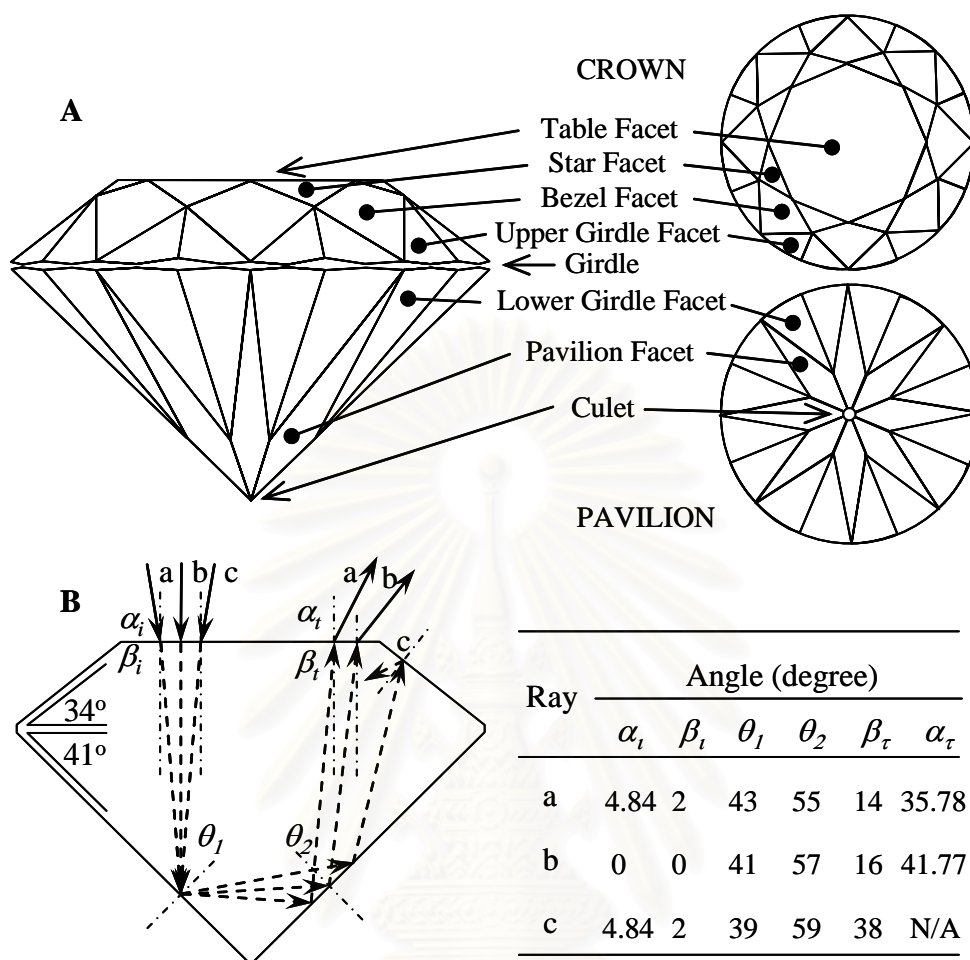


**Figure 2.14** A schematic drawing of a round brilliant cut diamond (A). Ray tracing of different radiations inside a round brilliant cut diamond (B). A summary of angles at diamond/air interface are shown.

สถาบันวิทยบริการ  
จุฬาลงกรณ์มหาวิทยาลัย

## CHAPTER III

### EXPERIMENTAL SECTION

The novel transreflectance technique for characterization of faceted gemstones was applied for faceted gemstones such as diamond, emerald, ruby and turquoise. In order to verify an efficiency of the technique, various classical infrared sampling techniques such as transmission, specular reflection and diffuse reflection were employed for comparison purpose. The spectra of natural, synthetic and treated gemstones were compared in order to identify characteristic of chemical compositions, impurities, and treatment processes. The applications of transreflectance technique for gems and jewelry characterization were subsequently demonstrated. The novel transreflectance technique is a nondestructive while sample preparation is not necessary. A novel accessory for adjusting the reflection plane of the faceted gemstone was constructed and was utilized with the infrared microscope.

#### 3.1. Materials and Equipments

##### 3.1.1 Gemstone Samples

The gems specimens were sets of reference gemstones achieved from the Department of Mineral Resources (DMR) and Burapha University Chanthaburi (BUCH) IT Campus, Thailand. The samples were varieties of facet gemstones with various cutting styles and carat weights including diamonds, sapphires, rubies, emeralds and turquoises. Diamonds with various types of treatments (*i.e.*, irradiation, heat, and high pressure-high temperature (HPHT) treatments) and its simulants were examined. The natural and synthetic gemstones such as flux-synthetic emerald, hydrothermal-synthesis emerald, flame fusion synthetic ruby and hydrothermal-synthetic ruby were also investigated. The physical and optical properties of the measured gemstones are summarized in table 3.1 [4]. The faceted gemstones were



characterized as received without additional sample preparation except cleaning with water and organic solvent (*i.e.*, methanol, ethanol, isopropanol and acetone). For the spectral acquisition of mounted gemstones on a jewelry (*i.e.*, ring, pendant, necklace and earring), the whole jewelry is placed on the sample holder without removing the gemstones from the jewelry setting.

**Table 3.1** Physical and optical properties of the measured gemstones.

<b>Gemstone</b>	<b>Diamond</b>	<b>Ruby</b>	<b>Emerald</b>	<b>Turquoise</b>
<b>Chemical composition</b>	Carbon	Al <sub>2</sub> O <sub>3</sub>	Be <sub>3</sub> Al <sub>2</sub> (SiO <sub>3</sub> ) <sub>6</sub>	CuAl <sub>6</sub> (PO <sub>4</sub> ) <sub>4</sub> (OH) <sub>8</sub> .5H <sub>2</sub> O
<b>Crystal system</b>	Cubic	Trigonal	Hexagonal	Triclinic
<b>Varieties</b>	Transparent, colorless and fancy color	pink to red to opaque	Green	Opaque, blue to green
<b>Refractive index</b>	2.417	1.76-1.77	1.56-1.59	1.61-1.65
<b>Birefringence</b>	-	0.008	0.005-0.008	-
<b>Dispersion</b>	High (0.044)	Low (0.018)	Low (0.014)	-
<b>Specific gravity</b>	3.52	3.99	2.7-2.8	2.6-2.9
<b>Hardness</b>	10	9.0	7.5-8.0	5.5-6.0
<b>Cleavage</b>	perfect	poor	poor (basal)	-

### 3.1.2 Instrument

1. Nicolet Magna 750 FT-IR spectrometer equipped with a mercury-cadmium telluride (MCT) detector
2. NICPLAN™ infrared microscope with 15X Cassegrain infrared objectives and 10X glass objectives
3. A diffuse reflectance accessory (The Collector™ DRIFT Accessory, Spectra Tech Inc. USA).
4. A novel accessory for reflecting plane adjustment with sample holder

### 3.1.3 Default Spectral Acquisition Parameters

#### FT-IR Spectrometer Setup

Source	Standard Globar™
Beam splitter	Germanium coat on KBr
Detector	MCT

#### Acquisition Parameters

Spectral resolution	4 cm <sup>-1</sup>
Number of scans	256
Signal gain	Auto
Spectral format	Absorbance or Kubellka-Munk unit

#### Infrared Microscope Parameters

Experimental Mode	Reflection
Spectral resolution	4 cm <sup>-1</sup>
Number of scans	256
Signal gain	Auto
Spectral format	Reflectance or Absorbance

## 3.2 The novel accessory

### 3.2.1 The optical design and fabrication procedure

Ideally, when a faceted gemstone is placed on the sample holder, the table facet must face up perpendicularly to the infrared radiation from the built-in 15X Cassegrain objective in order to achieve a high energy throughput for spectral acquisition. Thus, the novel accessory should be adjustable in order to manipulate the table facet perpendicular to the focusing infrared radiation. The novel accessory was designed and constructed. Components of the novel accessory are illustrated in Figure 3.1. This accessory is designed based on double thin plates in order to effectively utilize a small working area of microscope. Since the working area between microscope's stage and objective lens is usually restricted to 10-15 mm in height, the maximum thickness of the whole accessory was 10 mm. Each of these plates was lathed to a final dimension of 3 mm thick, 90 mm wide and 90 mm long. The center of both plates was perforated and then gouged out with diameters of 40 mm for placing the sample holder. The sample holders are different sizes and shape brass ring depends on the specific size of faceted gemstone and jewelry as shown in Figure 3.2. Figures 3.2 and 3.3 show accessory arrangements for nondestructive characterization of faceted gemstone and jewelry. The brass ring is a rotate-able holder mounted into the center of the accessory. Gemstones and jewelry of various sizes and shapes were placed on the brass ring. The three knobs setting on the corner of accessory (see Figure 3.1) were employed for adjustment of the reflecting plane. To investigate effect of sample orientation using the transmittance technique, the sample holder was rotated to desired degrees. With the combination of adjustable plane (upper plate) and the rotary sample holder (center of accessory), the table facet of a gemstone can be adjusted perpendicularly to the incident radiation.

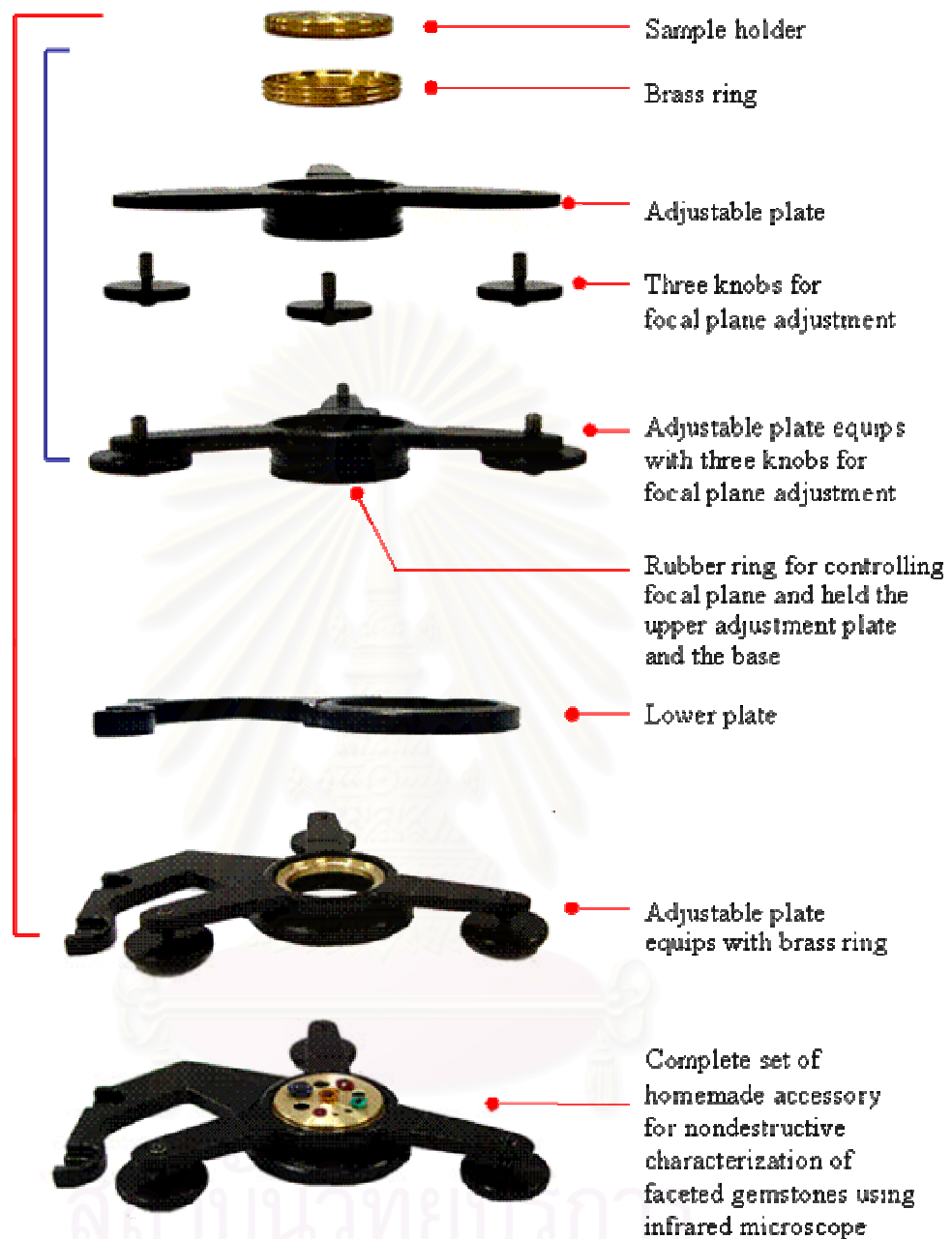


**Figure 3.1** Composition of a novel accessory for nondestructive characterization of faceted gemstone using infrared microscope.

The particular advantages of the novel accessory can be categorized as follows.

- ✓ Using an accessory with infrared microscope helps simplify the alignment of focal plane when performing with faceted gemstone and jewelry in order to produce high energy throughput of transreflectance radiation to detector.
- ✓ The accessory can be used with all commercially available microscopes.
- ✓ The transreflectance technique equipped with the novel accessory is non-destructive, requires no sample preparation, and has a short analysis time.
- ✓ For the spectral acquisition of a loose gemstone, the specimen was positioned on the sample holder of novel accessory with the table facet faced up. The accessory was available for various cut shapes and large samples.
- ✓ For the spectral acquisition of mounted gemstones on jewelry (*i.e.*, ring, pendant, necklace and earring), the whole jewelry is placed on the sample holder without removing the gemstones from the jewelry setting.

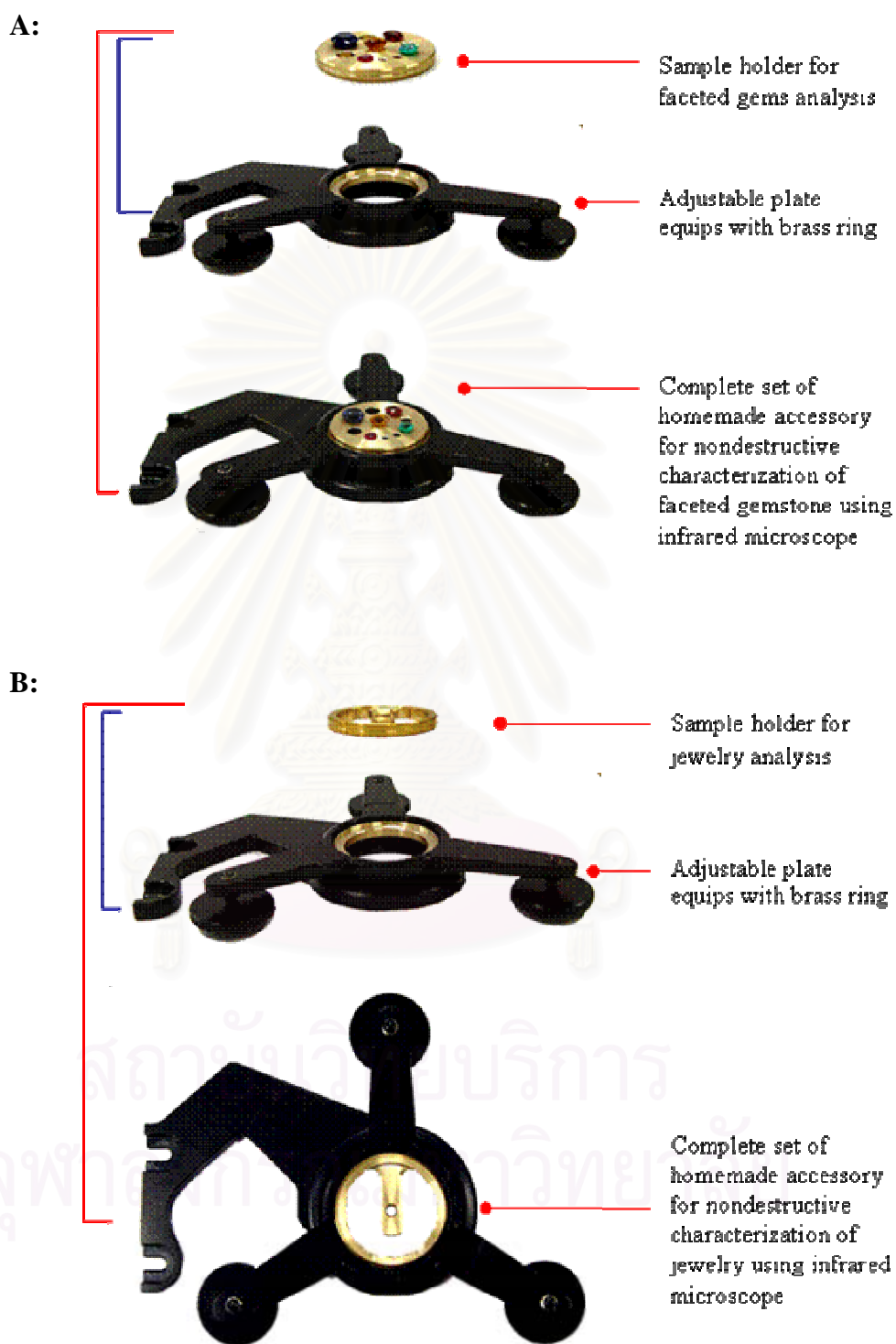


**Figure 3.2** Arrangement of the novel accessory for nondestructive characterization of faceted gemstone (A), and jewelry (B).

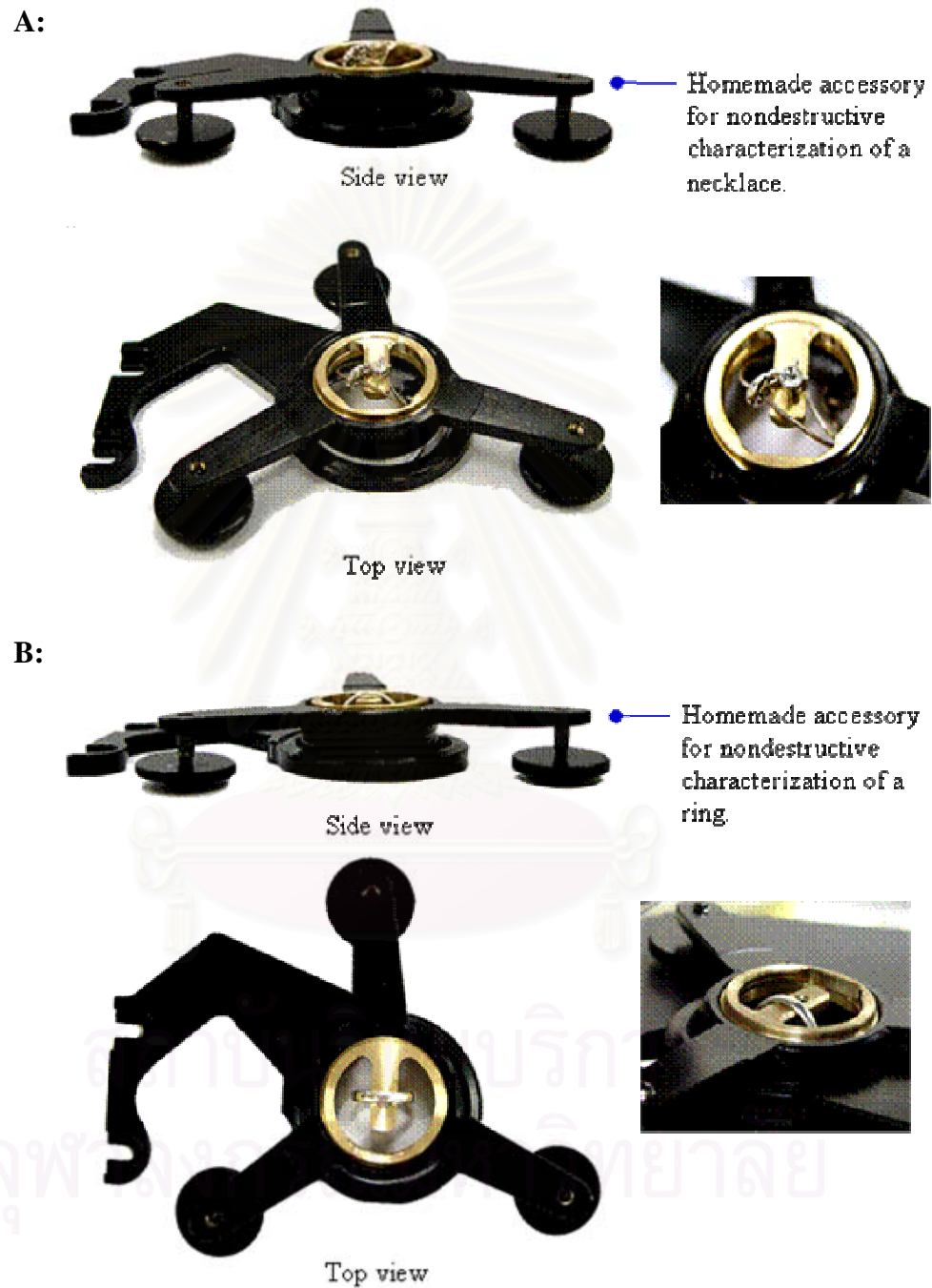


**Figure 3.3** Example of experimental procedures for spectral acquisition of gems on jewelries: a necklace (A), and a ring (B). The jewelry is placed on the sample holder of novel accessory without removing the gemstones from the jewelry setting.

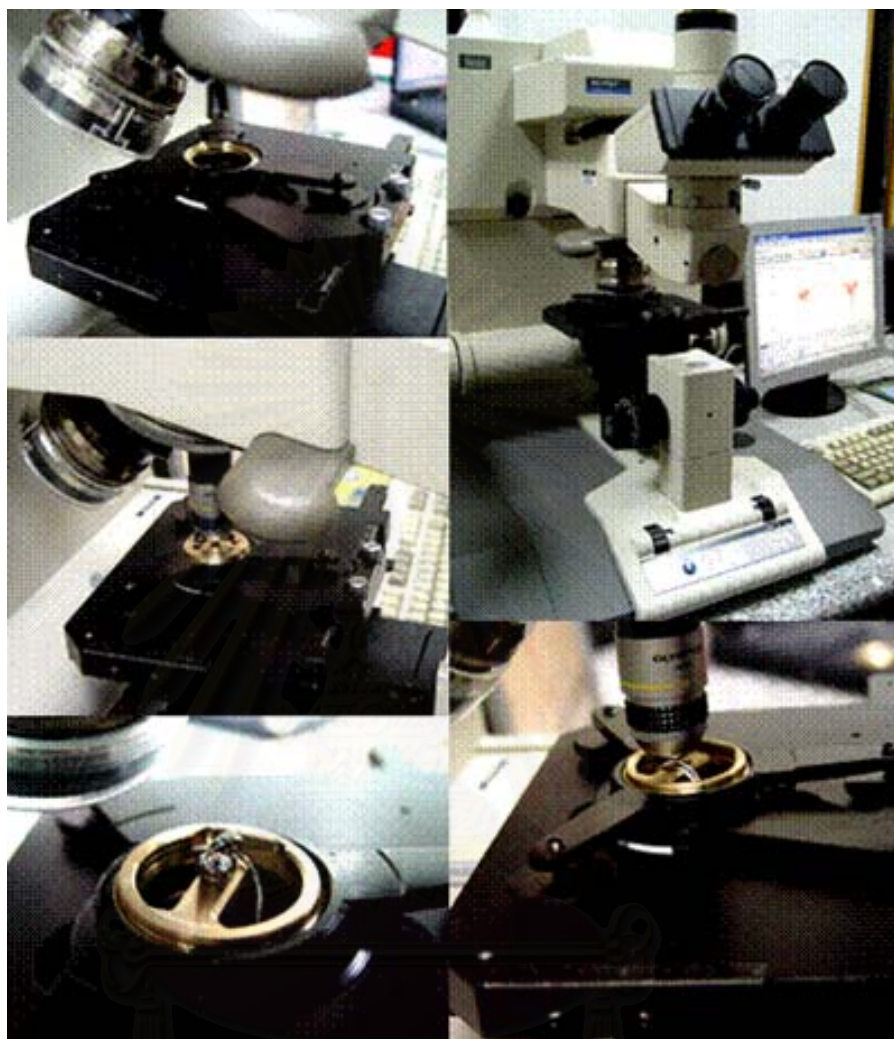


**Figure 3.4** Actual experimental setup for gem characterization using novel accessory with an infrared microscope.

### 3.2.2 Setting of the novel accessory with IR microscope

As illustrated in Figure 3.4, the novel accessory was placed onto the stage of infrared microscope. The NICPLAN<sup>TM</sup> infrared microscope equipped with a novel accessory is capable of analyzing sample in either transmittance or reflection mode. In practice, the incident IR beam from the infrared microscope's objective is perpendicular onto the planar surface of sample. The amount of light reaching the sample is controlled via the aperture of the microscope.



In case of the transmittance experiment, it is important that the image should be centered at the culet of the faceted gemstone. If the focus or image is not centered, the high energy throughput cannot be obtained and the transmittance radiation cannot be detected. In addition, while viewing the sample focus, adjust the three knobs of novel accessory to obtain a sharp image of sample surface. For large sample or jewelry, there are various sample holders suitable for specific item.

### **3.3 Experimental Procedures**

#### **3.3.1 Transmission Technique**

The widely used technique for gemstone samples is the pressing of an alkali halide (KBr) pellet. Transmission technique was employed for turquoise and emerald. They can be ground and pressed into a pellet because their hardness is not so high. Their spectra were collected for comparison with other techniques. The gemstone sample was grinded into fine powders and then placed a few milligram of spectroscopic-grade KBr in an agate mortar and grinded until there is no evidence of crystallinity. A very small quantity of sample was add into the ground KBr powders and grind again until the sample is uniformly distributed throughout the KBr, after that transferring the mixture to a die where it is pressed until the alkali halide particles coalesce into a transparent or translucent disk. A vacuum line connected to the die is used to remove entrained air and moisture. After removing the mixture pellet out of the die, the pellet was placed into the sample holder and then a transmission spectrum was collected.

#### **3.3.2 Diffuse Reflectance Technique**

The Collector<sup>TM</sup>, a diffuse reflectance attachment manufactured by Spectra Tech Inc., was employed for all diffuse reflectance spectral acquisitions. The number of accumulated scans depended mainly on the nature of the sample. Spectra are ratioed against a background of mirror alignment. The faceted gemstone was placed on the

sample holder with the table facet faced down. The position of the sample holder in the accessory was always optimized before the spectral acquisition. A beam blocker of diffuse reflectance attachment, a small gold coated blade, was placed across the sample surface during the diffuse reflectance measurement in order to avoid the specular reflection component. The infrared beam was coupled into the gemstone at the near normal angle of incidence, while the representative spectrum was collected from the diffuse reflected radiation. The spectral intensity of the diffuse reflectance spectrum was expressed in Kubelka-Munk units.

The main limitation of diffuse reflectance accessory is its working space. The sample stage must be small and lie close to the collector mirror, thus the big gemstones cannot be employed using the diffuse reflectance attachment. Since the diffuse reflectance spectrum was greatly influence by the arrangement of the sample on the sample holder, several spectra with different arrangements were collected. The observed spectrum with the best signal-to-noise ratio was employed for further analysis.

### **3.3.3 Specular Reflection Technique**

The specular spectrum of a faceted gemstone was performed by a NICPLAN<sup>TM</sup> infrared microscope attached to the FT-IR spectrometer. The microscope was operated in the reflectance mode. Reflection with normal incidence from a gold mirror was exploited as a background spectrum. Appropriate background was obtained for each series of measurements that is with equivalent apertures in place. A novel accessory was employed for all spectral acquisitions. The accessory was placed on the stage of microscope and then the sample holder was mounted onto the accessory. For the spectral acquisition of both loose gemstones and jewelries, the specimen was simply positioned on the sample holder with the table facet faced up. Prior to the measurement, a facet of the sample was aligned perpendicularly to the incident radiation by using the adjusting knobs of novel accessory in order to obtain a high energy throughput for spectral acquisition. The infrared radiation was coupled into the gemstone through the table facet by a built-in 15X Cassegrainian objective.

In all case the incident infrared beam was focused at a sample surface. The specularly reflected radiation was collected by the same objective while the observed spectrum was expressed in reflectance unit. Since the observed specular reflection spectrum exhibit the reflective-index-type feature, it was transform into an absorption-type spectrum by Kramers-Kronig (KK) transformation. The transformation process was easily performed by a built-in subroutine in the OMNIC<sup>TM</sup> software. The OMNIC<sup>TM</sup> software is the software using to control the spectrometer and to collect spectrum.

### 3.2.4 Transflectance Technique

The transflectance spectrum of a faceted gemstone was also collected by a NICPLAN<sup>TM</sup> infrared microscope attached to the FT-IR spectrometer. The novel accessory was employed for all spectral acquisitions using the microscope. The accessory was mounted on the stage of microscope. Reflection with normal incidence from a gold mirror was employed as a background for all spectral acquisitions. First, for the spectral acquisition of a loose gemstone, the specimen was positioned on the sample holder of novel accessory with the table facet faced up. For the spectral acquisition of mounted gemstones on jewelry (*i.e.*, ring, pendant, necklace and earring), the whole jewelry is placed on the sample holder without removing the gemstones from the jewelry setting (see Figure 3.3). The infrared radiation is coupled into the gemstone through the table facet by the built-in 15X Cassegrain objective. Second, prior to the measurement, a table facet of the sample was aligned perpendicular to the incident radiation by using the adjusting knobs of the novel accessory in order to obtain a high energy throughput. If no focus is visible, the accessory was adjusted until a sharp image of the table facet is obtained. Note that in the viewing position, the high energy throughput will be obtained at the focus image of table facet. When the focus at the table facet was obtained, the next step is raising the stage of microscope in order to bring the infrared radiation pass into the sample and then reflected at the pavilion facets before emerging to the air. In order to obtain the transflected radiation, the infrared beam must focus at the pavilion facets of the gemstone. The center point of the sample was always fixed in the holder, while

its position was adjusted both horizontally and vertically using x-y axis controlling stage of microscope to maximize the throughput of the infrared radiation.

For the transparent gemstone such as diamond, the images of its pavilion and culet can be observed with the objective, while those of translucent or semitransparent gemstone cannot. However, in case of the experiment to determine the transmittance spectrum of translucent gemstone we can notice the transmittance phenomenon from the return of energy throughput in OMNIC™ program when the infrared radiation reflected at the pavilion facet and then reaching to the infrared objective (see Figure 2.13, chapter 2). Of note is that the high energy throughput will be obtained again at the point above the focus of culet depend strongly on the cutting of the gemstone. Using the adjusting knobs of accessory and stage controls, a specific feature to be analyzed can be moved into position and into focus. The transmittance radiation was collected by the infrared objective and then the transmittance spectrum was acquired. The observed spectrum was expressed in absorbance unit.

### **3.4 Influence of Sample Arrangement**

#### ***Diffuse Reflectance Technique***

To study effect of sample arrangement, the diffuse reflectance spectrum was obtained by using a commercial DRIFT accessory. In order to maximize spectral quality, as well as to increase reproducibility, every sample applied onto the sample holder must be carefully placed with the pavilion facets faced up at the center point of the sample holder. The whole sample holder was rotated with the angles of 0° to 315° and the diffuse reflectance spectra were collected with every 45° rotation.

#### ***Specular Reflection Technique***

Two different sampling techniques equipped with infrared microscope were employed for spectral collections in order to determine how the spectral features with

the same novel accessory under different sample orientation. The first was specular reflection technique and the second was transreflectance technique. With both techniques, a sample was placed in the brass sample holder at the center of novel accessory with table facet faced up. Reflection with normal incidence from a gold mirror was employed as a background for all spectral acquisitions. The specular reflectance spectra were obtained by using the same procedure as express in section 3.2. The incident radiation was focus at the table facet of a gemstone and then specular reflectance spectrum was then collected. Towards the next process, whole sample holder was rotated with every  $45^\circ$  of rotational angles and then collected the spectrum.

### *Transreflectance technique*

The transreflectance measurements obtained with novel accessory and infrared microscope were compared with diffuse reflectance spectrum obtained by using a commercial DRIFT accessory. For the study of effect of the sample orientation, a sample was placed in the brass sample holder at the center of novel accessory with the table facet faced up. The spectral acquisition procedure with the transreflectance technique is the same as that mention in section 3.3. When the focal point at pavilion facet was achieved, the first transreflectance spectrum of the orientation series was then collected. Next, the sample arrangements were controlled by rotating the whole brass ring with various angles of rotation between  $0^\circ$  to  $315^\circ$ . The transreflectance spectra were then colleted with every  $45^\circ$ . For some spectral measurements, the position of the gemstone was slightly adjusted horizontally or vertically by using the adjusting knobs of the novel device and microscope's stage in order to optimize the measured throughput.

### **3.5 Influence of the varying Aperture Size in Transreflectance Technique**

One of the most important components of the scanning unit of infrared microscope is the field stop or aperture, which acts as a spatial filter at the image plane positioned directly upper position of the sample. The illumination area of the

sample with IR light is determined by setting this mechanical aperture of the microscope. These variable apertures are also very useful if the sample being studied is heterogeneous because it allows the operator to study different areas of the sample by closing the apertures around them. In case of transmittance technique, the aperture is positioned such that the radiation from the source is transmitted through the sample and then transmitted radiation was collected. Thus, the aperture size may affect to the obtained spectrum.

FT-IR spectra were obtained using a Nicolet Magna 750 FT-IR spectrometer with a NICPLAN<sup>TM</sup> microscope operating in reflectance mode. A narrow-band MCT detector was used to acquire data at  $4\text{ cm}^{-1}$  resolution with 256 scans. In case of the experiments to determine the effect of aperture size in transmittance spectrum, transmittance spectrum was performed as the same method that mentioned in section 3.3. Briefly, prior to the measurement, the gold alignment mirror was employed as a background for spectral acquisition. Since FT-IR spectroscopy employed a single-beam spectrometric method, one must always obtain a background spectrum. The spectrum of the sample is then ratioed to the background. It is therefore important that the aperture size be the same for both background and sample spectra. For the first spectral acquisition in this experiment, the size of aperture was set manually to  $100 \times 100\ \mu\text{m}$  and then collected the background spectrum. After removing the mirror off the microscope's stage, placed the novel accessory on the stage and then set the gemstone into the sample holder. The gemstone was visualized through the microscope lens and a sampling area was selected and positioned right on the table facet. The selected sampling area must focus at center of the specific facet. The projected image of an aperture, positioned at the first focus point of the table facet, determines the sampling area that will be probed. The size of the aperture was set to the same value of the background spectrum. When the focus at the table facet with the correct aperture size was obtained, the next step is raising the stage in order to couple the infrared radiation into the sample and then reflected at the pavilion facets before recording as transmittance spectrum.

Several apertures size was set of 200 x 200 to 5000 x 5000  $\mu\text{m}$  and then the same procedures were repeated in order to collect both background and transmittance spectra.

### 3.6 Unique Identification of a Gemstone

#### 3.6.1 Sample of Interest: A Type IaA Diamond.

#### 3.6.2 Instruments for Data Acquisition

1. FT-IR spectrometer:
  - 1.1 Nicolet Magna 750 FT-IR spectrometer equipped with NICPLAN<sup>TM</sup> infrared microscope.
  - 1.2 Bruker/Equinox-55/106S FT-IR spectrometer equipped with an infrared microscope.
2. The novel accessory for adjustment of focal plane with sample holder

#### 3.6.3 Default Instrumental Parameters

##### Instrumental Setup

Source	Standard Globar <sup>TM</sup>
Beam splitter	Multilayer coating on KBr
Detector	MCT

##### Acquisition Parameters

Spectral resolution	4 $\text{cm}^{-1}$
Number of scans	256
Signal gain	Auto
Spectral format	Absorbance

### **Infrared Microscope Parameters**

Experimental Mode	Reflection
Spectral resolution	4 cm <sup>-1</sup>
Number of scans	256
Signal gain	Auto
Spectral format	% Reflectance or Absorbance

### **3.6.4 Experimental Procedure**

Two different FT-IR spectrometers equipped with the different infrared microscopes were employed for spectral collections with the transmittance technique in order to determine the transmittance spectra under different spectrometers. The first was Nicolet Magna 750 infrared spectrometer equipped with NICPLAN<sup>TM</sup> infrared microscope. The second was Bruker/Equinox-55/106S FT-IR spectrometer with the infrared microscope. With the both spectrometer, it was possible to configure the optical system to allow use of the novel accessory with the infrared microscope for transmittance spectral acquisition. For purposes of spectral comparisons between different spectrometers, the same experimental parameters were utilized on a Bruker/Equinox-55/106S FT-IR spectrometer. Data collection was performed under Opus software with parameters mentioned above. The same procedures to acquire transmittance spectrum (see section 3.3) was performed with the Bruker FT-IR spectrometer. The result spectra express in absorbance unit.



## CHAPTER IV

### RESULTS AND DISCUSSION

Considering the objective of this research, in addition to introduction of a novel technique for non-destructive characterization of faceted gemstone, the limitation and benefit of different sampling techniques will be discussed. This chapter is divided into sections, each describing results of the investigation of the specific gemstones that acquired with different sampling techniques. The order of sections is determined by the sampling technique and also subdivided based on species of gems. The last section shows application of a novel transreflectance technique employed for jewelry analysis and unique identification of gemstone.

#### 4.1 Comparison of FT-IR Sampling Techniques

The novel transreflectance technique using an infrared microscope to acquire an infrared spectrum by collecting the transreflected radiation from the pavilion facets of cut diamonds was exploited. To ensure an efficiency of this novel transreflectance technique, the observed spectra were compared to the well-accepted diffuse reflectance and specular reflectance spectra. Spectra of a 0.1050 ct and a 0.1075 ct round brilliant cut diamonds show in Figure 4.1 and 4.2, respectively. The diffuse reflectance and transreflectance spectra clearly reveal the three principle absorption bands of diamond (*i.e.*, three-phonon absorption at  $3900 - 2650 \text{ cm}^{-1}$ , two-phonon absorption at  $2650 - 1500 \text{ cm}^{-1}$ , and one-phonon absorption at  $1400 - 900 \text{ cm}^{-1}$ ) [10,25]. The transreflectance technique provides spectrum with an equal or better spectral qualities to that of the well-accepted diffuse reflectance technique. Although the spectral envelop of the transreflectance spectrum is the same as that of the well-accepted diffuse reflectance spectrum, it seem to possess a superior spectral quality. The absorptions in all three principle regions are more prominent in the transreflectance spectrum. The high noise level at the peak maxima of the two-phonon region indicates saturated absorption. This is due to the high absorption coefficient of diamond in that region. The absorption bands associated with hydrogen impurity and

nitrogen impurity in the diamond crystal structure are clearly observed in diffuse reflectance and transmittance spectra [23-25]. The specular reflection spectrum, on the other hand, does not show any prominent absorption feature. It should be noted that the absorptions of water vapor (3900 - 3500 and 1800 - 1400  $\text{cm}^{-1}$ ) and carbon dioxide gas (2400 - 2300  $\text{cm}^{-1}$ ) can be noticed in all measured spectra. The variations of the absorption magnitudes are due to the fluctuation of the ambient air during the spectral acquisition.

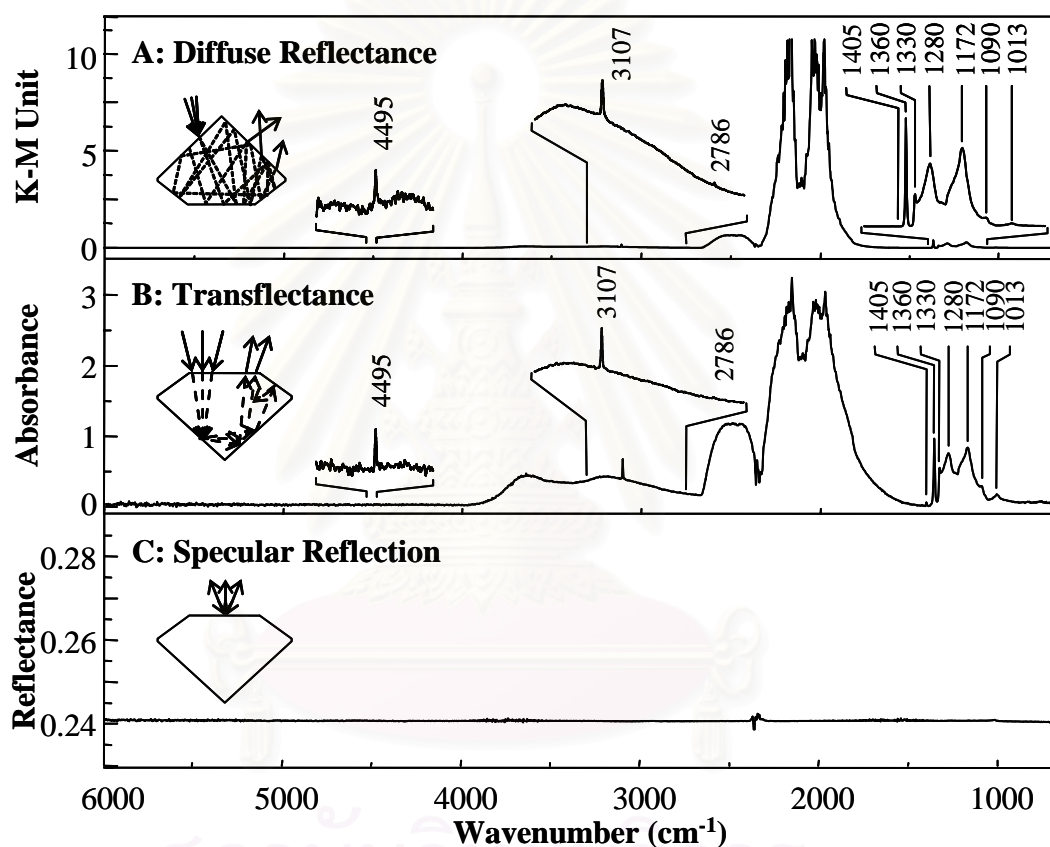


**Figure 4.1** FTIR spectra of a 0.1050 ct round brilliant cut type IaB natural diamond acquired by (A) diffuse reflectance, (B) transmittance, and (C) specular reflection techniques.

According to the diffuse reflectance and transmittance spectra, the natural diamond in Figure 4.1 was identified as a type IaB while that in Figure 4.2 is a type IaA. The type IaB diamond possesses a B-center defect (*i.e.*, an aggregate consists of four nitrogen atoms surrounding a vacancy) which shows absorption band at 1330, 1172 and 1013  $\text{cm}^{-1}$  [13]. An associated absorption band at 1360  $\text{cm}^{-1}$ , which referred

to the extended-planar-defect platelets, could also be noticed. For spectra with strong absorption at  $3107\text{ cm}^{-1}$ , weak absorption at  $2786\text{ cm}^{-1}$  was noticed in type IaB diamond. Both absorption bands are commonly observed as minor features in infrared spectra of hydrogen-containing natural diamonds. The absorption at  $2786\text{ cm}^{-1}$  is believed to be the first overtone of the absorption at  $1405\text{ cm}^{-1}$ . Regarding Figure 4.2, the unique absorption bands in the one-phonon region of the type IaA diamond associates with an A-center defect (*i.e.*, a defect consists of a pair of adjacent substitution nitrogen atoms in the diamond lattice) [31]. The main absorption has maximum at  $1282\text{ cm}^{-1}$  and additional weak absorptions at  $1362$ ,  $1208$  and  $1015\text{ cm}^{-1}$ .

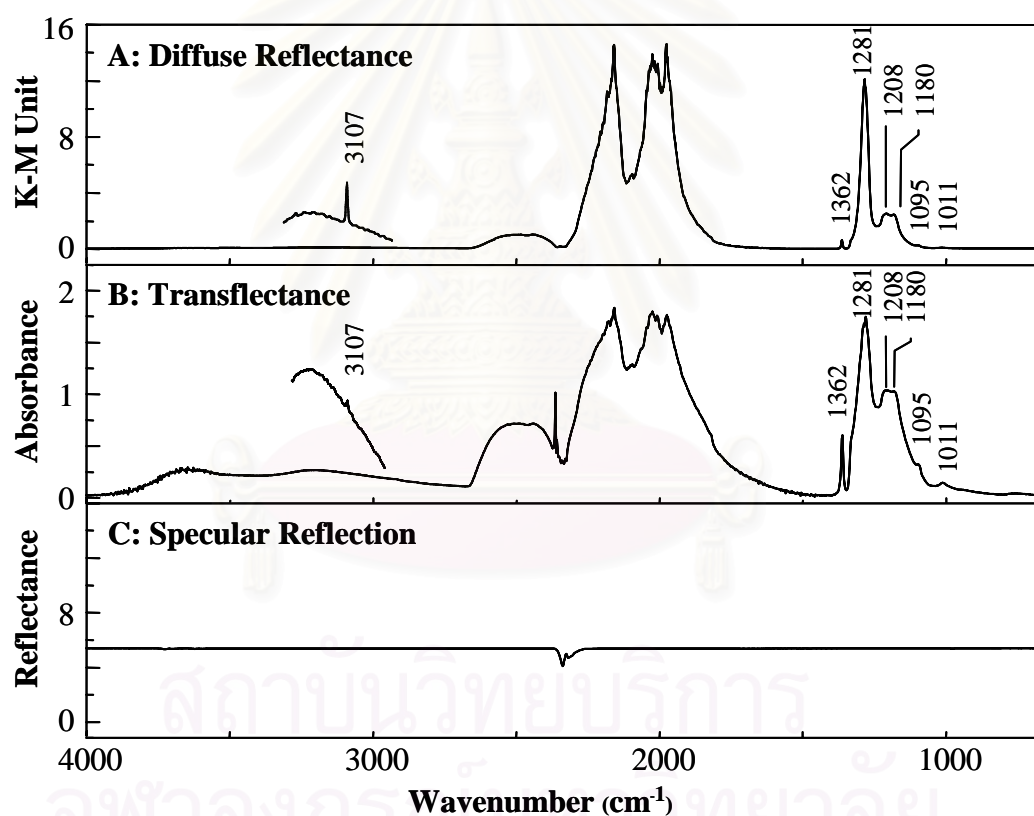


**Figure 4.2** FTIR spectra of a 0.1075 ct round brilliant cut type IaA natural diamond acquired by (A) diffuse reflectance, (B) transflectance, and (C) specular reflection techniques.

As a result, an infrared microscope can be utilized for a nondestructive transmittance spectral acquisition of faceted diamonds. Due to the nondestructive nature, short measurement time, simplicity, and spectral information directly related to chemical structures and compositions, transmittance technique could be employed for routine analysis of faceted diamonds. Although the shown results are those of the round brilliant cut diamonds, the techniques could be applicable for other types of diamond cuttings and/or gemstones.

## **4.2 Diffuse Reflectance Technique for Gem Characterization**

Prior to the investigation of the novel sampling technique, it is desirable to verify the sensitivity and reproducibility of well-accepted sampling techniques for gems analysis. In this section, characterization of various faceted gemstones was employed via diffuse reflectance technique. The unique spectral features associated with chemical compositions, impurities, and treatment processes were also discussed.

### **4.2.1 Diamond Characterization**

Diamond has long been a prime interest of gem and jewelry markets due to its popularity, mystic believes, and commercial values. Due to its high commercial value, various types of diamond simulants have been produced. Since diamond simulants do not share the same chemical compositions with natural diamond, they can be easily distinguished by appearances and/or physical properties. Beside the synthetics and simulants, various types of treatments (*i.e.*, irradiation, heat, and high pressure-high temperature (HPHT) treatments) were applied to the low quality diamonds in order to improve their appearances (*i.e.*, inclusion elimination, color enhancement, and clarity improvement) [1-4]. Due to the same chemical structure and composition, the synthetic or treated diamonds cannot be differentiated from the natural gemstones by the conventional characterization techniques (*i.e.*, refractive index, hardness, color, specific gravity, and light dispersion measurements). However, it is important for gemologist to correctly identify the diamonds because of the large price difference between the synthetic or treated diamonds and natural untreated diamonds.

FT-IR spectroscopy is well-known for its spectral information unique to molecular structure and chemical composition. The technique was widely employed for diamond classification based on impurities (*i.e.*, nitrogen, hydrogen and boron) in the crystal lattice. Spectral information associated with lattice defects (*i.e.*, changes or transitions of defect centers) and growth structures were determined and employed for differentiating natural, synthetic and treated diamonds. Different treatment processes can also be identified by FT-IR spectroscopy. For classical diamond characterization using transmission technique, a thin slab of diamond is required. Because the technique is destructive, it is not suitable for high commercial value faceted diamonds. Transmission measurement of a faceted diamond using a beam condenser is complicated by sample arrangement and the complex reflection at the cut and polished surface. In order to solve the problems associated with characterization of faceted diamond, diffuse reflectance technique is presented.

Figure 4.3 shows diffuse reflectance spectra of irradiated fancy color diamonds. The spectral feature unique to defects and impurities in each diamond crystal structure are clearly observed. The irradiated green diamond in Figure 4.3A was identified as a type IaB while the irradiated yellow diamond in Figure 4.3D is a type IaA. As mentioned before, the type IaB diamond possesses a B-center defect which shows absorption band at 1330, 1172 and 1013  $\text{cm}^{-1}$  while the unique absorption bands in the one-phonon region of the type IaA diamond associates with an A-center defect which the main absorption has maximum at 1282  $\text{cm}^{-1}$  and weak absorptions at 1362, 1208 and 1015  $\text{cm}^{-1}$  [10,13,40]. Due to the over absorption in the one-phonon region associated with high nitrogen concentration in Figure 4.3E, classification of the irradiated black diamond based on spectral information in the one-phonon region is not possible. It should be noted that the absorptions of nitrogen and hydrogen cannot be noticed in the diffuse reflectance spectrum of a pink diamond (see Figure 4.3C), thus the diamond is possibly assigned as type IIa. The obtained spectrum of a red diamond shows different characteristic absorption band in one phonon region which cannot be identify. However, these diffuse reflectance spectral features of irradiated fancy color diamonds could be employed for classification of diamond type.

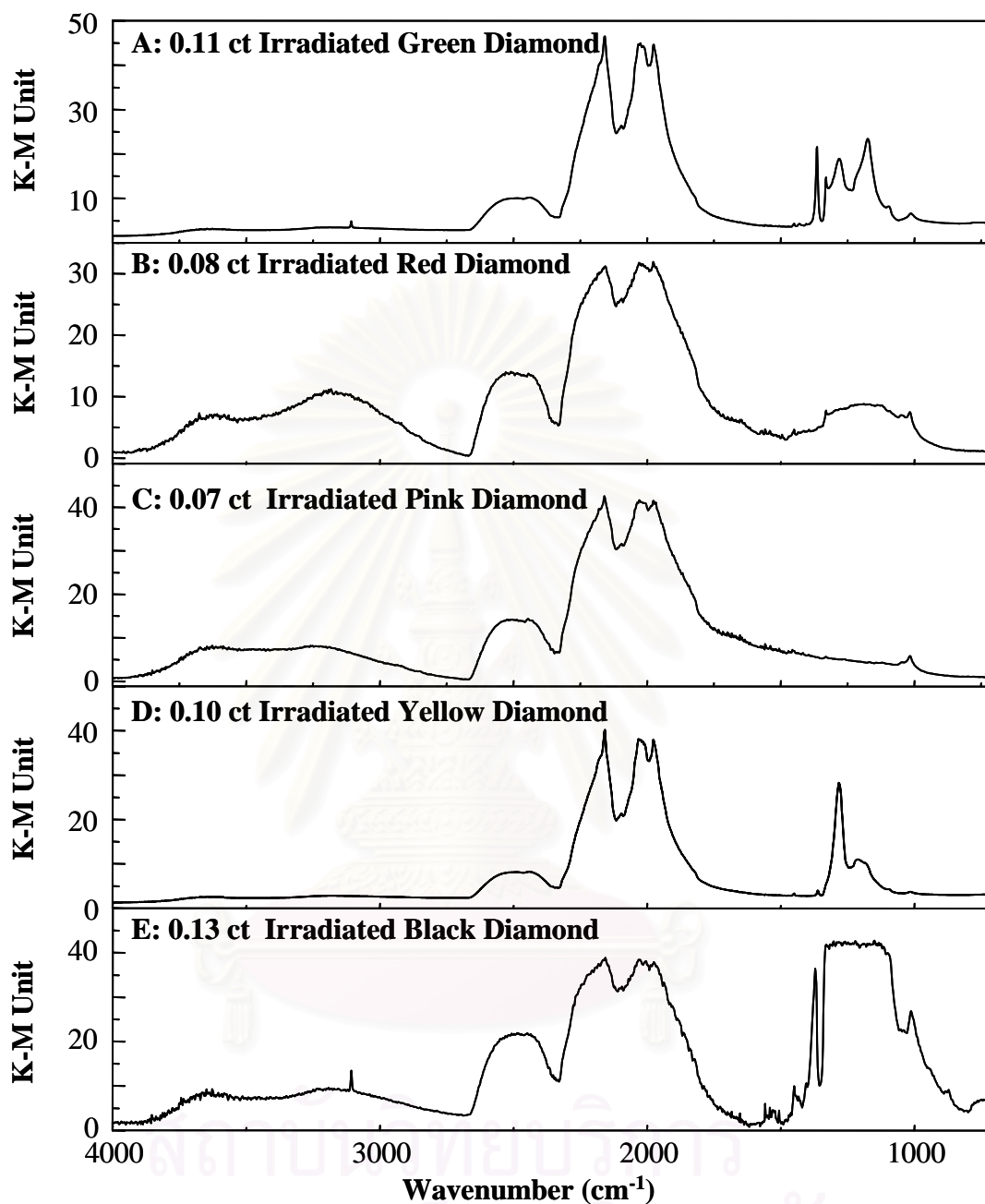


**Figure 4.3** Diffuse reflectance spectra of irradiated faceted diamonds: 0.11 ct irradiated green diamond (A), 0.08 ct irradiated red diamond (B), 0.07 ct irradiated pink diamond (C), 0.10 ct irradiated yellow diamond (D), and 0.13 ct irradiated black diamond (E).

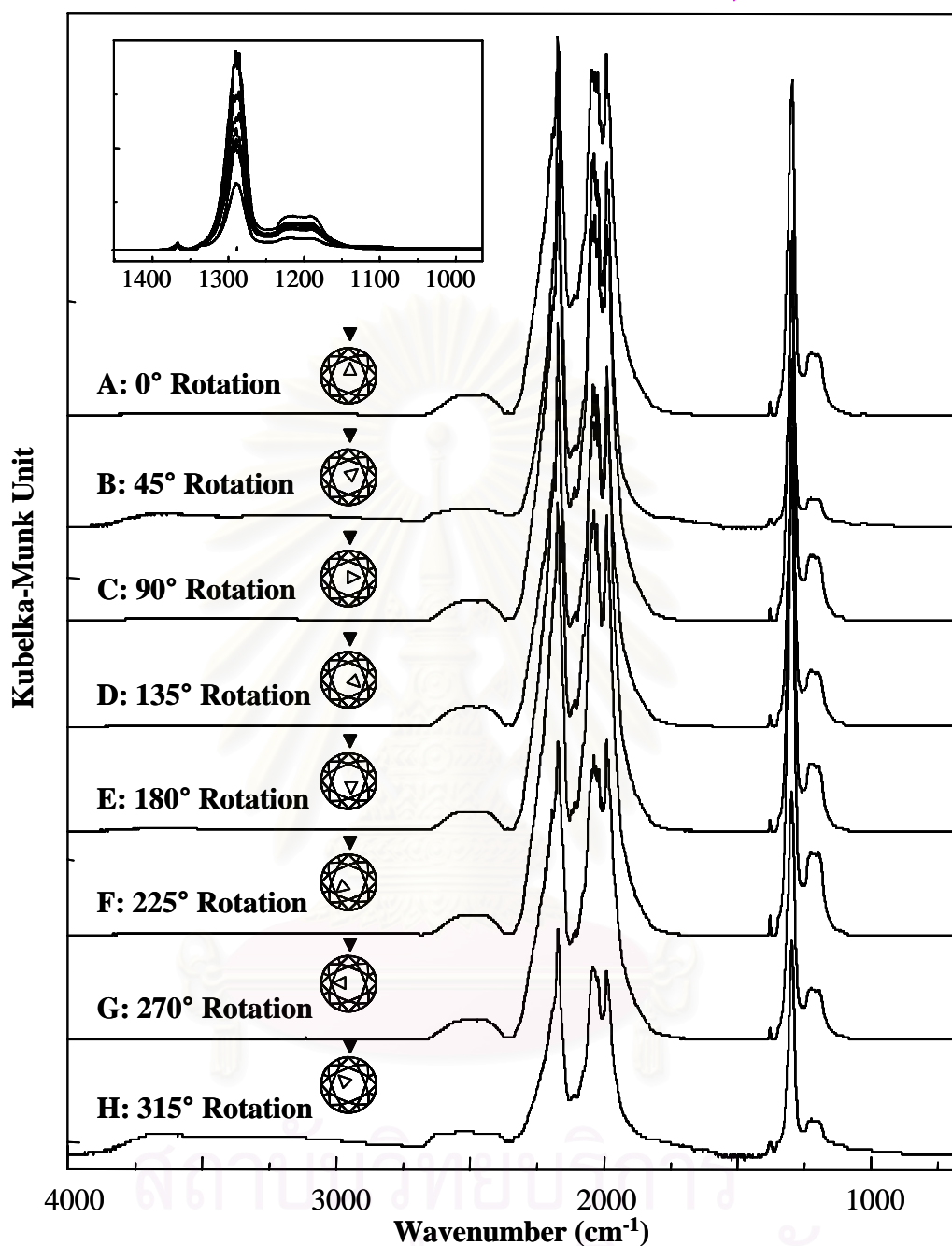


**Figure 4.4** Normalized diffuse reflectance spectra of the diamond in Figure 4.2 under different arrangements. The diamond was rotated: 0° (A), 45° (B), 90° (C), 135° (D), 180° (E), 225° (F), 270° (G), and 315° (H) with respect to a reference position. Due to a significant variation of absorption magnitudes, the observed spectra were normalized by the absorption at 2493 cm<sup>-1</sup>. The inset of absorptions in the one-phonon region was added for clarity.

It is well known that diffuse reflectance spectra of a faceted diamond are greatly influenced by the diamond arrangement on the sample holder [8,10]. As shown in Figure 4.4, diffuse reflectance spectra of the diamond with different arrangements (*i.e.*, different positions and/or angles of placement on the sample holder) are not exactly the same. Although the observed diffuse reflectance spectra clearly revealed the three principle absorption bands, their normalized spectra were not superimposed. Since a concentric rotational axes of a symmetrically faceted diamond and the sample holder is difficult to achieve, exact diffuse reflection patterns under different diamond arrangements cannot be obtained. As a result, a superimposition of diffuse reflectance spectra from the same faceted diamond is not normally observed.

As mentioned before, diamond is the most imitated of all gemstones. Common diamond simulants included cubic zirconia (CZ;  $ZrO_2$ ), synthetic colorless corundum (sapphire;  $Al_2O_3$ ), synthetic spinel, strontium titanate ( $SrTiO_3$ ), yttrium aluminium garnet (YAG), gadolinium gallium garnet (GGG), and synthetic moissanite [1-4]. Some of the simulants can be identified by standard gemological characterization techniques, others cannot. Spectra of faceted diamond simulants acquired by diffuse reflectance are shown in Figure 4.5. The weak absorption bands are clearly observed in the high wavenumber region while saturation is observed in the lower wavenumber region of diffuse reflectance spectra. Although the absorption bands of the synthetic moissanite in the  $2500 - 2200\text{ cm}^{-1}$  are interfered by that of carbon dioxide gas, their absorption maxima are clearly identified. Peak positions of the absorption bands of diamonds simulants deduced from the experimentally observed spectra are conformed to those reported elsewhere [11]. It can be seen that not only diffuse reflectance technique can be differentiated between diamond and diamond simulants but it can be employed for identification of each type of diamond simulants.



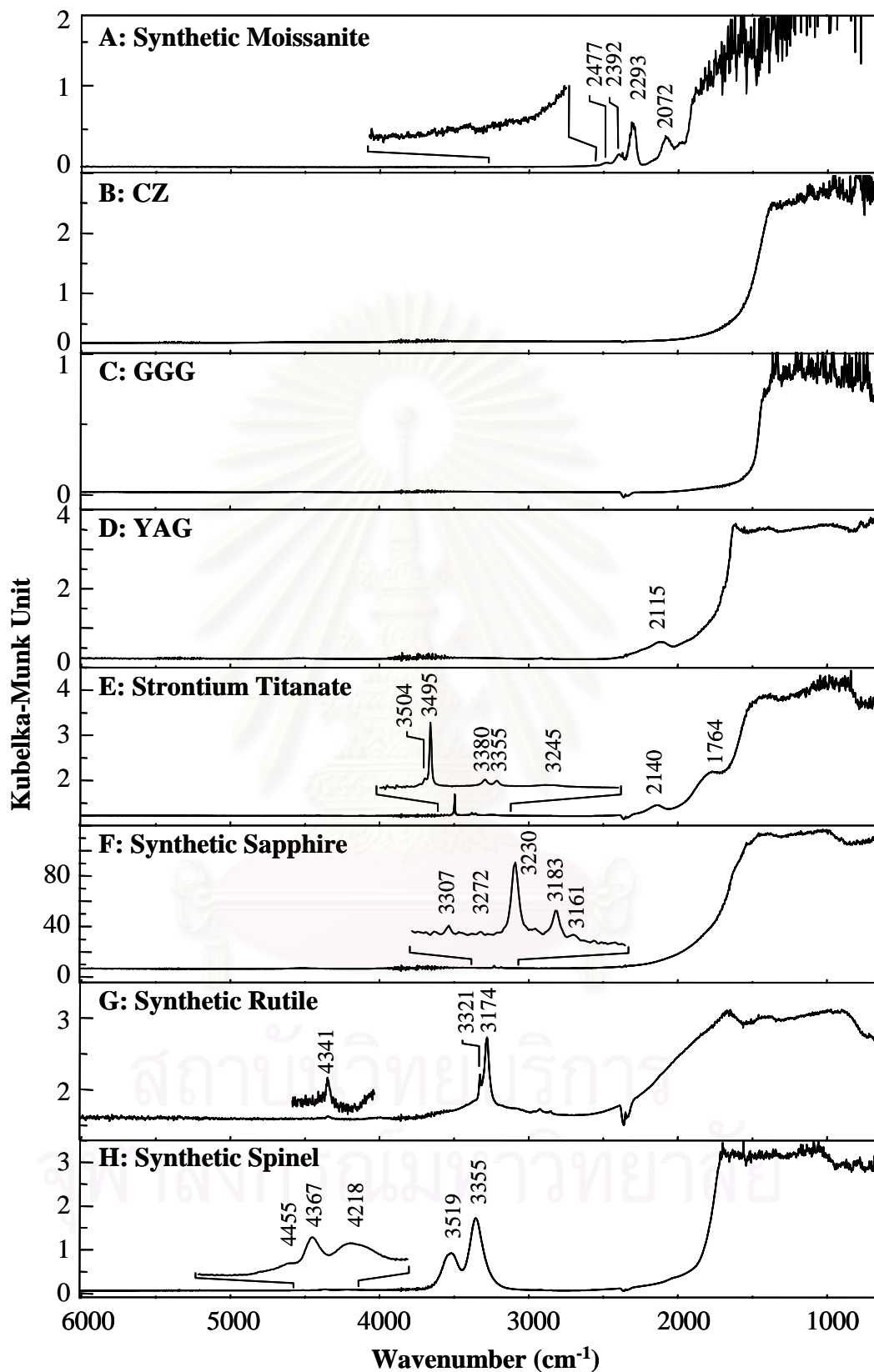


**Figure 4.5** FTIR spectra of round brilliant cut diamond simulants acquired by diffuse reflectance technique.

#### 4.2.2 Emerald Characterization

Emerald is a variety of beryl ( $\text{Be}_3\text{Al}_2\text{Si}_6\text{O}_{18}$ ), characterized by different shades of green. Beryl is a cyclosilicate in which the arrangement of  $\text{Si}_6\text{O}_8$  rings contains channels parallel to the c-axis, which can accommodate alkalis and molecules (such as  $\text{H}_2\text{O}$  and  $\text{CO}_2$ ), retained in the structure during crystallization [4,38].

Infrared spectroscopy has been applied to problem concerning the distinction of natural and synthetic emeralds since 1967. Winckersheim and Buchanan studied water in beryl and suggested that single molecule exists in the channels and alkali ions were present in some channels as well [38]. Wood and Nassau found that alkalis and free volatile molecules occupy variable positions in the channel and  $\text{H}_2\text{O}$  within the structure has been classified as type I or II, depending on the orientation of twofold axis of symmetry of the molecule relative to the c axis of beryl: perpendicular as type I and parallel as type II [39-40]. In flux-grown synthetic emeralds, no water absorption bands are observable, and in hydrothermal-grown synthetic emeralds water molecules that are not bound to alkali ions (type-I water molecules) are present. In natural emeralds, type-I water molecules as well as water molecules, which are bound to alkalies (type-II water molecules), are found. Hence,  $\text{H}_2\text{O}$  play a role helpful for discrimination between natural and synthetic beryl, given that (i) it is present in significantly different amounts, and (ii) it occurs as type I and II in the natural emerald, and as type I only in the hydrothermal emerald [38-42].

The FT-IR technique that widely employed for characterization of emeralds is transmission technique by means of KBr pellet method [38,40]. However, the technique is not suitable for faceted emerald because of the destructive nature of the sample preparation process. For this result, in this research the alternative non-destructive sampling technique for faceted emerald characterization based on FT-IR spectroscopy were introduced. In this section, infrared spectra of emerald that acquired by diffuse reflectance technique were employed, and differentiations between natural and synthetic emeralds were also exploited.

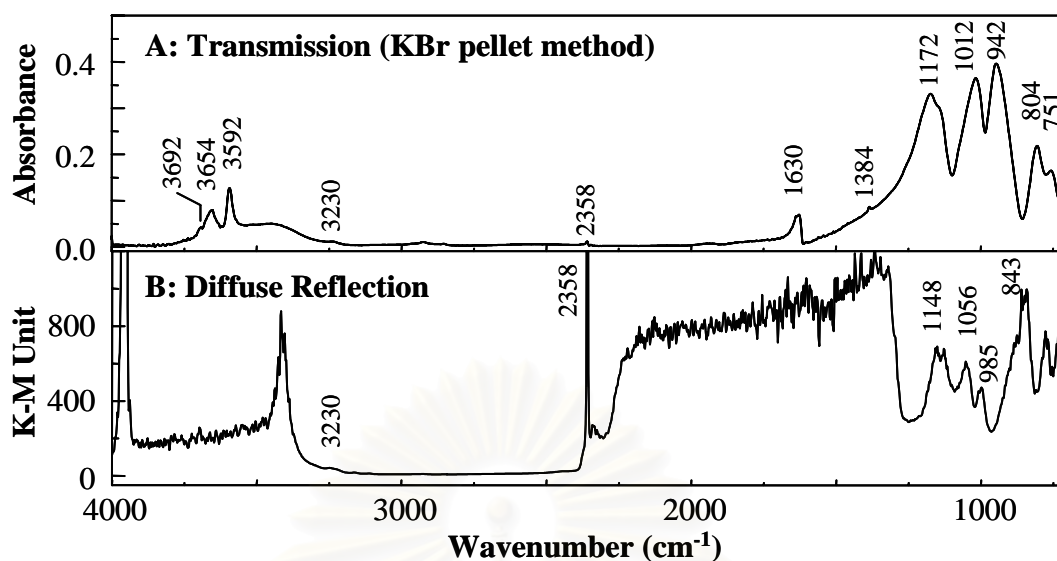


**Figure 4.6** FTIR spectra of a 0.730 ct oval cut emerald acquired by (A) transmission (KBr pellet method) and (B) diffuse reflectance techniques.

In order to investigate an efficiently of diffuse reflectance technique for characterization of faceted gemstone, the classical transmission technique was employed for its spectral comparison. Because of its low hardness, the emerald was ground with KBr powder and pressed into a pellet. Figure 4.6A and B shows infrared spectra of a 0.730 ct oval cut natural emerald acquired by transmission and diffuse reflectance techniques, respectively.

The transmission spectrum clearly reveals the strong absorption bands of emerald in low wavenumber ( $1500\text{-}700\text{ cm}^{-1}$ ), which are assigned to characteristic vibrations of beryl structure corresponding mainly to the stretching vibration of ring silicates. All peaks result from Si-O (symmetric ring deformation), Be-O, and Al-O bonding [40-44]. In addition, high absorption bands of molecular water in crystal structure of emerald can be noticed at  $3692$ ,  $3654$ ,  $3592$ ,  $3230$  and  $1630\text{ cm}^{-1}$  [38-42]. The three absorption bands in the OH stretching region ( $3800\text{-}3500\text{ cm}^{-1}$ ) are assigned to three different types of water molecules and/or hydroxyl group. In summary, an absorption band at  $3692\text{ cm}^{-1}$  is assigned to type-I water molecules which are not bound to the adjacent alkali ions. The others at  $3592$  and  $3654\text{ cm}^{-1}$ , respectively, are caused by symmetric and asymmetric stretching mode of type-II water molecules and/or hydroxyl groups, which are bound to alkali ions. Most probably, band at  $3592\text{ cm}^{-1}$  is due to water molecules which are bound to alkalies

(lithium and/or sodium) in the sequence  $\text{H}_2\text{O}-\text{Na}-\text{OH}_2$  (type-IIa water molecules), and another band at  $3654\text{ cm}^{-1}$  is assigned to water molecules or hydroxyl groups which are bound to alkalis in the sequence  $\text{H}_2\text{O}-\text{Na}-\square$  (type-IIb water molecules) or  $\text{HO}-\text{Na}-\square$  (hydroxyl group), which  $\square$  representing vacancies in channel sites of the beryl structure [38,40]. Another weak absorption at  $3230\text{ cm}^{-1}$  was assigned as overtone of water molecules. In the bending region, strong absorption band of water molecules at  $1630\text{ cm}^{-1}$  cannot be concluded because it was interfered by absorption band of bending vibration of water from KBr matrix. It should be noted that the broad band at  $3300-3000\text{ cm}^{-1}$  are observed. It can be seen that the main disadvantage of this method is water absorption band of KBr, which can interfere those of emerald absorption band in the region  $1680-1630$  and  $3200-3800\text{ cm}^{-1}$ . The peak assignment of water molecule in emerald lattice is summarized in Table 4.1.

**Table 4.1** Peak assignment of water molecules in emerald

Peak Position ( $\text{cm}^{-1}$ )	Peak Assignment
3692	Type I water
3654	Type II water: Asymmetric stretching of $\text{H}_2\text{O}$
3592	Type II water: Symmetric stretching of $\text{H}_2\text{O}$
3230	Overtone of OH bending
1630	OH bending of water molecule

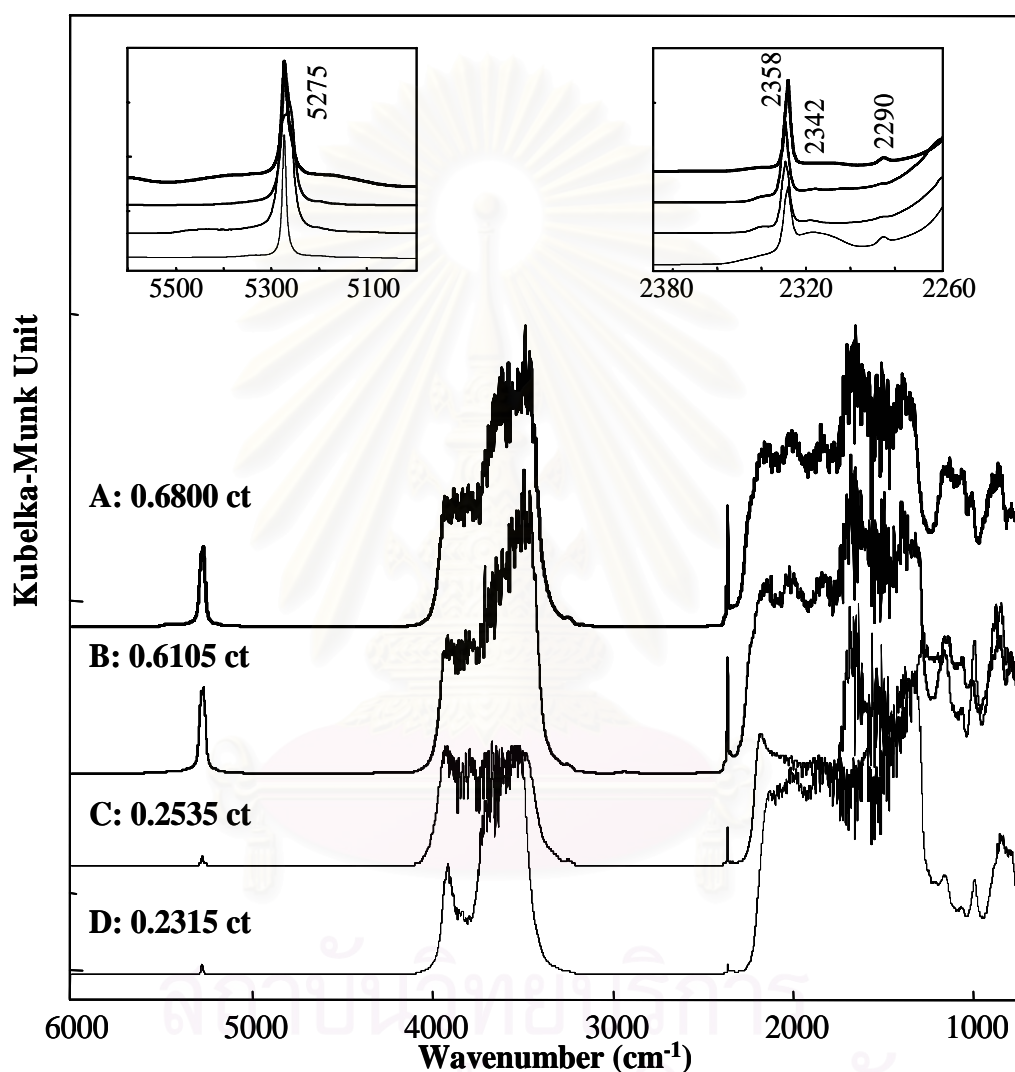
Regarding Figure 4.6B, the spectral envelop of diffuse reflectance spectrum is not similar to those of transmission spectrum. The diffuse reflectance spectrum of faceted emerald suffers from over absorption in both low and high wavenumber regions which corresponding to the stretching vibrations of beryl structure ( $1500-700\text{ cm}^{-1}$ ) and  $\text{H}_2\text{O}$  molecules ( $3700-3200\text{ cm}^{-1}$ ). The magnitude of absorption is associated with size of the faceted specimen. As mentioned before, absorption band in the low wavenumber region is the characteristic of beryl, which exhibit in all emerald spectra. Peak positions in this region are not similar to those of transmission spectrum. In KBr pellet technique, maxima of peak position were obtained for very restrictive crystal orientation regarding to the incident beam. Unlike transmission technique, infrared spectra of faceted emerald acquired by diffuse reflectance

technique are affected by the orientation of the sample to the incident beam. It should be remembered that emeralds are doubly refractive. Ideally, spectra should be taken at known crystallographic orientation in order to control these variations. However, the faceted gemstones rarely lend themselves to such conditions. While non-of the diagnostic features completely disappeared at any orientation tested, some did become quite weak or fail to detect the relevant features in some cases. It is, therefore, important that spectra be obtained at two or three different orientation before any conclusion is drawn as to the origins or types of a particular sample. Another reason is that the obtained spectrum suffers from specular reflectance component because of the smooth surface of the faceted emerald.

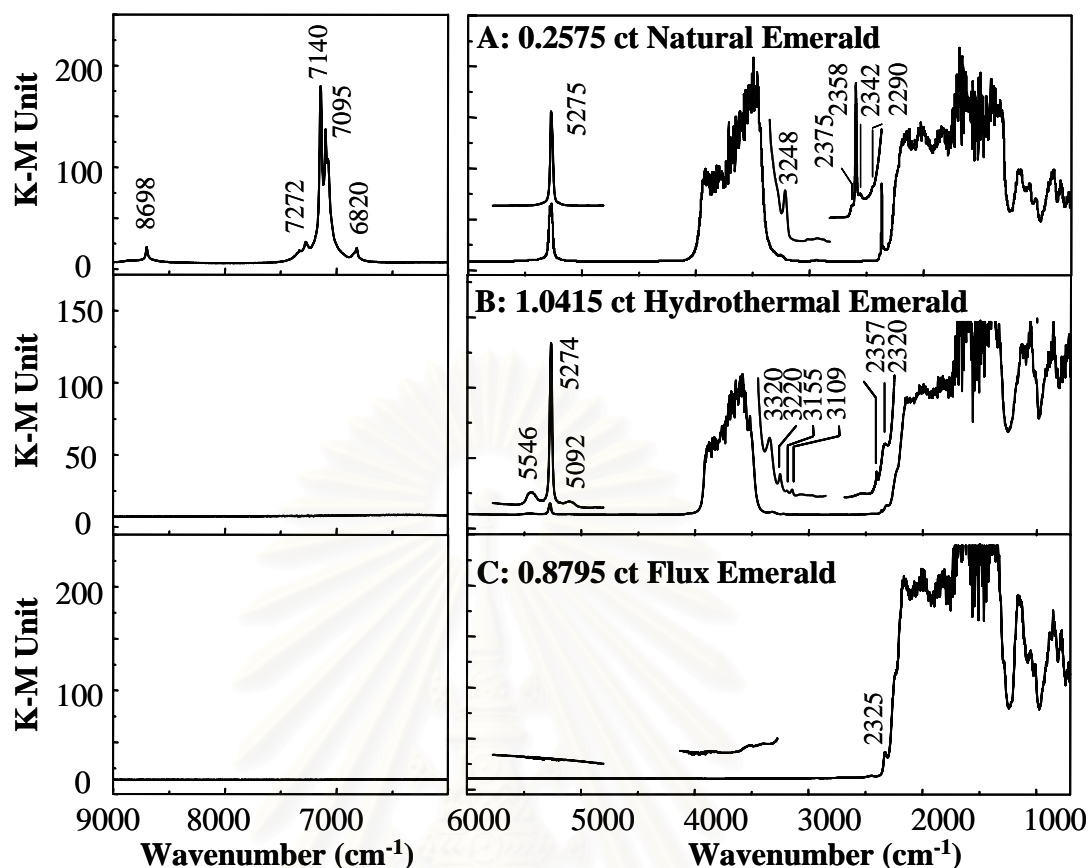
Due to the saturation of molecular water in the high wavenumber region, classification of the emerald acquired by diffuse reflectance technique in Figure 4.6B was not possible. In addition, the strong absorption bands of carbon dioxide ( $\text{CO}_2$ ) at  $2350\text{ cm}^{-1}$  is also clearly observed in diffuse reflectance spectrum. Although the channels of the emerald structure may contain  $\text{CO}_2$  molecules [40], it should be noted that the absorption at  $2350\text{ cm}^{-1}$  may be due to  $\text{CO}_2$  in the ambient air during spectral acquisition. Thus, classification of this absorption band can not be concluded. In order to investigate the origin of  $\text{CO}_2$  absorption band, we additionally identified many natural emeralds with different sizes and cuttings via diffuse reflectance technique. The representative absorbance spectra are presented in Figure 4.7.

Figure 4.7 shows diffuse reflectance spectra of four natural emeralds. The resulting spectra present over absorption bands at  $4000\text{-}3200$  and  $1500\text{-}700\text{ cm}^{-1}$ , which indicate the presence of molecular water and characteristic bands of emerald structure, respectively. The inset of Figure 4.7 indicates a prominent absorption band of  $\text{CO}_2$  in the  $2200\text{-}2240\text{ cm}^{-1}$  and combination bands of molecular water in the  $5500\text{-}5000\text{ cm}^{-1}$ . The observation in  $2200\text{-}2240\text{ cm}^{-1}$  shows distinct spectral features of  $\text{CO}_2$  different from the ambient air. All obtained spectra show strong absorption at  $2353\text{ cm}^{-1}$  and associated with a weak absorption band at  $2290\text{ cm}^{-1}$  and  $2340\text{ cm}^{-1}$ , which is typically caused by  $\text{CO}_2$  molecules either in the channel sites or in fluid inclusions [40]. The  $2290\text{ cm}^{-1}$  band was never observed in the synthetics, while it is

usually present in natural emeralds. Moreover, in natural emeralds the  $2358\text{ cm}^{-1}$  band identified as  $\text{CO}_2$  is always stronger than the  $2340\text{ cm}^{-1}$  feature. As a result, we can conclude that the strong absorption band in the  $2400\text{--}2200\text{ cm}^{-1}$  corresponding to the valence vibration of the trapped  $\text{CO}_2$  molecules in the crystal lattice of emerald [39-47].



**Figure 4.7** FTIR spectra of faceted natural emerald acquired by diffuse reflectance technique; 0.6800 ct (A), 0.6105 ct (B), 0.2535 ct (C), and 0.2315 ct (D). The absorption of  $\text{CO}_2$  in the ambient air was eliminated by purging the spectrometer with a dry nitrogen gas.



**Figure 4.8** FTIR spectra of natural and synthetic emeralds acquired by diffuse reflectance technique. Note: The near infrared spectra ( $9000\text{-}6000\text{ cm}^{-1}$ ) of the identical emeralds were acquired from separate measurement.

As mentioned before, we have now successfully identified natural emerald using diffuse reflectance technique. It should be noted that the presence of molecular species, such as  $\text{H}_2\text{O}$  and  $\text{CO}_2$  in emerald, can be easily recognized in the FTIR spectra [48-52]. In another our measurement, we additionally discriminated natural emerald and different synthetic emeralds. As shown in Figure 4.8, the infrared spectra of natural and hydrothermal synthetic emeralds are more similar to one another. Flux synthetic emerald can be readily distinguished from their natural and hydrothermal counterparts. The most obvious difference in the flux emerald is the absence of the strong absorption between  $3400$  and  $3800\text{ cm}^{-1}$ . This strong absorption has been identified as being associated with water molecules that is always present in natural and hydrothermal synthetic emeralds because of their growth condition [4]. Although the natural and hydrothermal emeralds cannot be distinguished differently

by water absorption band between 4000-3000  $\text{cm}^{-1}$  because of their over absorption feature, the combination band of water molecules in the 5600-5000  $\text{cm}^{-1}$  can be exploited for the identification. The tested hydrothermal emerald spectrum shows strong absorption at 5092, 5274 and 5546  $\text{cm}^{-1}$  while the natural emerald only present a strong absorption band at 5275  $\text{cm}^{-1}$ . The spectral features in near infrared region (9000-6000  $\text{cm}^{-1}$ ) can also used to distinguish these troublesome hydrothermal from natural emeralds. The near infrared spectrum of natural emerald shows strong absorption bands at 8698, 7272, 7140, 7095 and 6820  $\text{cm}^{-1}$  corresponding to the overtone and combination bands of type II water molecules related to the high amount of alkali ion [52]. In contrast, these absorption bands cannot be observed in the spectra of the tested hydrothermal emerald. Hence, water absorption bands in near infrared region plays a role available for discrimination between natural and synthetic emeralds.

The spectral features at 2200-2400  $\text{cm}^{-1}$  can also used to distinguish these troublesome hydrothermal from natural emeralds. The tested natural emerald shows at least two and, more commonly, three features in this region, at 2290, 2340 and 2358  $\text{cm}^{-1}$ . The 2290  $\text{cm}^{-1}$  band was never observed in the synthetics, while it is usually present in natural emeralds. Moreover, in natural emeralds the 2358  $\text{cm}^{-1}$  band identified as  $\text{CO}_2$  is always stronger than the 2340  $\text{cm}^{-1}$  feature, while in synthetics the relationship is reversed [39-40, 51].

The dependence of sample arrangement for faceted emerald characterization was additionally observed. An obtained data collection was performed under identical conditions with diamond characterization (see Section 4.2.2, Figure 4.4). To evaluate the influence of sample arrangement on the sample holder, diffuse reflectance spectra of princess cut hydrothermal emerald were employed for comparison purpose. In case of this anisotropic gemstone as emerald, the specimen was carefully applied at the central part of sampling cup (sample holder) to ensure the maximum sensitivity and reproducibility.



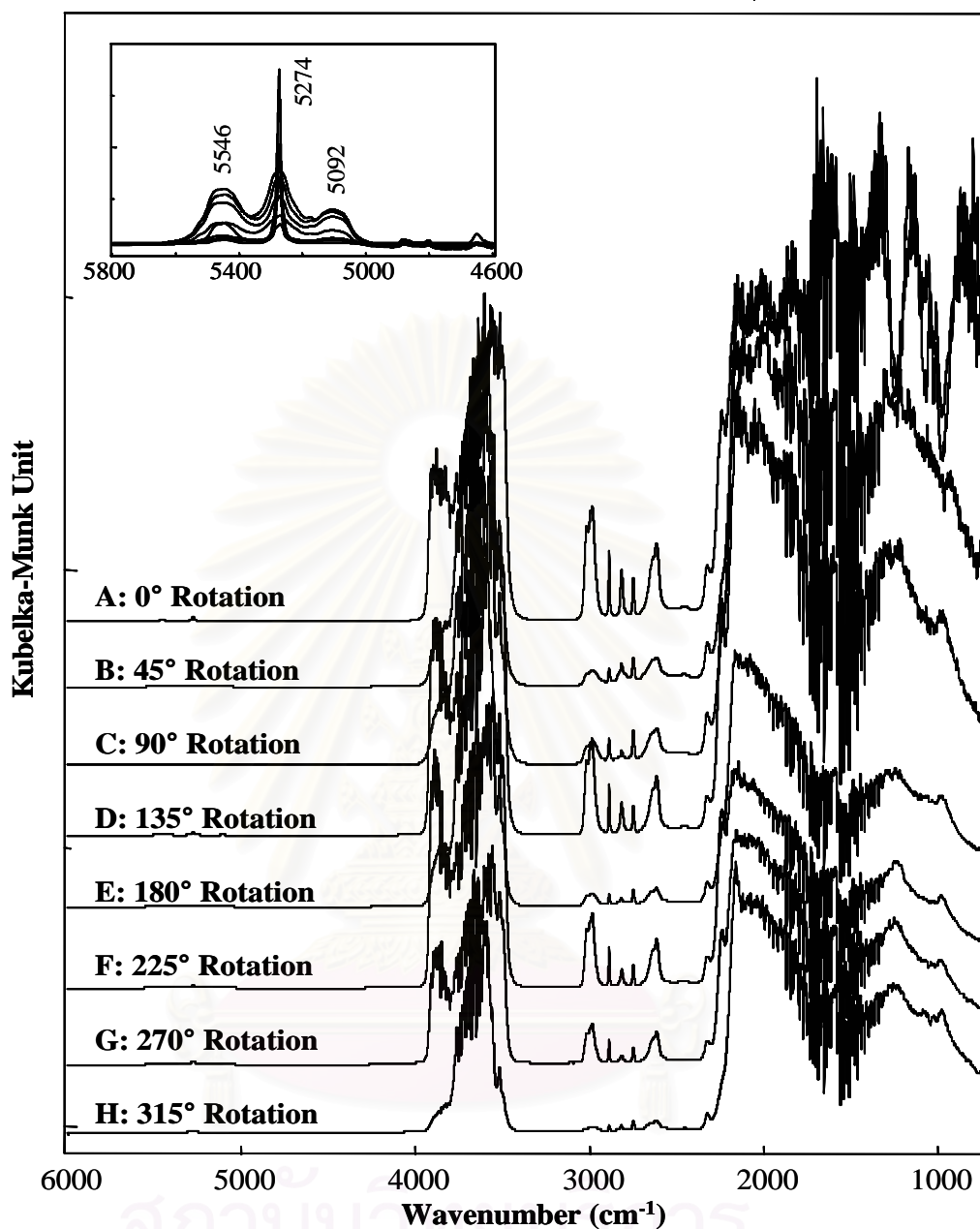


**Figure 4.9** Normalized diffuse reflectance spectra of 0.4960 ct hydrothermal emerald (princess cut) under different arrangement. The emerald was rotated: 0° (A), 45° (B), 90° (C), 135° (D), 180° (E), 225° (F), 270° (G), and 315° (H) with respect to a reference position.

Figure 4.9 shows normalized diffuse reflectance spectra of 0.4960 ct hydrothermal emerald (princess cut) under different arrangement (*i.e.*, different positions and/or angles of placement on the sample holder). By comparing the observed diffuse reflectance spectra, it is clearly seen that the obtained normalized

spectra of emerald were not superimposed. Since a concentric rotational axes of a symmetrically faceted emerald and the sample holder is difficult to achieve, exact diffuse reflection patterns under different emerald arrangements cannot be obtained [23-25]. As a result, a superimposition of diffuse reflectance spectra from the same faceted emerald is not normally observed. In each case, it should be noted that emeralds is an anisotropic gem material which has doubly refractive property. Their infrared spectra are affected by the orientation of the sample to the incident radiation. Difference sample orientation exhibits different spectral intensity, especially the bands that associated with water and carbon dioxide molecules. Therefore, it is important that spectra be obtained at two or three different orientation before any conclusion is drawn as to the origins of a particular sample.

In addition, the obtained spectra of this hydrothermal synthetic emerald exhibit a pattern of strong absorption features between 2600 and 3000  $\text{cm}^{-1}$  that readily distinguishes them from their natural counterparts. Most of the absorption features seen in this range for synthetics were also seen to some degree in natural emeralds, but never all together with relatively high magnitudes in the synthetics. Moreover, some features that were observed in most hydrothermal synthetics - for example, those at 2745, 2830, 2995, 3490, 4052, and 4375  $\text{cm}^{-1}$  - were never detected in natural emerald. This region (3100-2500  $\text{cm}^{-1}$ ) corresponds to the chlorine related band [42]. Thus, the majority of hydrothermal synthetic emeralds can be distinguished from its natural counterpart by the infrared absorption in this region.

#### **4.2.3 Ruby and Sapphire Characterization**

Ruby is a variety of corundum,  $\alpha\text{-Al}_2\text{O}_3$  colored red by chromium ions dispersed throughout its crystal structure [53-54]. The general analysis of ruby based on infrared spectroscopy cannot be employed by KBr pellet technique because of its extremely high hardness value. The sample must be polished and cut as a thin slab to allow the light to pass through the stones [54]. Thus, this technique is not suitable of faceted ruby. Recently, beam condenser was adapted for ruby and sapphire identification but the technique is complicated by sample arrangement and suffered from semitransparent property of specimen. Again, this section involves

characterization and differentiations natural and some synthetic ruby and sapphire by diffuse reflectance technique.

As described previously, since ruby is high hardness material, identification of faceted ruby cannot perform via transmission technique by means of KBr pellet method. Figure 4.10 shows infrared spectra of various types of rubies that acquired via diffuse reflectance technique. As clearly seen in the Figure, each spectrum represents the characteristic of each specimen. According to the diffuse reflectance spectra of all specimens, rubies possess the dominant over absorption features typical of corundum from Al-O stretching frequencies and lattice absorption in the region of approximately  $700\text{-}1100\text{ cm}^{-1}$  [55-57]. Their spectral features in this region are different depend on the size/thickness of sample and sample arrangement.

For comparison propose, samples of natural faceted rubies obtained from either DMR (0.9905 ct natural ruby) or BUCH (0.9810 ct natural ruby) were employed. Typical results are shown in Figure 4.10A and B. Each observed spectrum shows over absorption band at lower wavenumber assigned as Al-O stretching frequencies. A natural ruby in Figure 4.10A displays the predominant absorption bands at  $3400\text{-}3100$  and  $2340\text{ cm}^{-1}$  while that in Figure 4.10B presents only board band at  $3145\text{ cm}^{-1}$ . The peak at  $2340\text{ cm}^{-1}$  can be assign to the vibration of C-O bond in  $\text{CO}_2$  [54-55]. The series of sharp peaks observed in the  $3400\text{-}3100\text{ cm}^{-1}$  range are related to structural OH groups bonded within corundum lattice. As shown in Figure 4.10A, sharp absorption bands at  $3368$ ,  $3309$ ,  $3232$  and  $3186\text{ cm}^{-1}$  indicate the formation of OH group in the lattice [53]. Hydrogen can also exist in corundum as  $\text{H}_2\text{O}$ , leading to a board absorption band at  $3415\text{ cm}^{-1}$  (see Figure 4.10B). It can also be present as water within fluid inclusion, and, finally, it can exist as a component of an included solid phase, such as diaspore [53], which is one of the hydroxides of aluminum. Peak positions of the absorption bands of faceted natural ruby deduced from experimentally observed spectra are conformed those reported elsewhere [53-61]. By comparison, the natural ruby in Figure 4.10A and B can be classified as heat-treated ruby and non-heat treated ruby, respectively. As a consequence, these absorption bands may be used as an indicator of both heat-treated ruby and sapphire.

The diffuse reflectance spectra of different synthetic rubies were also shown in Figure 4.10. The series of sharp peaks observed in the 3400-3100  $\text{cm}^{-1}$  are related to hydroxyl stretching. Since differences in their synthetic process result in differences in their spectral features, the OH stretching absorption can be utilized as a means to identify and distinguish hydrous alumina phases [53,58-61]. From the observed spectra, diffuse reflectance technique can be employed for differentiating between natural and synthetic rubies.

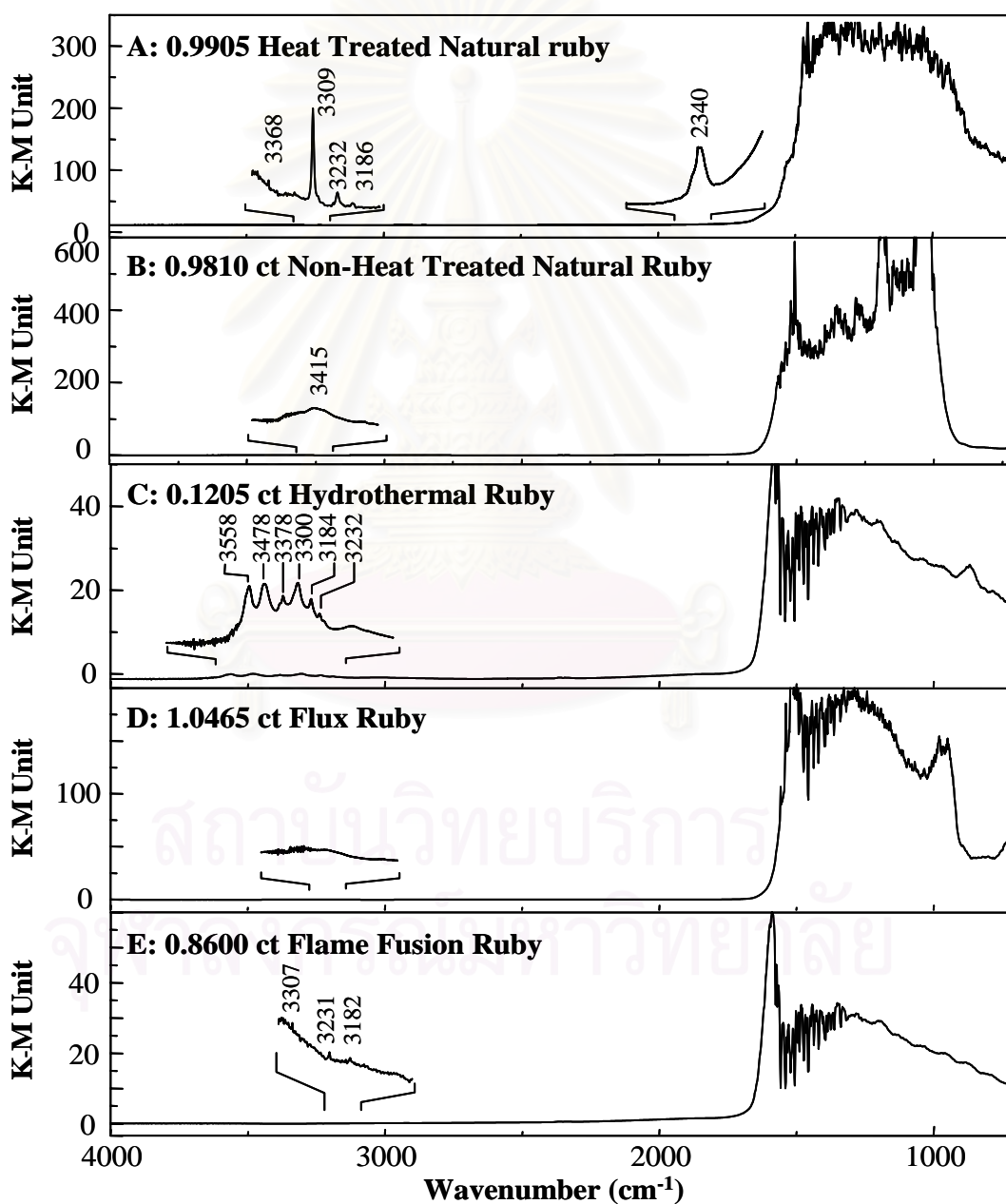


**Figure 4.10** FTIR spectra of natural and synthetic rubies acquired by diffuse reflectance technique.

Rubies and sapphires from different country of origin were also examined. The corresponding observed diffuse reflectance spectra are shown in Figure 4.11. Again, only the spectral feature above  $3000\text{ cm}^{-1}$  was observable because the low wavenumber region shows over absorption of Al-O. Each spectrum shows characteristic absorption in the  $3400\text{-}3100\text{ cm}^{-1}$  region which corresponding to structural OH stretching. For the diffuse reflectance spectra of Australian sapphire and African sapphire, the same spectral feature in OH frequencies region was observed. However, there are observable the difference of intensity ratio of those peak which imply the OH absorption from several hydrous alumina phases. This observation elucidates that not only diffuse reflectance spectra can be utilized for differentiating between natural and synthetic ruby but also for examining the sapphire from different the country of origin.

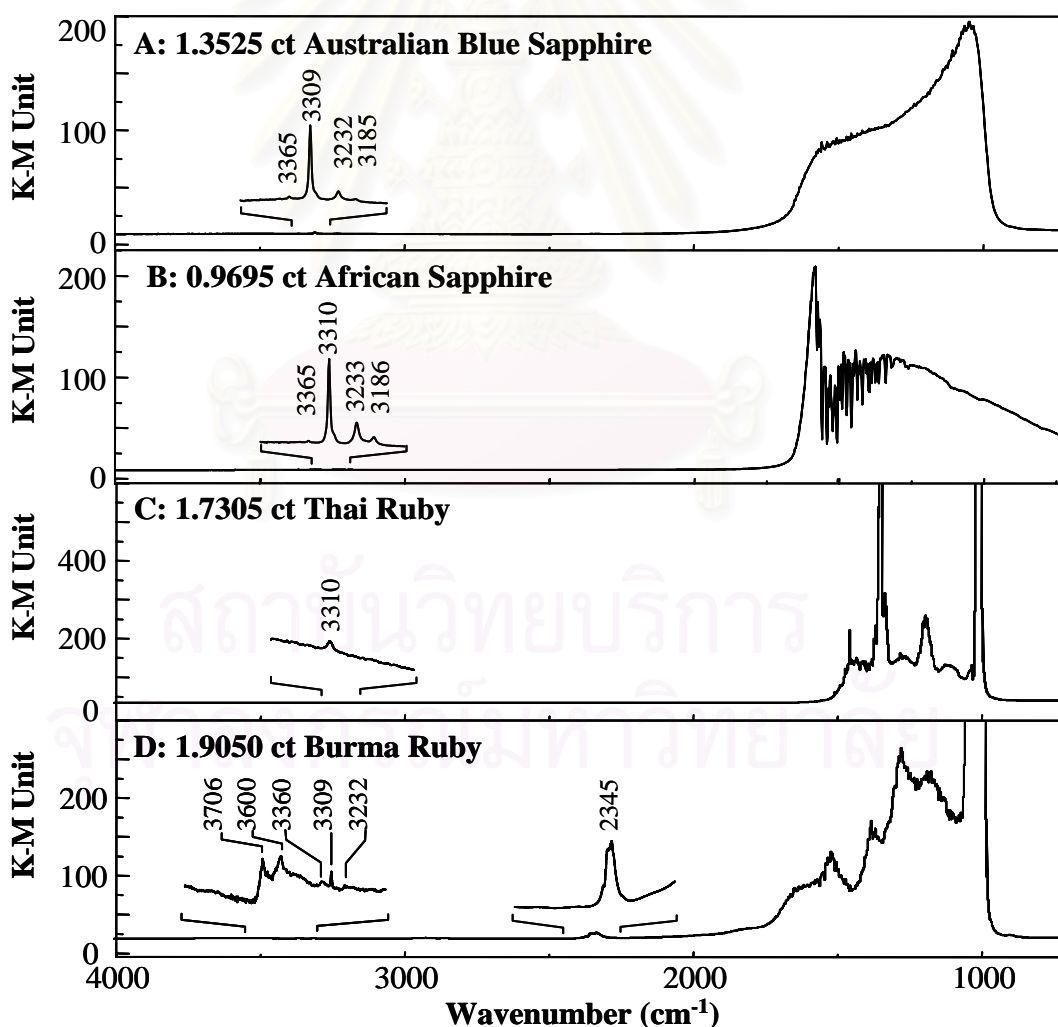


**Figure 4.11** FTIR spectra of rubies and sapphire from different country of origin acquired by diffuse reflectance technique.

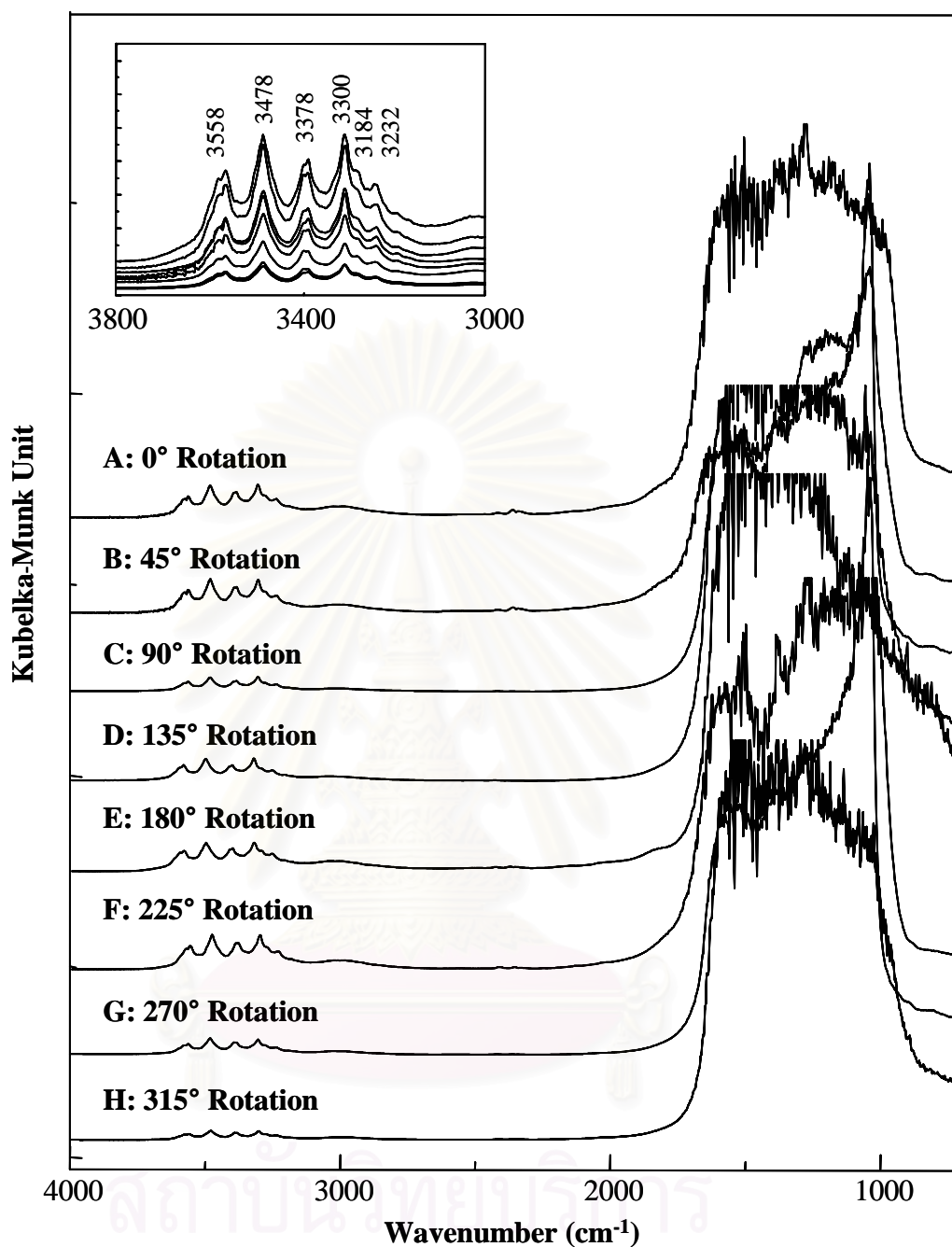


**Figure 4.12** Diffuse reflectance spectra of 1.1510 ct hydrothermal ruby (oval cut) under different arrangement. The ruby was rotated: 0° (A), 45° (B), 90° (C), 135° (D), 180° (E), 225° (F), 270° (G), and 315° (H) with respect to a reference position.

Effect of the sample arrangement was also investigated by a 1.1510 ct faceted hydrothermal ruby. As shown in Figure 4.12, each spectrum represents the diffuse reflectance spectra acquired under different arrangement. The normalized spectra of ruby were not superimposed.

#### 4.2.4 Turquoise Characterization

Turquoise is a hydrous copper aluminum phosphate with the chemical composition  $\text{CuAl}_6(\text{PO}_4)_4(\text{OH})_8 \cdot 5\text{H}_2\text{O}$ . Although the color of turquoise is variable, its main chemical constituents are  $\text{Al}_2\text{O}_3$ ,  $\text{P}_2\text{O}_5$  and  $\text{H}_2\text{O}$  relatively stable [62]. Turquoise is an opaque mineral, with color ranging from blue through shades of green to yellowish gray. Today turquoise remains popular in fine jewelry worldwide.

A number of turquoise imitations are found on the gemstone market. The supply of high quality turquoise is limited. However, most turquoise is adulterated. Turquoise has been subjected to various methods of treatment in order to improve its value as gem material, for example, enhanced color or reduced porosity. The methods include impregnating with plastic, paraffin and oil [63]. Moreover, turquoise is imitated by glass, plastic, enamel and dyed chalcedony. Of these some glass imitation may be difficult to detect. Touching a red-hot needle to the material will aid in detection, either by revealing the oil or paraffin, or by the acrid odor coming from the plastic. This technique is a destructive process which not suitable for high commercial value material. The separation of natural, untreated turquoise from its treated counterpart, and the unequivocal identification of imitation or synthetic turquoise is difficult with the routine gemological technique. Therefore, efficient methods to detect fraudulent loose and mounted gemstone on jewelry are required.

In case of turquoise, traditionally sampling technique is KBr-pellet method [62]. However, it's not suitable for polished gemstone or jewelry analysis because of destructive nature of the sample preparation process. Diffuse reflectance infrared Fourier transform (DRIFT) spectroscopy was shown to be a highly effective approach for the detection and identification of composition in gem materials that are non-destructive process. To investigate the efficiency of the technique, we performed comprehensive testing on a total of 16 samples included cabochon, beads and rough samples. Transmission and diffuse reflectance spectra of a natural turquoise are shown in Figure 4.13. The transmission spectrum in Figure 4.13A clearly reveals the characteristic peak of natural turquoise. The peak assignments are displayed in Table

4.2 [62]. The obtained transmission spectrum shows the strong and broad absorption of OH stretching at 4,000-3,300  $\text{cm}^{-1}$ . However, KBr can also absorb water, which may interfere or overlap with O-H stretching in the crystal structure of turquoise.

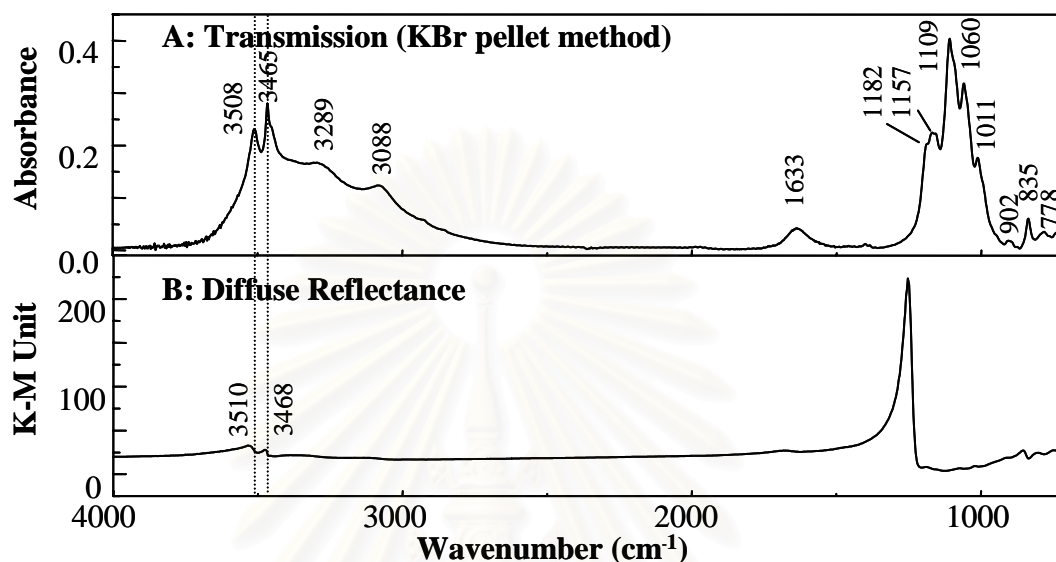


**Figure 4.13** FTIR spectra of natural turquoise acquired by (A) transmission (KBr pellet method) and (B) diffuse reflectance techniques.

**Table 4.2** Infrared absorption spectra of turquoise.

Peak Position ( $\text{cm}^{-1}$ )	Peak Assignment
3508	Stretching Vibration of OH and H <sub>2</sub> O
3465	
3289	
3088	
1633	Curving vibration of H <sub>2</sub> O
1182	Stretching vibration of P-O ( $\nu_3$ )
1157	
1109	
1060	
1011	
902	



As shown in Figure 4.13B, the spectral envelop of the diffuse reflectance spectrum is clearly different from that of the conventional transmission spectrum. The spectral features and the relative band intensities in the diffuse reflectance spectrum are different from those of the corresponding transmission spectrum. At the low wavenumber region, the resultant spectrum shows the fundamental absorption band around  $1,500\text{-}500\text{ cm}^{-1}$  which exhibits derivative band shape. This derivative band shape is known as *reststrahlen* [27-29]. These bands are due to the fact that diffuse reflectance technique based on incident radiation on a sample being scattered in all direction. The drawbacks of the technique arise from the specular reflectance component of the partial smooth surface, which the radiation does not penetrate the sample. This becomes a particular problem in spectral regions where there are functional groups that have high absorption coefficients. These species tend to absorb more radiation than they reflect and usually all the detailed spectral information is either lost or greatly distorted. This is particularly true for turquoise which strongly absorbs infrared radiation from  $1300\text{ to }700\text{ cm}^{-1}$  when studied by diffuse reflectance technique. Another reason is that cutting of most turquoise samples as a bead or cabochon which impossible to produce the suitable energy throughput at the detector. It is difficult to verify certain peak position of chemical composition in turquoise structure. Although the spectral envelop of the diffuse reflectance spectrum suffer with derivative shaped band, some peak positions defined at the center of the derivative peak in higher wavenumber region can be investigated such as OH stretching at  $3510\text{ and }3468\text{ cm}^{-1}$  (see dot line).

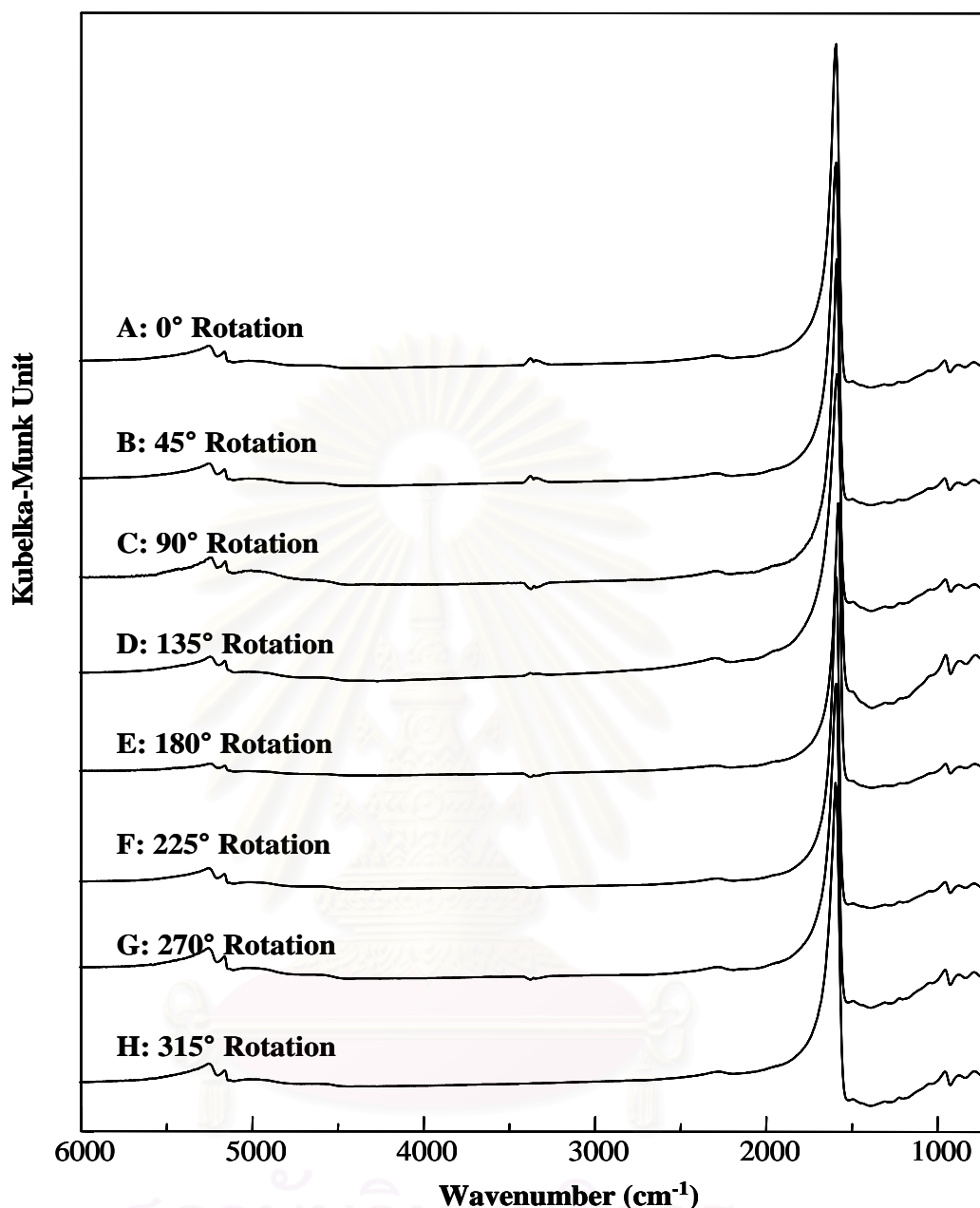


**Figure 4.14** Diffuse reflectance spectra of 6.3805 ct natural turquoise (rough stone) under different arrangement. The turquoise was rotated: 0° (A), 45° (B), 90° (C), 135° (D), 180° (E), 225° (F), 270° (G), and 315° (H) with respect to a reference position.

The above phenomenon indicates that spectral quality of the diffuse reflectance spectrum depends strongly on sample form, surface appearance, refractive index and absorption coefficient of the sample. In order to achieve a good spectral quality, spectrum should be collected several times. The spectrum with the

best signal-to-noise ratio should be selected for further analysis. The effect of sample arrangement was also examined. This operation may lead to additional information about chemical composition of the specimen. As shown in previous section, it is well known that diffuse reflectance spectrum of a faceted gemstone is greatly influenced by sample arrangement on the sample holder. Diffuse reflectance spectra of the turquoise with different arrangements are also not superimpose (see Figure 4.14). Due to the derivative band shape, the obtained spectra cannot be normalized. Although sample arrangements were changed, all diffuse reflectance spectra always show similar differential type peak shape.

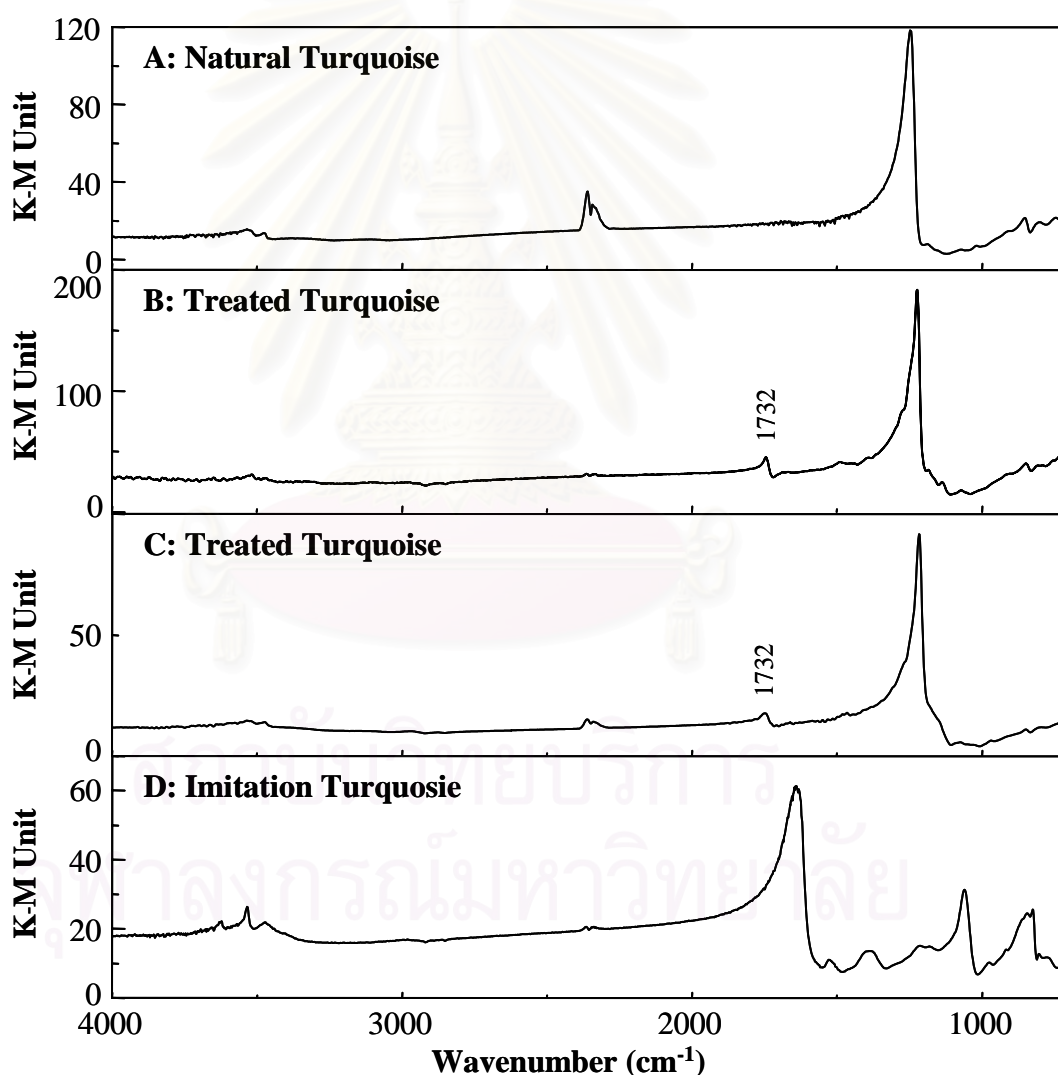


**Figure 4.15** FTIR spectra of natural, impregnated and imitation turquoises acquired by diffuse reflectance technique.

Since natural turquoise is very sensitive to chemical and has been known to suffer damage from simple perspiration, good-quality turquoise is also treated by plastic impregnation in order to improve the durability. At present, plastic impregnation (stabilization) is thought to be the best method for treating turquoise [63-64]. To investigate the efficiency of turquoise characterization, a number of natural and impregnated turquoises were performed via diffuse reflectance technique. Representative infrared spectra of turquoises show in Figure 4.15. Comparison the diffuse reflectance spectra, it should be note that the infrared spectra of natural and treated turquoise are more similar than its imitation. All the turquoise samples analyzed present strong differential type peak shape at the same position. Nevertheless, the spectra of treated turquoises or impregnated turquoises show compositional variations which corresponding to the filler within the specimens. A remarkable difference was small derivative shaped peak at  $1732\text{ cm}^{-1}$  [64]. This absorption band is probably due to a carbonyl species which corresponding to the organic substances filled in the treated turquoise because of their impregnation or treatment process. This absorption band was never observed in the natural turquoise. We do not know the certain compound but we can suggest that treatment substances of turquoise are wax, paraffin oil, polyacrylate resin, or polyester [63-64].

According to Figure 4.15, imitated turquoise can easily be distinguished from their natural counterpart. The most obvious difference is the strong absorption in the  $1600\text{-}900\text{ cm}^{-1}$  region. This strong absorption has been identified as clay-like aluminum hydroxide, which is a pattern produced matched that of gibbsite-imitated turquoise. Due to the difference chemical composition, their spectral features are also very different. Natural turquoise - a phosphate compound,  $\text{CuAl}_6(\text{PO}_4)_4(\text{OH})_8 \cdot 5\text{H}_2\text{O}$  - can be distinguished easily from its common substitutes, gibbsite - a hydroxide compound,  $\text{Al}(\text{OH})_3$  [59,64].

**Summary:**

In summary, the diffuse reflectance technique can be utilized for characterization of gemstones. It is possible to distinguish natural, treated and imitated gemstones. Advantages of the technique include:

- ✓ It is a non-destructive while no sample preparation is necessary. Therefore, it is faster and simpler than the transmission technique.
- ✓ It is applicable for opaque and semitransparent gemstones.
- ✓ Absorption bands unique to impurities, defects in the crystal structures, and treatment processes can be clearly identified. The measured spectrum can be exploited for classification and/or determination of the natural, treated gemstone and simulants.

However, the technique encounter some limitations associated with the physical and optical properties of the samples such as refractive index, homogeneity, cutting, and sample size. Disadvantages of the technique include:

- ✗ The accessory and its sample holder have small working area which restricts its application on large size gemstone or jewelry. If the physical dimension of the gemstone (*i.e.* cutting, sample size, surface appearance) are not suitable, the valuable diffuse-reflected light was throw away because the infrared beam cannot be properly coupled onto the sample.
- ✗ The measurements of faceted gemstone tend to be non-reproducible since the spectral intensity depends strongly on the gems orientation within the sample holder. It is important that result spectrum be obtained at two or three different orientation before any conclusion is drawn.
- ✗ In case of cabochon cutting, specularly reflected radiation from the surface of the gemstone is responsible for differential type peak shape.

### 4.3 Specular Reflection Technique for Gem Characterization

Another well-accepted sampling technique has been used for gems analysis is specular reflectance technique. The measurement for specular reflectance is much simpler than other techniques. It is a non-destructive and requires no sample preparation. As described before, it is particularly useful with polished gems. In order to analyze both loosed and mounted gemstone on jewelry, the reflectance spectra were recorded by the infrared microscope using the novel accessory.

#### 4.3.1 Diamond Characterization

Specular reflectance spectra of round brilliant cut natural and treated diamonds are shown in Figure 4.16. Comparing to the corresponding diffuse reflectance spectra, the specular reflection spectra, on the other hand, do not show any prominent absorption feature. This is because diamond has high refractive index with low absorption coefficient in the mid-infrared region. Therefore, specular reflection technique is not suitable for diamond characterization. It should be noted that the absorptions of water vapor ( $3900 - 3500$  and  $1800 - 1400 \text{ cm}^{-1}$ ) and carbon dioxide gas ( $2400 - 2300 \text{ cm}^{-1}$ ) can be noticed in all measured spectra. The variations of the absorption magnitudes are due to the fluctuation of the ambient air during the spectral acquisition.

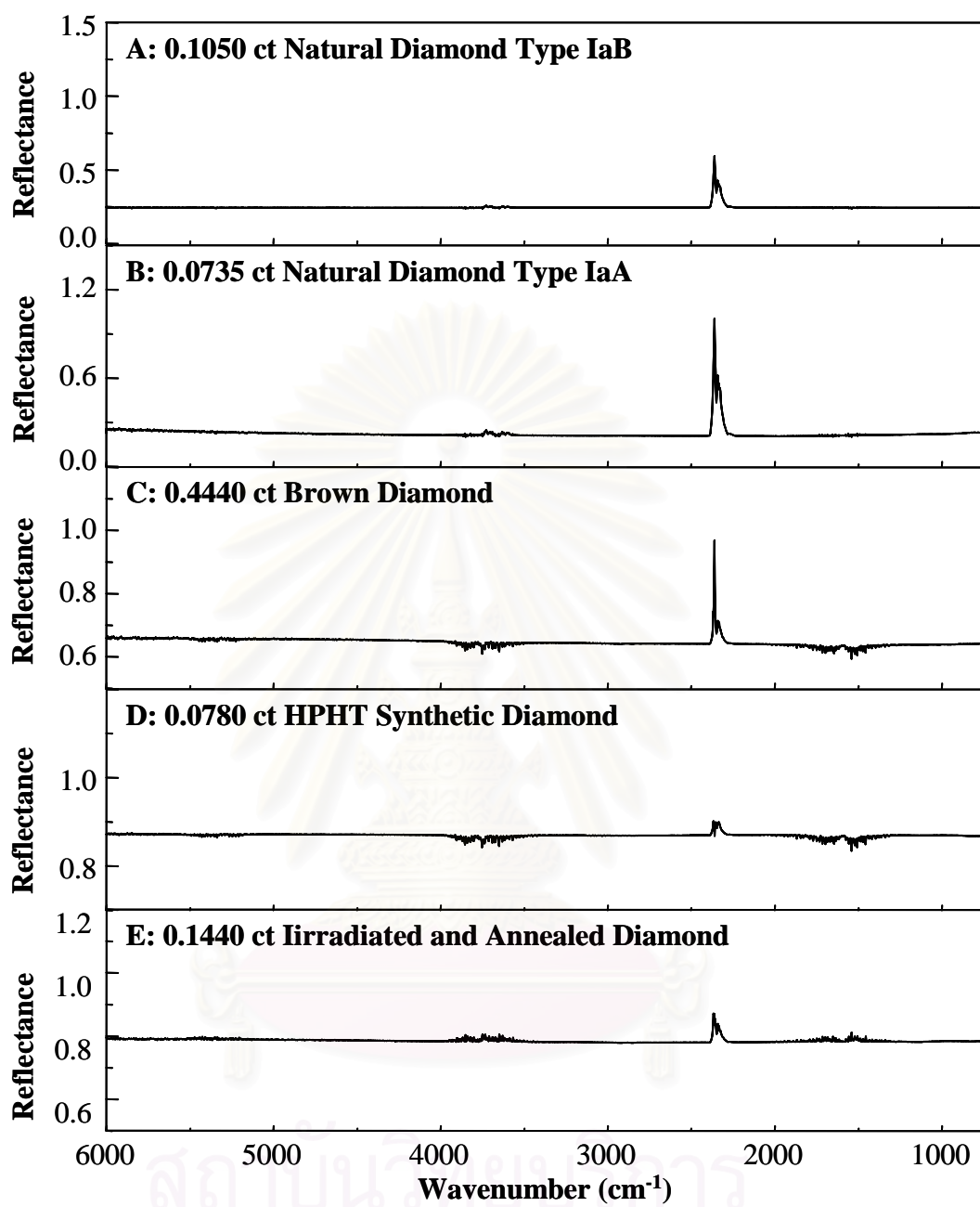


**Figure 4.16** FTIR spectra of round brilliant cut diamonds acquired by specular reflectance technique.

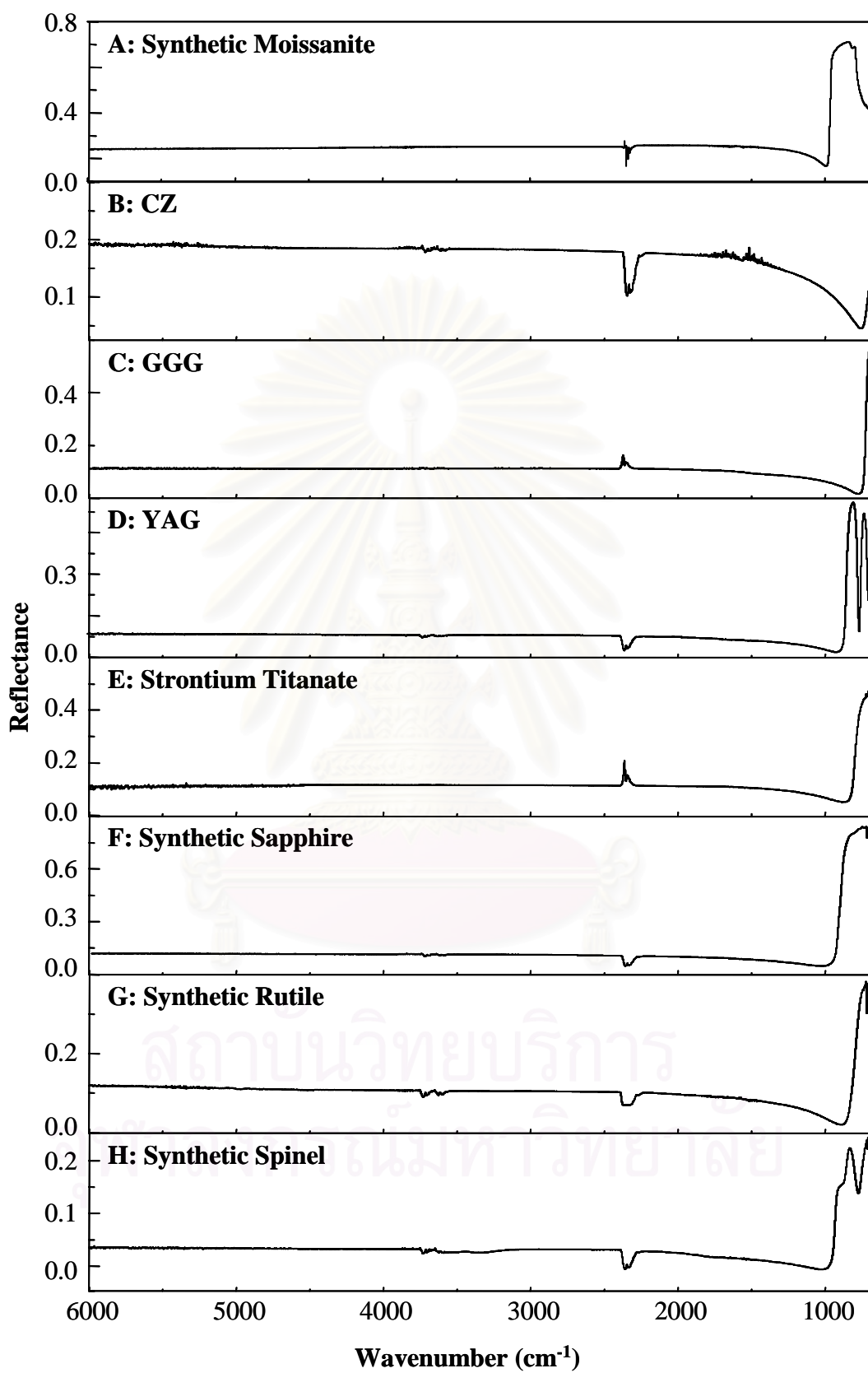


**Figure 4.17** FTIR spectra of round brilliant cut diamond simulants acquired specular reflection technique.



Spectra of faceted diamond simulants acquired by specular reflection technique are shown in Figure 4.17. The spectral envelopes of the specular reflectance spectra are different from those of the diffuse reflectance spectra. Due to the high absorption coefficient of the gemstones in the low wavenumber region, specular reflectance spectra show refractive-index type spectral features [25]. Although the exact positions of the absorption maxima in that region cannot be identified, they can be noticed from the specular reflectance spectra. It should be noted that Kramers-Kronig transformations of the specular reflection spectra cannot be performed since the absorption maxima are too close to the low wavenumber end of the observed spectra. Unlike the diffuse reflectance spectra, the weak absorption bands in the high wavenumber region cannot be observed in specular reflectance spectra. Although the peak positions of the absorption bands of diamonds simulants correspond to their chemical composition cannot be noticed in specular reflectance spectra, their spectral feature can be utilized for identification purpose based on their types from their onset around  $1000\text{ cm}^{-1}$ .

#### 4.3.2 Emerald Characterization

The emerald specimens were also investigated via specular reflection technique. We subsequently analyzed the effect of sample arrangement. Figure 4.18 displays emerald spectra acquired from specular reflectance technique with different sample orientation. According to the observed spectra, refractive index type spectral features appear at low wavenumber region. This is due to the high absorption coefficient of the gemstones. Although the exact positions of the absorption maxima in that region cannot be identified from the diffuse reflectance spectrum, they can be noticed from the specular reflectance spectra. It should be noted that absorption bands at higher wavenumber region ( $3800\text{-}3200\text{ cm}^{-1}$ ) which correspond to water molecule in the crystal lattice cannot be noticed.

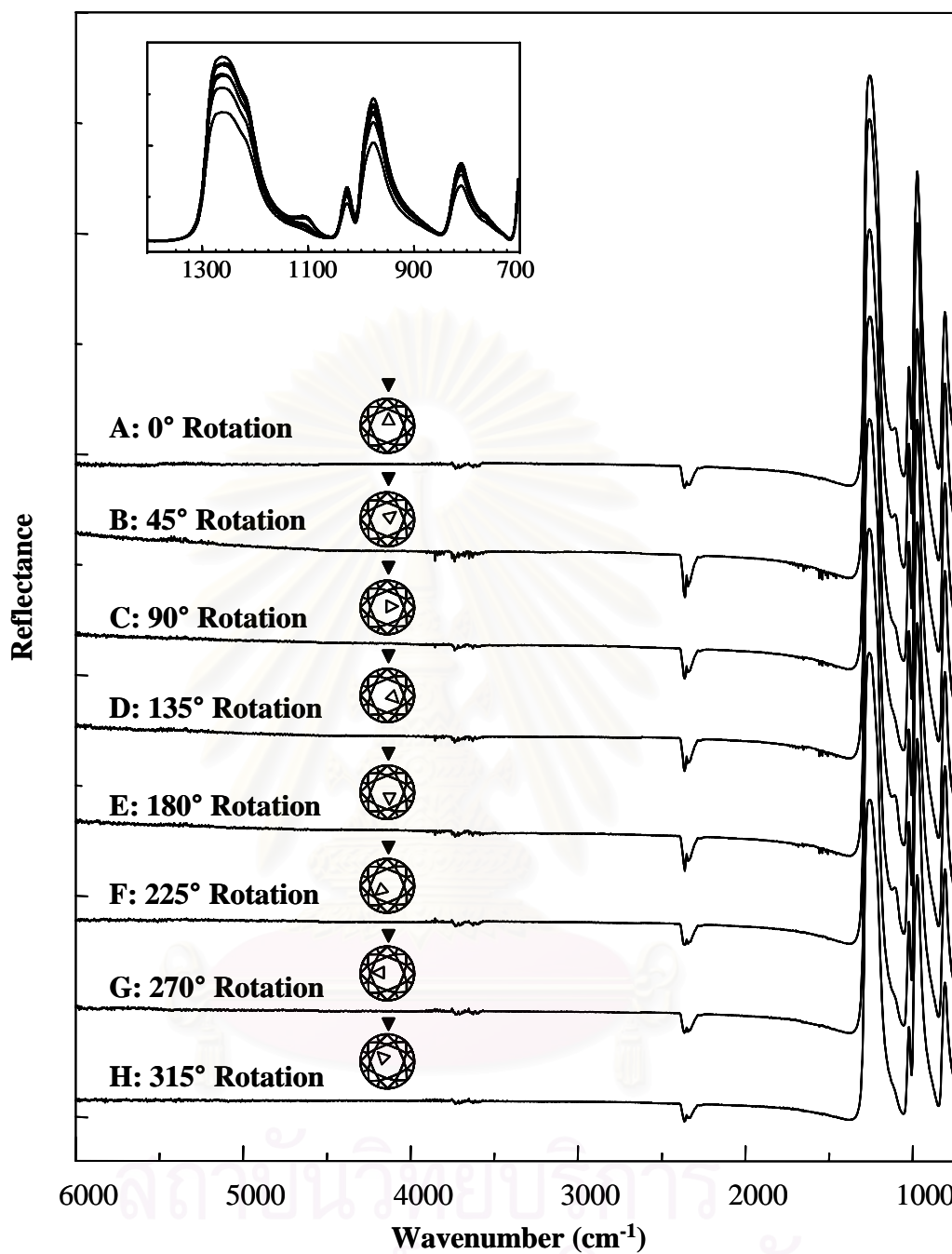


**Figure 4.18** Specular reflection spectra of the 0.7520 ct hydrothermal emerald under different arrangements. The emerald was rotated: 0° (A), 45° (B), 90° (C), 135° (D), 180° (E), 225° (F), 270° (G), and 315° (H) with respect to a reference position. The inset was added for clarity.

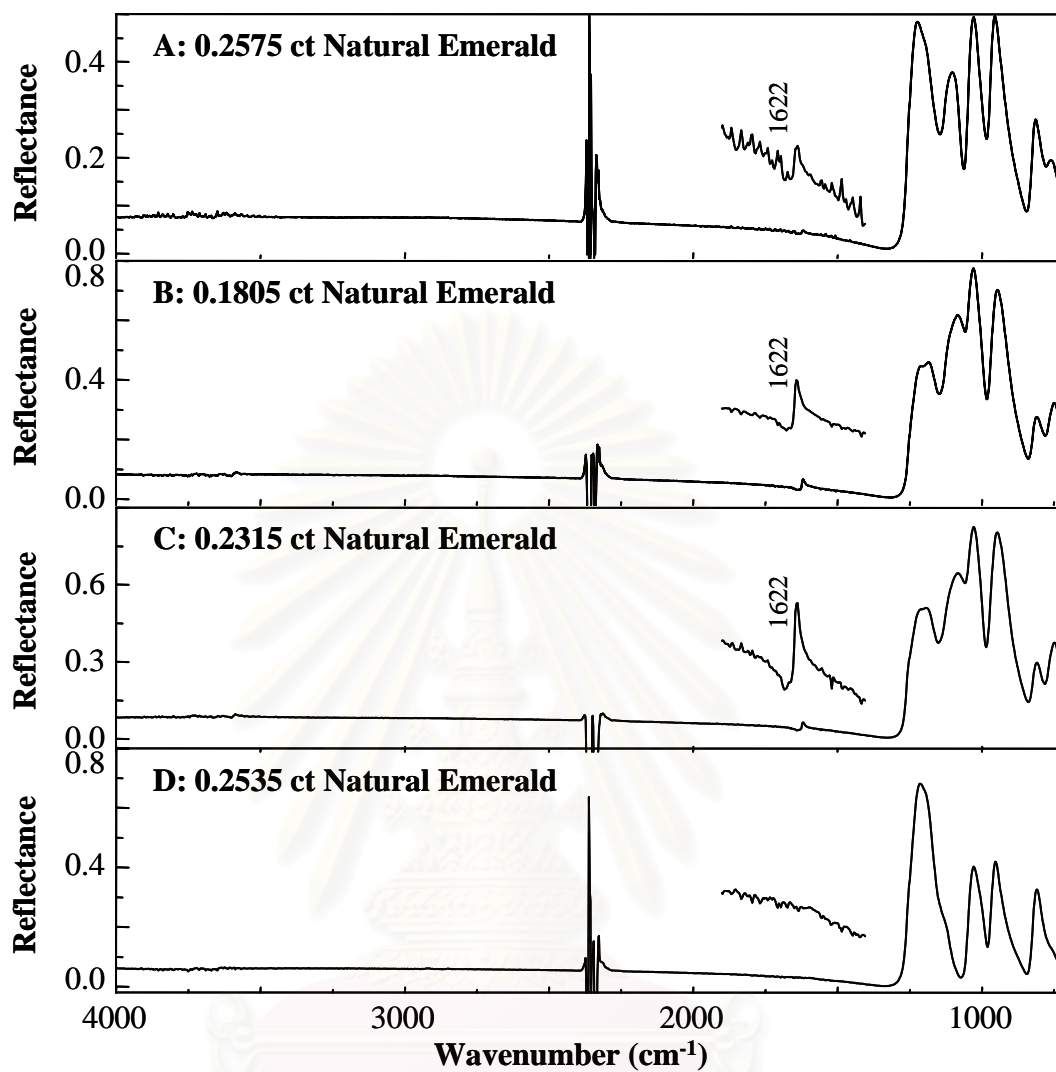


**Figure 4.19** FTIR spectra of natural emeralds acquired by specular reflection technique.

สถาบันวิทยบริการ  
จุฬาลงกรณ์มหาวิทยาลัย

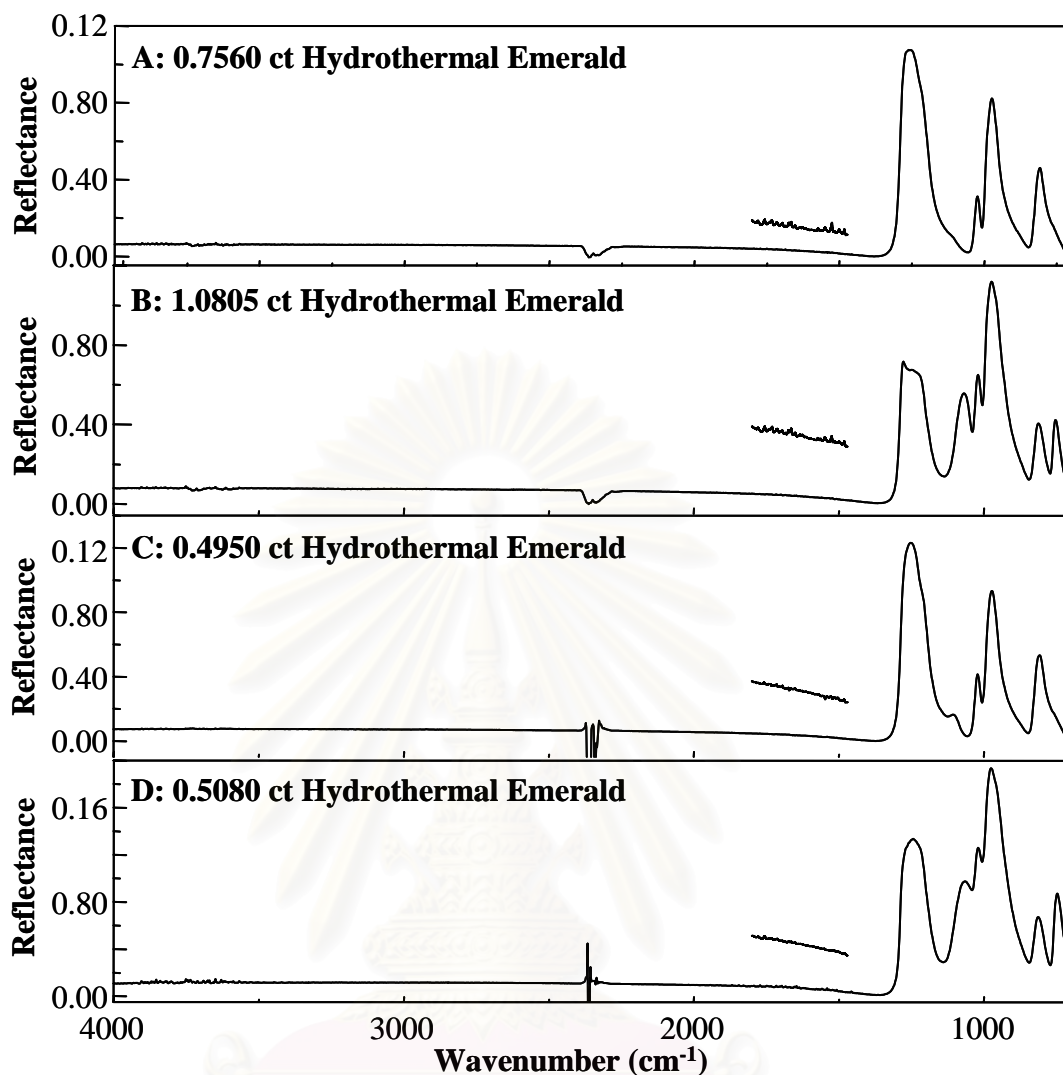


**Figure 4.20** Specular reflectance spectra of hydrothermal emeralds acquired by specular reflection technique.

As mention previously, it is well known that diffuse reflectance spectrum of a faceted emerald is greatly influenced by emerald arrangement on the sample holder. Similar to the diffuse reflectance spectrum, the specular reflectance spectrum was slightly affected by the emerald arrangements (as shown in Figure 4.18). Although the observed specular reflectance clearly revealed the absorption bands at low wavenumber, their spectra were not superimposed. Due to minor variations of the alignment with respect to the incident radiation, discrepancies among specular reflectance spectra can be noticed. This is because emerald is anisotropic material which its crystals have two refractive indices, the incident beam is partially polarized thus the observed reflectance spectrum depends strongly on crystal orientation [8].

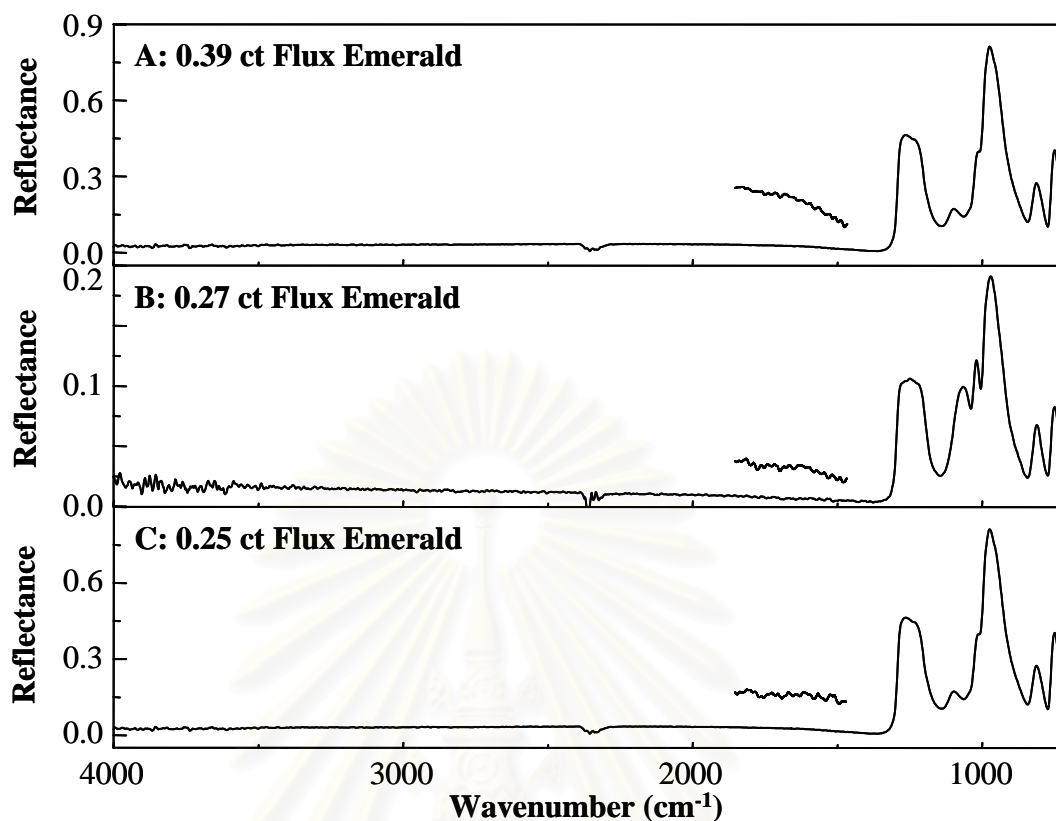


**Figure 4.21** FTIR spectra of flux emeralds acquired by specular reflection technique.

For identification purpose, the applicability of specular reflectance has been demonstrated. Experiment observed reflectance spectra of natural, hydrothermal and flux emeralds acquired via specular reflection technique were shown in Figures 4.19-4.21, respectively. Unlike the diffuse reflectance spectra, the weak absorption bands in the high wavenumber region cannot be observed in the specular reflectance spectra because of their low absorption coefficient. However, the exact positions of the absorption maxima in the low wavenumber region, which cannot be identified from the diffuse reflectance, can be noticed from the specular reflectance spectra. All specular reflection spectra show refractive-index type spectral features. Moreover, each spectrum that acquired from individual specimen present different spectral feature in this region. This may be because that emerald is an anisotropic gem material which has doubly refractive property. Their infrared spectra are affected by the orientation of the sample to the incident radiation.

In case of natural emerald, most of the spectra show derivative-type peak shapes at  $1622\text{ cm}^{-1}$ . This absorption band was never observed in the specular reflectance spectra of synthetic emerald (see Figures 4.20 and 4.21). These became clearer in the absorption index spectra when each obtained spectrum was converted to absorbance by KK transformation as shown in Figure 4.22. It clearly seen that natural emerald reveals a small absorption band at  $1622\text{ cm}^{-1}$  which assigned as OH bending of water molecular in its crystal lattice. The absorption band cannot be noticed in synthetic emeralds. Thus, it is possible to differentiate natural emerald from its synthetic counterparts by using specular reflectance technique. Unfortunately, we cannot differentiate between flux and hydrothermal emeralds by using specular reflection technique because the spectral feature is similar.

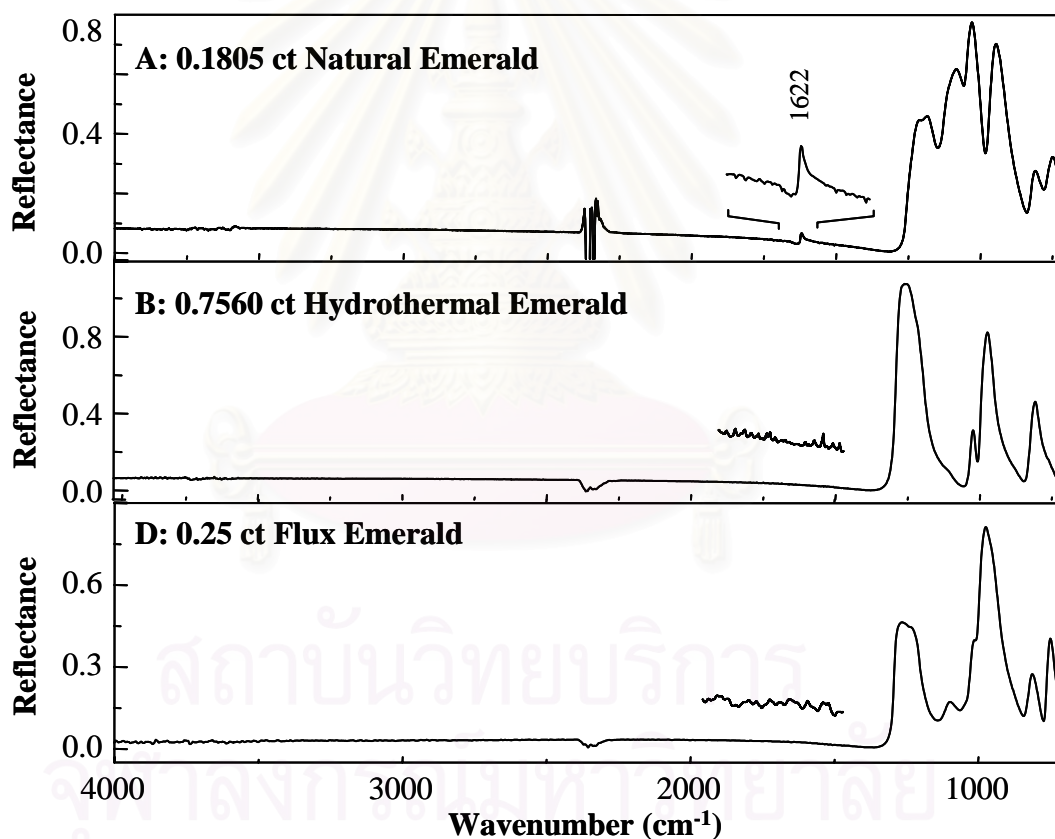


**Figure 4.22** FTIR spectra of the same specimens in Figure 4.19-4.21. The spectra are Kramer-Kronig transformations.

### 4.3.3 Ruby and Sapphire Characterization

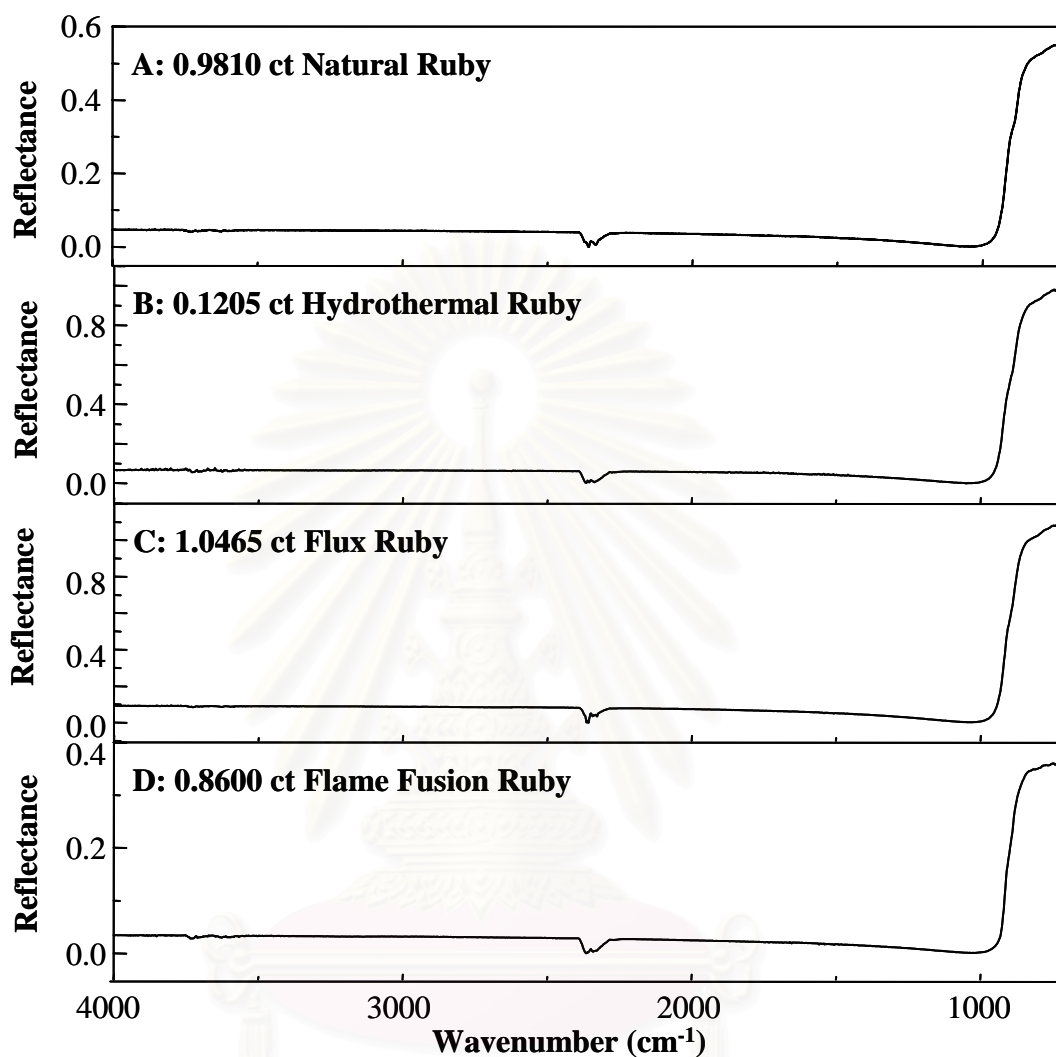


**Figure 4.23** FTIR spectra of natural and synthetic ruby acquired by specular reflection technique.

Specular reflectance spectra of faceted natural and synthetic rubies are shown in Figure 4.23 while those of sapphire from different country display in Figure 4.24. By comparison, all specular reflectance spectra in both Figures are similar. The specular reflection spectra do not show any prominent absorption feature in that region. Unlike the diffuse reflectance spectra (see Section 4.2.3), the weak absorption bands in the high wavenumber region which refer to the vibrational absorption of OH stretching cannot be observed in specular reflectance spectra. Since the high absorption coefficient of the gemstones in the low wavenumber region, the specular

reflection spectra show refractive-index type spectral features. This band is assigned as Al-O vibraional band of corundum lattice. It should be noted that Kramers-Kronig transformations of the specular reflection spectra cannot be performed since the absorption maxima are too close to the low wavenumber end of the observed spectra. Regarding the spectra reported in this section, we cannot differentiate between natural and synthetic ruby, and the sapphire from different country of origin.

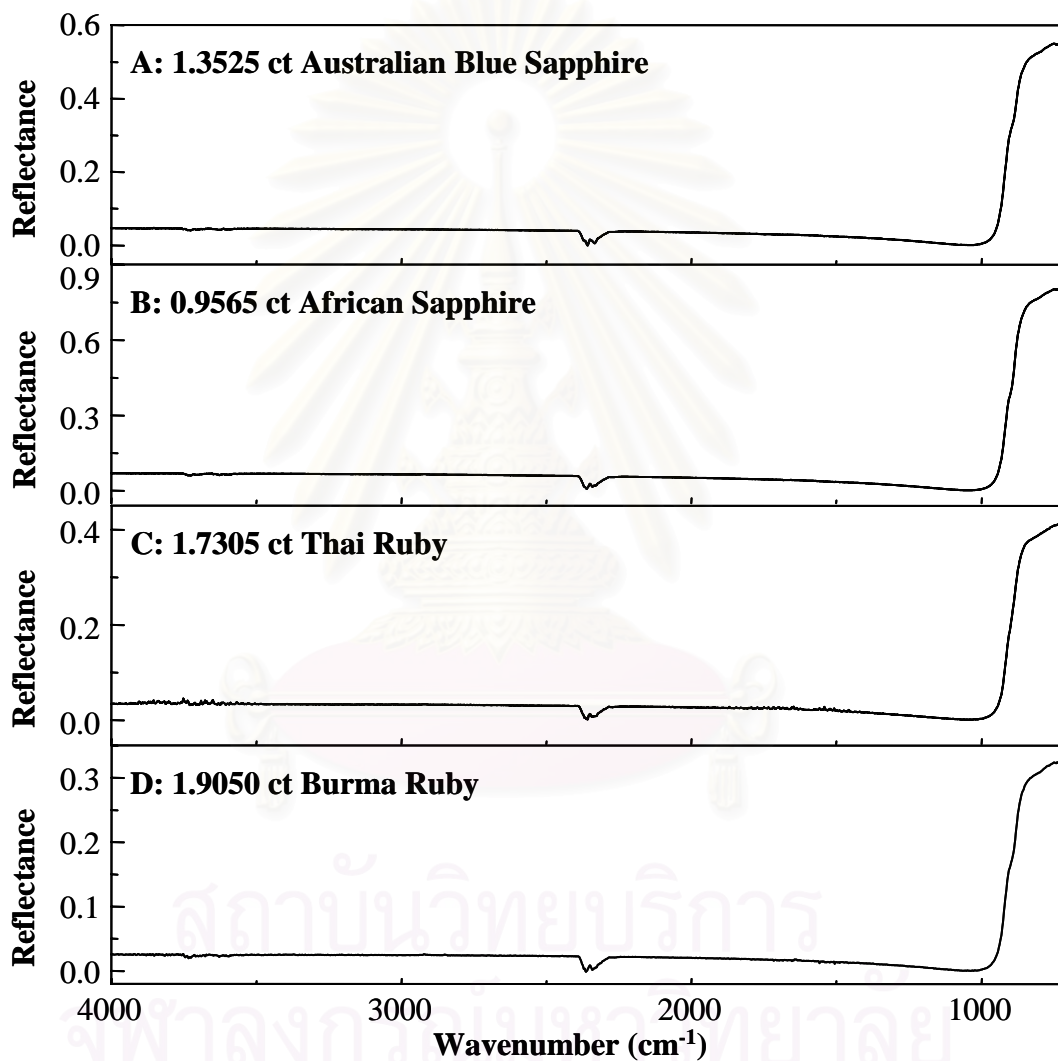


**Figure 4.24** FTIR spectra of ruby and sapphires from different mine acquired by specular reflectance technique.



#### 4.3.4 Turquoise Characterization

Since turquoise is an opaque gemstone, it represents a challenge for infrared sampling technique when non-destructive sampling process is required. In general, it has been investigated mainly by transmission technique [62]. As mentioned in Section 4.2.4, characterization of turquoise acquired by diffuse reflectance technique is limited by its physical properties that make their spectra suffered from the derivative-type peak shape. As a result, it turns to be of interest to determine via specular reflection technique. We performed the polished turquoise analysis simply by FT-IR microscopy specular reflectance method without additional sample preparation. To evaluate the efficiency of the technique, natural, treated and imitated turquoise was employed for comparison purpose.

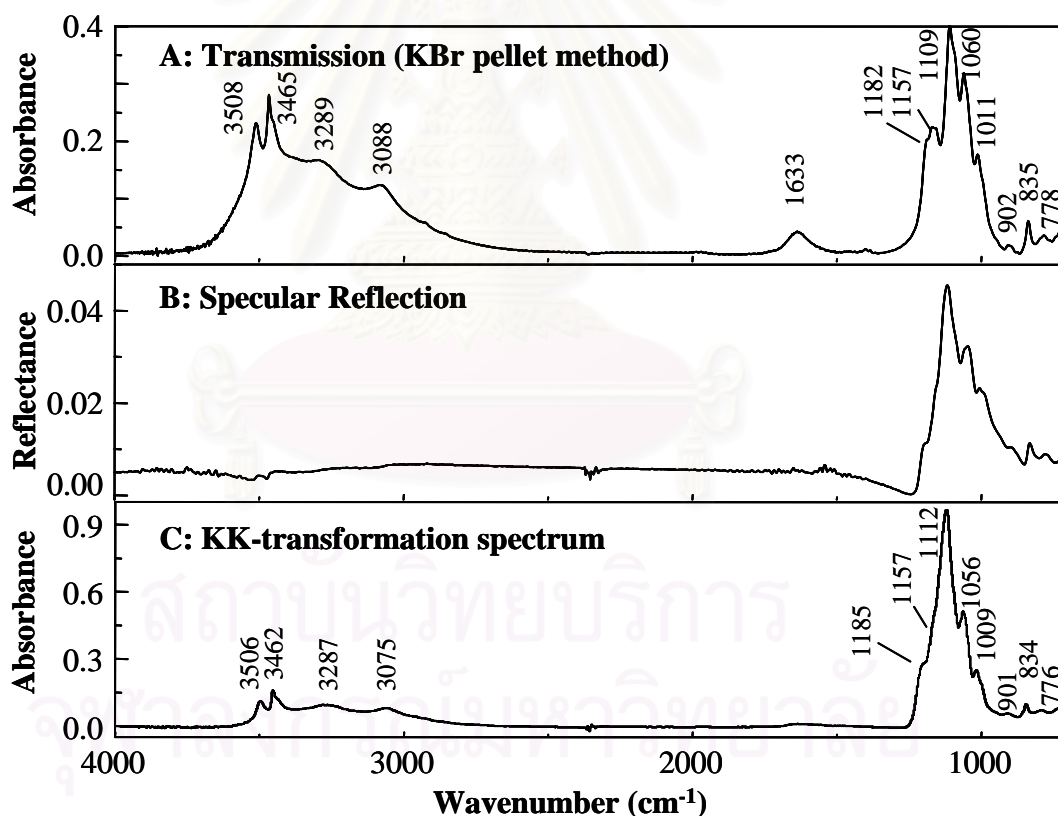


**Figure 4.25** FTIR spectra of natural turquoise (cabochon) acquired by (A) transmission (KBr pellet method), (B) specular reflection, and (C) KK transformation of spectrum (B).

Figure 4.25 shows infrared spectra of a natural turquoise (cabochon) acquired via transmission and specular reflection technique. In case of specular reflectance, the observed spectrum typically shows derivative-type peak shape in the low wavenumber region attributable to characteristic absorption of turquoise and small absorption bands at higher wavenumber attributed to OH stretching absorption. Figure 4.25C shows the KK-derived spectrum of the specimen. The quality of KK-transformed spectrum (see Figure 4.25C) is comparable to or better than that of the well-accepted diffuse reflectance spectrum (see Figure 4.13). Clearly, the agreement between infrared spectra of turquoise obtained by transmission and KK-transformed spectrum is very good and certainly very satisfactory. As pointed out in the Theory Section, the total amount of incident energy is the sum of reflected, scattered, transmitted, and absorbed light. The intensity of each beam depends on the intensity and wavelength of the incident radiation, the optical properties of the specimen, and the geometry of the experimental setup. Since turquoise is an opaque material, the incident beams cannot be transmitted, most of the coupled radiations were absorbed by the matter and the remaining component will be reflected or scattered [27-29]. In this experiment, infrared microscope was set in reflection mode. Thus, only pure reflected beam can be observed. In principle, if the recorded spectra are pure specular reflectance and free from artifacts, the KK-transform will work ideally, then the measured absorption bands and peak positions should correlate directly correlated with chemical composition of material [28-30].

By comparing the transmission and KK-transformed spectra of turquoise, it is clearly seen that remarkable difference is their relative intensity. In each spectrum, there are several peaks in OH stretching region ( $3600\text{-}3000\text{ cm}^{-1}$ ) corresponding to absorption of water molecule in the sample [62]. However, it should be noted that transmission spectrum is also present a predominant absorption band at  $1633\text{ cm}^{-1}$  attributable to OH bending absorption of water molecule, while it cannot be observed in KK-transformed spectrum. This indicates that OH bending band in transmission spectrum arise from water molecule which absorbed in KBr powder. As a result, another advantage of specular reflection technique is that the method is free from interfering bands from water molecules.

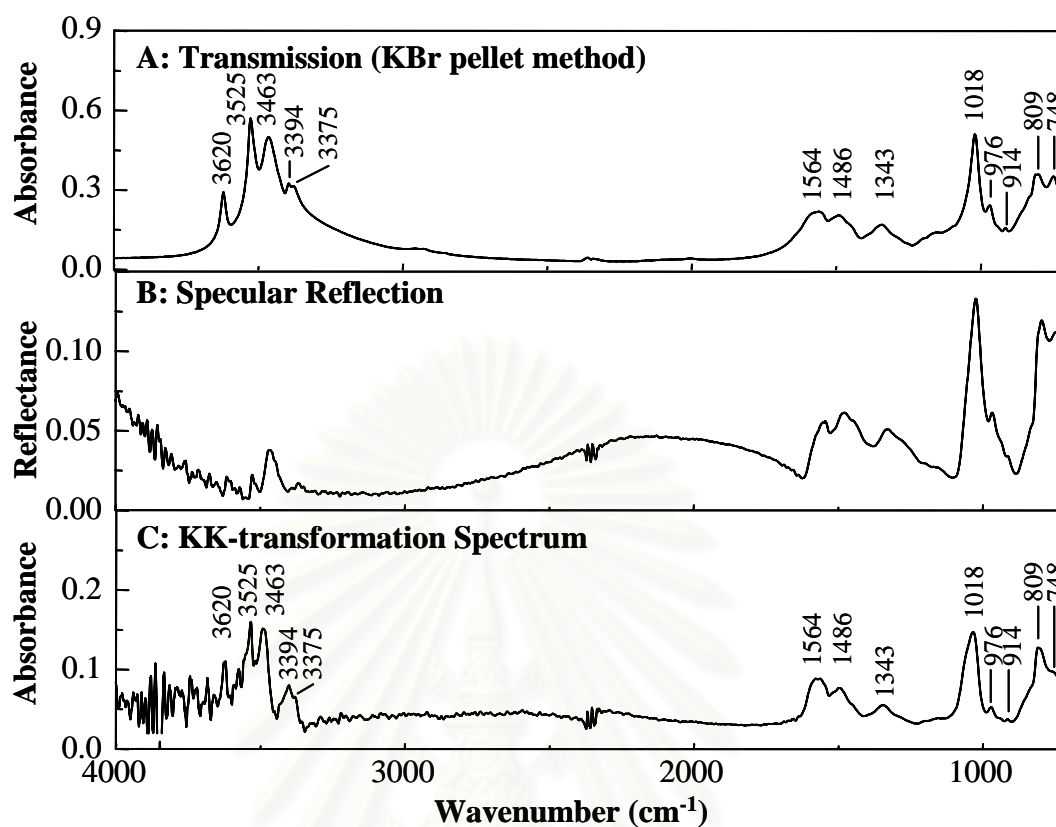


**Figure 4.26** FTIR spectra of imitation turquoise (Gibbsite) acquired by (A) transmission (KBr pellet method), (B) specular reflection, and (C) KK transformation of spectrum (B).

Figure 4.26A and B show infrared spectra of imitation turquoise acquired via transmission and specular reflection techniques, respectively. The result of KK transformation on the spectrum in Figure 4.26B is shown in Figure 4.26C. Its spectral feature is similar to those of transmission spectrum. Regarding the obtained spectrum reported above, the sample was assigned as gibbsite [64]. The specular reflectance spectrum possessed the lower S/N ratio than that of the transmission spectrum. In case of KK-transformed spectrum, very high noise level clearly reveals especially in high wavenumber region. This is because specular reflectance technique is a surface characterization which the infrared beam is bounced off the sample instead of passing through the sample. Since, it is difficult to capture all the light reflected off of a sample's surface, reflection spectra may be noisier than transmission spectra for a given number of scans and resolution. As a result, it is necessary to use more scans with reflectance sample to get the S/N ratio of an

appropriate level or by increasing an aperture size of infrared microscope. Although the specular reflection method using infrared microscope is simple, adjusting the optics in practice is very delicate. Because of the curved surface of cabochon, a small shift in focus of turquoise surface may give rise to a drastic change in energy throughput.

Regarding the overall observations reported above, it indicates that FT-IR microscopy specular reflectance measurements can provide a very convenient means of determining turquoise as far as monitoring opaque gemstone with non-destructive process is concerned.

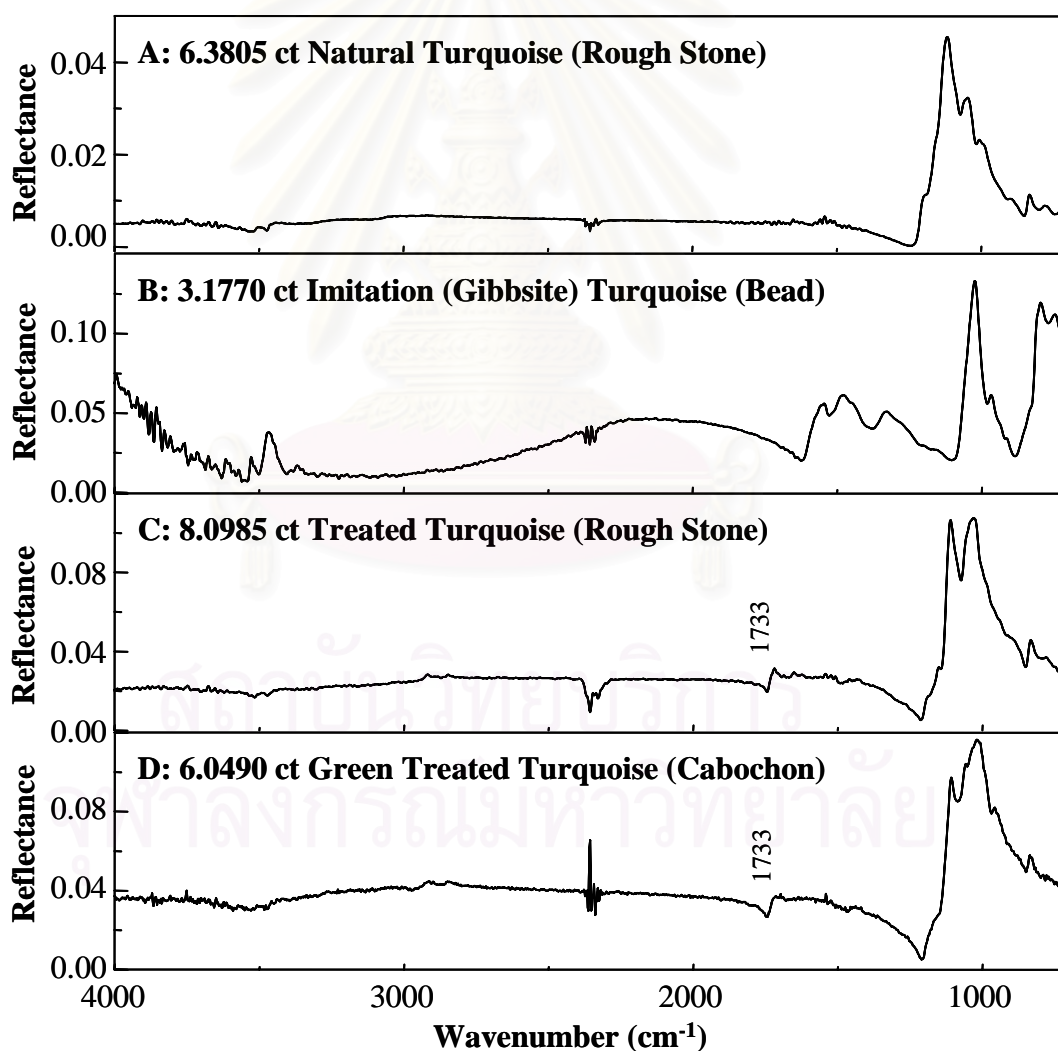


**Figure 4.27** FTIR spectra of natural, impregnated and imitation turquoises acquired by specular reflection technique.

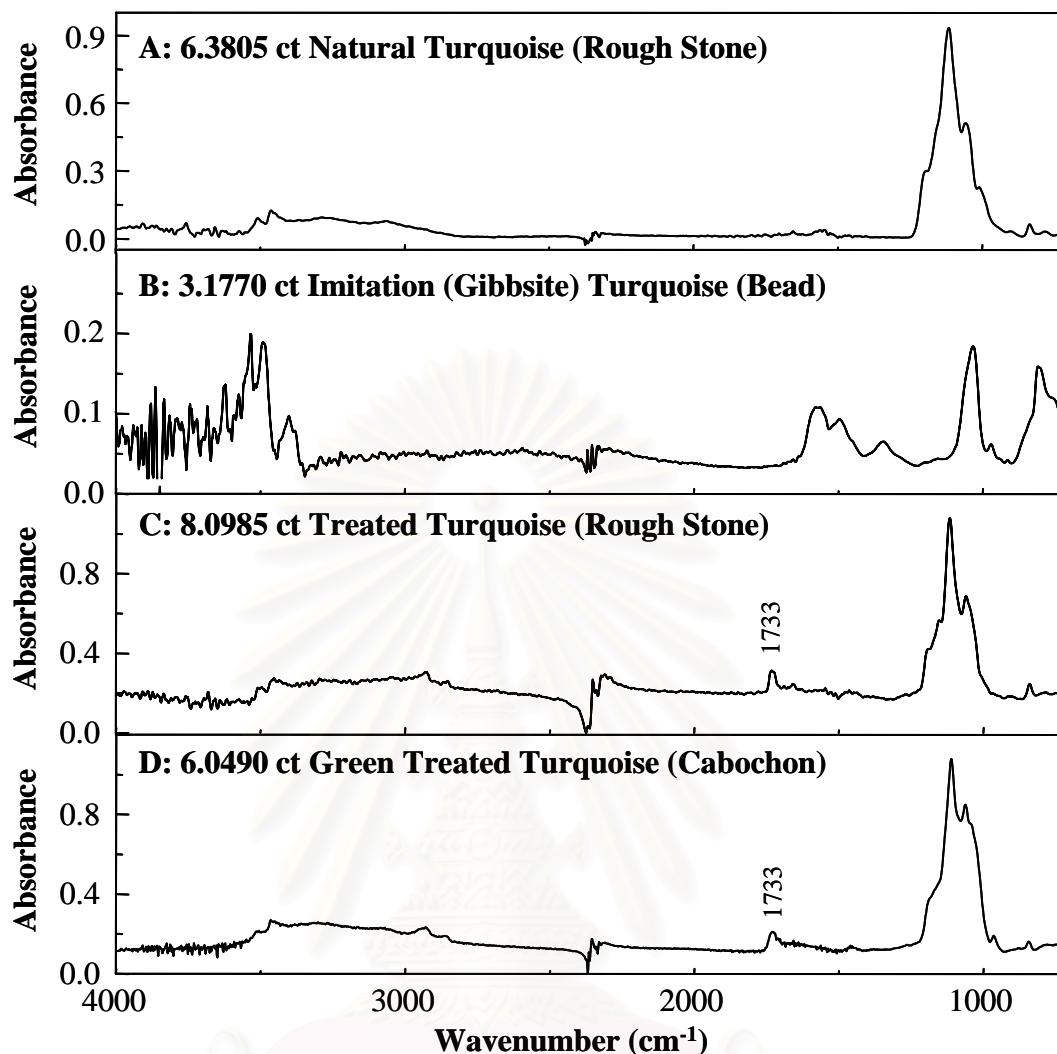


**Figure 4.28** FTIR spectra of the same natural, impregnated and imitation turquoises shown in Figure 4.27 acquired by specular reflection technique and then corrected by KK transformation.

Figure 4.27 shows reflectance spectra of turquoises that acquired via specular reflection technique. Once again, the reflectance spectra in Figure 4.27 were KK-transformation. Typical results are shown in Figure 4.28. As clearly seen in Figure 4.27, imitated turquoise (Gibbsite) spectrum is distinctly different from others while the reflectance spectra of natural and treated turquoises are similar. Thus, it can be easily differentiated initiation from natural counterpart by using specular reflectance technique. By comparing untreated-natural with treated-natural turquoise spectra, the most obvious different in the treated turquoise spectrum is the presence of small derivative shaped peak and at  $1733\text{ cm}^{-1}$  (see Figure 4.27). The KK-transformed

spectra of treated turquoise are also show this prominent peak at the same position (see Figure 4.28). As mentioned before, this absorption band has been identified as C=O vibration of organic substances such as wax, paraffin oil, polyacrylate resin, or polyester which is present in treated turquoise because of their impregnation or treatment process [64]. This absorption band was never observed in the untreated-natural turquoise. It should be noted that absorption of carbon dioxide gas ( $2400 - 2300 \text{ cm}^{-1}$ ) can be noticed in all measured spectra. The variations of the absorption magnitudes are due to the fluctuation of the ambient air during the spectral acquisition.

In order to show additional advantage of the technique, different sampling areas of each specimen were carefully sampled while obtained spectra were converted by KK transformation. Figures 4.29 and 4.30 show KK transformed spectra of an untreated natural and a treated natural turquoise, respectively. Regarding infrared spectra of untreated natural turquoise in Figure 4.29, the observation shows the same spectral feature. Because of the homogeneity, all obtained spectra that acquired with different sampling area do not present any characteristic absorption bands of filler or treated substance. Spectra of treated turquoise shown in Figure 4.30, on the other hand, show different spectral feature depends on the selected sampling area. The prominent peak at  $1735 \text{ cm}^{-1}$  was observed in all spectra. Moreover, the relative intensities of this band acquired from different sampling area is different, which indicates that treated turquoise is not homogenous.

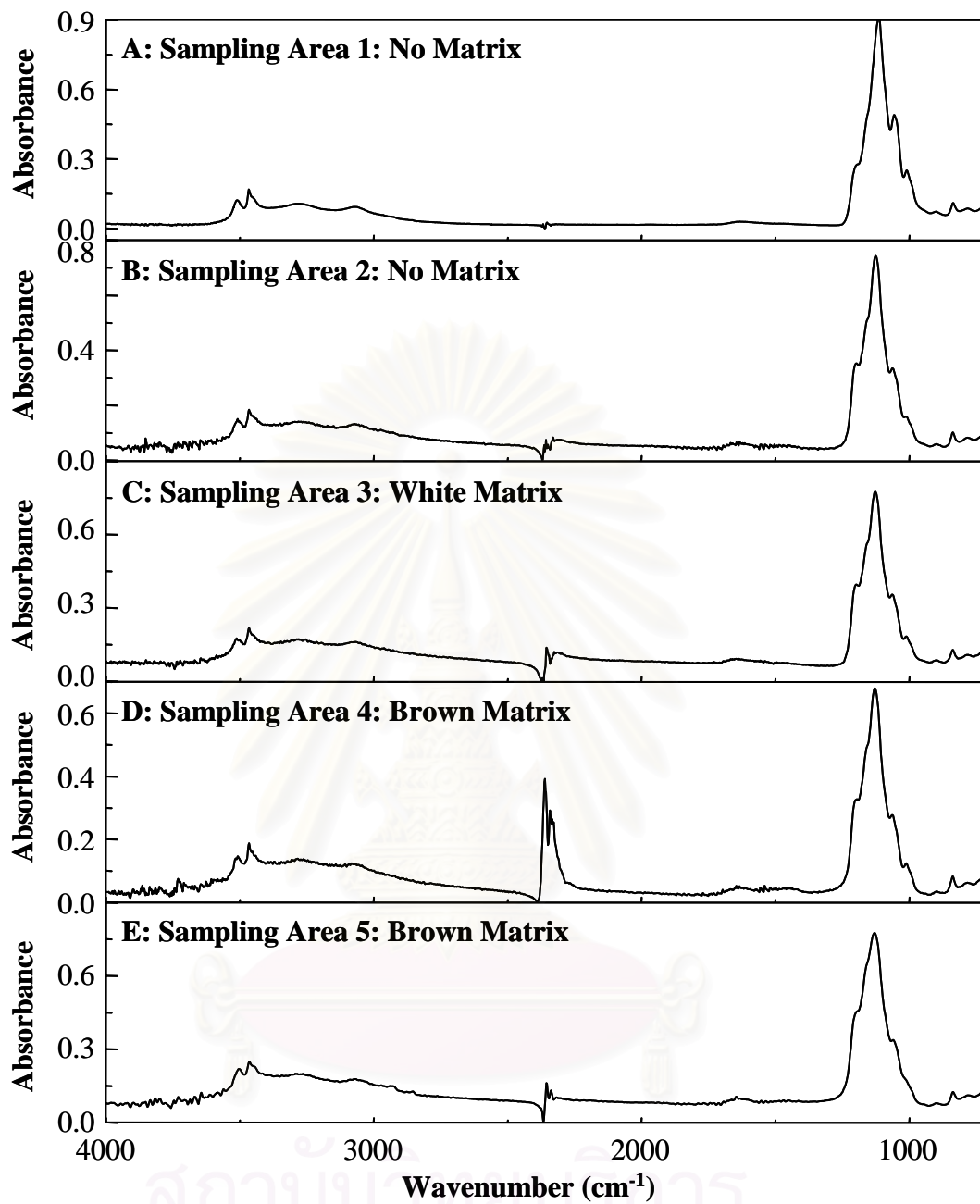


**Figure 4.29** FTIR spectra of 6.3805 ct natural turquoise at different sampling areas acquired by specular reflection technique. The observed spectra are KK-transformed.

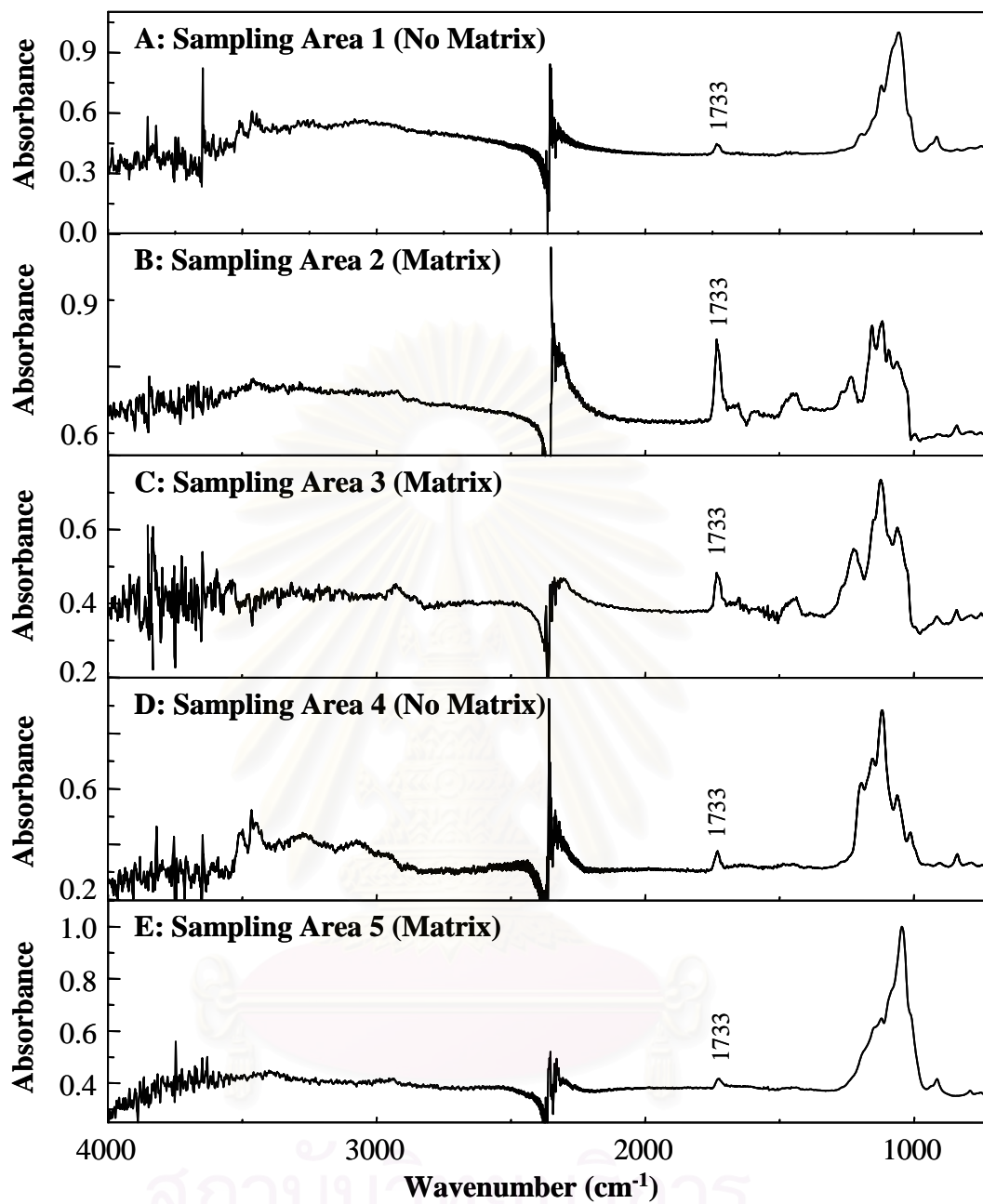


**Figure 4.30** FTIR spectra of a treated turquoise at different sampling areas acquired by specular reflection technique. The shown spectra are KK-transformed.



**Summary:**

The specular reflectance is an available FTIR sampling technique for characterization of opaque gemstone because it is a non-destructive technique and requires no sample preparation. The method does not have the problem of thickness of sample. As shown in this section, the technique can be employed for characterization of opaque gemstone such as turquoise. However, the technique is not suitable for some gemstones (*i.e.*, diamond, ruby, and emerald). This is because turquoise is an opaque gemstone, when incident radiation impinges on turquoise's surface, the reflected radiation presents pure specular reflection, thus the KK transformation works ideally. The KK-transformed spectrum agrees very well with transmission spectrum.

Since diamond is a high refractive index material and have low absorption coefficient in mid-IR region, its specular reflectance spectrum does not show any prominent absorption feature. As a result, specular reflection technique cannot be employed for diamond analysis. The obtained spectrum of emerald can be easily differentiated natural from synthetic counterpart but it cannot be employed for identifying its synthetic process. In case of ruby, specular reflection technique is not suitable for characterization of ruby and synthetic ruby because all observed spectra show the same spectral feature.

#### **4.4 Transflectance Technique for Gem Characterization**

As clearly seen in previous sections, infrared spectra of faceted gemstones can be nondestructively acquired by diffuse reflectance or specular reflection technique. However, the techniques suffer from the difficulties associated with the measurement processes. The observed spectra are greatly influenced by gemstone arrangements. Moreover, the techniques are not normally applicable to mounted gemstones. As a result, the novel transflectance technique using an infrared microscope to acquire an infrared spectrum by collecting the transflected radiation from the pavilion facets of cut gemstone was exploited [23-25].

##### **4.4.1 Parameter Affecting Transflectance Spectrum**

Prior to the characterization of faceted gemstones, it is desirable to verify several parameters affecting transflectance spectrum in order to evaluate the sensitivity and reproducibility of the novel technique. In addition to introduction of a novel technique for non-destructive characterization of faceted gemstone, the limitation and benefit of techniques will be discussed. The quality of transflectance spectrum is compared with those of the well-accepted diffuse reflectance and specular reflectance spectra.

###### **4.4.1.1 Effect of Cutting**

In principle, a faceted gemstone was cut in such a proportion that total internal reflection within the gemstone is enhanced. To increase the number of total internal reflection, the cutting proportion of the gemstone is carefully design with respect to refractive index, size, shape, and carat weight. The number of transflected radiation will depend strongly on the angle and positions that light enter the gemstone. It is equally important that the angle of pavilion facets must appropriate to reflect the incident rays back to the crown facets or diamond/air interface [34]. In order to evaluate the influence of cut proportions affecting to the transflectance spectrum, emeralds with various cutting styles and cut proportions (*i.e.*, well-cut proportion and unconventional proportion) were employed for comparison purpose.

In this case, the well-cut proportion was defined as the symmetrical pavilion facets which assessed visually while the poor-cut proportion was defined as asymmetrical pavilion facets or imperfect cutting.

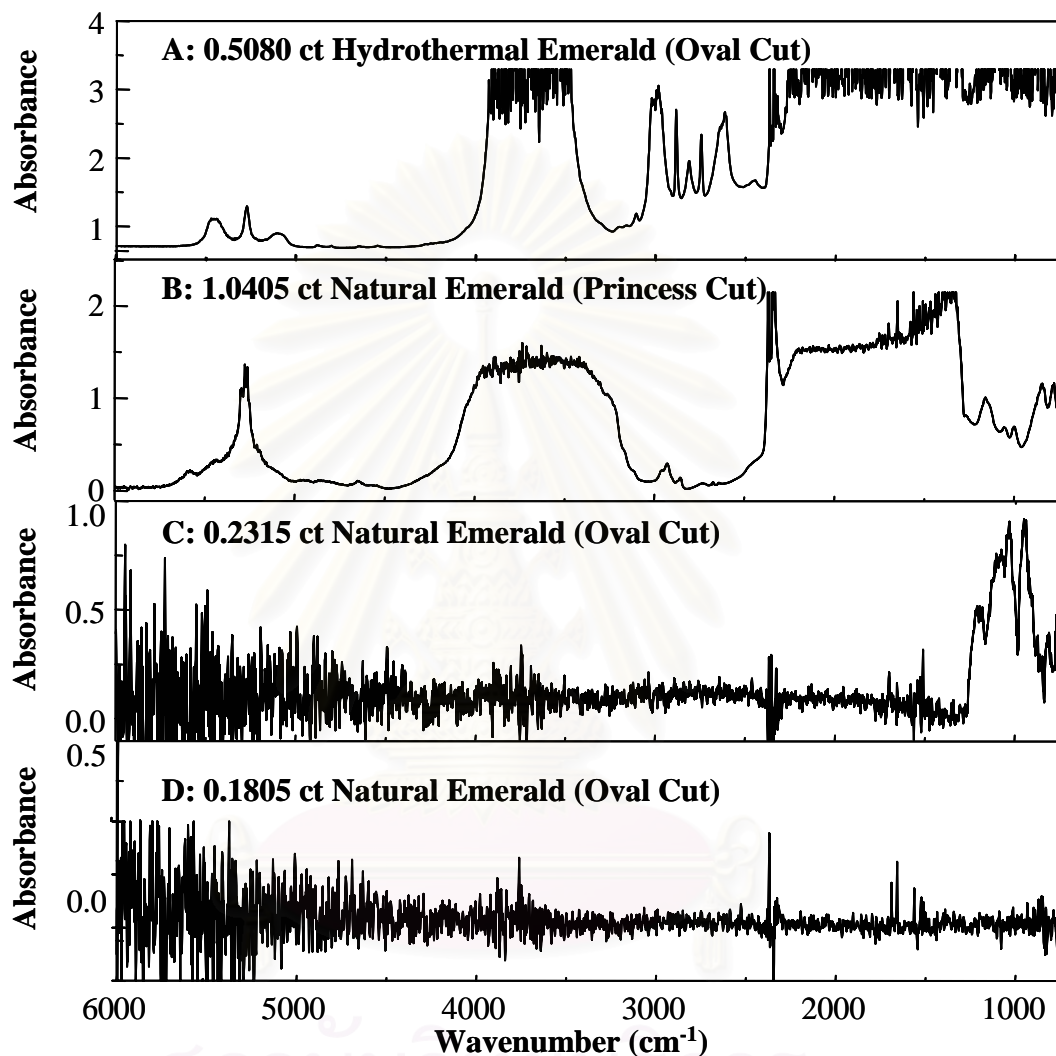


**Figure 4.31** FT-IR spectra of faceted emerald with various cutting styles and shapes. Note. (A) and (B) are well-cut proportion emeralds, (C) and (D) are poor-cut proportion emeralds.

Figure 4.31 shows transmittance spectra of emeralds with various cuts and shapes. Figure 4.31A and B, respectively, are the transmittance spectra of well-cut proportion hydrothermal and natural emeralds while Figure 4.31 C and D are those of poor-cut proportions natural emeralds. In case of well-cut proportions, the spectral features unique to defect and impurities in each emerald are clearly observed. It

should be noted that both emeralds are different cuttings. Although the spectral envelop of the transreflectance spectrum is the same as that of the well-accepted diffuse reflectance spectrum, it seem to possess a superior over absorption in low wavenumber and OH stretching in the high wavenumber regions. The transreflectance radiation undergoes transmission-like travel through the faceted emerald before reflecting back to the objective. A large emerald with inherently long transreflected path length benefits the weak absorption bands [11,25]. The weak absorption bands unique to its impurity can be clearly observed in the transreflectance spectra in higher wavenumber. Due to the saturation of molecular water observed in the OH stretching region, classification of the emerald acquired by transreflectance technique was difficult. However, the overtone absorption of molecular water can be easily recognized and utilized for emerald characterization. Regarding this observations, we have successfully accomplished a novel transreflectance technique for characterization of well-cut proportion emeralds with all cutting styles.

Regarding the Figure 4.31C, the specular reflectance spectral feature in low wavenumber region which corresponding to the vibration of beryl structure can be noticed in the observed transreflectance spectrum of a poor-cut proportion natural emerald. This is because the radiation which reflecting back to detector does not undergoes total internal reflected radiation. The overall spectral feature shows high noise level because there is very low energy throughput of reflected radiation at the detector. The transreflectance spectrum of another poor-cut proportion emerald does not show any prominent absorption feature (Figure 4.31D). The spectrum also present very high noise level because it does not have any transreflected radiations coupling back to the detector. As mentioned before, if the angles of the facet are wrong, many of the incident rays will pass out through the pavilion facets or being refracted out through the back of the stone (see Figure 2.13A). Since the position where the coupled radiation entering the emerald can be controlled while the transreflected radiation through the asymmetrical pavilion facet cannot be collected, the observed transreflectance spectra of poor-cut proportion emerald does not reveal absorption-like spectral feature. As a result, the transreflectance technique is not suitable for gemstones with poor-cut proportion.

#### 4.4.1.2 Effect of Defect in Gemstone

It is well known that gemstone may have some structural defects and inclusion in its structures. In this section, we additionally observed the influence of defect in gemstone affecting to transreflectance spectrum. Again, emerald is the representative gemstone for this study because emerald often contains defect, inclusion and other flaws. Difference number of defect of some emeralds was employed for spectral comparison. It should be noted that the number of accumulated scans depend on the nature of the sample. For the higher amount of defects, the greater number of scans was required. In most specimens an approximate thickness (including sample height of faceted stones) of 4 mm was maintained. Figure 4.32 shows transreflectance spectra of emeralds with different number of defects. The order of emeralds showing in the figure was arranged from minimum to maximum number of defects.

Although the samples have different number of defects, all obtained transreflectance spectra clearly reveal the characteristic of beryl, as shown in Figure 4.32. It should be noted that the samples are of different cuttings. The spectral envelopes of transreflectance spectra are similar to those of the diffuse reflectance spectra. The transreflectance spectra of all faceted emeralds suffer from over absorption in both low and high wavenumber regions which corresponding to the stretching vibrations of beryl structure ( $1500\text{-}700\text{ cm}^{-1}$ ) and  $\text{H}_2\text{O}$  molecules ( $3700\text{-}3000\text{ cm}^{-1}$ ) [37-39]. The magnitude of absorption is associated with its defects and size of the faceted specimen. A large emerald with inherently long transreflected path length benefits the weak absorption bands. The weak absorption bands unique to impurity can be clearly observed in higher wavenumber. Although the natural and hydrothermal emeralds cannot be distinguished via water absorption band at  $4000\text{-}3000\text{ cm}^{-1}$  due to their over absorption, the combination band of water molecules in the  $5600\text{-}5000\text{ cm}^{-1}$  can be exploited for the identification. When comparing Figure 4.32A and D, a hydrothermal emerald is bigger than natural emerald, on the other hand, relative intensity of hydrothermal emerald (Figure 4.32A) is lower than that of natural emerald (Figure 4.32D). This is because the natural emerald contains more defects than others. Because of its defect, the majority of incident radiation is lost

while the minority of tranflected radiation was coupled back to the detector. Therefore, the high internal defect gemstone can be analyzed via transfectance technique. If the stone has a lot of defects, the high number of scans was required in order to receive the better spectral quality.

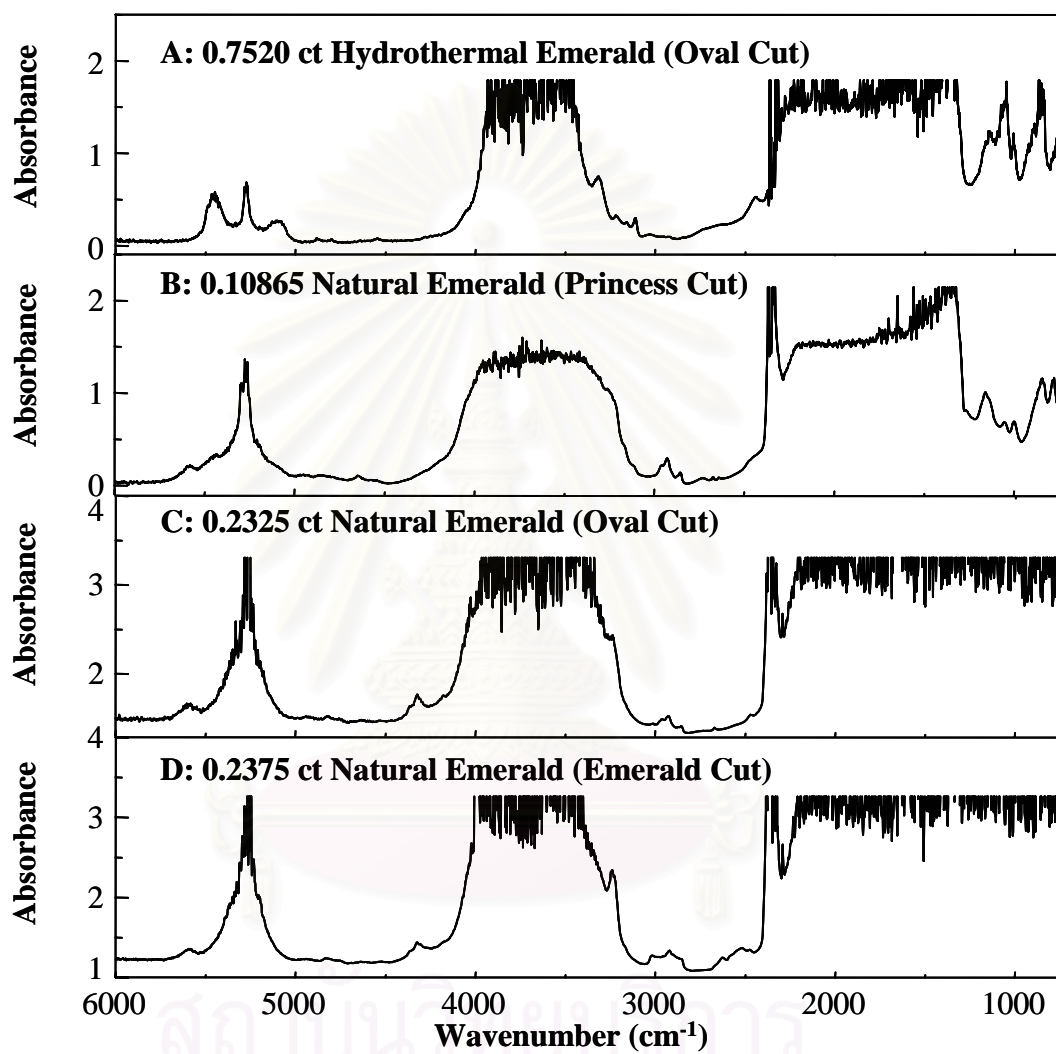


**Figure 4.32** FTIR spectra of emeralds with different number of defects acquired by transfectance techniques. Note: Number of defect D>C>B>A

#### 4.4.1.3 Effect of Transparency

Figure 4.33 shows infrared spectra of various gemstone species that acquired by transfectance technique. The natural diamond, hydrothermal emerald and natural ruby were representative gemstones for transparent, semi-transparent, and translucent gemstone, respectively. Since turquoise is an opaque gemstone, it cannot be analyzed by this technique. According to the Figure 4.33, all obtained transfectance spectra clearly reveal the characteristic absorption of each item which is the same as that of the well-accepted diffuse reflectance spectra (see Section 4.3). Although the tested gemstones different species but it can be concluded that transfectance technique can be employed for characterization both of transparent and translucent gemstones.

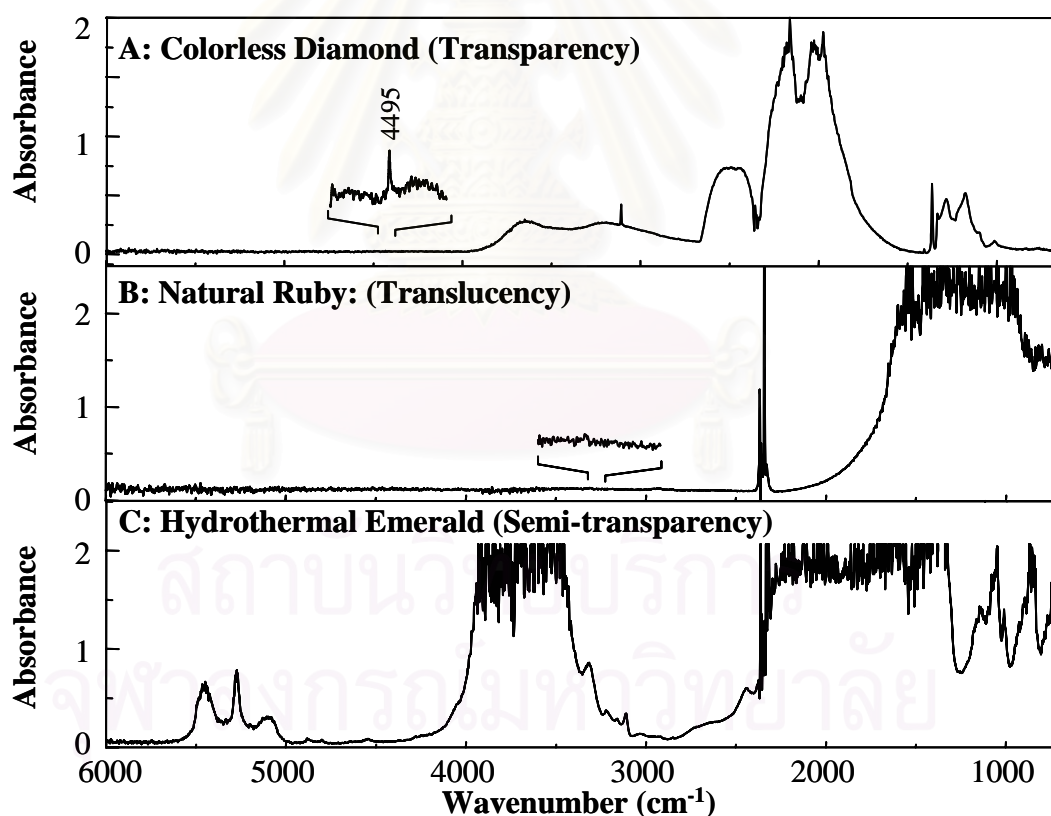


**Figure 4.33** Transflectance spectra of various gemstones with different diaphaneity: (A) diamond: transparency, (B) natural ruby: translucency, and (C) hydrothermal emerald: semi-transparency.

However, with increasing thickness of specimen the absorbance increased and *vice versa*. Likewise, in faceted gemstones, both the transparency and its associated total internal reflections were responsible for varying transflected radiation in different directions within the gemstone. The thickness of most specimens that can be analyzed by transreflectance technique was approximately 5-8 mm, depending on its diaphaneity. As the transparency of gemstones decrease, the absorption increases giving very high absorption intensity or over absorption. In such specimens the quality of their IR spectra is much reduced, due to considerable noise, thereby emerald and ruby require higher number of scans than diamond. The higher the number of scans the better the quality of the observed spectra.

#### **4.4.1.4 Effect of Sample Arrangement**

It is well known that diffuse reflectance spectrum of a faceted gemstone is greatly influenced by sample arrangement on the sample holder [10,23-24]. For comparison purpose, in this section we additionally observed the dependence of sample arrangement for faceted gemstones characterization. An obtained data collection was performed under identical specimens with diffuse reflectance technique (see Section 4.2.2).

Figure 4.34 shows transreflectance spectra of a 0.1075 ct round brilliant cut diamond under different arrangements. Unlike the diffuse reflectance spectrum, the transreflectance spectrum was not affected by the diamond arrangements. Superimposition of the transreflectance spectra with different diamond arrangements are shown in the inset. The coupled radiation from the microscope is non-polarized while the incident radiation covers a wide range of angles due to the focusing optics of the built-in 15X Cassegrainian objective [23-24]. The radiation undergoes transmission-like traveling through the faceted diamonds. Since the position where the coupled radiation entering the diamond can be controlled while the transflected radiation through the symmetrical table facet can be collected, the influences of diamond orientations are eliminated. Thus, the observed transreflectance spectra of a diamond are reproducible and are superimposed. Due to minor variations of the alignment with respect to the incident radiation, negligible discrepancies among



transflectance spectra can be noticed. It should be noted that the shown transflectance spectra were not normalized.

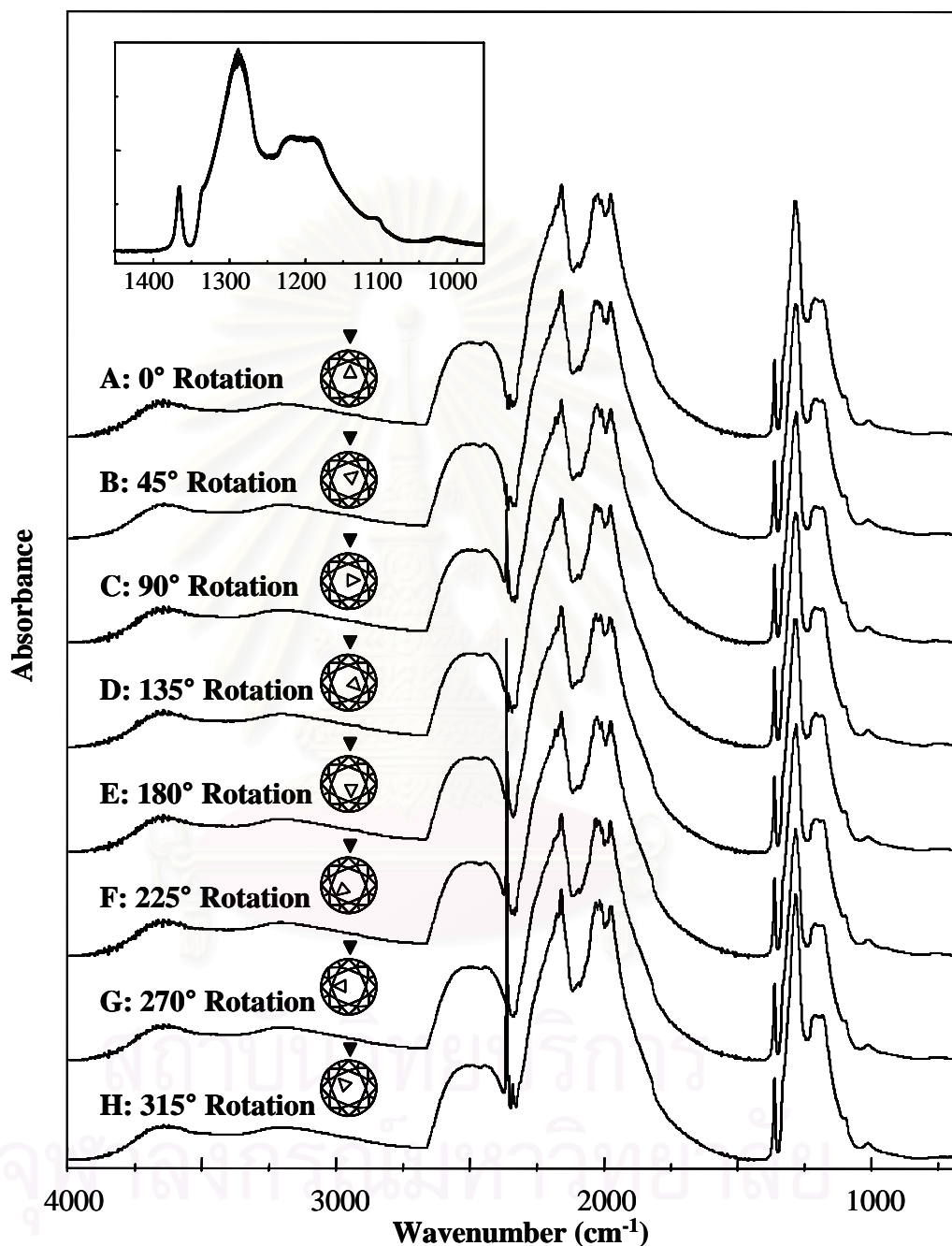


**Figure 4.34** Transflectance spectra of a 0.1075 ct round brilliant cut diamond under different arrangement. The diamond was rotated:  $0^\circ$  (A),  $45^\circ$  (B),  $90^\circ$  (C),  $135^\circ$  (D),  $180^\circ$  (E),  $225^\circ$  (F),  $270^\circ$  (G), and  $315^\circ$  (H) with respect to a reference position. The inset of absorptions in the one-phonon region was added for clarity.

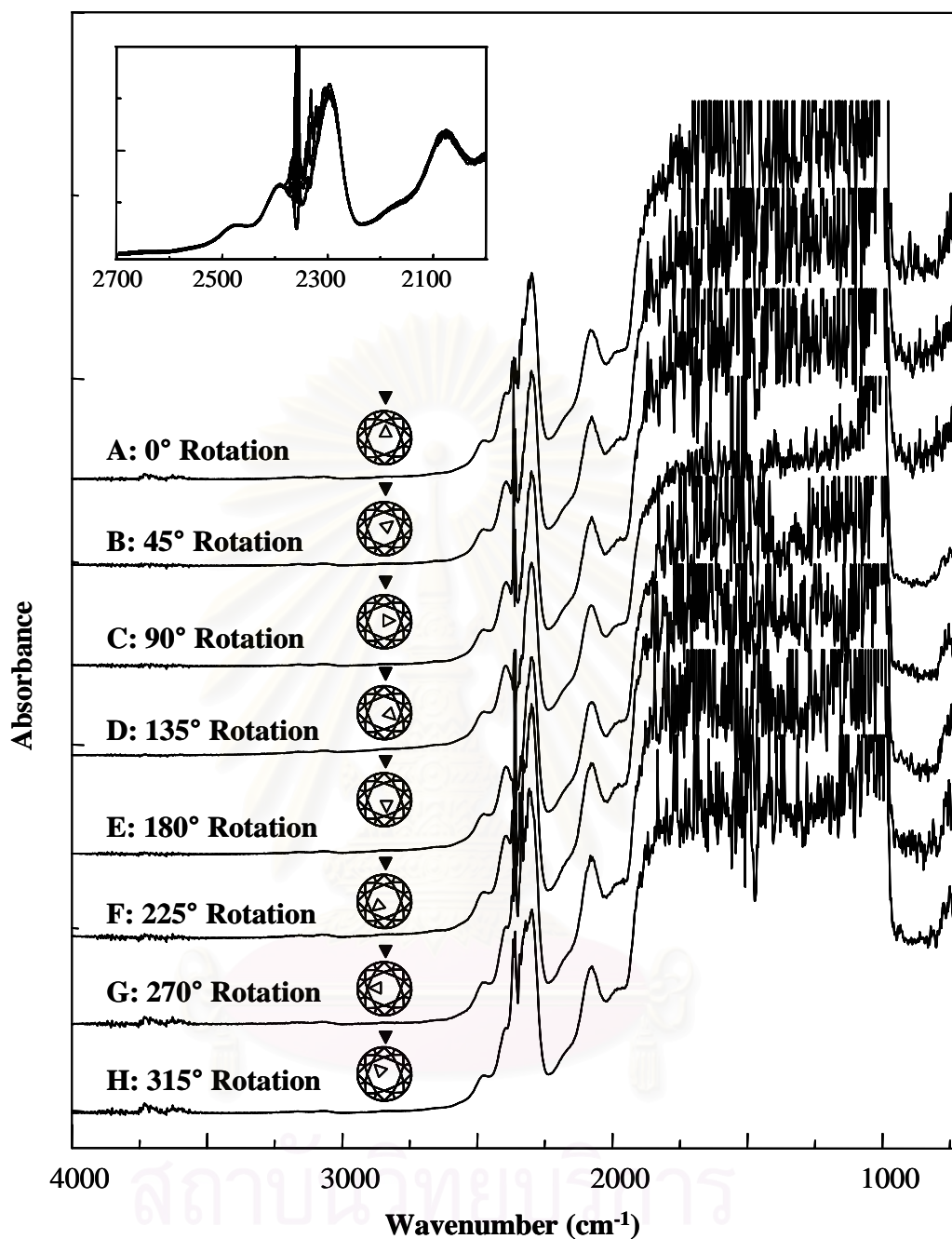


**Figure 4.35** Transflectance spectra of the 1.0595 ct moissanite under different arrangement. The diamond was rotated:  $0^\circ$  (A),  $45^\circ$  (B),  $90^\circ$  (C),  $135^\circ$  (D),  $180^\circ$  (E),  $225^\circ$  (F),  $270^\circ$  (G), and  $315^\circ$  (H) with respect to a reference position. The inset of absorptions in the one-phonon region was added for clarity.

Since diamond is an isotropic material which have only one refractive index, light entering the diamond produces a single refracted ray. The transflectance spectrum may receive small effect of sample arrangement. However, most gemstones

are anisotropic which exhibits a slight to pronounced variation in the intensity of their infrared absorption with their pleochroic direction. To ensure the reproducibility of the transmittance technique, effect of the sample arrangement was also investigated on anisotropic gemstones such as moissanite, emerald and ruby. Moissanite, a new man-made gemstone material having properties overall closer to those of diamond than any other simulant, is a representative material of transparent anisotropic gemstone while hydrothermal emerald and ruby are those of anisotropic colored gemstones. An anisotropic material has two refractive indices. When a ray of light enters these gemstones it is split into two rays which are polarized at right angles to each other. Their infrared spectra may be affected by the orientation of the sample to the incident radiation [4].

Transmittance spectra of the moissanite, hydrothermal emerald and hydrothermal ruby under different sample arrangement are shown in Figures 4.35, 4.36 and 4.37, respectively. The inset of each Figure shows superimposition of the transmittance spectra with different arrangement. The spectral features of all specimens show characteristic bands similar to those of the diffuse reflectance spectra. In the lower wavenumber region, saturation is observed in the obtained transmittance spectra of all specimens. The weak absorption bands in the high wavenumber region are clearly observed in their transmittance spectra. Although the absorption bands of the synthetic moissanite in the  $2500 - 2200 \text{ cm}^{-1}$  are interfered by that of carbon dioxide gas, their absorption maxima are clearly identified (see Figure 4.35). According to the observed transmittance spectra of emerald and ruby in Figure 4.36 and 4.37, it is clearly seen that the obtained spectra were superimposed. Although all specimens are anisotropic materials, their transmittance spectra were not affected by the sample arrangements. It should be noted that all specimens are of different cutting. Since a concentric rotational axis of a symmetrically faceted gemstones and the sample holder of novel accessory is easily achieved, exact transmittance patterns under different sample arrangements can be obtained. Moreover, the influences of anisotropic material orientations are also eliminated because the coupled radiation from the microscope is non-polarized while the incident radiation covers a wide range of angles due to the focusing optics of the built-in 15X Cassegrainian objective. Thus, their observed transmittance spectra are

reproducible and are superimposed. However, the negligible discrepancies among transmittance spectra can be noticed because of minor variations of the alignment.

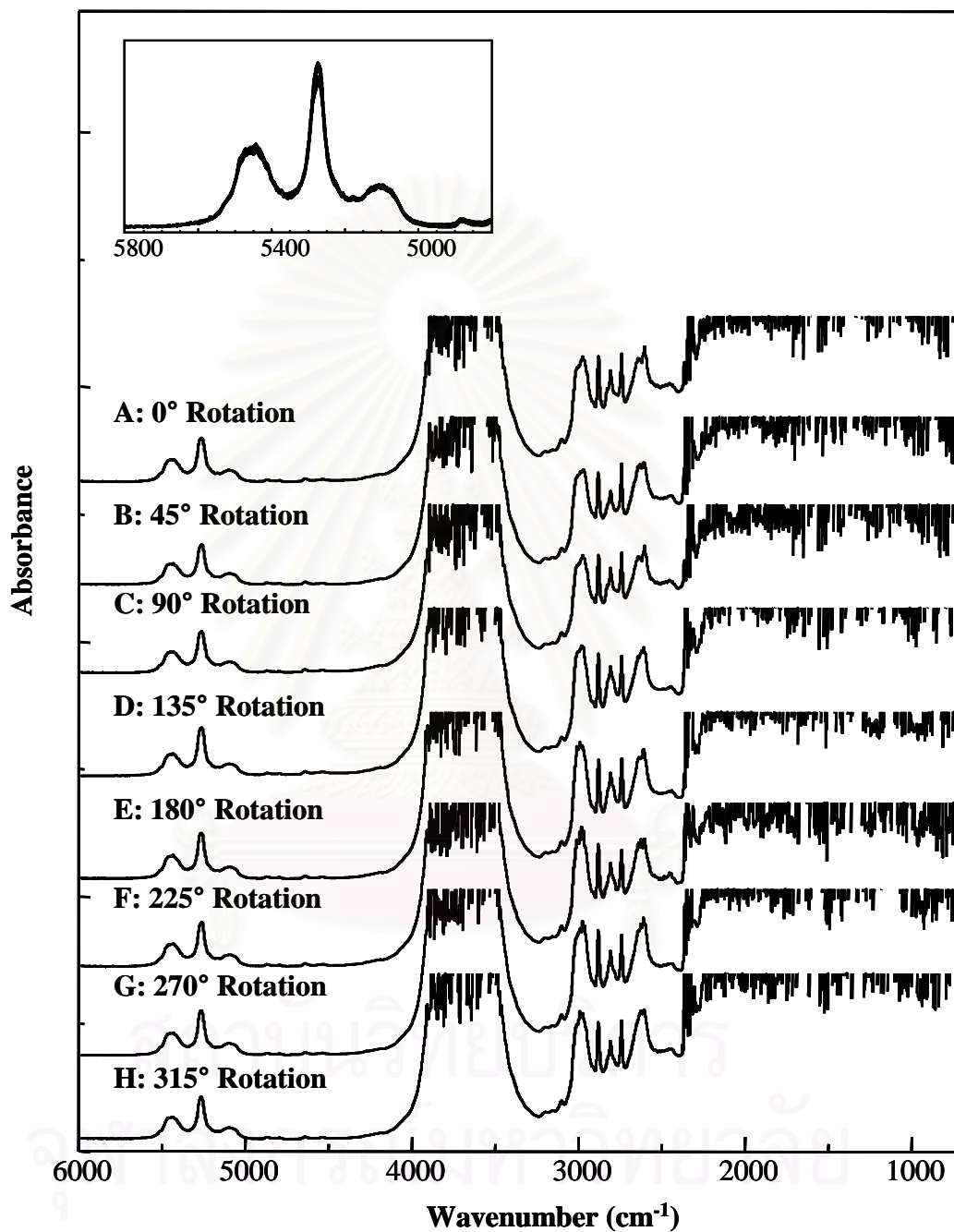


**Figure 4.36** Transmittance spectra of the 0.4960 ct hydrothermal emerald (princess cut) under different arrangement. The emerald was rotated: 0° (A), 45° (B), 90° (C), 135° (D), 180° (E), 225° (F), 270° (G), and 315° (H) with respect to a reference position.

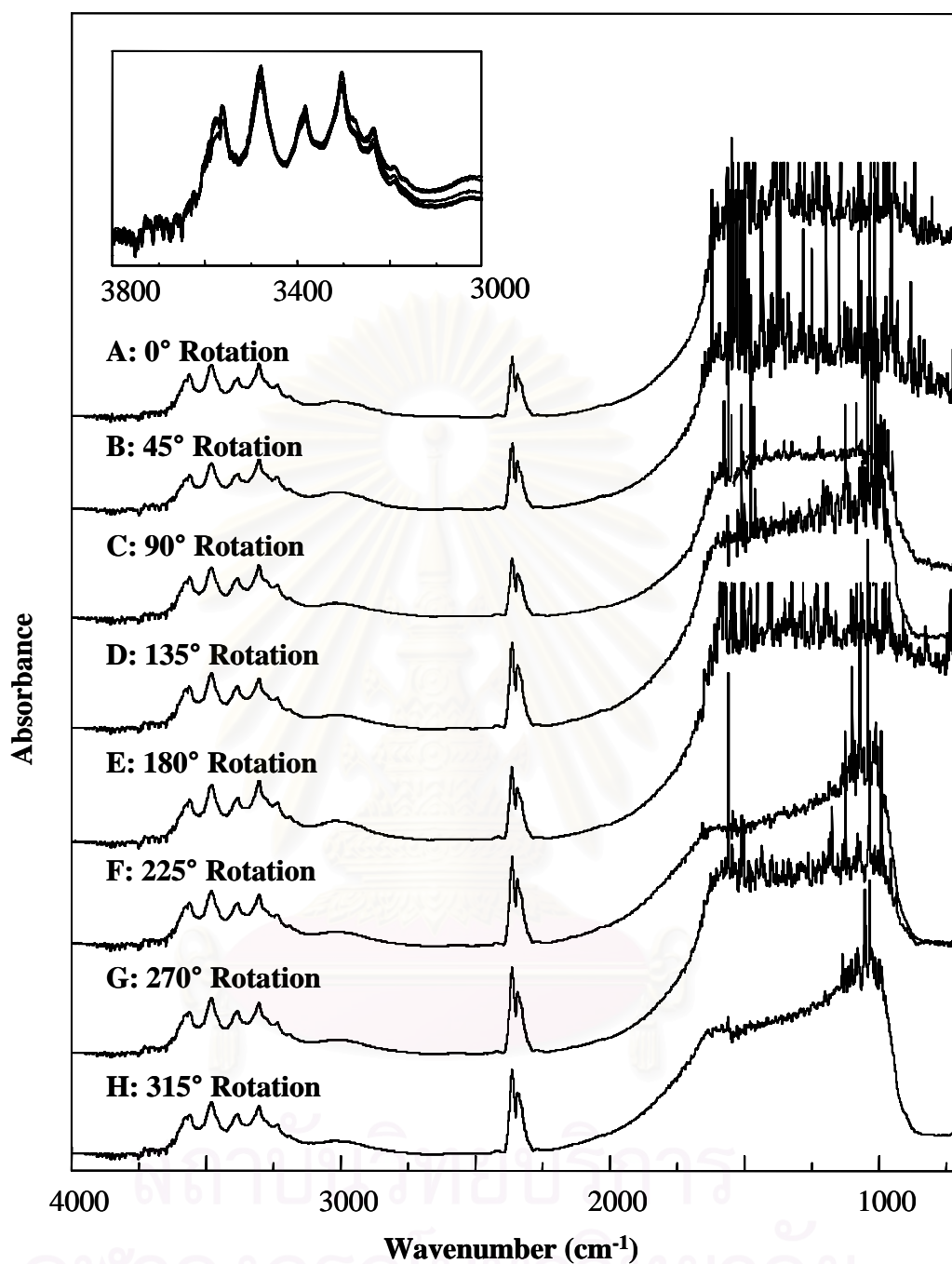


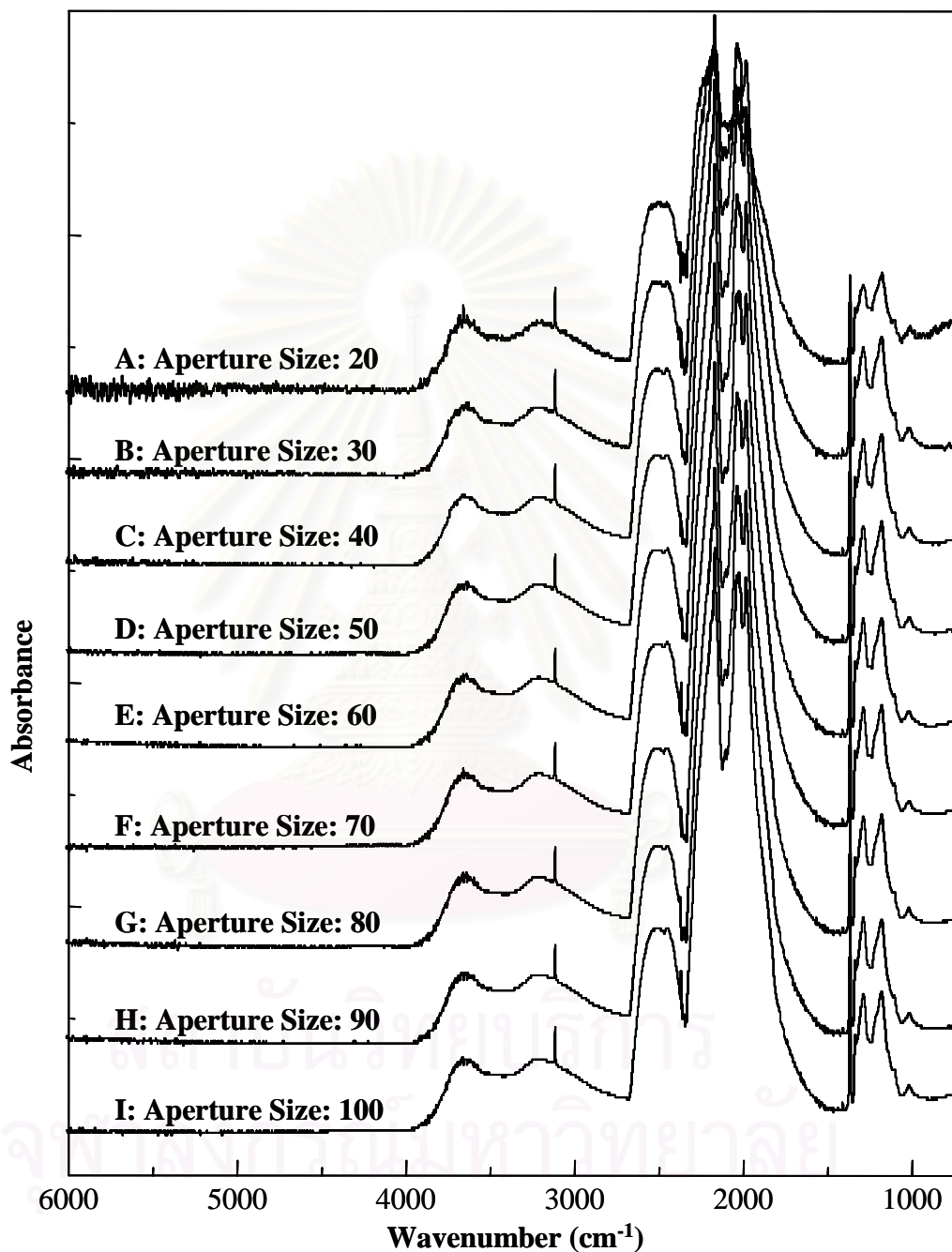
**Figure 4.37** Transflectance spectra of the 1.1510 ct hydrothermal ruby (oval cut) under different arrangement. The ruby was rotated: 0° (A), 45° (B), 90° (C), 135° (D), 180° (E), 225° (F), 270° (G), and 315° (H) with respect to a reference position.

#### 4.4.1.5 Effect of Aperture Size

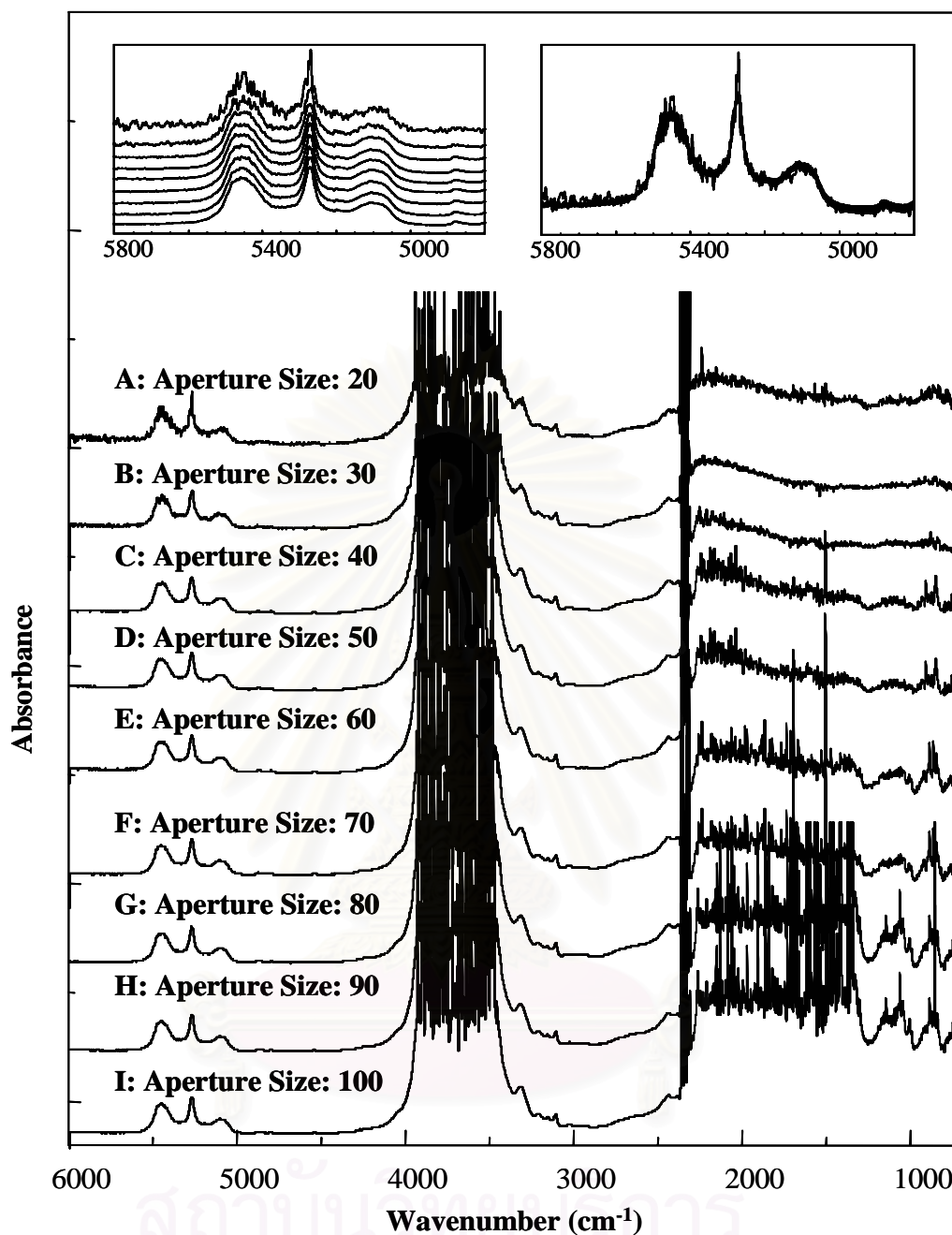
In case of infrared microscopy, the variable aperture is useful if the sample being studied is heterogeneous because it allows the operator to study different areas of the sample. For comparison purpose, all transmittance spectra were acquired with 256 co-added scans. Figure 4.38 shows spectra of a diamond acquired with different sizes of the aperture. Since all obtained transmittance spectra clearly reveal the same spectral feature, it can be concluded that the diamond is a homogenous material. An obvious difference of the obtained spectra is their S/N ratio. Although, all obtained spectra show prominent characteristic absorptions of the diamond, the larger the size of aperture the better the S/N ratio and spectral quality. In case of aperture size lower 40  $\mu\text{m}$ , the spectrum shows baseline shift and high noise level in the higher wavenumber. It should be noted that some absorption bands of hydrogen impurity in the diamond lattice appear at the high wavenumber was the indicator for treatment process. These data show that the higher number of scans needs to be used when using size selection of aperture smaller than 40  $\mu\text{m}$ .

Figure 4.39 illustrated transmittance spectra of a hydrothermal emerald that acquired with identical procedure. The inset A and B was added for clarity. Similar to the transmittance spectra of diamond, the obtained spectra of emerald that acquired with the larger aperture size presenting the better S/N ratio. The transmittance spectra obtained with different aperture sizes clearly reveal the characteristic absorption bands of hydrothermal emerald. The spectra suffer from over absorption in both low and high wavenumber regions which corresponding to the stretching vibrations of beryl structure ( $1500\text{-}700\text{ cm}^{-1}$ ) and  $\text{H}_2\text{O}$  molecules ( $3700\text{-}3200\text{ cm}^{-1}$ ). Considering the low wavenumber, all transmittance spectra of emerald obtained from the aperture size smaller than 70  $\mu\text{m}$  show the saturation. As seen in Figure 4.39G - 4.39I, the transmittance spectrum at lower wavenumber suffers from the specular reflection. According to the optical design of the objective, the coupled radiation is inherently convergence. When using large sizes of aperture, the radiations impinge the table facet with different angles undergoes different reflections before emerging into the air. Some radiations may not undergo transmittance phenomenon but they may emerge from the table facet. The out going

radiation from the table facet is the specular reflection. Since both specular reflection and transflected radiation were collected by the built-in 15X Cassegrainian objective, the spectral distortion in transmittance spectrum was observed.



**Figure 4.38** Transmittance spectra of the 0.105 ct Type IaB diamond under different aperture size setting. The aperture of infrared microscope was 20 (A), 30 (B), 40 (C), 50 (D), 60 (E), 70 (F), 80 (G), 90 (H) and 100 (I).



**Figure 4.39** Transflectance spectra of the 0.752 ct hydrothermal emerald under different aperture size setting. The aperture of infrared microscope was 20 (A), 30 (B), 40 (C), 50 (D), 60 (E), 70 (F), 80 (G), 90 (H) and 100 (I).

Regarding all observation in this section, it reveals the transflectance technique can be analyzed both transparent and translucent gemstone. Whatever gemstone is isotropic or anisotropic, the obtained spectrum was not affected from sample arrangements. Nevertheless, the technique can not be performed with poor-cut proportion gemstone.



## 4.4.2 Identification of Gemstones

As shown in previous section, the novel transreflectance technique using infrared microscope was successfully employed for spectral acquisition of faceted gemstone such as diamond, emerald, and ruby. The technique is nondestructive, provides unambiguous results, requires no sample preparation, and has short analysis time. The same spectral features with better spectral quality as those from the well-accepted diffuse reflectance technique are observed. Unlike the diffuse reflectance spectrum, the transreflectance spectrum is not affected by the gemstone arrangements. In this section, characterization of various faceted gemstones was performed by the transreflectance technique.

### 4.4.2.1 Diamond Characterization

With our results described in Section 4.1, it can be seen that the novel transreflectance technique was successfully employed for spectral acquisition of faceted diamond. The quality of transreflectance spectrum is comparable to or better than that of the well-accepted diffuse reflectance spectrum. To introduce another utilization of the novel transreflectance technique, characterization and differentiation of treated diamond and diamond stimulant were explored.

Transreflectance spectra of brown diamonds and treated diamonds are shown in Figure 4.40. The absorptions in all three principle regions are prominent in the observed spectra. The treatment history and/or unique characters of the faceted diamonds can be drawn from the observed transreflectance spectra [23-25]. The spectra exhibited spectral features associated with nitrogen defect-induced one-phonon absorption. According to the absorption in the one-phonon region, the diamond in Figure 4.40A is classified as a type IaA diamond while that in Figure 4.40B is a type IaB. Both spectra contain a well defined amber center at  $4166\text{ cm}^{-1}$ , which is a typical absorption for natural brown diamonds. Absorption bands associated with hydrogen impurity in the three-phonon region can also be observed. The absorption bands in the one-phonon region of the HPHT-treated diamond in Figure 4.40C indicate that the diamond is type Ib synthetic diamond. A sharp peak at

$1344\text{ cm}^{-1}$  is the characteristic absorption of HPHT-treated synthetic diamond attributed to the local vibration induced by the C-centered single nitrogen substitution. A broad absorption band at  $1128\text{ cm}^{-1}$  implies the presence of low concentration B-centered substitution [10,12,65-70]

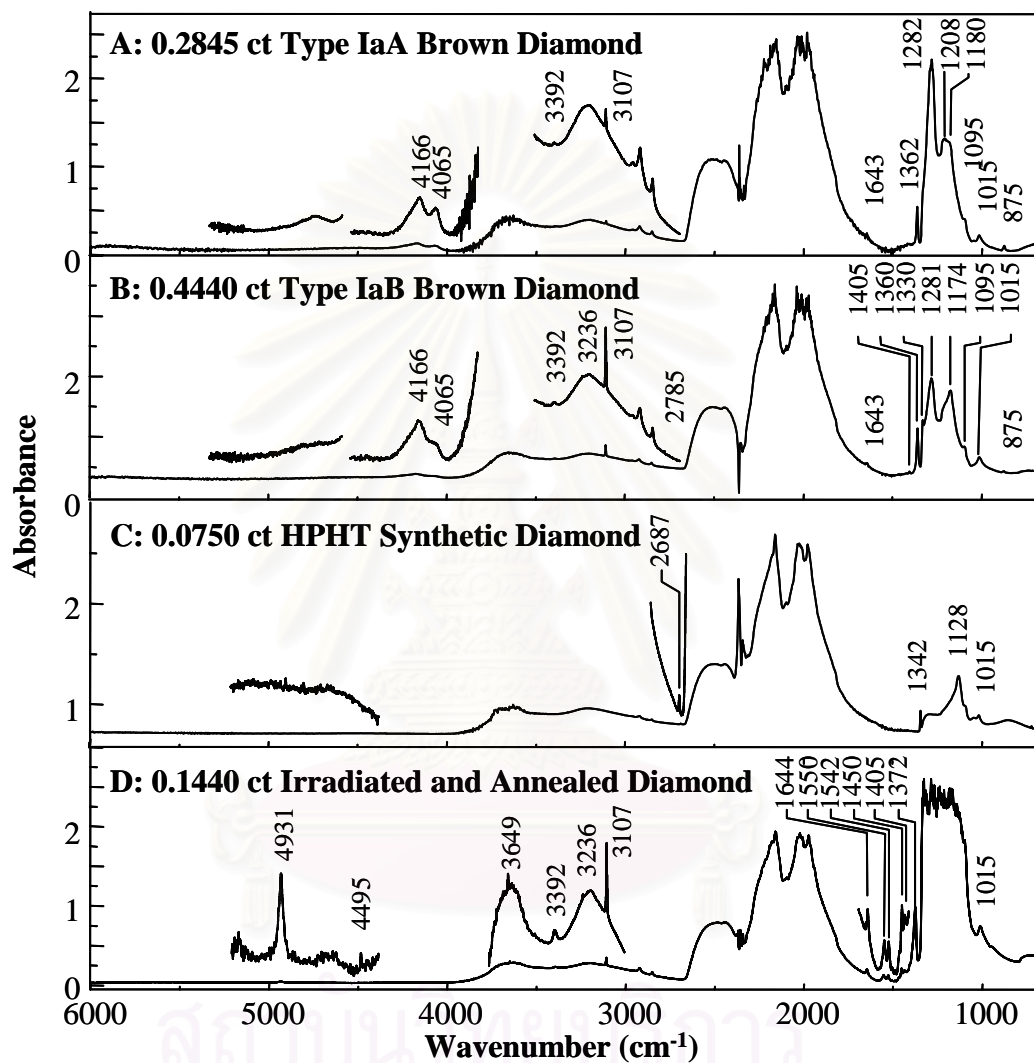


**Figure 4.40** Transflectance spectra of colored and treated diamonds: 0.2845 ct type IaA brown diamond (A), 0.4440 ct type IaB brown diamond (B), 0.0750 ct HPHT type Ib diamond (C), and 0.1440 ct irradiated and annealed diamond (D).

Due to the over absorption in the one-phonon region associated with high nitrogen concentration of the irradiated and annealed diamond in Figure 4.40D, classification of the diamond based on the spectral information in the one-phonon region is not possible. However, absorption bands in the high wavenumber region

associated with defect centers can be exploited for characterization purposes. The H1a absorption at  $1450\text{ cm}^{-1}$  is the local vibrational mode associated with interstitial nitrogen. The H1b absorption at  $4931\text{ cm}^{-1}$  seen in type IaA diamonds is related to the A-center [66-69]. The absorption centers, H1a and H1b, observed in the figure are the unique characteristics of irradiated-and-annealed type I diamond [67-71]. It should be noted that absorption bands in this region are not observed in un-irradiated type I natural diamonds. The sharp absorption bands associated with vinylidene at  $3107\text{ cm}^{-1}$  and that with N-H stretching at  $3236\text{ cm}^{-1}$  are clearly observed. Another vinylidene-related absorption at  $1405\text{ cm}^{-1}$  are observed as a shoulder of the strong absorption at  $1372\text{ cm}^{-1}$  [15,72]. It should be noted that absorption at  $2350\text{ cm}^{-1}$  is due to carbon dioxide in the ambient air. Due to fluctuation of carbon dioxide in the ambient air during spectral acquisition, both positive and negative bands were observed.

Spectra of faceted diamond simulants acquired by transreflectance technique are shown in Figure 4.41. The spectral envelopes of the transreflectance spectra are similar to those of the diffuse reflectance spectra (see Figure 4.5). In the lower wavenumber region, saturation is also observed transreflectance spectra. The weak absorption bands in the high wavenumber region are clearly observed in the diffuse reflectance and transreflectance spectra. Although the absorption bands of the synthetic moissanite in the  $2500 - 2200\text{ cm}^{-1}$  are interfered by that of carbon dioxide gas, their absorption maxima are clearly identified. Spectral quality of the transreflectance spectra seem to be better than that of the diffuse reflectance spectra. Two small absorption bands of the synthetic moissanite at  $3157$  and  $3071\text{ cm}^{-1}$  can be noticed in the transreflectance spectra while the same bands could not be observed in the diffuse reflectance spectra [25]. Since the faceted moissanite has a long transreflected path length, the weak absorption band can be clearly observed in the transreflectance spectrum. Peak positions of the absorption bands of diamonds simulants deduced from the experimentally observed spectra are conformed to those reported elsewhere [8].

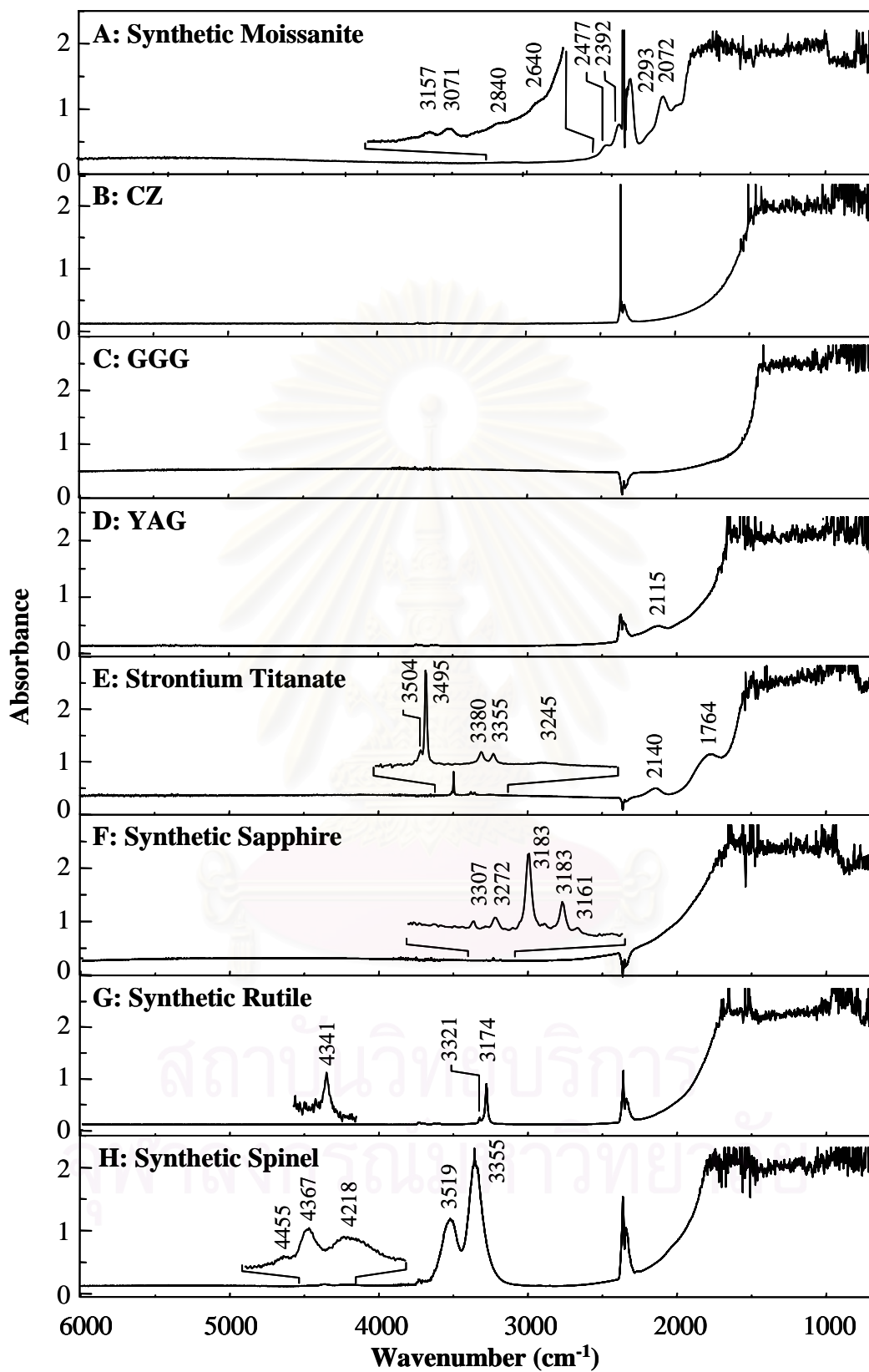


**Figure 4.41** FTIR spectra of round brilliant cut diamond simulants acquired transmittance techniques.

#### 4.4.2.2 Emerald Characterization

Regarding the observations reported in Section 4.4.1, we have successfully accomplished characterization of faceted emerald by novel transreflectance technique. Additionally, the technique can be employed for discrimination of natural emerald and different synthetic emeralds. Figure 4.42 shows observed spectra of natural and synthetic emeralds that acquired via transreflectance technique.

As expected, the spectral envelopes of the transreflectance spectra in Figure 4.42 are similar to those of the diffuse reflectance spectra (see Figure 4.8). In the lower wavenumber region, saturation is observed in transreflectance spectra while specular reflection bands are also observed in diffuse reflectance spectra. The weak absorption bands in the high wavenumber region are clearly observed in the transreflectance spectra. As shown in Figure 4.42, flux synthetic emerald can be readily distinguished from their natural and hydrothermal counterparts. The most obvious difference in the flux emerald is the absence of the strong absorption between 3400 and 3800  $\text{cm}^{-1}$ . The infrared spectra of natural and hydrothermal synthetic emeralds are more similar to one another [48-51]. As described in diffuse reflectance spectra, the natural and hydrothermal emeralds cannot be distinguished by water absorption band between 4000-3000  $\text{cm}^{-1}$  because of their over absorption feature. However, the combination band of water molecules in the 5600-5000  $\text{cm}^{-1}$  can be exploited for the identification. The hydrothermal emerald shows strong absorption at 5092, 5274 and 5546  $\text{cm}^{-1}$  while natural emerald only present a strong absorption band at 5275  $\text{cm}^{-1}$  [47]. It should be noted that the presence of  $\text{CO}_2$  in emerald can be easily recognized in the diffuse reflectance spectra but those absorption does not utilize in the transreflectance spectra. The absorption band of  $\text{CO}_2$  suffers from over absorption feature because of the thickness of the sample. From all observation, it can be concluded that transreflectance technique is viable technique for differentiating between natural and synthetic emeralds.

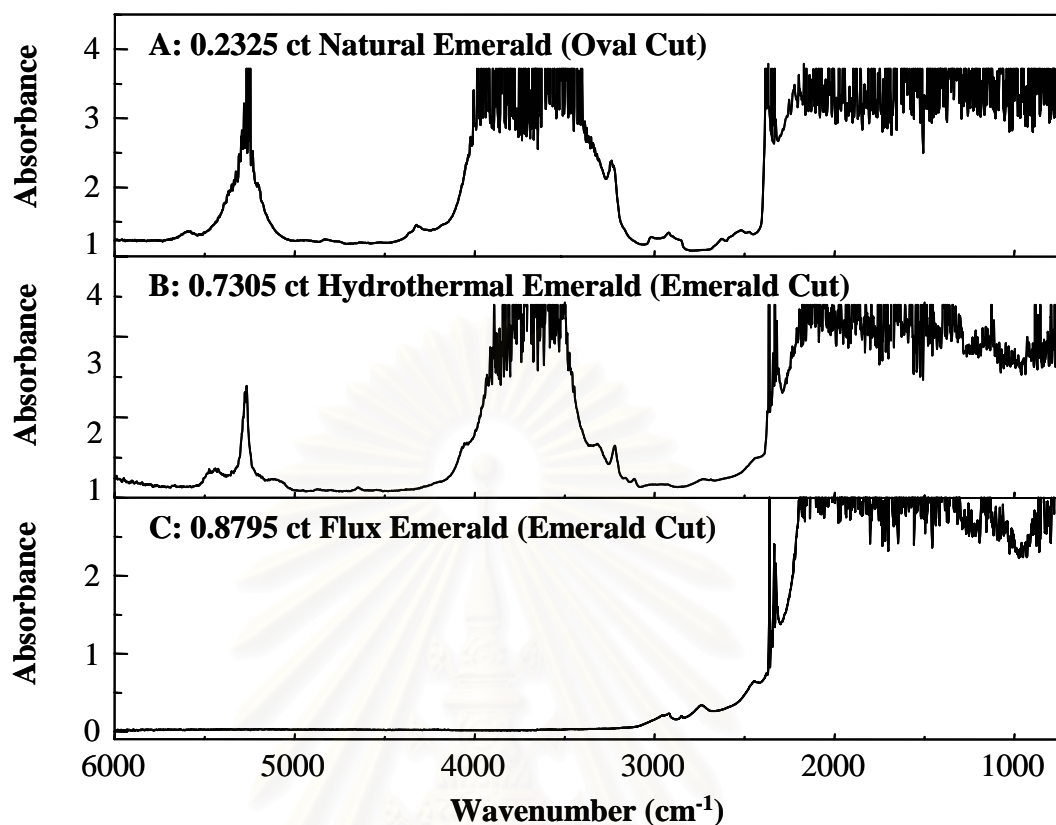


**Figure 4.42** FTIR spectra of natural and synthetic emeralds acquired by transmittance technique.

#### 4.4.2.3 Ruby and Sapphire Characterization

Figure 4.44 shows infrared spectra of natural and different synthetic rubies acquired by transmittance technique. The obtained spectra exhibit the same spectral features as those acquired by diffuse reflectance technique. When comparing with diffuse reflectance spectra, it is clearly seen that remarkable difference is their S/N ratio. Some obtained spectra of ruby present higher noise than those of diffuse reflectance under the same number of scans. This is because the optical properties of the specimens, thickness of sample, and the geometry of the experimental setup. Since ruby and sapphire is transparent/translucent material, most of the incident beams are not translected back to the detector, most of them were absorbed by the matter and the remaining component undergoes transmittance phenomenon. Thus, the low energy throughput was observed. To obtained high spectral quality, the higher number of scan is necessary in these particular gemstones.

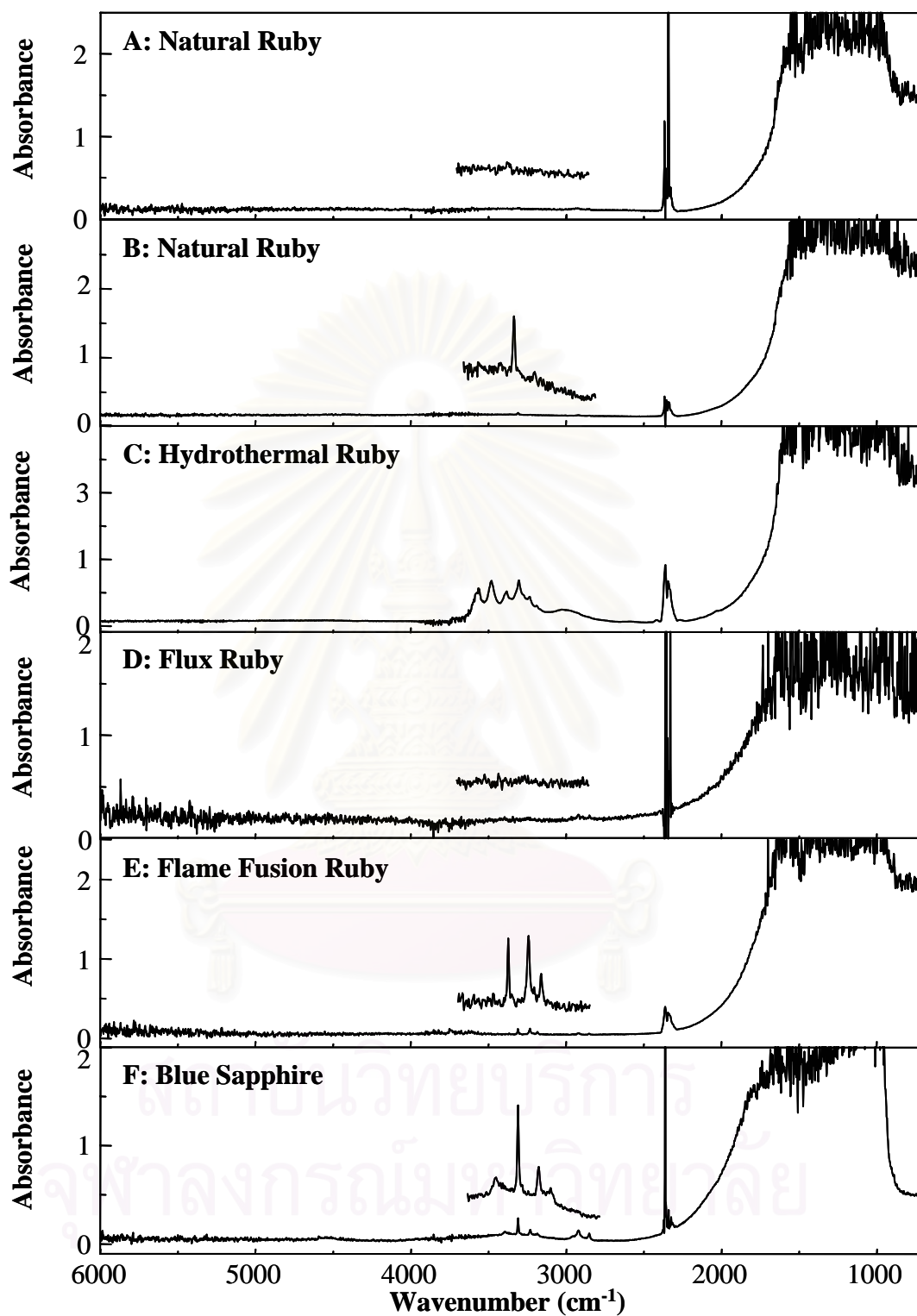


**Figure 4.43** FTIR spectra of natural and synthetic rubies acquired by transmittance technique.

As clearly seen in the Figure 4.43, each spectrum represents the characteristic of each specimen. According to the diffuse reflectance spectra of all specimens, rubies possess the dominant over absorption features typical of corundum from Al-O stretching frequencies and lattice absorption in the region of approximately  $700\text{-}1100\text{ cm}^{-1}$ . Their spectral features in this region are different depend on the size/thickness of sample and sample arrangement. The transmittance spectra of different synthetic rubies exhibited the series of sharp peaks in the  $3400\text{-}3100\text{ cm}^{-1}$  which related to hydroxyl stretching. Since differences in their synthetic process result in differences of their spectral features, the OH stretching absorption can be utilized as a means to identify and distinguish hydrous alumina phases. From the observed spectra, transmittance technique can be employed for differentiating between natural and synthetic rubies. By comparison, the natural ruby in Figure 4.43A and B can be classified as heat-treated ruby and non-heat treated ruby, respectively [52-53]. As a consequence, these absorption bands may be used as an indicator of both heat-treated ruby and sapphire.

The color sapphires were additionally examined by transmittance technique. The observed spectra are shown in Figure 4.44. Again, only the spectral feature above  $3000\text{ cm}^{-1}$  was observable because the low wavenumber region shows over absorption of Al-O stretching frequencies. Each spectrum shows characteristic absorption in the  $3400\text{-}3100\text{ cm}^{-1}$  region which corresponding to structural OH stretching. Therefore, it was possible to employ the spectral feature in this region for positively identify their impurity. By comparing the spectra of color sapphires, it is clearly seen that each item shows different spectral feature in the OH frequencies region. Furthermore, there are observable the difference of intensity ratio of those peak which imply the OH absorption from several hydrous alumina phases [52,57]. By comparison, the natural ruby in Figure 4.44D and E can be classified as natural orange colored sapphire and stimulant of orange colored sapphire, respectively. That distinctive difference is clearly revealed in the  $2500\text{ - }2000\text{ cm}^{-1}$ .



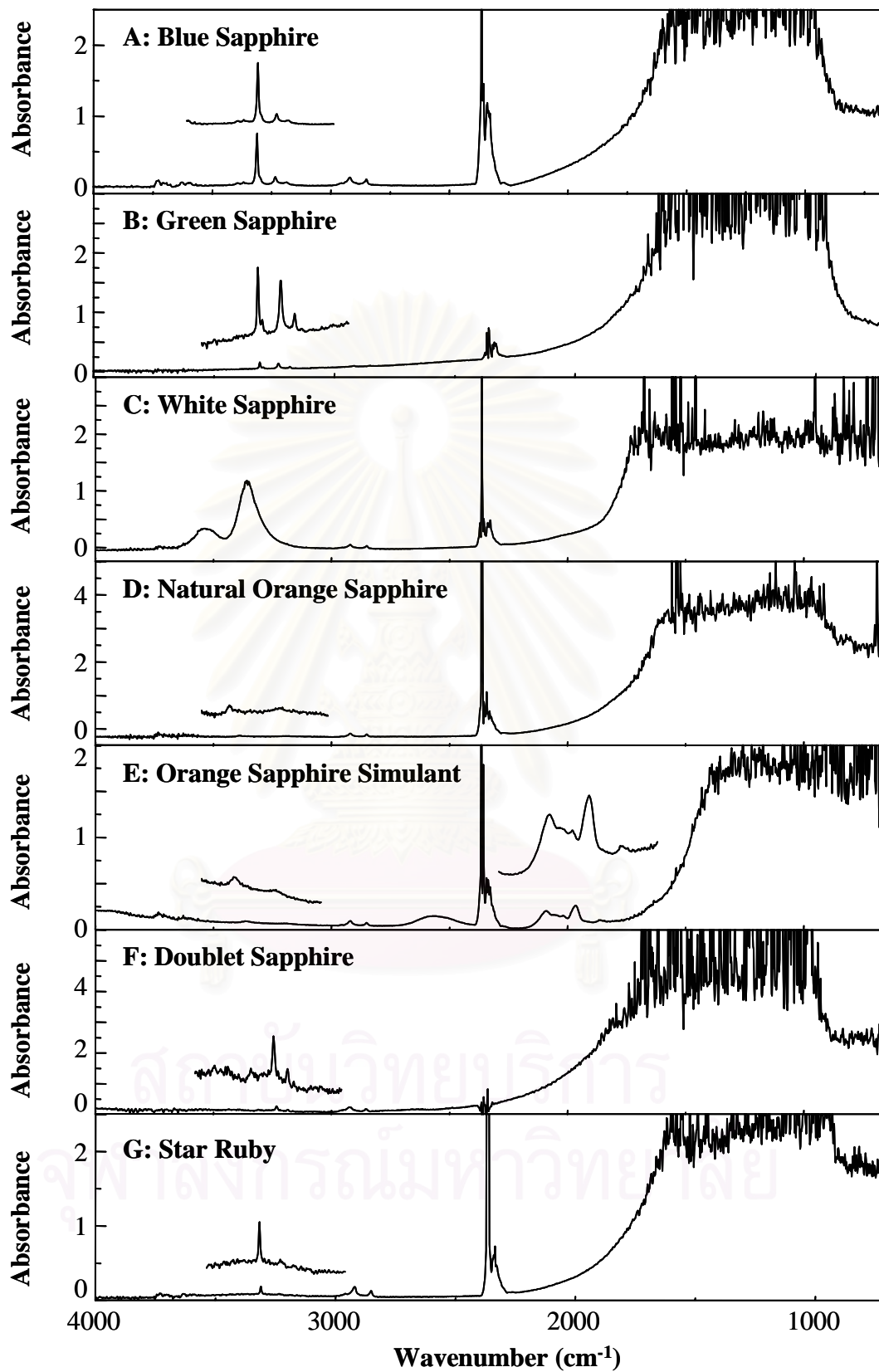


**Figure 4.44** FTIR spectra of fancy color sapphires acquired by transmittance technique.

A somewhat surprising result is that the transmittance spectrum of doublet sapphire and star ruby were observed. Doublet is a gemstone sandwich made in layered sections. The lower, larger portion is made from glass or an inexpensive stone and has a smaller layer of a more valuable stone adhered to the top of it [4]. When the doublet gemstone was mounted in jewelry, it cannot be examined by conventional FT-IR accessory without taking the gemstone out of the jewelry. The transmittance spectrum of the doublet sapphire show characteristic absorption in the 3400-3100  $\text{cm}^{-1}$  region which corresponding to structural OH stretching. Nevertheless, the type of synthetic sapphire used as lower layer of the doublet cannot identify. The OH stretching absorption bands present the same peak position with those of flame fusion synthetic ruby while the intensity ratio of each absorption bands is different. Star ruby, a phenomenal gemstone which cut cabochon and occasionally produces a six-legged star, was also investigated with transmittance technique. The obtained spectrum of star ruby shows in Figure 4.44G. In the practice, the star ruby was placed with the star facet face down. The infrared incident beam was coupled into the bottom of star and impinging inside hemispherical facet before emerging to the air. Thus, the technique utilized only the loose star gemstone or cabochon.

***Summary:***

The novel transmittance technique using infrared microscope was successfully employed for spectral acquisition of loose faceted gemstone. The incident radiation is coupled to the gemstone via the table facet while the transmittance radiation is collected by the built-in 15X Cassegrainian objective. The same spectra features with better spectral quality than those from the well-accepted diffuse reflectance technique are observed. This observation indicates that not only transmittance technique can be utilized for characterization of various gemstones but also to differentiate between their natural and synthetic counterpart. It is viable for distinguishing natural, treated and imitated gemstones. Several advantages of the technique can be concluded as follow:

- ✓ The technique is nondestructive, provides unambiguous results, requires no sample preparation, and has short analysis time.
- ✓ It can be employed for transparent, semitransparent and translucent gemstones.
- ✓ Because of the internal scattering of radiation that occurs, the effective pathlength of the infrared radiation is increase many fold by this scattering. Therefore, it is possible to detect very low concentrations of species in the sample.
- ✓ The technique can be employed for both of isotropic and anisotropic gemstones. The measurement of faceted gemstone is reproducible since the transmittance spectrum is not altered by the sample arrangements.
- ✓ The novel accessory composes of several sample holder which suitable for various sizes of loosed gemstones and jewelries. The technique is applicable for various type of gemstone and cutting. Although the shown results in this section are those of the loose gemstones, the technique can be employed for mounted gemstone on jewelries without taking the gems out of the jewelry setting.
- ✓ Absorption bands unique to impurities, defects in the crystal structures, and treatment processes can be clearly observed. The measured spectrum can be exploited for classification and/or determination of the natural, treated gemstone and simulants.

Nevertheless, the technique encounter some limitation depends strongly on the physical and optical properties of analyzed sample. Disadvantages of the technique can be categorized as follows.

- ✗ The maximum thickness that can be performed with transmittance technique is approximately 8 mm.
- ✗ The transmittance technique can not be employed for opaque gemstone.
- ✗ In case of cabochon, the sample was placed on the sample holder with the table face down. The infrared incident beam was coupled into the bottom of cabochon and impinging inside hemispherical facet before emerging to the

air. Thus, the technique cannot be performed with the cabochon in jewelry setting.

- ✘ The transreflectance technique cannot be employed for poor-cut proportion gemstones because the transreflected radiation cannot be collected.

#### **4.4.3 Other Applications of Transreflectance Technique**

The purpose of this section is to employ the combination of observed transreflectance spectra of faceted diamond and its physical cut proportion (*i.e.*, cutting, table size, girdle diameter, crown height) as the unique identification of the diamond. The technique takes advantage of the defects and impurities in the diamond crystal lattice, which exhibit unique absorption bands in the infrared spectrum as the unique signature of individual diamond. The unique spectral features associated with chemical compositions, impurities, and treatment processes will be discussed.

##### **4.4.3.1 Unique Identification of Diamonds**

In order to exhibit unique identification of a faceted diamond, different color and treated diamonds were chosen for spectral acquisition. Six round brilliant diamonds, some with unconventional proportions, were employed (see table 4.3). It should be noted that the proportion of diamonds are different. Transreflectance spectra of the employed diamonds are shown in Figure 4.45. The spectral features unique to defects and impurities in diamond crystal structure are clearly observed in the transreflectance spectra of six faceted diamonds. Since infrared spectrum is unique to type of a diamond, absorptions at the characteristic frequencies of each diamond are different. These spectral features could be employed for diamond classification. According to spectral envelopes in the one-phonon region, diamonds number 1-5 are classified as type IaB, IaA, IaA/B, IaA and Ib, respectively. Since, the transreflectance spectrum of diamond number 6 suffers from over absorption in one phonon region, a specific type of the diamond cannot be identified.

**Table 4.3** Proportional values of faceted diamond examined in this section

Sample	Color	Weight (ct)	Table (mm)	Crown (mm)	Pavillion (mm)
A	colorless	0.0910	1.85	0.65	2.90
B	colorless	0.1030	1.85	0.70	3.15
C	brown	0.2845	1.70	0.75	3.05
D	brown	0.4440	1.65	0.70	2.85
E	yellow	0.0750	1.45	0.75	2.65
F	yellow	0.1440	1.45	0.50	2.85

It should be noted that the same color diamonds are not only different proportions but also unique transmittance spectrum. Comparing between colorless diamonds, the natural colorless diamond in Figure 4.45A was identified as a type IaB while that in Figure 4.45B is a type IaA. The type IaB diamond possesses a B-center defect (*i.e.*, an aggregate consists of four nitrogen atoms surrounding a vacancy) which shows absorption band at 1330, 1172 and 1013  $\text{cm}^{-1}$ . An associated absorption band at 1360  $\text{cm}^{-1}$ , which referred to the extended-planar-defect platelets, could also be noticed in Figure 4.45A. Transmittance spectrum of colorless diamond in Figure 4.45B clearly reveals the unique absorption bands in the one-phonon region of the type IaA diamond associated with an A-center defect (*i.e.*, a defect consists of a pair of adjacent substitution nitrogen atoms in the diamond lattice). The main absorption has maximum at 1282  $\text{cm}^{-1}$  and additional weak absorptions at 1362, 1208 and 1015  $\text{cm}^{-1}$  [10,12,36].

The transmittance spectra of two brown diamonds shown in Figure 4.45C and Figure 4.45D exhibited absorptions associated with nitrogen defect-induced one-phonon absorption. According to the absorption in the one-phonon region, the diamond in Figure 4.45C is classified as a type IaA diamond while that in Figure 4.45D is a type IaB diamond. Both spectra contain a well defined amber center at 4166  $\text{cm}^{-1}$ , which is a typical absorption for natural brown diamonds. Absorption bands associated with hydrogen impurity in the three-phonon region can also be observed.

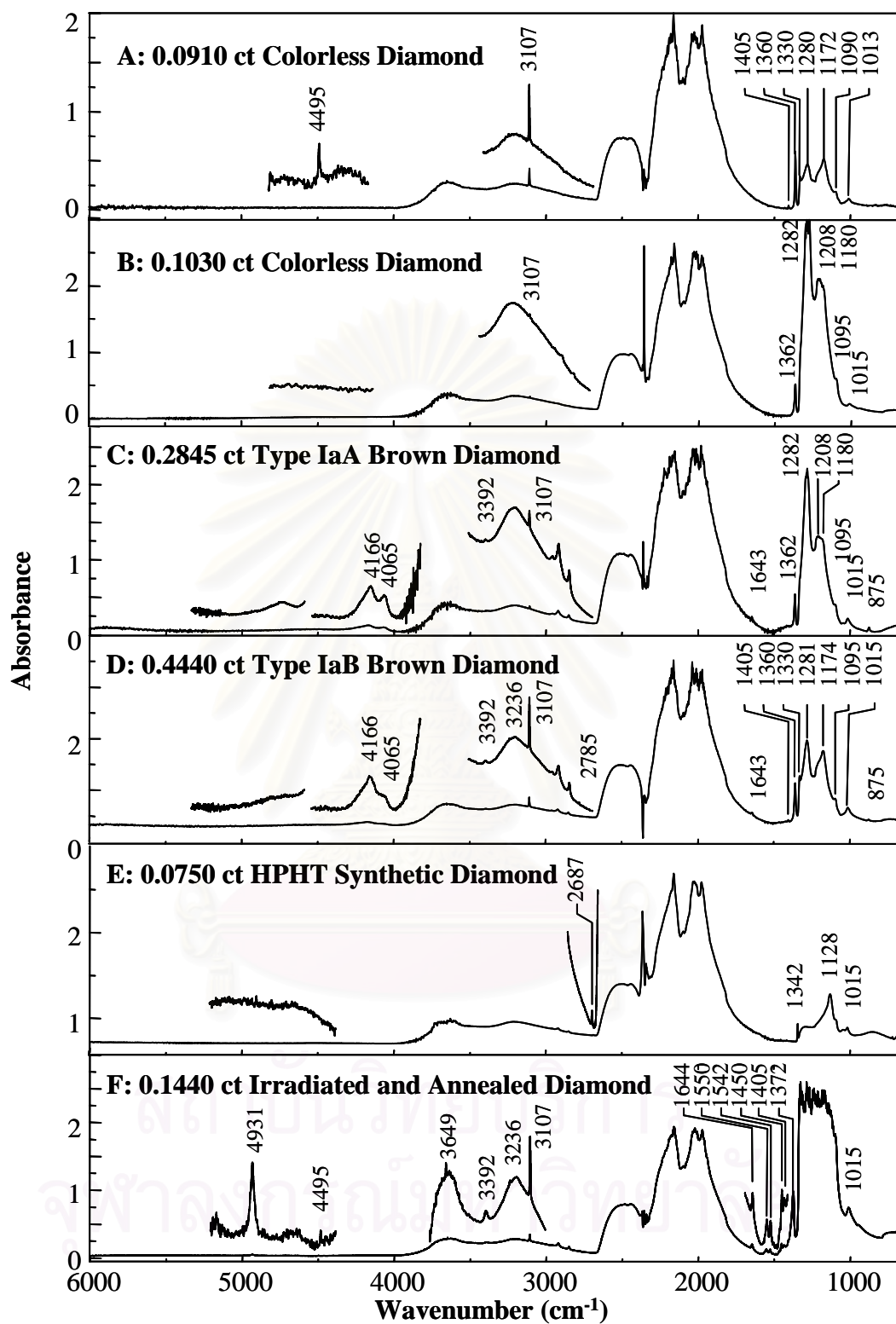


**Figure 4.45** FT-IR spectra of different types of diamonds acquired by transmittance technique.

The absorption bands in the one-phonon region of the HPHT-treated synthetic diamond in Figure 4.45E indicate that the diamond is type Ib. A sharp peak at  $1344\text{ cm}^{-1}$  is the characteristic absorption of HPHT-treated synthetic diamond attributed to the local vibration induced by the C-centered single nitrogen substitution. A broad absorption band at  $1128\text{ cm}^{-1}$  implies the presence of low concentration B-centered substitution. Due to the over absorption in the one-phonon region associated with high nitrogen concentration of the irradiated and annealed diamond in Figure 4.45F, classification of the diamond based on the spectral information in the one-phonon region is not possible. However, absorption bands in the high wavenumber region associated with defect centers can be exploited for characterization purposes. As mention before, the spectrum exhibited absorption band of H1a and H1b centers which are unique character of irradiated and annealed type I diamond [65-70].

In addition to the nitrogen-related absorptions, diamonds also exhibited sharp absorption bands related to hydrogen impurity at 4495, 3236, 3107, 2785 and  $1405\text{ cm}^{-1}$ . A sharp peak at  $3107\text{ cm}^{-1}$ , which attribute to C-H stretching vibration of vinylidene group [8], presented in the transmittance spectra of some diamonds. The intensity of this band varied considerably depending on concentration of hydrogen impurity. For spectra with strong absorption at  $3107\text{ cm}^{-1}$  (*i.e.*, Figure 4.45A, B, C and F), weak absorptions at 3236 and  $2785\text{ cm}^{-1}$  were noticed. Both absorption bands are commonly observed as minor features in infrared spectra of hydrogen-containing natural diamonds. The absorption at  $2785\text{ cm}^{-1}$  is believed to be the first overtone of the absorption at  $1405\text{ cm}^{-1}$  while the sharp peak at  $3236\text{ cm}^{-1}$  was assigned to N-H stretching absorption [13,69].

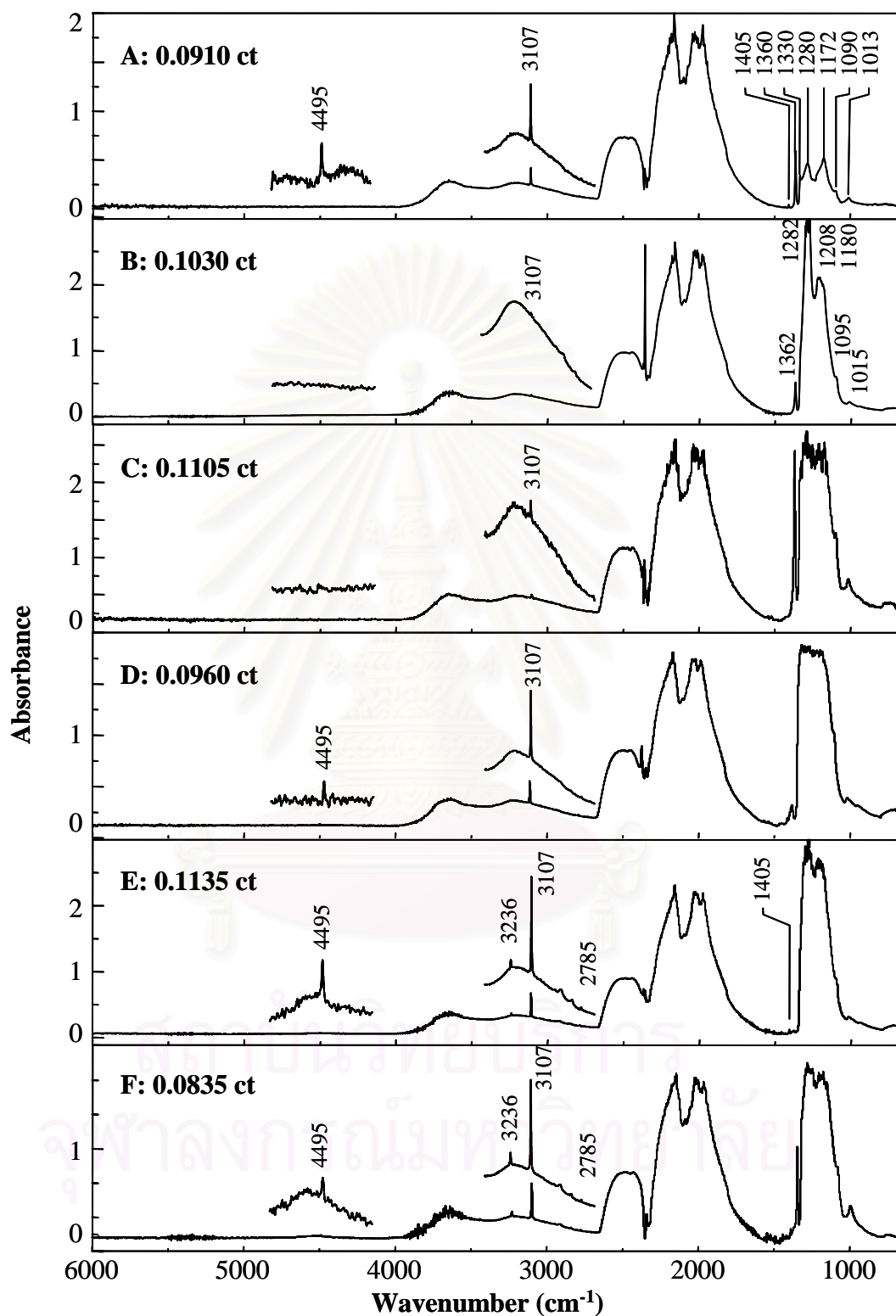


**Figure 4.46** FT-IR spectra of different types of colorless diamonds acquired via transfectance technique.



To ensure the purpose of this section, we additionally measured six colorless faceted diamonds which have the same visual appearance. The spectral feature unique to defects and impurities in diamond crystal structure are clearly observed in the transmittance spectra of six faceted colorless diamonds shown in Figure 4.46. These spectral features could be employed for diamond classification. The natural colorless diamond in Figure 4.46A was identified as a type IaB while that in Figure 4.46B is a type IaA. The type IaB diamond possesses a B-center defect (*i.e.*, an aggregate consists of four nitrogen atoms surrounding a vacancy) which shows absorption band at 1330, 1172 and 1013  $\text{cm}^{-1}$  [13]. An associated absorption band at 1360  $\text{cm}^{-1}$ , which referred to the extended-planar-defect platelets, could also be noticed. The unique absorption bands in the one-phonon region of the type IaA diamond associates with an A-center defect (*i.e.*, a defect consists of a pair of adjacent substitution nitrogen atoms in the diamond lattice). The main absorption has maximum at 1282  $\text{cm}^{-1}$  and additional weak absorptions at 1362, 1208 and 1015  $\text{cm}^{-1}$  [10,37]. Due to the over absorption in the one-phonon region associated with high nitrogen concentration in Figure 4.46C-4.46F, classifications of the diamonds based on spectral information in the one-phonon region are not possible.

According to the transmittance spectrum in Figure 4.45 and 4.46, the unique identification of faceted diamond is derived from their unique carat weight, proportions and transmittance spectrum. Although it is possible that two diamonds have the same physical properties (*i.e.*, color, carat weight, cutting, cut proportions), their transmittance spectra are different. The unique absorption in one-phonon region of transmittance spectrum is strongly dependent on the impurities and/or defect in crystal lattice of diamonds. It should be noted that it is difficult to find two samples with the same number and kind of defects.

In addition, we subsequently determined the transmittance spectra of a diamond under different spectrometers. There are Nicolet Magna 750 infrared spectrometer and Bruker/Equinox-55/106S FT-IR spectrometer. For purposes of spectral comparisons between different spectrometers, the same experimental parameters were utilized on both FT-IR spectrometers. Transmittance spectra of a 0.1075 ct round brilliant cut diamond acquired by the two different FT-IR

spectrometers are shown in Figure 4.47. The observed transmittance spectra from both spectrometers show the same spectral feature. It should be noted that only obvious difference is their spectral intensity. In order to make a comparison, both transmittance spectra were normalized by the absorption at  $2493\text{ cm}^{-1}$  and the normalized spectra was shown in Figure 4.48. The inset of absorptions in one-phonon region shows almost superimposition of their spectral features. The magnitude of absorption is associated with energy throughput and alignment of the instrument. Due to minor variations of the alignment with respect to the incident radiation, negligible discrepancies among transmittance spectra can be noticed. It should be noted that the noticeable different is in the one phonon region with over absorption (*i.e.*, absorption at  $1280\text{ cm}^{-1}$ ). Besides the observed transmittance spectra from two different spectrometers show the same spectral features, the spectra were not affected by the diamond arrangements, as shown in Figure 4.49. It should be noted that the shown transmittance spectra were not normalized.

As all mentioned above, the transmittance spectra of a diamond from different instruments under various gemstones orientation are superimposed. Absorption bands in an infrared spectrum are directly corrected to chemical composition of the diamond. Impurities and defects in an individual diamond make the observed infrared spectrum its unique signature [12,37]. Spectral feature associated with treatment processes (*i.e.*, irradiation and high temperature – high pressure treatments), defects, and impurities in the diamond crystal lattice were clearly observed in the transmittance spectra. When the contribution of its transmittance spectrum was developed, the unique identification of the diamond was revealed. If the combination of the transmittance spectrum and physical properties of a diamond such as color, carat weight, cutting and cut proportions are considered, we will obtain the unique signature of an individual diamond can be established.

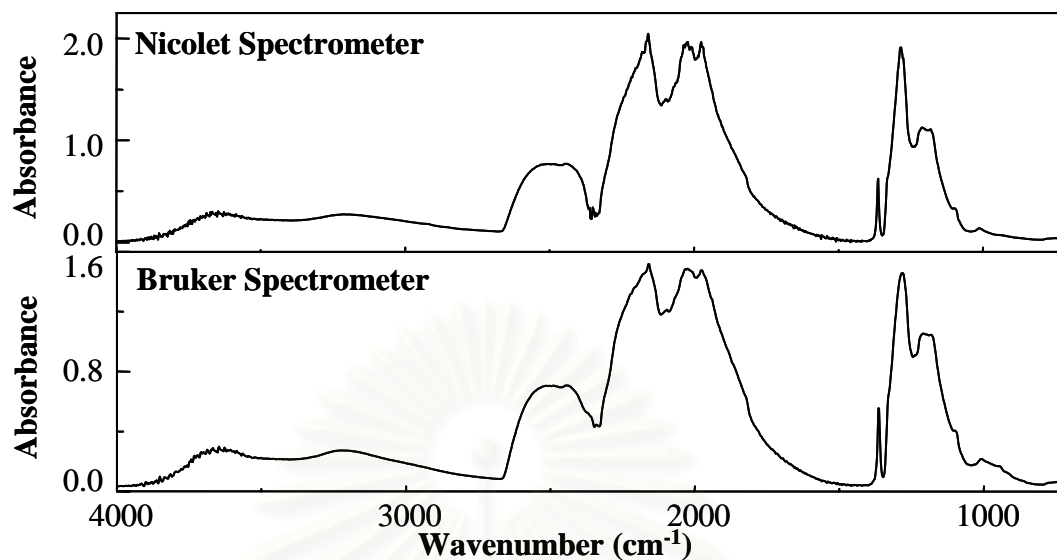


**Figure 4.47** FTIR spectra of a 0.1075 ct round brilliant cut diamond acquired by transmittance technique from different spectrometers.

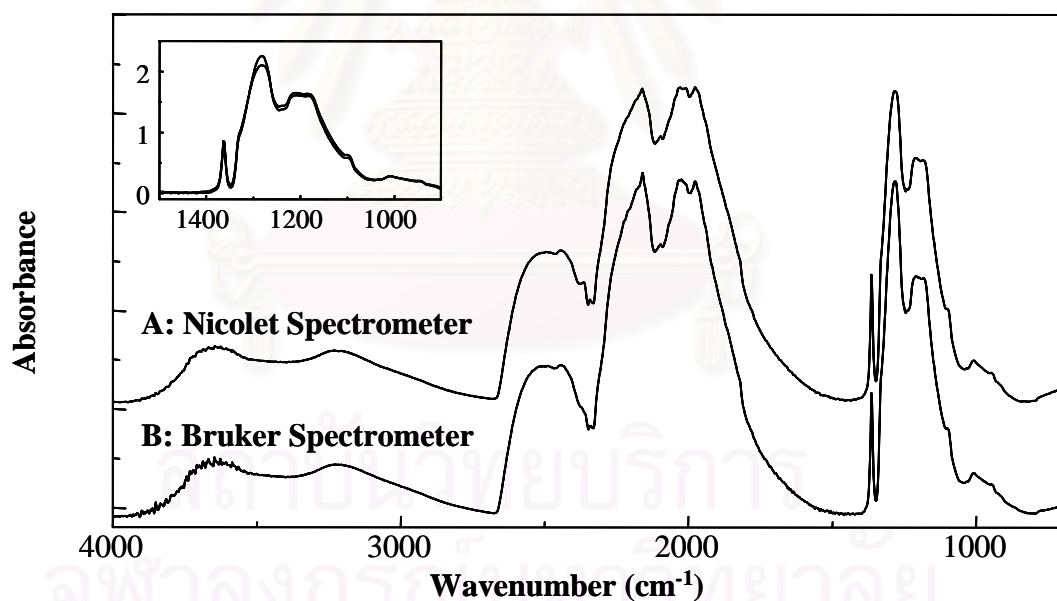


**Figure 4.48** Normalized spectra of the 0.1075 ct round brilliant cut diamond acquired by transmittance technique from different spectrometers. The observed spectra were normalized by the absorption in the two-phonon at  $2493\text{ cm}^{-1}$ . The inset of absorptions in one-phonon region was added for clarity.

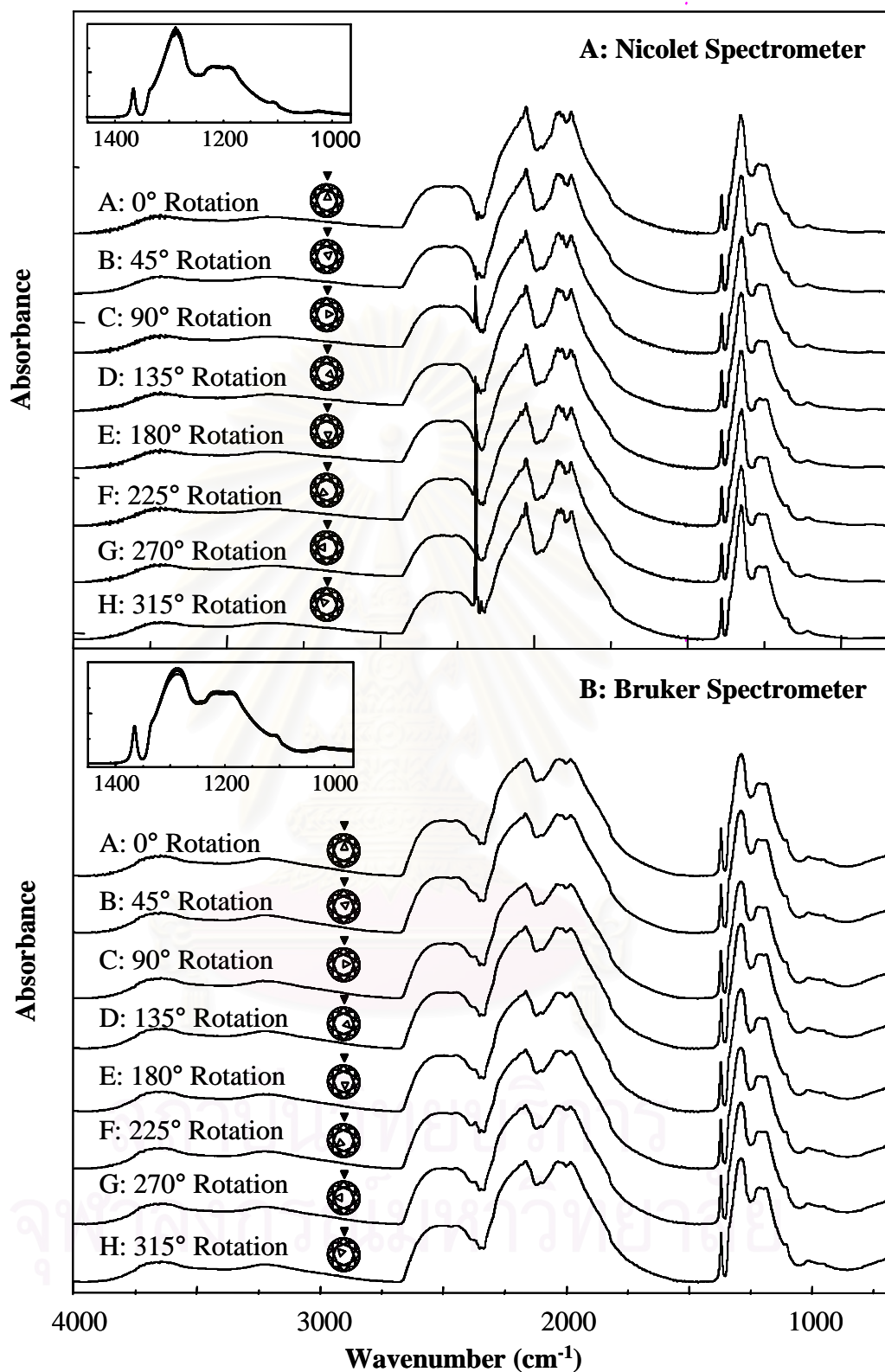


**Figure 4.49** Transflectance spectra of the 0.1075 ct round brilliant cut diamond under different arrangement. The diamond was rotated: 0° (A), 45° (B), 90° (C), 135° (D), 180° (E), 225° (F), 270° (G), and 315° (H) with respect to a reference position. The inset of absorptions in the one-phonon region was added for clarity.

#### 4.4.3.2 Jewelry Analysis

Regarding all observations above, the novel transflectance technique using infrared microscope was successfully employed for spectral acquisition of loose faceted gemstone. Absorption bands unique to impurities, defects in the crystal structures, and treatment processes can be clearly observed [23-25]. The measured spectrum can be exploited for classification and/or determination of the treatment history of the various gemstones [7-12]. Since, the incident radiation is coupled to the faceted gemstone via the table facet, the technique can be employed for characterization of mounted faceted gemstone on jewelry [23]. This section will present the major advantage of the technique for direct spectra acquisition of mounted gemstones on jewelries without taking the gemstones out of the jewelry bodies.

For diamonds with complex setting on jewelry, spectrum of an individual diamond can be selectively measured by the novel transflectance technique. As shown in Figure 4.50, there are five diamonds on the ring: four small diamonds (0.05 ct) and a big diamond (0.20 ct). According to the ring design, the four small diamonds are imbedded in the metal setting. The only observable parts of the diamonds are the table facet, the star facet and parts of the upper girdle facet. As a result, their infrared spectra cannot be acquired by diffuse reflectance or transmission technique. However, the novel transflectance technique enables the collection of all FT-IR spectra of the mounted diamonds. Similar to spectral features of the loose diamond, the three principle absorption bands of the mounted diamonds are clearly observed. Since the spectra in Figure 4.50A were collected without cleaning, strong absorption of accumulate substances on the surface of diamonds due to prolong wearing were clearly observed [23].

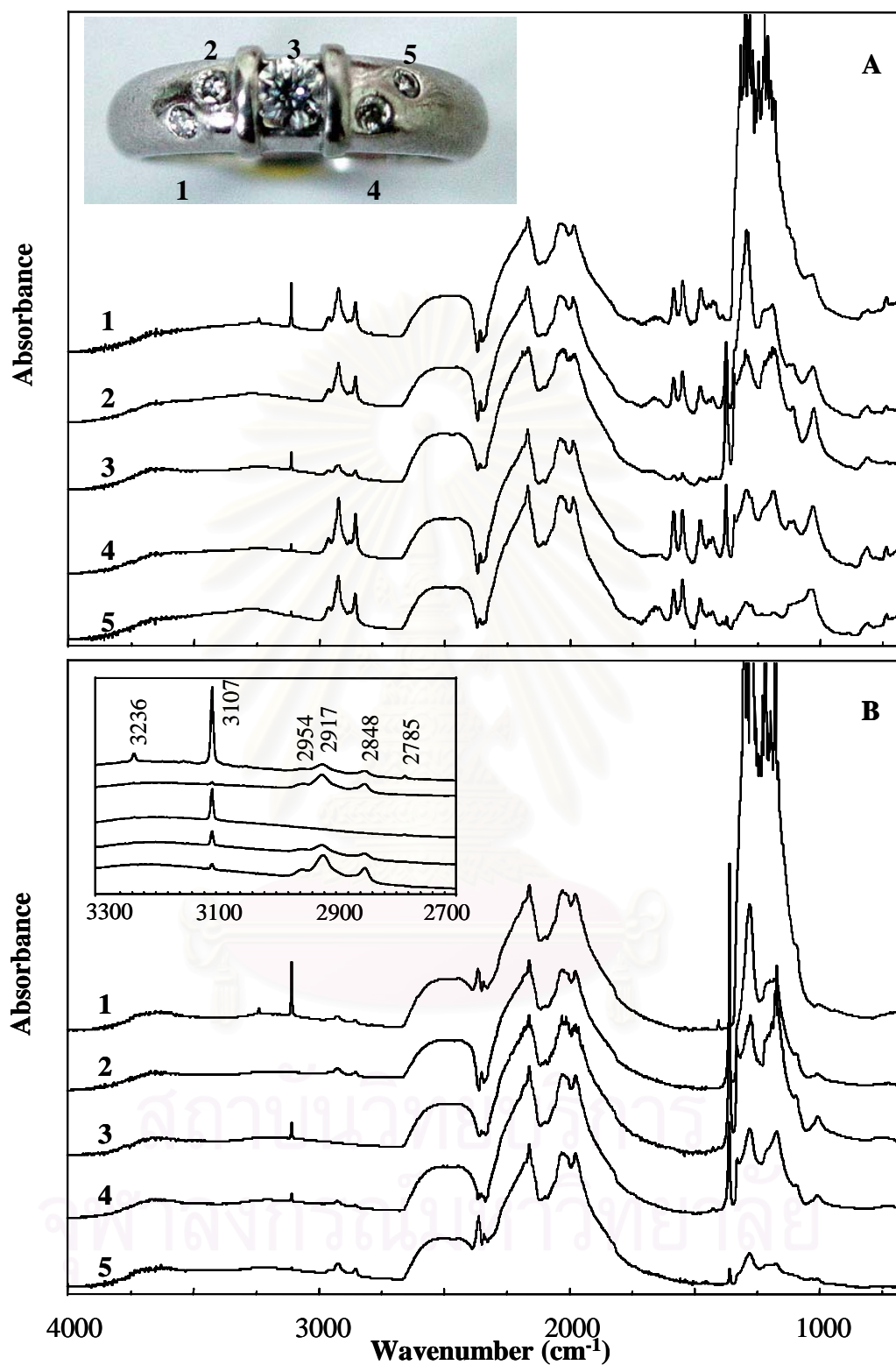


**Figure 4.50** Normalized transfectance spectra of mounted round brilliant cut diamonds on a ring before cleaning (A) and after cleaning (B). The observed spectra were normalized by the absorption in the two-phonon at  $2493 \text{ cm}^{-1}$ . The inset of absorptions in C-H stretching region was added for clarity.

When the big diamond (diamond number 3) was carefully cleaned, the absorption associated with aliphatic hydrocarbon at 2954, 2917, 2848, 1645, 1541 and 1468  $\text{cm}^{-1}$  were disappeared. The small diamonds were more difficult to be cleaned due to ring design with small opening near culet. The unclean surfaces of faceted diamonds are responsible for residual absorptions in the C-H stretching region in Figure 4.50B. According to the spectral feature in the one-phonon region, all diamonds are of different types. The over absorption in the one-phonon region of diamond number 1 indicated that the diamond contains high nitrogen impurity. Although other weak absorption bands associated with hydrogen and nitrogen impurities can be clearly observed, type of the diamond cannot be identified. According to spectral envelopes in the one-phonon region, diamonds number 2-5 are classified as type IaA, IaA/B, IaA/B and IaB, respectively [10-12].

In order to verify the utilization of novel transreflectance technique for characterization of faceted gemstones on jewelry, various types of complex jewelry were also investigated with the technique. The typical results are shown in Figure 4.51, there are one yellow gemstone and five diamonds on the ring. The spectrum of a yellow gemstone can be assigned as the natural yellow sapphire. Similar to spectral features of the loose diamond, the three principle absorption bands of the mounted diamonds are clearly observed. Figure 4.52 compares the obtained spectra of faceted gemstones on a brooch and a ring acquired via transreflectance technique. As clearly be seen, the transreflectance spectrum obtained from a brooch (Figure 4.52A) corresponding to the spectrum of cubic zirconia (CZ), while those obtained from the ring (Figure 4.52B) indicates the characteristic absorption bands of natural diamond. Since the jewelry were collected without cleaning, strong absorption of accumulate substances on the surface of diamonds due to prolong wearing were clearly observed.

Therefore, the distinct advantage of the transreflectance technique over the diffuse reflectance or transmission techniques is its ability to acquire infrared spectra of mounted gemstones on the jewelry without taking the gemstone out of the jewelry setting. An infrared spectrum of an individual gemstone on the complex jewelry setting can be selectively measured. Moreover, the spectral features of the mounted gemstones were not interfered by the metal setting. Although the shown results are

those of the mounted round brilliant cut gemstones, the technique is applicable for any types of gemstones, jewelries, and/or cuttings.

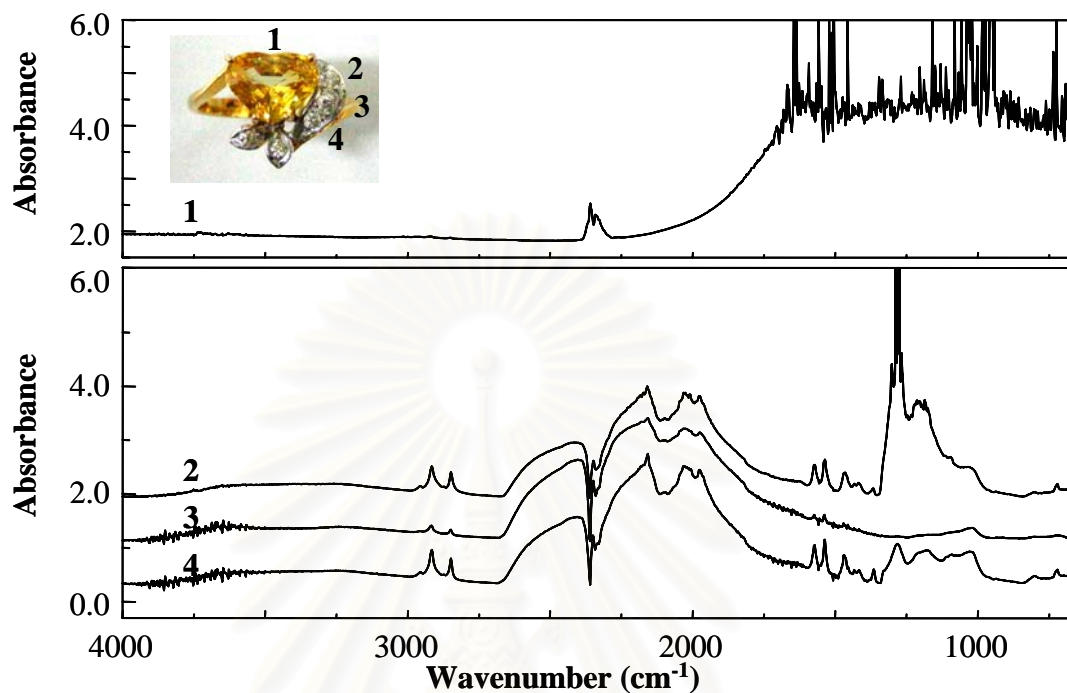


**Figure 4.51** Transflectance spectra of faceted sapphire and diamonds on a ring.

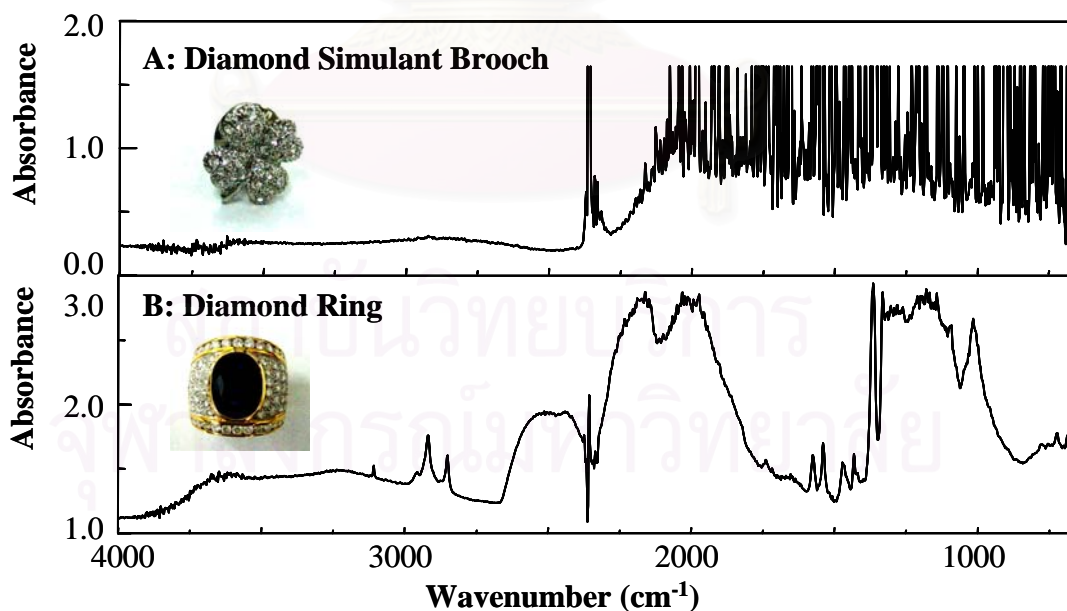


**Figure 4.52** Transflectance spectra of faceted diamond simulant on a brooch and natural diamond on a ring.



## CHAPTER V

### CONCLUSIONS

FT-IR spectroscopy has proven to be a valuable contributor to the characterization of gemstone due to the molecular specific fingerprints of the vibrational spectra. Various FT-IR sampling techniques and accessory designed for specific application and sample form are available. However, different sampling techniques encounter different difficulties.

Transmission is not applicable for faceted gemstone because of its destructive nature and complex reflections of the cut and polished surfaces. Diffuse reflectance measurements of faceted gemstone tend to be non-reproducible since the observed spectral intensity depends strongly on the sample arrangement. Moreover, both transmission and diffuse reflectance techniques are not applicable for mounted gemstones on jewelry bodies. The specular reflectance technique is an available non-destructive technique for characterization of opaque gemstone such as turquoise. The KK transformed spectrum agrees very well with transmission spectrum.

The novel transflectance technique using infrared microscope was successfully employed for spectral acquisition of loose and mounted faceted gemstones. A homemade accessory for adjusting the reflection plane of the faceted gemstone was constructed and was utilized with the infrared microscope. The technique is nondestructive, provides unambiguous results, requires no sample preparation, and has short analysis time. The incident radiation is coupled to the diamond via the table facet while the transflectance radiation is collected by the built-in 15X Cassegrainian objective. The same spectra features with better spectral quality as those from the well-accepted diffuse reflectance technique are observed. Unlike the diffuse reflectance spectrum, the transflectance spectrum is not altered by the sample arrangements. The technique can be employed for both isotropic and anisotropic gemstones. Absorption bands unique to impurities, defects in the crystal structures, and treatment processes can be clearly observed. The measured spectrum can be

exploited for classification and/or determination of the treatment history of the gemstones. As a result, the transfectance technique can be employed for characterization of various gemstones and differentiating between their natural, simulant, and synthetic counterpart.

Nevertheless, the technique encounter some limitation depends strongly on the physical and optical properties of analyzed sample. The maximum thickness that can be performed with transfectance technique is approximately 8 mm. The technique can not be employed for opaque gemstone and poor-cut proportion gemstones because the translected radiation cannot be collected.

A novel technique of gemstone identification using the combination of infrared spectrum and physical properties of a diamond (i.e., carat weight, cut shape, cut proportions) as the unique signature of the diamond was developed. The transfectance spectra of a diamond from different instruments under various gemstones orientation are superimposed. Impurities and defects in an individual diamond make the observed infrared spectrum its unique signature. When combine the transfectance spectrum and physical properties of a diamond such as color, carat weight, cut shape and cut proportions, the unique identification of the diamond was revealed. This procedure can apply to other gemstones and jewelry to identify the individual specimen.

Finally, the distinct advantage of the transfectance technique over the diffuse reflectance or transmission techniques is its ability to acquire infrared spectra of mounted gemstones on the jewelry without taking the gemstone out of the jewelry setting. The homemade accessory composes of several sample holder which suitable for various sizes of loosed gemstones and jewelries. An infrared spectrum of an individual gemstone on the complex jewelry setting can be selectively measured. Moreover, the spectral features of the mounted gemstone were not interfered by the metal setting. The technique is applicable for any types of gemstones, jewelries, and/or cut shape.

## REFERENCES

1. Petkewich, A. Finding a Real Gem. Anal. Chem. 75 (2003): 71A-74A.
2. Jayaraman, A. A Brief Overview of Gem Materials: Natural and Synthetic. Curr. Sci. 79 (2000): 1555-1565.
3. Shigley, J. E. Treated and Synthetic Gem Materials. Curr. Sci. 79 (2000): 1566-1571.
4. Read, P. G. Gemmology. Oxford: Butterworth-Heinemann, 1995.
5. Liddicoat, R. T. Jr. Handbook of Gem Identification. 12<sup>th</sup> ed. California: Gemological Institute of America, 1987.
6. Nassau, K. Synthetic Moissanite: A New Man Made Jewel. Curr. Sci. 79 (2000): 1572-1577.
7. Fritsh, E.; and Stockton, C. M. Infrared Spectroscopy in Gem Identification. Gems. Gemology. Spring (1987): 18-26.
8. Tretyakova, L. I.; Reshetnyak, N. B.; and Yu. Tretyakova, V. A Combined Spectroscopic Method for Non-destructive Gem Identification. J. Gemm. 25 (1997): 532-539.
9. Martin, F.; Merigoux, H.; and Zecchini, P. Reflectance Infrared Spectroscopy in Gemology. Gems. Gemology. Winter (1989): 226-231.
10. Ferrer, N.; and Jogués-Carulla, J. M. Characterization Study of Cut Gem Diamond by IR Spectroscopy. Diam. Relat. Mater. 5 (1996): 598-602.
11. Fernandes, S.; Khan, M.; and Choudhary, G. A. Compilation of Infrared Absorption Spectra of Some Specific Gemstones. Australian Gemmologist 1Q (2003): 361-367.
12. Mendelssohn, M. J.; and Milledge, H. J. Geologically Significant Information from Routine Analysis of the Mid-Infrared Spectra of Diamonds. Int. Geol. Rev. 37 (1995): 95-110.
13. Iakoubovskii, K.; and Adiaenssens, G. J. Optical Characterization of Natural Argyle Diamond. Diam. Relat. Mater. 11 (2002): 125-131.
14. Jenkins, A. L.; and Larsen, R. A. Gemstone Identification Using Raman Spectroscopy. Spectroscopy 19 (2004): 20-25.

15. Kirui, J. K.; Van Wyk, J. A.; and Hoch, M. J. R. ESR Studies of the Negative Deviancy in Irradiated Type-I Diamonds. Diam. Relat. Mater. 8 (1999): 1569-1571.
16. Lai, P. F.; Prawer, S.; and Noble, C. Electron Spin Resonance Investigation of Ion-Irradiated Diamond. Diam. Relat. Mater. 11 (2002): 1391-1396.
17. Kupriyanov, I. N.; Gusev, V. A.; Borzdov, Y. M.; Kalinin, A. A. and Palyamov, Y. N. Photoluminescence Study of Annealed Nickel and Nitrogen-Containing Synthetic Diamond. Diam. Relat. Mater. 8 (1999): 1301-1309.
18. Lindblom, J.; Hölsä, J.; Papunen, H.; Häkkänen, H.; and Mutanen, J. Differentiation of Natural and Synthetic Gem-Quality Diamond by Luminescence Properties. Opt. Mater. 24 (2003): 243-251.
19. Collins, A. T. Spectroscopy of Defects and Transition Metals in Diamond Diam. Relat. Mater. 9 (2000): 417-423.
20. Clark, C. D.; Collins, A. T.; and Woods, G. S. The Properties of Natural and Synthetic Diamond. London: Academic Press, 1992.
21. Woods, G. S.; and Collins, A. T. The  $1450\text{ cm}^{-1}$  Infrared Absorption in Annealed, Electron-Irradiated Type I Diamonds. J. Phys. C: Solid State Phys. 15 (1982): L949-L952.
22. Reinitz, I. M.; Fritsch, E.; and Shigley, J. E. An Oscillating Visible Light Optical Center in Some Natural Green to Yellow Diamonds. Diam. Relat. Mater. 7 (1998): 313-316.
23. Egkasit, S.; and Thongnopkun, P. Transflectance Spectra of Faceted Diamonds Acquired by Infrared Microscopy. Appl. Spectrosc. 59 (2005): 1160-1165
24. Egkasit, S.; and Thongnopkun, P. Novel Attenuated Total Reflection Fourier Transform Infrared Microscopy Using a Gem Quality Diamond as an Internal Reflection Element. Appl. Spectrosc. 59 (2005): 1236-1241.
25. Thongnopkun, P.; and Egkasit, S. FTIR Spectra of Faceted Diamonds and Diamond Simulants. Diam. Relat. Mater. 14 (2005): 1592-1599.
26. Urban, M. W. Attenuated Total Reflectance Spectroscopy of Polymer: Theory and Practice. Washington: American Chemical Society, 1996.

27. Smith, B. C. Fundamentals of Fourier Transform Infrared Spectroscopy. New York: CRC Press, 1996.
28. Coleman, P. B. Practical Sampling Techniques for Infrared Analysis. London: CRC Press, 1993.
29. Chalmers, J. M.; Overall, N. J.; and Ellison, S. Specular Reflectance: A Convenient Tool for Polymer Characterization by FTIR-Microscopy. Micron. 27 (1996): 315-328.
30. Fuller, M. P.; and Griffiths, P. R. Diffuse Reflectance Measurements by Infrared Fourier Transform Spectrometry. Anal. Chem. 50 (1978): 1906-1910.
31. Katon, J. E. Infrared Microspectroscopy: A Review of Fundamentals and Applications. Micron. 27 (1996): 303-314.
32. Wilhelm, P. Application of FT-IR Microscopy with Materials Analyse. Micron. 27 (1996): 341-344.
33. Yan, G.; Jingzhi, L.; and Beili, Z. The Infrared Microscope and Rapid Identification of Gemstones. J. Gemm. 24 (1995): 411-415.
34. Green, B.; Reinitz, I.; Johnson, M.; and Shigley, J. Diamond Optics Part 1: Reflection, Refraction and Critical Angle. [Online] (n.d.). Available from: [www.gia.edu/html](http://www.gia.edu/html).
35. Hemphill, T. C.; Reinitz, I. M.; Johnson, M. L.; and Shigley, J. E. Modeling the Appearance of the Round Brilliant Cut Diamond: An Analysis of Brilliance Gems. Gemology. 34 (1998): 158-183.
36. Reinitz, I. M.; Johnson, M. L.; Hemphill, T. C.; Gilbertson, A. M.; Geurts, R. H.; and Green, D. B. Modeling the Appearance of the Round Brilliant Cut Diamond: An Analysis of Fire, and More About Brilliance. Gems. Gemology. 37 (2001): 174-197.
37. Briddon, P. R.; and Jones, R. Theory of Impurities in Diamond. Physica. B 185 (1993): 179-189.
38. Karl, S.; and Lore, K. Water in Beryl – a Contribution to the Separability of Natural and Synthetic Emeralds by Infrared Spectroscopy. J. Gemm. 22 (1990): 215-223.
39. De Donato, P.; Cheilletz, A.; Barres, O.; and Yvon, J. Infrared Spectroscopy of OD Vibrators in Minerals at Natural Dilution: Hydroxyl Groups in

- Talc and Kaolinite, and Structural Water in Beryl and Emerald. Appl. Spectrosc. 58 (2004): 521-527.
40. Charoy, B.; De Donato, P.; Barres, O.; and Pinto-Coelho, C. Channel Occupancy in an Alkali-Poor Beryl from Serra Branca (Goias, Brazil): Spectroscopic Characterization. Am. Mineral. 81 (1996): 395-403.
  41. Koivula, J. I.; Kammerling, R. C.; DeGhionno, D.; Reinitz, I.; Fritsch, E.; and Johnson, M. L. Gemological Investigation of a New Type of Russian Hydrothermal Synthetic Emerald. Gems. Gemology. Spring (1996): 32-29.
  42. Mashkovtsev, R. I.; and Solntsev, V. P. Channel Constituents in Synthetic Beryl: Ammonium. Phys. Chem. Minerals. 29 (2002): 65-71.
  43. George, M.; Karanth, R. V.; Gundu Rao, T. K.; Deshpande, R. S. Maxixe-Type Colour Centre in Natural Colourless Beryl from Orissa, India: An ESR and OA Investigation. J. Gemm., 26 (1998): 238-251.
  44. John, I. K.; Robert, C. K.; Dino, D.; Ilene, R.; Emmanuel, F.; and Mary, L. J. Gemological Investigation of a New Type of Russian Hydrothermal Synthetic Emerald. Gems. Gemology. Spring (1996): 32-40.
  45. Gordon, E. B.; and Bradford, A. High-Temperature Structure and Crystal Chemistry of Hydrous Alkali-Rich Beryl from the Harding Pegmatite, Taos Count, New Mexico. Am. Mineral. 71 (1986): 547-556.
  46. Pulz, G. M.; Rey Silva, L. J. H.; and Silva, J. J. The Chemical Signature of Emeralds from the Campos Verdes-Santa Terezinha Mining District, Goias, Brazil. J. Gemm. 26 (1998): 252-261.
  47. Kiefert, L.; Hänni, H.A.; Chalain, J-P.; and Weber, W. Identification of Filler Substances in Emeralds by Infrared and Raman Spectroscopy. J. Gemm. 26 (1999): 501-520.
  48. Stockton, C. M. The Separation of Natural from Synthetic Emeralds by Infrared Spectroscopy. Gems. Gemology. Summer (1987): 96-99.
  49. Charoy, B.; De Donato, P.; Barres, O.; and Pinto-Coelho, C. Channel Occupancy in an Alkali-Poor Beryl from Serra Branca (Goias, Brazil): Spectroscopic Characterization. Am. Mineral. 81 (1996): 395-403.
  50. Henn, U.; and Milisenda, C. C. Synthetic Red Beryl from Russia. J. Gemm. 26 (1999): 481-486.

51. Marcos-Pascual, C.; and Moreiras, D. B. Characterization of Alexandrite, Emerald and Phenakite from Franqueira (NW Spain). J. Gemm. 25 (1997): 340-357.
52. Fumagilli, M.; Proserpi, L.; Pavese, A.; and Bordiga, S. Natural versus Hydrothermal Synthetic Russian Red Beryl: Chemical Composition and Spectroscopic Measurements. J. Gemm. 28 (2003): 291-301.
53. Smith, C. P. A Contribution to Understanding the Infrared Spectra of Rubies from Mong Hsu, Myanmar. J. Gemm. 24 (1995): 321-335.
54. Siripaisarnpipat, S.; Pattharakorn, T.; Pattharakorn, S.; Sanguanruang, S.; Koonsaeng, N.; Achiwawanich, S.; Promsurin, M.; and Hanmungthum, P. Spectroscopic Properties of Mong Hsu Ruby. Australian Gemmologist. 21 (2002): 236-241.
55. Koivula, J. I. Carbon Dioxide Fluid Inclusions as Proof of Natural-Colored Corundum. Gems. Gemmology. Fall (1986): 152-155.
56. Kubichki, J. D.; and Apitz, S. E. Molecular Cluster Models of Aluminum Oxide and Aluminum Hydroxide Surface. Am. Mineral. 83 (1998): 1054-1066.
57. Ruan, H. D.; Frost, R. L.; and Klorpogge, J. T. Application of Near-Infrared Spectroscopy to the Study of Alumina Phases. Appl. Spectrosc. 55 (2001): 190-196.
58. Frost, R. L.; Klorpogge, J. T.; Kussell, S. C.; and Szetu, J. L. Vibrational Spectroscopy and Dehydroxylation of Aluminum (Oxo)hydroxides: Gibbsite. Appl. Spectrosc. 53 (1999): 423-434.
59. Wang, S. L.; and Johnston, C. T. Assignment of the Structural OH Stretching Bands of Gibbsite. Am. Mineral. 85 (2000): 739-744.
60. Kronenberg, A. K.; Castaing, J.; Mitchell, T. E.; and Kirby, S. H. Hydrogen Defect in  $\alpha$ -Al<sub>2</sub>O<sub>3</sub> and Water Weakening of Sapphire and Alumina Ceramics between 600 and 1000°C – I: Infrared Characterization of Defects. Acta. Mater. 48(2000): 1481-1494.
61. Frederickson, L. D. Jr. Characterization of Hydrated Aluminas by Infrared Spectroscopy: Application to Study of Bauxite Ores. Anal. Chem. 26 (1954): 1883-1885.

62. Lijian, Q.; Weixuan, Y.; and Mingxin, Y. Turquoise from Hubei Province, China. J. Gemm. 26 (1998): 1-12.
63. Daniel, W. A.; Xiande, W.; Beesley, C. R.; and Ronald, R. Analysis of Fissure – Filled Turquoise, Emeralds, and Rubies by Near – Infrared Spectroscopy. American Laboratory October (1999): 41-47.
64. Lind, Th.; Schmetzer, K.; and Bank, H. The Identification of Turquoise by Infrared Spectroscopy and X-ray Powder Diffraction. Gems. Gemology. Fall (1983): 164-168.
65. Clark, C. D.; and Davey, S. T. Defect-Induced One-Phonon Absorption in Type Ia Diamonds. J. Phys. C: Solid State Phys. 17 (1984): L399-L403.
66. Kiflawi, I.; Mainwood, A.; Kanda, H.; and Fisher, D. Nitrogen Interstitials in Diamond. Phys. Rev. B 54 (1996): 16719-16726.
67. Kiflawi, I.; Davies, G.; Fisher D.; and Kanda, H. New Infrared Absorption Centres in Electron Irradiated and Annealed Type Ia Diamonds. Diam. Relat. Mater. 8 (1999): 1576-1580.
68. Collins, A. T.; Davies, G.; and Woods, G. S. Spectroscopic Studies of the H1b and H1c Absorption Lines in Irradiated, Annealed Type-Ia Diamonds. J. Phys. C 19 (1986): 3933-3944.
69. De Weerd, F.; Palyanov, Y. N.; and Collins, A. T. Absorption Spectra of Hydrogen in <sup>13</sup>C Diamond Produced by High-Pressure, High-Temperature Synthesis. J. Phys: Condens. Matter. 15 (2003): 3163-3170.
70. De Weerd, F.; and Van Royen, J. Investigation of Seven Diamonds, HPHT Treated by NovaDiamond. J. Gemm. 27 (2000): 201-208.
71. Vins, V. G.; and Kononov, O. V. A Model of HPHT Color Enhancement Mechanism in Natural Gray Diamonds. Diam. Relat. Mater. 12 (2003): 542-545.
72. De Weerd, F.; and Van Royen, J. Defects in Colored Natural Diamonds. Diam. Relat. Mater. 10 (2001): 474-479.





**APPENDICES**

สถาบันวิทยบริการ  
จุฬาลงกรณ์มหาวิทยาลัย

**APPENDIX A**

FTIR Spectra of Faceted Diamonds and Diamond Simulants

Pimthong Thongnopkun and Sanong Ekgasit

Diamond and Related Materials (2005) 14: 1592 – 1599.

สถาบันวิทยบริการ  
จุฬาลงกรณ์มหาวิทยาลัย



# FTIR Spectra of faceted diamonds and diamond simulants

Pimthong Thongnopkun, Sanong Ekgasit \*

*Sensor Research Unit, Department of Chemistry, Faculty of Science, Chulalongkorn University, Bangkok 10330, Thailand*

Received 6 January 2005; received in revised form 23 March 2005; accepted 26 March 2005

Available online 27 June 2005

## Abstract

FTIR spectra of faceted diamonds and diamond simulants collected by diffuse reflectance, transreflectance, and specular reflection techniques were compared. The transreflectance technique exploited total internal reflection phenomenon within the faceted diamond for the spectral acquisition. The transreflectance spectra were similar to the well-accepted diffuse reflectance spectra with equal or better spectral qualities. Based on the observed spectral features of the faceted diamond, classification of the diamond, determination of defects, impurities, and treatment process (i.e., irradiation and high pressure and high temperature) can be performed.

© 2005 Elsevier B.V. All rights reserved.

*Keywords:* Faceted diamond; Diamond simulant; Infrared spectroscopy; Diffuse reflectance; Transreflectance; Specular reflection

## 1. Introduction

In the recent years, synthetic gemstones with the same chemical composition as the natural gemstones were encountered. In many cases, they cannot be differentiated from their natural counterparts by the conventional characterization techniques such as refractive index, hardness, color, specific gravity, and light dispersion measurements. Beside the synthetic gemstones, there are various gemstone simulants of different chemical composition with similar appearances to those of the natural gemstones. Moreover, various treatments (i.e., irradiation, heat, and high pressure-high temperature (HPHT) treatments) were normally applied to the low quality gemstones in order to improve their appearances (i.e., eliminate inclusion, enhance color, and improve clarity) [1–3]. Due to their distinct commercial values, it is important for gemologist to correctly identify synthetic, natural, and treated gemstones.

Owing to its mystic belief, popularity and commercial value, diamond is probably the most imitated of all

gemstones. Common diamond simulants included cubic zirconia (CZ), colorless synthetic corundum (sapphire), synthetic spinel, strontium titanate, yttrium aluminium garnet (YAG), gadolinium gallium garnet (GGG), and synthetic moissanite. Some of the simulants can be identified by standard gemological characterization techniques, others cannot [4]. HPHT treatment, where diamond color is altered due to changes of defects in the diamond crystal lattice, has brought a completely new threat to the gems and jewelry industry [1,3]. Detection of the treatment processes has become a major task for diamond grading laboratories, especially faceted diamonds where nondestructive characterization techniques are required. Advance analytical techniques providing information associated with chemical structures and compositions such as Fourier transform infrared (FTIR) spectroscopy [5–8], Raman spectroscopy [9], electron spin resonance (ESR) spectroscopy [10,11], and photoluminescence spectroscopy [8,12–14] are necessary for gemstone characterization.

FTIR spectroscopy is well known for its molecular related spectral information. FTIR spectral fingerprints provide information directly related to chemical structure, chemical compositions and impurities in the analyzed materials. The technique was employed for diamond

\* Corresponding author. Tel.: +662 218 7585; fax: +662 254 1309.

*E-mail address:* [sanong.e@chula.ac.th](mailto:sanong.e@chula.ac.th) (S. Ekgasit).

classification based on impurities (i.e., nitrogen, hydrogen and boron) in the diamond crystal lattice [5,7]. It was also employed for differentiating diamond simulants from natural diamonds as well as determining the treatment processes applied onto the diamonds [15,16]. However, conventional infrared characterization techniques encountered several problems that make them unsuitable for routine analysis of faceted diamond. The classical transmission measurement using a thin slab of diamond [5–8] is not suitable for faceted diamonds due to its destructive nature and complex reflections of the cut and polished surfaces. Transmission measurement of a faceted diamond using beam condenser is complicated by sample arrangement where the coupled infrared radiation must pass through girdle [17,18]. Diffuse reflectance measurements of faceted diamonds tend to be non-reproducible since the spectral intensity depends strongly on the diamond orientation within the sample holder [5,19].

In order to solve the problems associated with characterization of faceted diamond and diamond simulants, a novel nondestructive transfectance technique for FTIR spectral acquisition using an infrared microscope was developed. The transfectance spectra were compared to the well-accepted diffuse reflectance and specular reflectance spectra. Spectral features associated with structures, impurities, and treatment processes were discussed.

## 2. Experimental

The measured samples were gems quality faceted diamonds (0.105 ct type IaB, 0.207 ct type IaA, 0.078 ct HPHT-treated and 0.144 ct irradiated and annealed diamonds) and diamond simulants (0.150 ct synthetic moissanite, 1.880 ct CZ, 2.010 ct GGG, 1.480 ct YAG, 1.780 ct strontium titanate, 1.100 ct synthetic sapphire, 1.350 ct synthetic rutile, and 1.250 ct synthetic spinel). The gemstones were characterized as received without an additional sample preparation except cleaning. All FTIR spectra were acquired by a Nicolet Magna 750 FTIR spectrometer equipped with a mercury–cadmium–telluride (MCT) detector. A spectral resolution of  $4\text{ cm}^{-1}$  with 512 co-addition scans was employed. The observed spectra ( $6000\text{--}650\text{ cm}^{-1}$ ) were baseline corrected before further analysis.

A commercial diffuse reflectance accessory (Collector, Spectra-Tech Inc., USA) was employed for all diffuse reflectance measurements. A faceted gemstone was placed on the sample holder with the table facet faced down, the infrared radiation was coupled into the gemstone at a near normal angle of incidence. The diffuse reflected radiation was then collected while the absorption of the gemstone was expressed in terms of Kubelka-Munk unit [20,21]. Since the observed diffuse reflectance spectrum

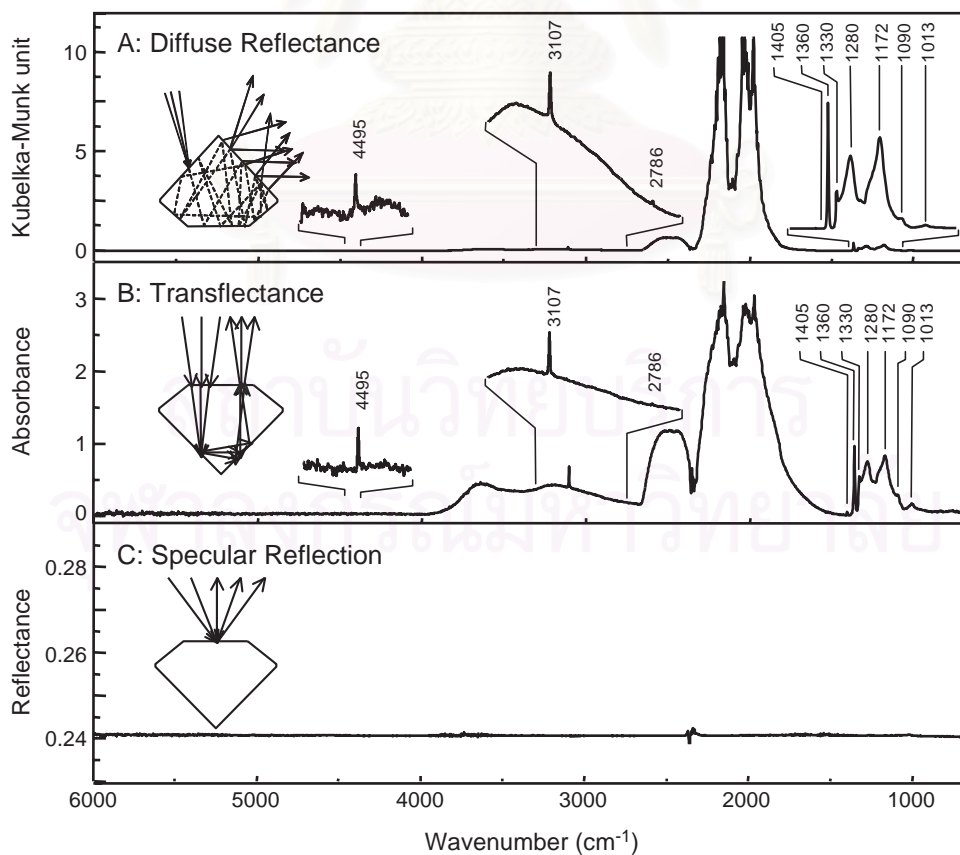


Fig. 1. FTIR spectra of a 0.105 ct round brilliant cut type IaB natural diamond acquired by (A) diffuse reflectance, (B) transfectance, and (C) specular reflection techniques.

was greatly influenced by the gemstone arrangements, several spectra with different gemstone arrangements were collected. The observed spectrum with the best signal-to-noise ratio was employed for further spectral analysis.

The transreflectance and specular reflection spectra of the same gemstone were collected by a NICPLAN infrared microscope attached to the FTIR spectrometer. The microscope was also equipped with an MCT detector. A home-made accessory was employed for all spectral acquisitions

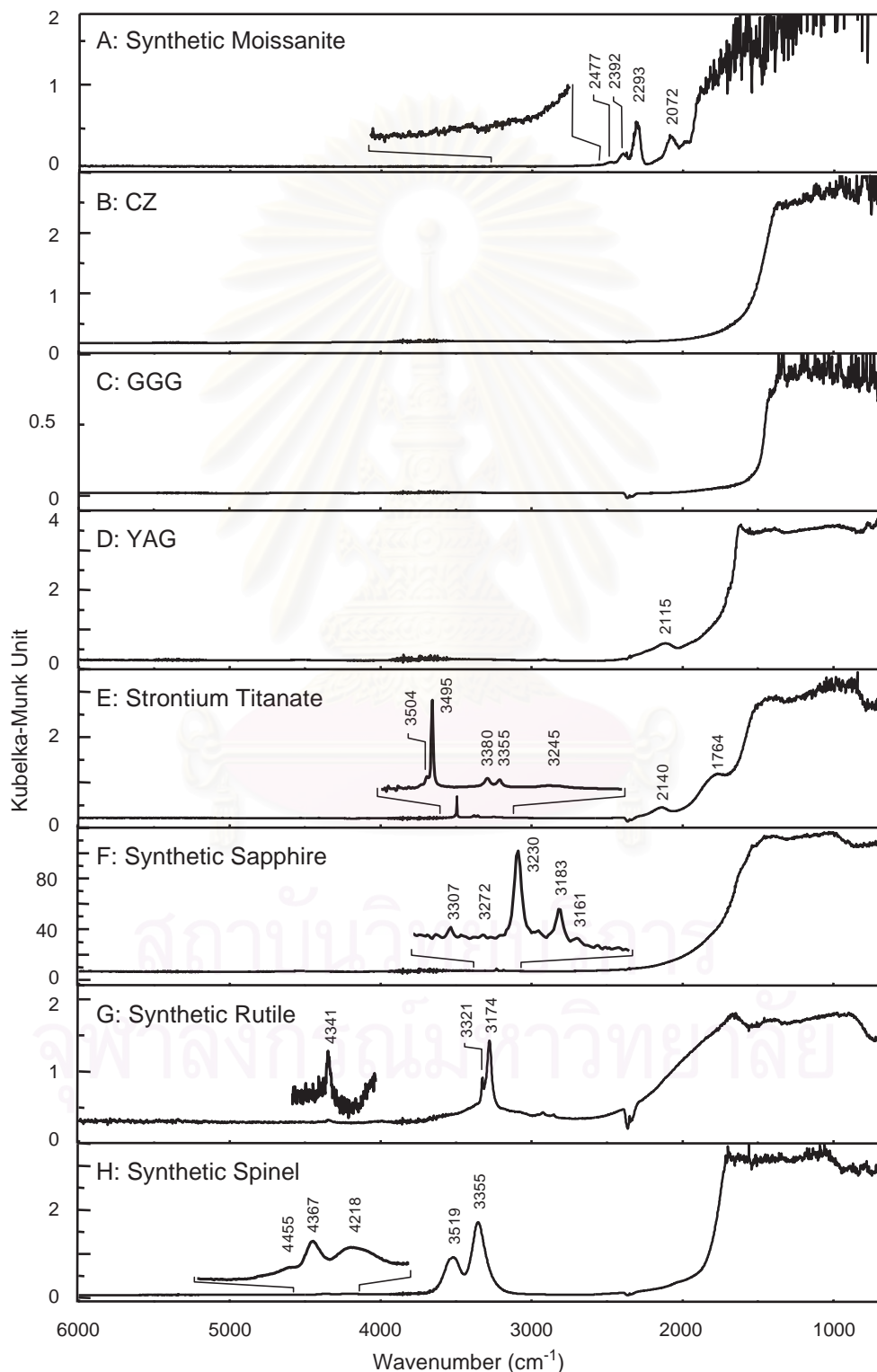


Fig. 2. FTIR spectra of round brilliant cut diamond simulants acquired by diffuse reflectance technique.

using the microscope. The faceted gemstone was placed on the sample holder with the table facet faced up perpendicularly to the infrared radiation from the built-in 15X Cassegrainian objective. The incident radiation is coupled into the gemstone while the reflected radiation from the

gemstone is collected by the objective. The specular reflection spectrum at the table facet was collected from the reflected radiation while the transmittance spectrum was collected from the total internal reflected radiation at the normal angle of incidence.

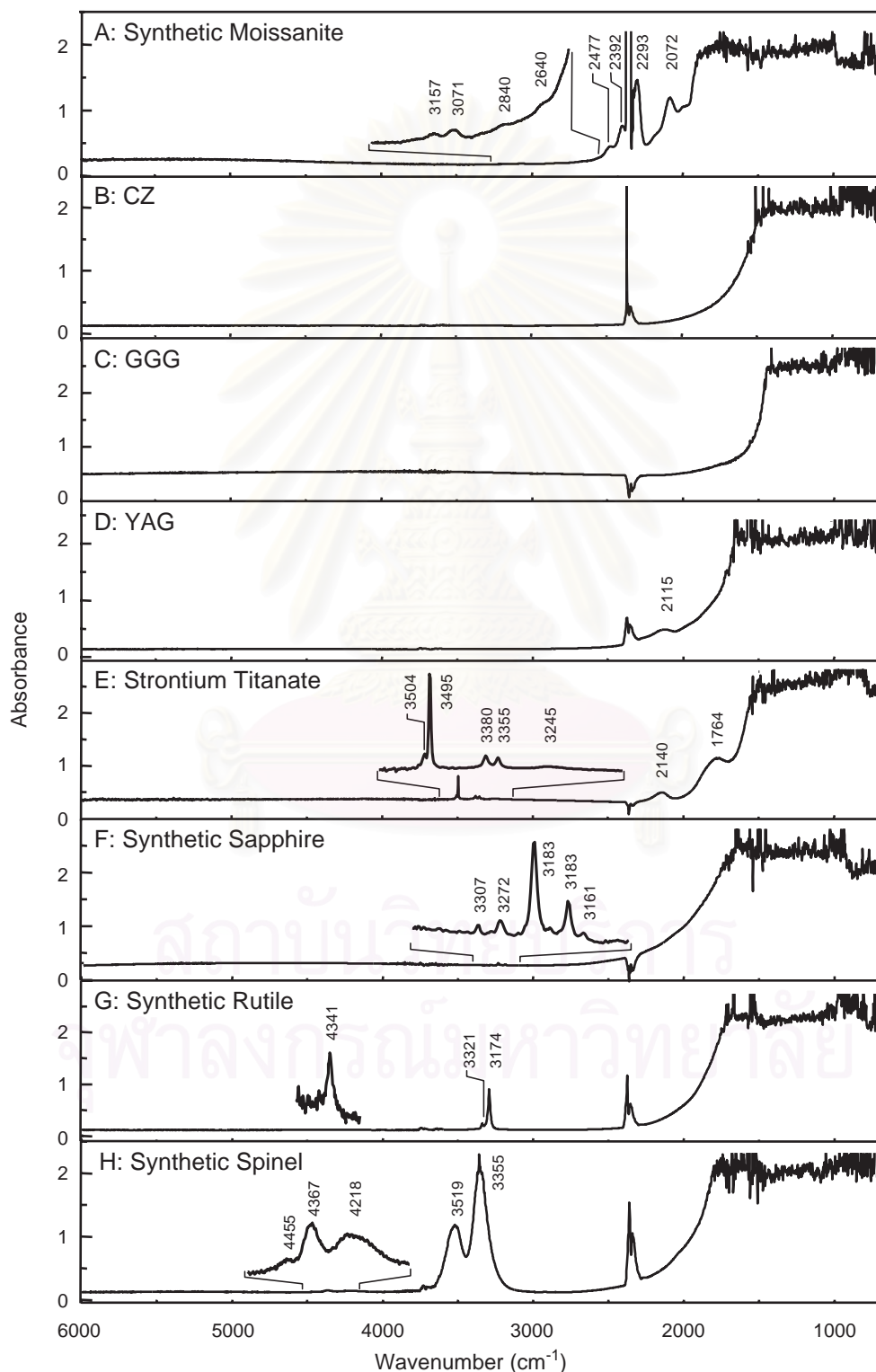


Fig. 3. FTIR spectra of round brilliant cut diamond simulants acquired by transmittance technique.

### 3. Results and discussion

Spectra of a 0.105 ct type IaB round brilliant cut diamond are shown in Fig. 1. The diffuse reflectance and transmittance spectra clearly reveal the three principle

absorption bands of diamond (i.e., three-phonon absorption at  $3900\text{--}2650\text{ cm}^{-1}$ , two-phonon absorption at  $2650\text{--}1500\text{ cm}^{-1}$ , and one-phonon absorption at  $1400\text{--}900\text{ cm}^{-1}$ ) [22]. The high noise level at the peak maxima of the two-phonon region indicates saturated absorption. This is due to the high

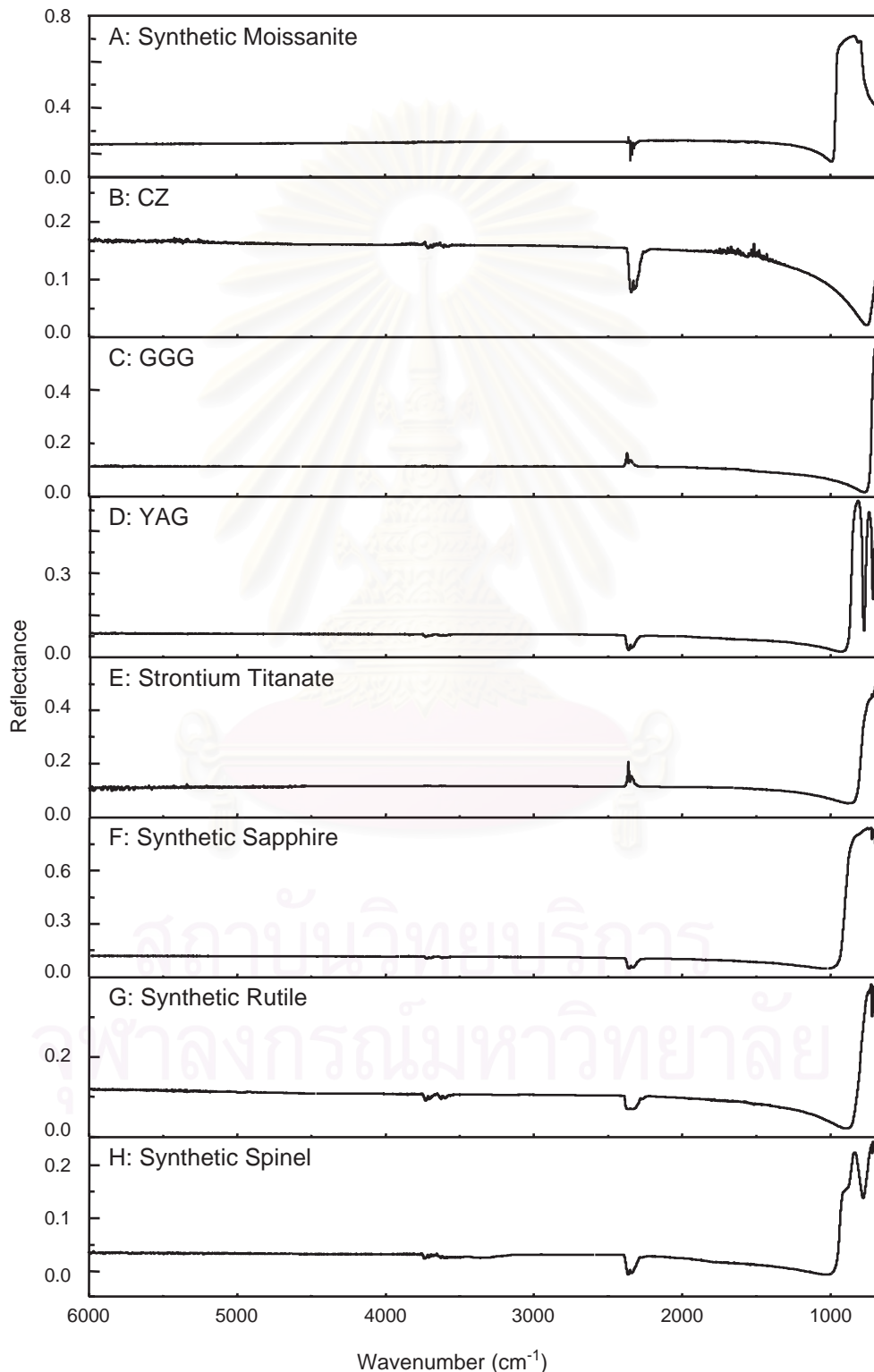


Fig. 4. FTIR spectra of round brilliant cut diamond simulants acquired by specular reflection technique.

absorption coefficient of diamond in that region. The absorption bands associated with hydrogen impurity and nitrogen impurity in the diamond crystal structure are clearly observed in diffuse reflectance and transmittance spectra. The hydrogen-impurity-related absorptions at 4495, 3107, 2786 and 1405  $\text{cm}^{-1}$  are assigned to the vinylidene group. The weak absorptions at 1330, 1172 and 1013  $\text{cm}^{-1}$  are due to B-nitrogen complex [8]. An associated absorption band at 1360  $\text{cm}^{-1}$ , which referred to the extended-planar-defect platelets, could also be noticed. The specular reflection spectrum, on the other hand, does not show any prominent absorption feature. It should be noted that the absorptions of water vapor (3900–3500 and 1800–1400  $\text{cm}^{-1}$ ) and carbon dioxide gas (2400–2300  $\text{cm}^{-1}$ ) can be noticed in all measured spectra. The variations of the

absorption magnitudes are due to the fluctuation of the ambient air during the spectral acquisition.

Spectra of faceted diamond simulants acquired by diffuse reflectance, transmittance and specular reflection techniques, respectively, are shown in Figs. 2–4. The spectral envelopes of the transmittance spectra are similar to those of the diffuse reflectance spectra. In the lower wavenumber region, saturation is observed in the diffuse reflectance and transmittance spectra. The specular reflection spectra, on the other hand, show refractive-index type spectral features. This is due to the high absorption coefficient of the gemstones in the low wavenumber region. Although the exact positions of the absorption maxima in that region cannot be identified from the diffuse reflectance nor transmittance spectra, they can be noticed from the specular

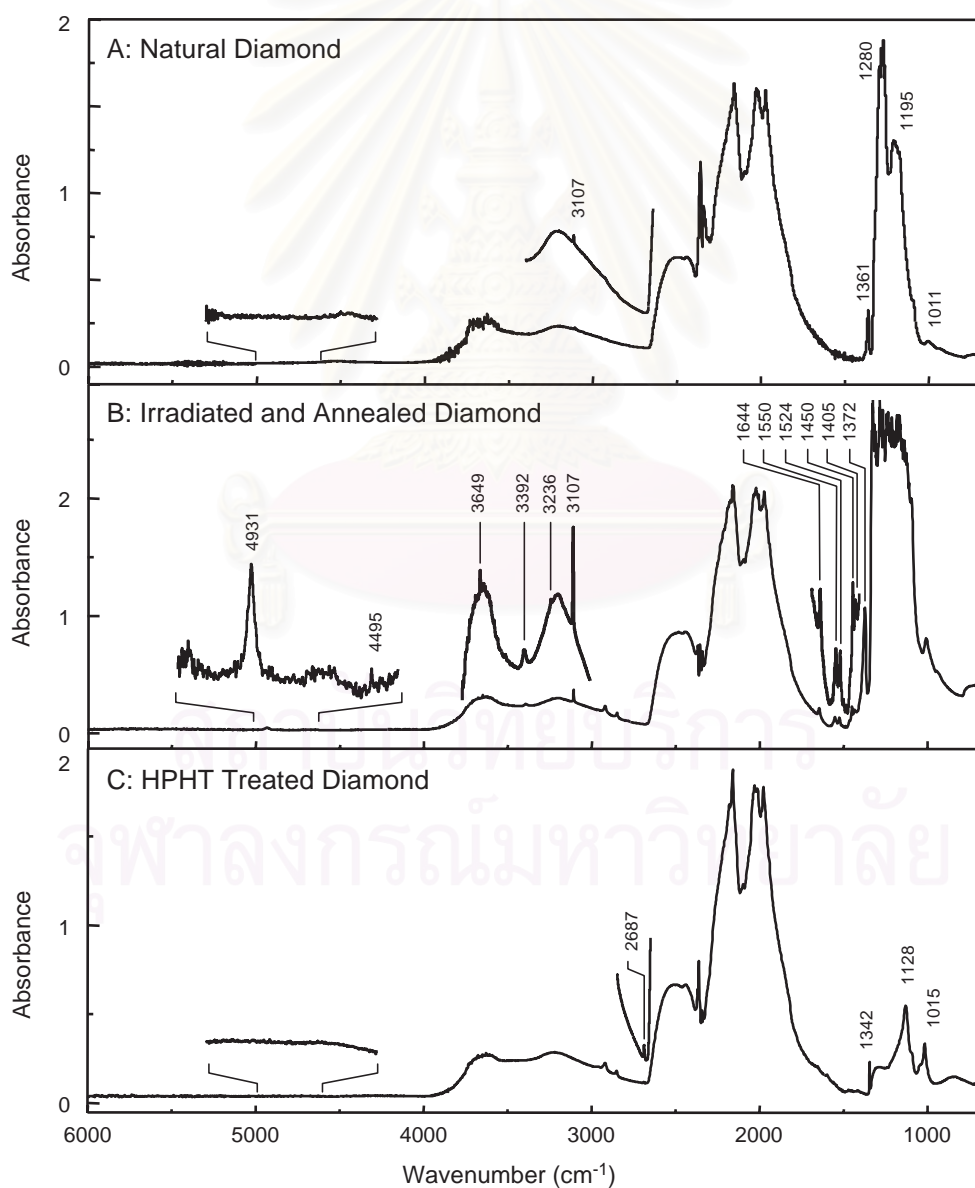


Fig. 5. FTIR spectra of round brilliant cut diamonds acquired by transmittance technique: (A) a 0.207 ct natural diamond, (B) a 0.144 ct irradiated and annealed diamond, and (C) a 0.078 ct HPHT-treated diamond.



reflectance spectra. It should be noted that Kramers-Kronig transformations of the specular reflection spectra cannot be performed since the absorption maxima are too close to the low wavenumber end of the observed spectra. The weak absorption bands in the high wavenumber region are clearly observed in the diffuse reflectance and transmittance spectra. Although the absorption bands of the synthetic moissanite in the 2500–2200  $\text{cm}^{-1}$  are interfered by that of carbon dioxide gas, their absorption maxima are clearly identified. Spectral quality of the transmittance spectra seem to be better than that of the diffuse reflectance spectra. Two small absorption bands of the synthetic moissanite at 3157 and 3071  $\text{cm}^{-1}$  can be noticed in the transmittance spectra while the same bands could not be observed in the diffuse reflectance spectra. Peak positions of the absorption bands of diamonds simulants deduced from the experimentally observed spectra in Figs. 2–4 are conformed to those reported elsewhere [6].

FTIR spectra of natural, HPHT-treated, and irradiated and annealed diamonds are shown in Fig. 5. The absorption bands unique to type of diamond and treatment processes are clearly observed. All diamonds exhibited an absorption band associated with defect-induced one-phonon absorption caused by nitrogen impurities. According to the spectral envelop and the main absorption at 1280  $\text{cm}^{-1}$ , the diamond in Fig. 5A was classified as type IaA diamond. Since the spectral features are associated with an A-centered defect (i.e., a defect consists of a pair of adjacent substituting nitrogen atoms in the diamond crystal lattice) [22].

Due to the saturation in the one-phonon region associated with high concentration of nitrogen, classification of the irradiated and annealed diamond in Fig. 5B was not possible. Since absorptions in the high wavenumber region (4000–5000  $\text{cm}^{-1}$ ) are clearly observed, the associated defect centers could be employed for characterization purpose. It should be noted that absorption bands in this region are not observed in un-irradiated type I natural diamonds. The H1a absorption at 1450  $\text{cm}^{-1}$  involves the creation of a local vibrational mode due to interstitial nitrogen. The H1b absorption at 4931  $\text{cm}^{-1}$  seen in type IaA diamonds is related to the A-center. The absorption centers, H1a and H1b, are unique to the irradiated and annealed type I diamond [16,23–25]. The sharp absorptions associated with the vibration of the vinylidene group at 3107  $\text{cm}^{-1}$  and 1405  $\text{cm}^{-1}$  and that with NH stretching at 3236  $\text{cm}^{-1}$  are clearly observed [26].

The absorptions in the one-phonon region of the HPHT-treated diamond in Fig. 5C indicates that the diamond was type Ib. Absorptions at 1342 and 1128  $\text{cm}^{-1}$  are typical for HPHT-treated diamond and are attributed to defect center with a single substituting nitrogen atom [5,7,27]. It should be pointed out that the weak absorptions at 2920 and 2849  $\text{cm}^{-1}$  in Fig. 5B and C are due of aliphatic hydrocarbon on the surfaces of the faceted diamond. The absorption bands were disappeared when the faceted diamond were carefully cleaned (see Fig. 5A).

#### 4. Conclusions

FTIR spectra of faceted diamonds and diamonds simulants measured by three different techniques were compared. The transmittance technique provides spectrum with an equal or better spectral qualities to that of the well-accepted diffuse reflectance technique. An infrared microscope can be utilized for a nondestructive transmittance spectral acquisition of faceted diamonds and diamond simulants. The observed spectra can be employed for classification purpose as well as for identification the treatment processes applied onto the diamonds. Due to the nondestructive nature, short measurement time, simplicity, and spectral information directly related to chemical structures and compositions, transmittance technique could be employed for routine analysis of faceted diamond. Although the shown results are those of the round brilliant cut diamonds, the techniques are applicable for other types of diamond cuttings and/or gemstones.

#### Acknowledgments

The authors gratefully acknowledge supports from Chulalongkorn University through the University Research Unit and the Ratchadaphidek Somphot Endowment, from the National Research Council of Thailand (NRCT) through the Nanopolymer Project (kor-sor-sor 52/2547), and a fellowship for Miss Pimthong Thongnopkun from the University Development Committee (UDC).

#### References

- [1] A. Petkewich, *Anal. Chem.* 75 (2003) 71A.
- [2] A. Jayaraman, *Curr. Sci.* 79 (2000) 1555.
- [3] J.E. Shigley, *Curr. Sci.* 79 (2000) 1566.
- [4] K. Nassau, *Curr. Sci.* 79 (2000) 1572.
- [5] N. Ferrer, J.M. Jugués-Carulla, *Diamond Relat. Mater.* 5 (1996) 598.
- [6] S. Fernandes, M. Khan, G. Choudhary, *Aust. Gemmol.* 1Q (2003) 361.
- [7] M.J. Mendelssohn, H.J. Milledge, *Int. Geol. Rev.* 37 (1995) 95.
- [8] K. Iakoubovskii, G.J. Adiaenssens, *Diamond Relat. Mater.* 11 (2002) 125.
- [9] A.L. Jenkins, R.A. Larsen, *Spectroscopy* 19 (2004) 20.
- [10] C.J. Noble, Th. Pawlik, J.M. Spaeth, *J. Phys., Condens. Matter* 10 (1998) 11781.
- [11] P.F. Lai, S. Praver, C. Noble, *Diamond Relat. Mater.* 11 (2002) 1391.
- [12] I.N. Kupriyanov, V.A. Gusev, Y.M. Borzdov, A.A. Kalinin, Y.N. Palyamov, *Diamond Relat. Mater.* 8 (1999) 1301.
- [13] J. Lindblom, J. Hölsä, H. Papunen, H. Häkkänen, J. Mutanen, *Opt. Mater.* 24 (2003) 243.
- [14] A.T. Collins, *Diamond Relat. Mater.* 9 (2000) 417.
- [15] F. de Weerd, J. van Royen, *Diamond Relat. Mater.* 10 (2001) 474.
- [16] I. Kiflawi, G. Davies, D. Fisher, H. Kanda, *Diamond Relat. Mater.* 8 (1999) 1576.
- [17] G.S. Woods, A.T. Collins, *J. Phys. C. Solid State Phys.* 15 (1982) L949.
- [18] I.M. Reinitz, E. Fritsch, J.E. Shigley, *Diamond Relat. Mater.* 7 (1998) 313.

- [19] L.I. Tretyakova, N.B. Reshetnyak, Y.V. Tretyakova, *J. Gemmol.* 25 (1997) 532.
- [20] R.G. Messerschmidt, *Appl. Spectrosc.* 39 (1985) 737.
- [21] M.P. Fuller, P.R. Griffiths, *Anal. Chem.* 50 (1978) 1906.
- [22] C.D. Clark, A.T. Collins, G.S. Woods, in: J.E. Field (Ed.), *The Properties of Natural and Synthetic Diamond*, Academic Press, London, 1992, p. 35, Chapter 2.
- [23] I. Kiflawi, A. Mainwood, H. Kanda, D. Fisher, *Phys. Rev., B* 54 (1996) 16719.
- [24] G.S. Woods, A.T. Collins, *J. Phys. C. Solid State Phys.* 15 (1982) L949.
- [25] A.T. Collins, G. Davies, G.S. Woods, *J. Phys. C* 19 (1986) 3933.
- [26] F. de Weerd, Y.N. Palyanov, A.T. Collins, *J. Phys., Condens. Matter.* 15 (2003) 3163.
- [27] A. Yelisseyev, Yu. Babich, V. Nadolinny, D. Fisher, B. Feigelson, *Diamond Relat. Mater.* 11 (2002) 22.



สถาบันวิทยบริการ  
จุฬาลงกรณ์มหาวิทยาลัย

## APPENDIX B

### Transflectance Spectra of Faceted Diamonds Acquired by Infrared Microscopy

Sanong Ekgasit and Pimthong Thongnopkun

Applied Spectroscopy (2005) 59: 1160 – 1165.

สถาบันวิทยบริการ  
จุฬาลงกรณ์มหาวิทยาลัย

# Transflectance Spectra of Faceted Diamonds Acquired by Infrared Microscopy

SANONG EKGASIT\* and PIMTHONG THONGNOPKUN

*Sensor Research Unit, Department of Chemistry, Faculty of Science, Chulalongkorn University, Bangkok 10330, Thailand*

A novel transflectance technique using an infrared microscope was employed for spectral acquisition of loose and mounted faceted diamonds. The observed transflectance spectrum shows the same spectral features as those of the well-accepted diffuse reflectance spectrum. Unlike the diffuse reflectance spectrum, the transflectance spectrum was not affected by the diamond arrangements. The technique can be employed for direct spectra acquisition of mounted diamonds without taking the diamonds out of the jewelry bodies. Moreover, an individual diamond on a complex jewelry setting can be selectively measured. Infrared absorption bands unique to the chemical compositions, impurities, and treatment processes of the diamonds are discussed. The observed transflectance spectra can be exploited for diamond classification.

Index Headings: **Faceted diamonds; Infrared spectrum; Transflectance; Diffuse reflectance.**

## INTRODUCTION

Diamond has long been the prime interest of gem and jewelry markets due to its popularity, mystic beliefs surrounding it, and commercial value. Due to its high commercial value, various types of diamond simulants have been produced. Since diamond simulants do not share the same chemical composition as natural diamond, they can be easily distinguished by appearance and/or physical properties. Diamonds are also synthesized by high temperature, high pressure, and chemical vapor deposition processes. Due to the small size of synthetic diamonds, their major utilization is in industrial applications. Recently, large gem-quality synthetic diamonds have also become available in the jewelry market. Beside the synthetics and simulants, various types of treatments (i.e., irradiation, heat, and high pressure–high temperature (HPHT) treatments) are applied to the low-quality diamonds in order to improve their appearance (i.e., inclusion elimination, color enhancement, and clarity improvement). Because they possess the same chemical structure and composition the synthetic or treated diamonds cannot be differentiated from natural gemstones by conventional characterization techniques (i.e., refractive index, hardness, color, specific gravity, and light dispersion measurements).<sup>1–4</sup> The enhanced or treated diamonds are more difficult to detect or to exclude from their natural untreated counterparts. Due to the large price difference between the synthetic or treated diamonds and natural untreated diamonds, it is important for gemologists to correctly identify the diamonds. As a result, gemologists and jewelry traders are increasingly dependent on chemical-based analytical techniques to defend the integrity of their trade against aggressive tampering.<sup>1</sup>

Modern technology is increasing its impact on diamond trading. Methods for changing the color, and consequently the value, of diamonds are becoming more and more advanced and complicated. The treatment processes are difficult to detect via conventional gemological characterization techniques. Detection of treatment processes becomes a major task for diamond grading laboratories, especially those of the faceted diamonds and diamonds on jewelry bodies where nondestructive and/or noninvasive characterization is required. Irradiation and HPHT treatments improve clarity and color of low-quality diamonds by altering defects in the diamond crystal lattice. Advanced analytical techniques such as Fourier transform infrared (FT-IR) spectroscopy,<sup>5–8</sup> Raman spectroscopy,<sup>9</sup> electron spin resonance (ESR) spectroscopy,<sup>10,11</sup> and photoluminescence spectroscopy<sup>8,12–14</sup> are employed for diamond characterization. Raman spectroscopy has been employed to identify inclusions within diamond and to separate naturals from simulants,<sup>9</sup> and ESR spectroscopy has been employed for detecting the Ni-related centers (i.e., nickel–nitrogen complex) in diamonds, especially those synthesized by the high pressure–high temperature process.<sup>10</sup> Photoluminescence is used to differentiate natural and synthetic diamonds and to detect certain color centers.<sup>8,12,13</sup>

Fourier transform infrared spectroscopy is well known for obtaining spectral information unique to molecular structure and chemical composition. The technique is widely employed for diamond classification based on impurities (i.e., nitrogen, hydrogen, and boron) in the crystal lattice.<sup>5,7</sup> Spectral information associated with lattice defects (i.e., changes or transitions of defect centers) and growth structures are determined and employed for differentiating natural, synthetic, and treated diamonds. Different treatment processes can also be identified by FT-IR spectroscopy.<sup>13,14</sup>

For classical diamond characterization using the transmission technique, a thin slab of diamond is required.<sup>7</sup> Since the technique is destructive, it is not suitable for faceted diamonds of high commercial value. Transmission measurement of a faceted diamond using a beam condenser is complicated by the sample arrangement and the complex reflections at the cut and polished surfaces.<sup>17,18</sup> Diffuse reflectance measurements of a faceted diamond, on the other hand, tend to be non-reproducible since the observed spectral intensity depends strongly on the diamond arrangement on the sample holder.<sup>5,19</sup> Moreover, both transmission and diffuse reflectance techniques are not applicable for mounted diamonds on jewelry bodies.

In order to solve the problems associated with characterization of faceted diamonds and diamonds on jew-

Received 10 May 2005; accepted 29 June 2005.

\* Author to whom correspondence should be sent. E-mail: sanong.e@chula.ac.th.

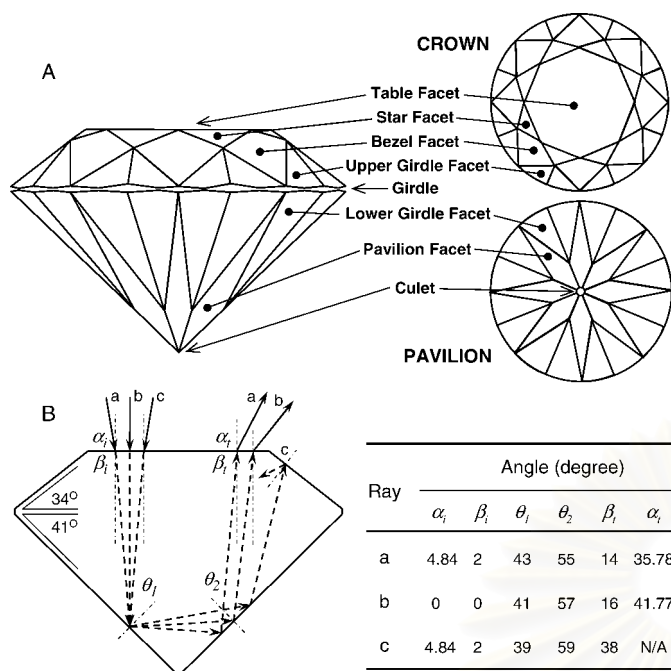


FIG. 1. (A) A schematic drawing of a round brilliant cut diamond. (B) Ray tracing of different radiations inside a round brilliant cut diamond. A summary of angles at the diamond/air interface is shown.

ely, a novel transreflectance technique using infrared microscopy is introduced. The technique is applicable for both loose and mounted diamonds. The observed transreflectance spectrum will be compared with the corresponding diffuse reflectance spectrum. The unique spectral features associated with chemical compositions, impurities, and treatment processes will also be discussed.

## THEORY

A modern brilliant cut diamond consists of  $57 + 1$  facets depending on the presence of the culet (see Fig. 1). Since the refractive index of diamond ( $n_{\text{diamond}} = 2.417$ ) is greater than that of air ( $n_{\text{air}} = 1.0$ ), total internal reflection at the diamond/air interface is observed when radiation traveling inside the diamond impinges on the interface with an angle greater than the critical angle. The critical angle,  $\theta_c$ , is given in terms of the refractive indices by  $\theta_c = \sin^{-1}(n_{\text{air}}/n_{\text{diamond}})$  and is equal  $24.44^\circ$  for the diamond/air interface. In principle, a faceted diamond is cut in such a proportion that the total internal reflection within the diamond is enhanced. To increase the number of total internal reflections, the cutting proportion of the diamond is carefully designed with respect to refractive index, size, shape, and carat weight. The number of total internal reflections depends on the angle and positions at which light enters the diamond. The greater the number of reflections within the diamond, the better the *fire* and *brilliance* of the faceted diamond.<sup>20,21</sup>

In order to collect transreflectance spectra of a faceted diamond using an infrared microscope, the infrared radiation is coupled into while the transreflected radiation is collected from the table facet by the built-in  $15\times$  Cassegrain objective. According to the optical design of the objective, the coupled radiation is inherently converging.<sup>22</sup> For the coupled infrared radiation with a normal

incidence to the table facet, the radiation totally reflects at the pavilion facet. Under the employed cut proportion shown in Fig. 1 (i.e., a set of Tolkowsky's recommended cut proportion with pavilion angle of  $41^\circ$  and crown angle of  $34^\circ$ ), the reflecting angles at the pavilion facet are  $41^\circ$  and  $57^\circ$ , respectively, for the first and second reflections. The radiation reaches the diamond/air interface at the table facet with a  $16^\circ$  angle of incidence and refracts into air with an angle of  $41.77^\circ$ . Due to the complex cut surfaces of the faceted diamond and the convergence of the coupled radiations, the radiations impinge the table facet with different angles and undergo different reflections before emerging into the air. However, some radiations may not emerge from the table facet but undergo multiple internal reflections before emerging into the air at any other facet.

According to the traveling path of the coupled radiation in Fig. 1, the outgoing radiation from the table facet is defined as the *transflected radiation*. Since diamond has absorption bands in the mid-infrared region, attenuations of the infrared radiation at characteristic absorption frequencies of diamond are expected. As a result, by collecting the transflected radiation, the absorption spectra of the diamonds can be measured. Since the absorption bands in an infrared spectrum are directly associated with chemical structures and compositions, they can be employed for diamond classification, characterization, and determination of the impurities and/or inclusions in the diamonds. Moreover, the spectrum can be exploited for the determination of the treatment processes applied to the diamond.<sup>13,14</sup>

## EXPERIMENTAL

The measured specimens were gem quality round brilliant cut diamonds with carat weights of 0.08 to 0.45 ct. The diamonds were characterized as received without additional sample preparation except cleaning. All FT-IR spectra were collected using a Nicolet Magna 750 FT-IR spectrometer equipped with a mercury-cadmium-telluride (MCT) detector. A spectral resolution of  $4\text{ cm}^{-1}$  with 512 coadded scans was employed. The observed spectra in the mid-infrared region were baseline corrected before further analysis.

The transreflectance spectrum of a faceted diamond was collected by a NICPLAN infrared microscope (also equipped with an MCT detector) attached to the FT-IR spectrometer. A homemade accessory was employed for all spectral acquisitions using the microscope. For the spectral acquisition of a loose diamond, the specimen was positioned on the sample holder with the table facet face up. For the spectral acquisition of mounted diamonds on jewelry (i.e., ring, pendant, necklace, earring, etc.), the whole piece of jewelry is placed on the sample holder without removing the diamonds from the jewelry body. The infrared radiation is coupled into the diamond through the table facet by a built-in  $15\times$  Cassegrain objective while the transflected radiation was collected by the same objective. The observed spectrum was expressed in absorbance units.

For comparison purposes, a commercial diffuse reflectance accessory (the Collector, Spectra-Tech Inc.) was employed for all diffuse reflectance spectral acquisitions.

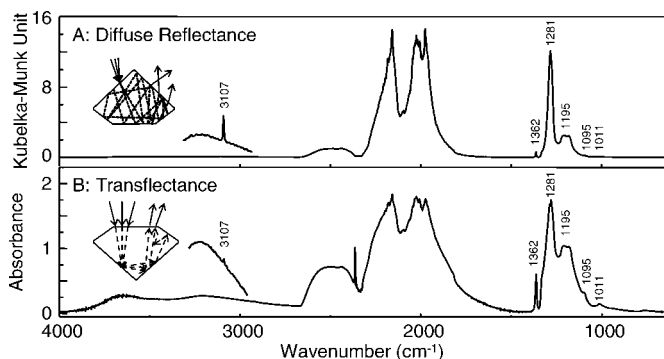


FIG. 2. (A) Diffuse reflectance and (B) transmittance spectra of a 0.1075 ct round brilliant cut type IaA natural diamond.

The same faceted diamond was placed on the sample holder with the table facet face down, and the infrared beam was coupled into the diamond at the near normal angle of incidence, while the representative spectrum was collected from the diffusely reflected radiation. The spectral intensity of the diffuse reflectance spectrum was expressed in Kubelka-Munk units.<sup>23</sup> Since the diffuse reflectance spectra were greatly influenced by the arrangement of the diamond on the sample holder,<sup>5,19</sup> several spectra with different arrangements were collected. The observed spectrum with the best signal-to-noise ratio was employed for further analysis.

## RESULTS

Diffuse reflectance and transmittance spectra of a 0.1075 ct round brilliant cut type IaA natural diamond are shown in Fig. 2. The three principal absorption bands of natural diamonds (i.e., three-phonon absorption at 3900–2650  $\text{cm}^{-1}$ , two-phonon absorption at 2650–1500  $\text{cm}^{-1}$ , and one-phonon absorption at 1400–900  $\text{cm}^{-1}$ )<sup>23</sup> are clearly observed. Absorption bands associated with hydrogen (3107  $\text{cm}^{-1}$ ) and nitrogen impurities (1362, 1281, 1208, 1180, 1095, and 1011  $\text{cm}^{-1}$ ) in the diamond crystal structure could be clearly identified. Although the spectral envelope of the transmittance spectrum is the same as that of the well-accepted diffuse reflectance spectrum, it seems to possess a superior spectral quality. The absorptions in all three principal regions are more prominent in the transmittance spectrum. It should be noted that the absorption at 2350  $\text{cm}^{-1}$  is due to carbon dioxide in the ambient air. Due to fluctuation of carbon dioxide in the ambient air during spectral acquisition, both positive and negative bands were observed.

It is well known that diffuse reflectance spectra of a faceted diamond are greatly influenced by the diamond arrangement on the sample holder.<sup>5,19</sup> Diffuse reflectance spectra of the diamond with different arrangements (i.e., different positions and/or angles of placement on the sample holder) are not exactly the same. As shown in Fig. 3, although the observed diffuse reflectance spectra clearly revealed the three principal absorption bands, their normalized spectra were not superimposed. Unlike the diffuse reflectance spectrum, the transmittance spectrum was not affected by the diamond arrangement. Superimpositions of the transmittance spectra with different diamond arrangements are shown in Fig. 4. Due to minor variations in the alignment with respect to the incident

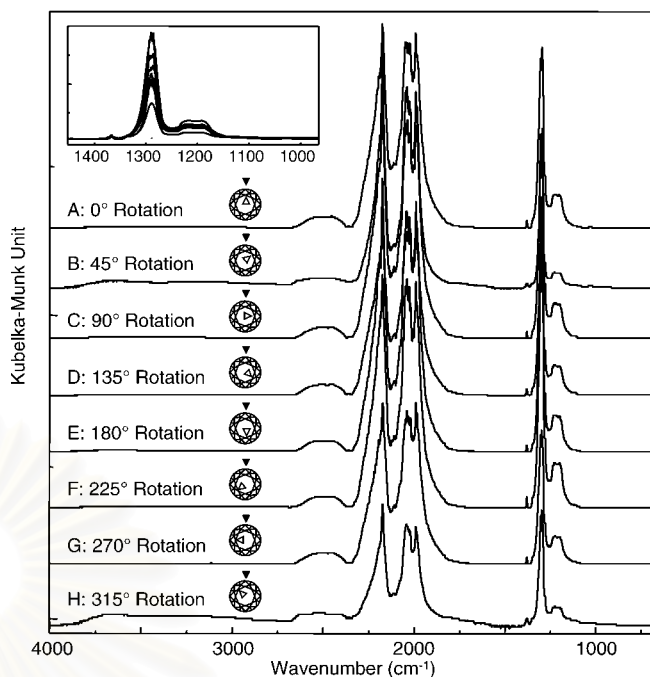


FIG. 3. Normalized diffuse reflectance spectra of the diamond in Fig. 2 under different arrangements. The diamond was rotated: (A) 0°, (B) 45°, (C) 90°, (D) 135°, (E) 180°, (F) 225°, (G) 270°, and (H) 315° with respect to a reference position. Due to a significant variation of absorption magnitudes, the observed spectra were normalized by the absorption at 2493  $\text{cm}^{-1}$ . The inset of absorptions in the one-phonon region was added for clarity.

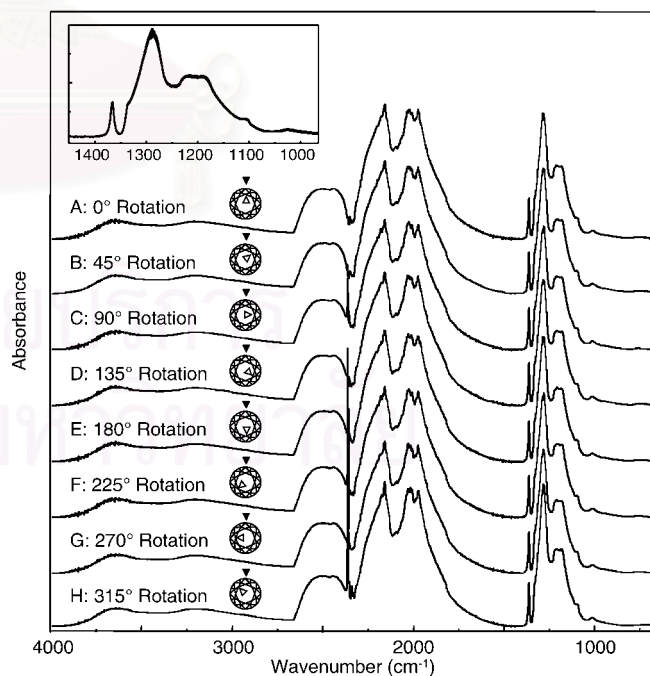


FIG. 4. Transmittance spectra of the diamond in Fig. 2 under different arrangements. The diamond was rotated: (A) 0°, (B) 45°, (C) 90°, (D) 135°, (E) 180°, (F) 225°, (G) 270°, and (H) 315° with respect to a reference position. The inset of absorptions in the one-phonon region was added for clarity.

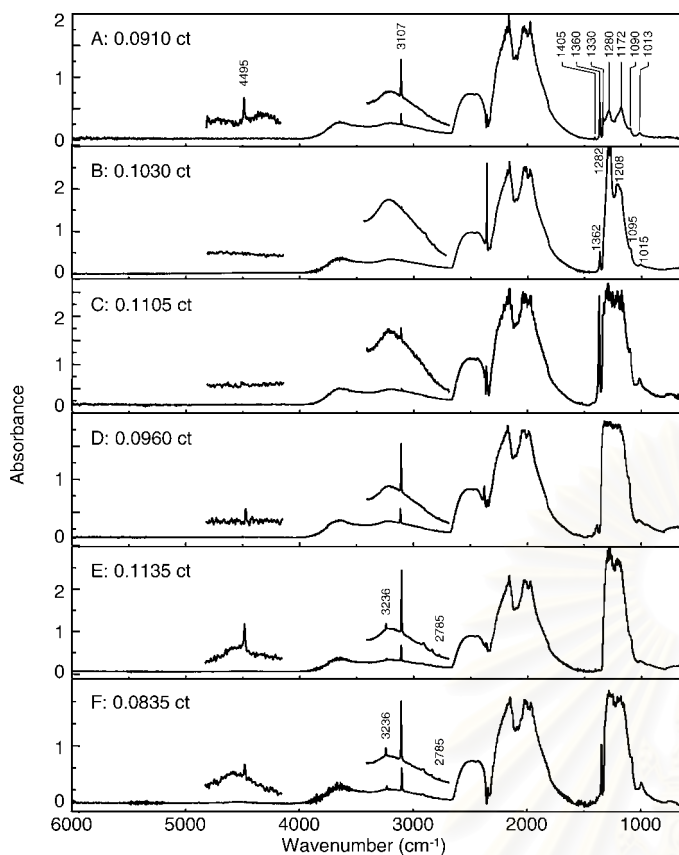


FIG. 5. Transflectance spectra of round brilliant cut natural colorless diamonds: (A) 0.0910 ct, (B) 0.1030 ct, (C) 0.1105 ct, (D) 0.0960 ct, (E) 0.1135 ct, and (F) 0.0835 ct.

radiation, negligible discrepancies among transflectance spectra can be noticed. It should be noted that the displayed transflectance spectra were not normalized.

The spectral features unique to defects and impurities in diamond crystal structure are clearly observed in the transflectance spectra of six faceted white diamonds shown in Fig. 5. These spectral features could be employed for diamond classification. The natural white diamond in Fig. 5A was identified as a type IaB, while that in Fig. 5B is a type IaA. The type IaB diamond possesses a B-center defect (i.e., an aggregate consists of four nitrogen atoms surrounding a vacancy), which shows absorption bands at 1330, 1172, and 1013  $\text{cm}^{-1}$ .<sup>8</sup> An associated absorption band at 1360  $\text{cm}^{-1}$ , which refers to the extended-planar-defect platelets, could also be noted. The unique absorption bands in the one-phonon region of the type IaA diamond are associated with an A-center defect (i.e., a defect consists of a pair of adjacent nitrogen atoms in the diamond lattice). The main absorption has a maximum at 1282  $\text{cm}^{-1}$  and additional weak absorptions at 1362, 1208, and 1015  $\text{cm}^{-1}$ .<sup>5,24</sup> Due to the over absorption in the one-phonon region associated with high nitrogen concentrations in Figs. 5C–5F, classifications of the diamonds based on spectral information in the one-phonon region are not possible.

In addition to the nitrogen-related absorptions, the diamonds also exhibited sharp absorption bands related to hydrogen impurities at 4495, 3236, 3107, 2785, and 1405  $\text{cm}^{-1}$ . A sharp peak at 3107  $\text{cm}^{-1}$ , which is attributed to

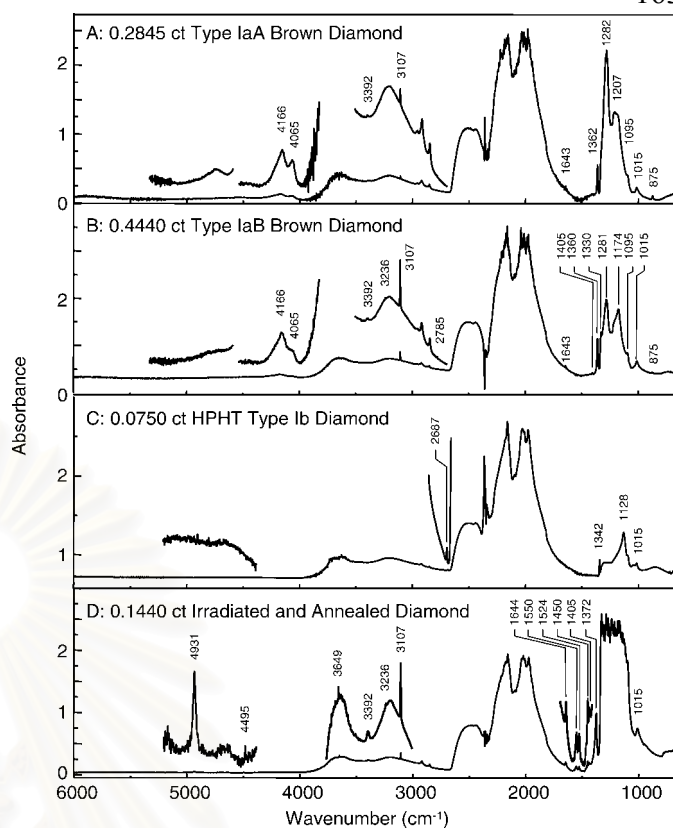


FIG. 6. Transflectance spectra of colored and treated diamonds: (A) 0.2845 ct type IaA brown diamond, (B) 0.4440 ct type IaB brown diamond, (C) 0.0750 ct HPHT type Ib diamond, and (D) 0.1440 ct irradiated and annealed diamonds.

the C–H stretching vibration of a vinylidene group,<sup>8</sup> is present in the transflectance spectra of all diamonds examined. The intensity of this band varied considerably depending on the concentration of the hydrogen impurity. The C–H bending absorption at 1405  $\text{cm}^{-1}$  was detected when the concentration of hydrogen was very high. The band can be clearly observed when interference from water vapor in the ambient air does not obscure the absorption band. For spectra with a strong absorption at 3107  $\text{cm}^{-1}$  (i.e., Figs. 5E and 5F), weak absorptions at 3236 and 2785  $\text{cm}^{-1}$  were noticed. Both absorption bands are commonly observed as minor features in infrared spectra of hydrogen-containing natural diamonds. The absorption at 2785  $\text{cm}^{-1}$  is believed to be the first overtone of the absorption at 1405  $\text{cm}^{-1}$  while the sharp peak at 3236  $\text{cm}^{-1}$  was assigned to the N–H stretching absorption.<sup>8,25</sup>

All transflectance spectra of brown diamonds and treated diamonds shown in Fig. 6 exhibited absorptions associated with nitrogen-defect-induced one-phonon absorption. According to the absorption in the one-phonon region, the diamond in Fig. 6A is classified as a type IaA diamond while that in Fig. 6B is a type IaB diamond. Both spectra contain a well-defined amber center with an absorption at 4166  $\text{cm}^{-1}$ , which is a typical absorption for natural brown diamonds.<sup>26</sup> Absorption bands associated with hydrogen impurity in the three-phonon region can also be observed.

The absorption bands in the one-phonon region of the HPHT-treated diamond in Fig. 6C indicate that the diamond is type Ib. A sharp peak at 1344  $\text{cm}^{-1}$  is the char-

acteristic absorption of HPHT-treated diamond, attributed to the local vibration induced by the C-centered single nitrogen substitution. A broad absorption band at  $1128\text{ cm}^{-1}$  implies the presence of low-concentration B-centered substitution.<sup>5,7,27</sup>

Due to the over absorption in the one-phonon region associated with high nitrogen concentration of the irradiated and annealed diamond in Fig. 6D, classification of the diamond based on the spectral information in the one-phonon region is not possible. However, absorption bands in the high wavenumber region associated with defect centers can be exploited for characterization purposes. The H1a absorption at  $1450\text{ cm}^{-1}$  is the local vibrational mode associated with interstitial nitrogen. The H1b absorption at  $4931\text{ cm}^{-1}$  seen in type IaA diamonds, on the other hand, is related to the A-center.<sup>28</sup> The absorption centers, H1a and H1b, observed in the figure are the unique characteristics of irradiated-and-annealed type I diamond.<sup>16,26–30</sup> It should be noted that absorption bands in this region are not observed in un-irradiated type I natural diamonds. The sharp absorption bands associated with vinylidene at  $3107\text{ cm}^{-1}$  and that with N–H stretching at  $3236\text{ cm}^{-1}$  are clearly observed. Another vinylidene-related absorption at  $1405\text{ cm}^{-1}$  is observed as a shoulder of the strong absorption at  $1372\text{ cm}^{-1}$ .<sup>10,15</sup>

For diamonds with complex settings on jewelry, a spectrum of an individual diamond can be selectively measured by the novel transreflectance technique. As shown in Fig. 7, there are five diamonds on the ring: four small diamonds (0.05 ct) and a big diamond (0.20 ct). According to the ring design, the four small diamonds are embedded in the metal body. The only observable parts of the diamonds are the table facet, the star facet, and parts of the upper girdle facet. As a result, their infrared spectra cannot be acquired by the diffuse reflectance or transmission technique. However, the novel transreflectance technique enables the collection of all FT-IR spectra of the mounted diamonds. Similar to spectral features of the loose diamond, the three principal absorption bands of the mounted diamonds are clearly observed. Since the spectra in Fig. 7A were collected without cleaning, strong absorptions of accumulated substances on the surface of the diamonds due to prolonged wearing were clearly observed. When the big diamond (diamond number 3) was carefully cleaned, the absorptions associated with aliphatic hydrocarbon at  $2954$ ,  $2917$ ,  $2848$ ,  $1645$ ,  $1541$ , and  $1468\text{ cm}^{-1}$  disappeared. The small diamonds were more difficult to clean due to the ring design, having only a small opening near the culet. The uncleaned surfaces of faceted diamonds are responsible for residual absorptions in the C–H stretching region in Fig. 7B. According to the spectral features in the one-phonon region, all diamonds are of different types. The over absorption in the one-phonon region of diamond number 1 indicates that the diamond contains high levels of nitrogen impurity. Although other weak absorption bands associated with hydrogen and nitrogen impurities can be clearly observed, the type of the diamond cannot be identified. According to spectral envelopes in the one-phonon region, diamonds number 2–5 are classified as type IaA, IaA/B, IaA/B, and IaB, respectively.

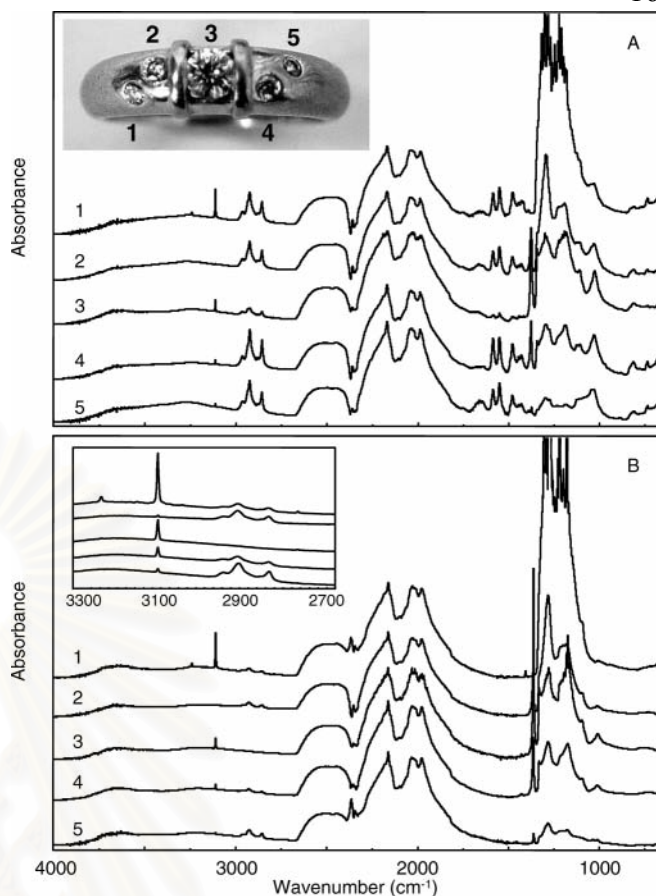


Fig. 7. Normalized transreflectance spectra of mounted round brilliant cut diamonds on a ring (A) before cleaning and (B) after cleaning. The observed spectra were normalized by the absorption in the two-phonon region at  $2493\text{ cm}^{-1}$ . The inset of absorptions in the C–H stretching region was added for clarity.

## DISCUSSION

In general, infrared spectra of faceted diamonds are nondestructively acquired by the diffuse reflectance technique or transmission technique using a beam condenser. However, the techniques suffer from the difficulties associated with the measurement processes. The transmission of the faceted diamonds is not always applicable due to complex reflections at the cut and polished surfaces. Moreover, the technique is not normally applicable to mounted diamonds, where the metal part of the jewelry body covers most of the faceted surfaces except the table facet, the star facet, and part of the bezel facet. The observed diffuse reflectance spectra, on the other hand, are greatly influenced by diamond arrangements on the sample holder. Since a concentric rotational axis of a symmetrically faceted diamond and the sample holder is difficult to achieve, exact diffuse reflection patterns under different diamond arrangements cannot be obtained. As a result, a superimposition of diffuse reflectance spectra from the same faceted diamond is not normally observed.

The novel transreflectance technique using an infrared microscope to acquire an infrared spectrum by collecting the transreflected radiation from the pavilion facets of cut diamonds was exploited. The quality of the transreflectance spectrum is comparable to or better than that of the well-accepted diffuse reflectance spectrum. Unlike the diffuse



reflectance spectrum, the transmittance spectrum was not affected by the diamond arrangements. The coupled radiation from the microscope is non-polarized while the incident radiation covers a wide range of angles due to the focusing optics of the built-in 15× Cassegrain objective. The radiation undergoes transmission-like travel through the faceted diamonds. Since the position at which the coupled radiation entering the diamond can be controlled while the transacted radiation through the symmetrical table facet can be collected, the influences of diamond orientations are eliminated. Thus, the observed transmittance spectra of a diamond are reproducible and are superimposed.

The diffuse reflectance and transmittance spectra of diamonds suffer from over absorption in the one-phonon and two-phonon regions. The magnitude of absorption is associated with size and concentration of nitrogen impurities in the diamond crystal structure. However, a large diamond with an inherently long transacted path length enhances the weak absorption bands. The weak absorption bands unique to defect centers can be clearly observed in the transmittance spectra. As a result, the treatment history and/or unique characters of the faceted diamonds can be drawn from the observed transmittance spectra.

The distinct advantage of the transmittance technique over the diffuse reflectance or transmission technique is its ability to acquire infrared spectra from mounted diamonds on jewelry without taking the diamond out of the jewelry body. An infrared spectrum of an individual diamond on a complex jewelry setting can be selectively measured. Moreover, the spectral features of the mounted diamonds were not interfered with by the metal body.

## CONCLUSION

The novel transmittance technique using an infrared microscope was successfully employed for spectral acquisition of loose and mounted faceted diamonds. The technique is nondestructive, provides unambiguous results, requires no sample preparation, and has a short analysis time. The incident radiation is coupled to the diamond via the table facet while the transmittance radiation is collected by the built-in 15× Cassegrain objective. The same spectral features with better quality as those from the well-accepted diffuse reflectance technique are observed. Unlike the diffuse reflectance spectrum, the transmittance spectrum is not altered by the diamond arrangements. Absorption bands unique to impurities, defects in the crystal structures, and treatment processes can be clearly observed. The measured spectrum can be exploited for classification and/or determination of the treatment history of the diamond. Although

the shown results are those of the loose diamonds and mounted round brilliant cut diamonds on a ring, the technique is applicable for other types of gemstones, jewelry, and/or cut shape.

## ACKNOWLEDGMENTS

The authors gratefully acknowledge support from Chulalongkorn University through University Research Unit and Ratchadaphisek Somphot Endowment, partial funding from the National Research Council of Thailand (NRCT) through the Nanopolymer Project (contract number Kor-Sor-Sor 52/2547), and a fellowship from the University Development Committee (UDC) for Miss Pimthong Thongnopkun.

1. A. Petkewich, *Anal. Chem.* **75**, 71A (2003).
2. A. Jayaraman, *Curr. Sci.* **79**, 1555 (2000).
3. J. E. Shigley, *Curr. Sci.* **79**, 1566 (2000).
4. K. Nassau, *Curr. Sci.* **79**, 1572 (2000).
5. N. Ferrer and J. M. Jugués-Carulla, *Diam. Relat. Mater.* **5**, 598 (1996).
6. S. Fernandes, M. Khan, and G. Choudhary, *Australian Gemmologist* **10**, 361 (2003).
7. M. J. Mendelssohn and H. J. Milledge, *Int. Geol. Rev.* **37**, 95 (1995).
8. K. Iakoubovskii and G. J. Adiaenssens, *Diam. Relat. Mater.* **11**, 125 (2002).
9. A. L. Jenkins and R. A. Larsen, *Spectroscopy* **19**, 20 (2004).
10. J. K. Kirui, J. A. Van Wyk, and M. J. R. Hoch, *Diam. Relat. Mater.* **8**, 1569 (1999).
11. P. F. Lai, S. Praver, and C. Noble, *Diam. Relat. Mater.* **11**, 1391 (2002).
12. I. N. Kupriyanov, V. A. Gusev, Y. M. Borzdov, A. A. Kalinin, and Y. N. Palyamov, *Diam. Relat. Mater.* **8**, 1301 (1999).
13. J. Lindblom, J. Hölsä, H. Papunen, H. Häkkänen, and J. Mutanen, *Opt. Mater.* **24**, 243 (2003).
14. A. T. Collins, *Diam. Relat. Mater.* **9**, 417 (2000).
15. F. De Weerd and J. Van Royen, *Diam. Relat. Mater.* **10**, 474 (2001).
16. I. Kiflawi, G. Davies, D. Fisher, and H. Kanda, *Diam. Relat. Mater.* **8**, 1576 (1999).
17. G. S. Woods and A. T. Collins, *J. Phys. C: Solid State Phys.* **15**, L949 (1982).
18. I. M. Reinitz, E. Fritsch, and J. E. Shigley, *Diam. Relat. Mater.* **7**, 313 (1998).
19. L. I. Tretyakova, N. B. Reshetnyak, and Y. V. Tretyakova, *J. Gemm.* **25**, 532 (1997).
20. T. C. Hemphill, I. M. Reinitz, M. L. Johnson, and J. E. Shigley, *Gem. Gemology* **34**, 158 (1998).
21. I. M. Reinitz, M. L. Johnson, T. C. Hemphill, A. M. Gilbertson, R. H. Geurts, and D. B. Green, *Gem. Gemology* **37**, 174 (2001).
22. J. E. Katon, *Micron* **27**, 303 (1996).
23. M. P. Fuller and P. R. Griffiths, *Anal. Chem.* **50**, 1906 (1978).
24. P. R. Briddon and R. Jones, *Physica B* **185**, 179 (1993).
25. F. De Weerd, Y. N. Palyamov, and A. T. Collins, *J. Phys: Condens. Matter.* **15**, 3163 (2003).
26. F. De Weerd and J. Van Royen, *J. Gemm.* **27**, 201 (2000).
27. C. D. Clark and S. T. Davey, *J. Phys. C: Solid State Phys.* **17**, L399 (1984).
28. I. Kiflawi, A. Mainwood, H. Kanda, and D. Fisher, *Phys. Rev. B* **54**, 16719 (1996).
29. V. G. Vins and O. V. Kononov, *Diam. Relat. Mater.* **12**, 542 (2003).
30. A. T. Collins, G. Davies, and G. S. Woods, *J. Phys. C* **19**, 3933 (1986).

## APPENDIX C

Novel Attenuated Total Reflection Fourier Transform  
Infrared Microscopy Using a Gem Quality Diamond as  
an Internal Reflection Element

Sanong Ekgasit and Pimthong Thongnopkun

Applied Spectroscopy (2005) 59: 1236 – 1241.

สถาบันวิทยบริการ  
จุฬาลงกรณ์มหาวิทยาลัย

# Novel Attenuated Total Reflection Fourier Transform Infrared Microscopy Using a Gem Quality Diamond as an Internal Reflection Element

SANONG EKGASIT\* and PIMTHONG THONGNOPKUN

Sensor Research Unit, Department of Chemistry, Faculty of Science, Chulalongkorn University, Bangkok 10330, Thailand

A novel technique for attenuated total reflection Fourier transform infrared (ATR FT-IR) spectral acquisition by an infrared microscope with a gem-quality faceted diamond as an internal reflection element (IRE) is introduced. Unlike conventional IREs, the novel diamond IRE has a sharp tip configuration instead of a flat tip configuration. Light at normal incidence was coupled into the diamond while the transflected radiation from the diamond was collected through the table facet by the built-in 15× Cassegrainian objective. The number of reflections in the novel diamond IRE equals two. The evanescent field generated under total internal reflection at the pavilion facet was exploited for ATR spectral acquisition of materials attached to the IRE. The observed ATR spectra were compared to those obtained via a traditional zinc selenide IRE.

Index Headings: Faceted diamond; Attenuated total reflection; ATR spectrum; Fourier transform infrared; ATR FT-IR; Micro-ATR; Internal reflection element; Diamond IRE.

## INTRODUCTION

Attenuated total reflection Fourier transform infrared (ATR FT-IR) spectroscopy is a molecular spectroscopic technique with unique surface-sensitive properties derived from the rapid decay of the strong evanescent field generated under the total internal reflection (TIR) phenomenon.<sup>1-5</sup> Although the rapid decay characteristic of the evanescent field makes the ATR spectrum sensitive to physicochemical phenomena near the interface, restrictions associated with the decay characteristic impose limitations on the application of the technique. The sample must optically contact the internal reflection element (IRE) in order to exploit the strong evanescent field near the interface. A small air gap can significantly deteriorate the observed spectra.<sup>6</sup> In most cases, ATR spectra of a hard and rigid solid sample cannot be observed, even though the sample is mirror flat, due to insufficient contact. The ATR technique is most effective for the spectral acquisition of liquids, soft solids, or thin films that can be cast onto the IRE since optical contact can be easily achieved. In order to improve the contact of hard and rigid solid samples, force is applied onto the sample against the IRE.<sup>7-10</sup> However, this operation must be performed with extreme care since the excessive force might damage the surface of the IRE. Another approach is to use an ATR accessory with an IRE with a small contact area in order to minimize the effect of local unevenness or roughness of the surface attached to the IRE.<sup>11-13</sup> There are numerous commercially available accessories designed for counteracting the contact problem. The hardest

rare type II natural diamond is employed in those accessories. Optical contact between the flat surface of the diamond IRE and a rigid solid sample can be easily achieved by simply pressing the two together.<sup>14,15</sup>

This paper introduces a novel ATR FT-IR microscopy method using a gem-quality round brilliant cut diamond (~0.1 carat weight) as an IRE for spectral acquisition with an infrared microscope under the reflection mode. Unlike conventional IREs<sup>7-13</sup> and commercially available diamond IREs,<sup>14,15</sup> the novel approach employs a sharp-tip diamond IRE. The observed ATR spectra acquired with the diamond IRE will be compared to those acquired with a traditional zinc selenide (ZnSe) IRE.

## THEORY

When electromagnetic radiation traveling within a denser medium (i.e., an IRE) impinges at the interface with a rarer medium of lower refractive index (i.e., a sample) at an angle of incidence greater than the critical angle, a strong evanescent field is generated at the interface. The evanescent field is strongest at the interface and decays exponentially as a function of the distance into the rarer medium. If the rarer medium is absorbing at the coupled frequency, the intensity of the reflected radiation becomes smaller than that of the incident radiation. The magnitude of reflection loss (or absorption) is proportional to the product between the imaginary part of the complex dielectric constant and the evanescent field amplitude. The absorbance  $A(\theta, \nu)$  can be expressed in terms of the experimental conditions and material characteristics as:<sup>6,16</sup>

$$A(\theta, \nu) = \frac{(2\pi\nu)^2}{\ln(10)k_{z,\text{IRE}}(\theta, \nu)} \cdot \frac{d_p(\theta, \nu)}{2} \times \text{Im}[\hat{\epsilon}_{\text{sample}}(\nu)] \langle E_0^2(\theta, \nu) \rangle \quad (1)$$

where  $\theta$  is the angle of incidence,  $\nu$  is the frequency of the incident radiation,  $\hat{\epsilon}_{\text{sample}}(\nu)$  is the complex dielectric constant of the sample,  $d_p(\theta, \nu)$  is the penetration depth,  $\langle E_0^2(\theta, \nu) \rangle$  is the mean square evanescent field (MSEvF) at the IRE/sample interface, and  $k_{z,\text{IRE}}(\theta, \nu)$  is the  $z$ -component wave-vector within the IRE. The wave-vector can be expressed in terms of the  $x$ -component wave-vector  $k_{x,\text{IRE}}(\theta, \nu)$  by  $k_{z,\text{IRE}}(\theta, \nu) = [(2\pi\nu)^2 \epsilon_{\text{IRE}} - k_{x,\text{IRE}}^2(\theta, \nu)]^{1/2}$ , where  $k_{x,\text{IRE}}(\theta, \nu) = 2\pi[\epsilon_{\text{IRE}} \sin^2\theta]$  and  $\epsilon_{\text{IRE}}$  is the dielectric constant of the prism. The detailed derivations of the MSEvF are given elsewhere.<sup>17,18</sup> The penetration depth, defined as the distance at which the MSEvF decays to 1/e of that at the interface, is given in terms of experimental conditions and material characteristics by  $d_p(\theta, \nu)$

Received 22 April 2005; accepted 6 July 2005.

\* Author to whom correspondence should be sent. E-mail: sanong.e@chula.ac.th.

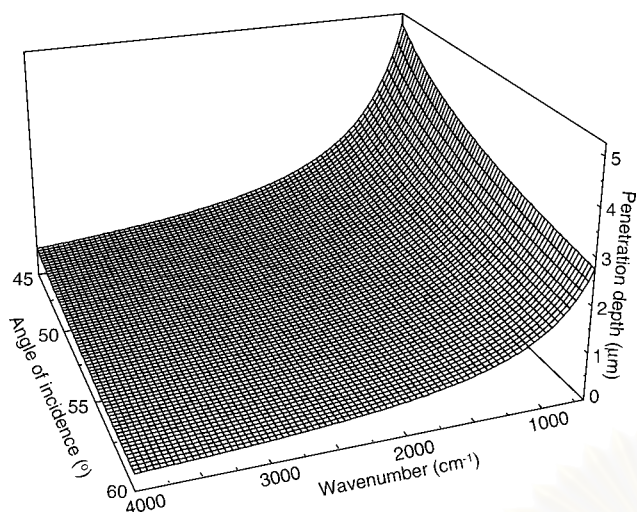


FIG. 1. Penetration depth in the mid-infrared region at various angles of incidence with a ZnSe IRE.

$= 1/[k_{x,IRE}(\theta, \nu) - (2\pi\nu)^2\epsilon_{IRE}]^{1/2}$ . Although the penetration depth is not the actual distance from the interface where the evanescent field interacts with the sample, it is the figure that indicates relative depth-dependent information acquired under various experimental conditions. The actual distance at which the spectral information was acquired (i.e., the sampling depth) is greater than the penetration depth.<sup>19</sup> The penetration depth profile in the mid-infrared region shown in Fig. 1 implies that absorption bands at various frequencies in an ATR spectrum do not provide information up to the same depth. The greater the frequency and/or the angle of incidence, the shallower is the depth of the acquired spectral information. An observed ATR spectrum is the collective molecular information from the IRE/sample interface up to the depth (i.e., sampling depth) at which the MSEvF decays to an insignificant level. The sampling depth in an ATR FT-IR spectrum is varied depending on the experimental conditions (i.e., angle of incidence and frequency of the coupled radiation) and material characteristics (i.e., refractive indices of the IRE and sample). In general, the value is approximately a few micrometers from the IRE/sample interface. However, it should be noted that the majority of the spectral information comes from chemical moieties near the interface, where the MSEvF is strongest. The spectral contribution at a greater depth decreases exponentially as the evanescent field decays.

Diamond can be employed as an IRE due to its high refractive index ( $n_{\text{Diamond}} = 2.417$ ) and partial optical transparency in the mid-infrared region. Diamond has three major absorption bands in the mid-infrared region, namely one-phonon ( $1400\text{--}900\text{ cm}^{-1}$ ), two-phonon ( $2650\text{--}1500\text{ cm}^{-1}$ ), and three-phonon ( $3900\text{--}2650\text{ cm}^{-1}$ ) absorptions.<sup>20</sup> The absorption magnitude in the one-phonon region depends strongly on the concentration of nitrogen impurities. Diamond with a high nitrogen content always shows over-absorption in this region.<sup>21</sup> Although the two-phonon region is always over-absorbing, it has little effect on the analysis of organic materials since most of the materials do not absorb in this region. The three-phonon absorption, on the other hand, is very weak. It imposes insignificant interference on the absorption of

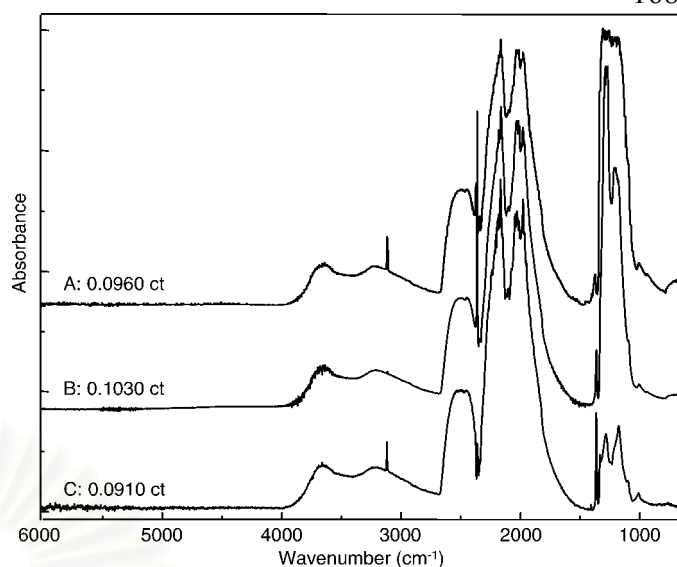


FIG. 2. Transmittance spectra of round brilliant cut natural diamonds with different levels of nitrogen impurities: (A) 0.0960 ct, (B) 0.1030 ct type IaA, and (C) 0.0910 ct type IaB. An absorption band at  $2350\text{ cm}^{-1}$  is due to a fluctuation of atmospheric carbon dioxide during the spectral acquisition.

the materials. Transmittance spectra of round brilliant cut diamonds with different magnitudes of nitrogen and hydrogen impurities are shown in Fig. 2. Absorption bands associated with impurities are clearly observed. The observed spectral envelopes in the one-phonon region indicate that the diamonds are of different types. The diamonds in Figs. 2B and 2C are of type IaA and IaB, respectively, while that in Fig. 2A cannot be identified due to the over-absorption in the one-phonon region. A sharp peak at  $3107\text{ cm}^{-1}$  is assigned to the vinylidene vibration of the hydrogen impurities in the diamond crystal structure. The intensity of the peak varies considerably with the concentration of hydrogen impurity in the diamond crystal structure.<sup>20,21</sup>

In principle, a faceted diamond is cut in such a proportion that the number of total internal reflections within the diamond is enhanced. To increase the number of total internal reflections, the cutting proportion of the diamond is carefully designed with respect to its refractive index, size, shape, and carat weight. The number of reflections depends on the angle and positions at which light enters the diamond. The greater the number of total internal reflections, the better is the fire and brilliance of the diamond. This phenomenon is due to the dispersion of light associated with its traveling distance and the total internal reflection inside the diamond.<sup>22,23</sup> A schematic illustration of ray tracings within a round brilliant cut diamond is shown in Fig. 3. In order to collect transmittance spectra of a faceted diamond using an infrared microscope, the infrared radiation is coupled into and is collected from the table facet by the built-in  $15\times$  Cassegrainian objective.<sup>24</sup> For the coupled radiation with a normal incidence to the table facet, the radiation totally reflects at the pavilion facet. Under the employed cut proportion (i.e., a set of Tolksowsky's recommended proportion with pavilion angle of  $41^\circ$  and crown angle of  $34^\circ$ ),<sup>20,21</sup> the angles of reflection at the pavilion facet are  $41^\circ$  and  $57^\circ$  for the first and second reflections, respectively. The radiation

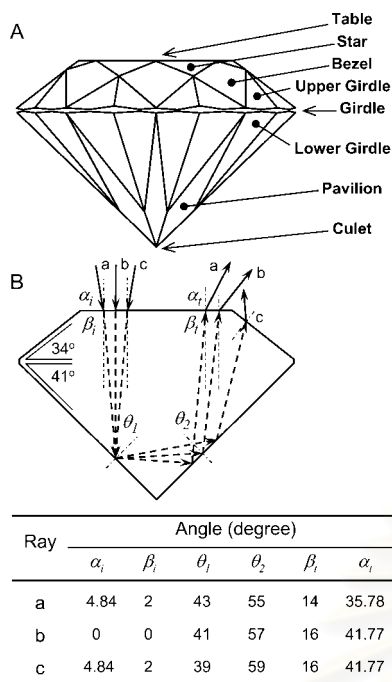


FIG. 3. (A) A schematic illustration of a round brilliant cut diamond with Tolkowsky's recommended proportion. (B) Ray tracing of the coupled radiations within the faceted diamond. Angles of reflection and refractions defined with respect to the direction normal to the reflecting surfaces are summarized.

reaches the diamond/air interface at the table facet with an angle of  $16^\circ$  and refracts into air with an angle of  $41.77^\circ$ . Due to the complex cut surfaces of the faceted diamond, the coupled radiations that impinge the table facet with different angles and/or positions undergo different reflections inside the faceted diamond before emerging into air at any facet. According to the traveling path of the coupled radiation, the outgoing radiation from the table facet is defined as the *transflected radiation*. The evanescent field generated under total internal reflection at the pavilion facets can interact with a material attached to the diamond. By collecting the transreflectance spectrum, absorption of the material under ATR conditions can be observed.

## EXPERIMENTAL

All FT-IR spectra were collected using a Nicolet Magna 750 FT-IR spectrometer equipped with a mercury-cadmium-telluride (MCT) detector. Spectra in the mid-infrared region ( $4000\text{--}650\text{ cm}^{-1}$ , unless otherwise specified) with a spectral resolution of  $4\text{ cm}^{-1}$  with 512 coadded scans were employed. A commercial single-reflection ATR accessory (The Seagull™, Harrick Scientific) with a 25 mm hemispherical ZnSe IRE was employed for all conventional ATR FT-IR spectral acquisitions. For the novel ATR FT-IR spectral acquisition using an infrared microscope, a gem-quality round brilliant cut natural diamond type IaB (0.0910 carat) was employed as an IRE. The defect-free diamond was mounted onto a homemade micro-ATR accessory. The homemade accessory has a sample holder whereby a solid sample can be brought into contact with the culet of the diamond IRE. Infrared radiation from the infrared microscope (Model NIC-

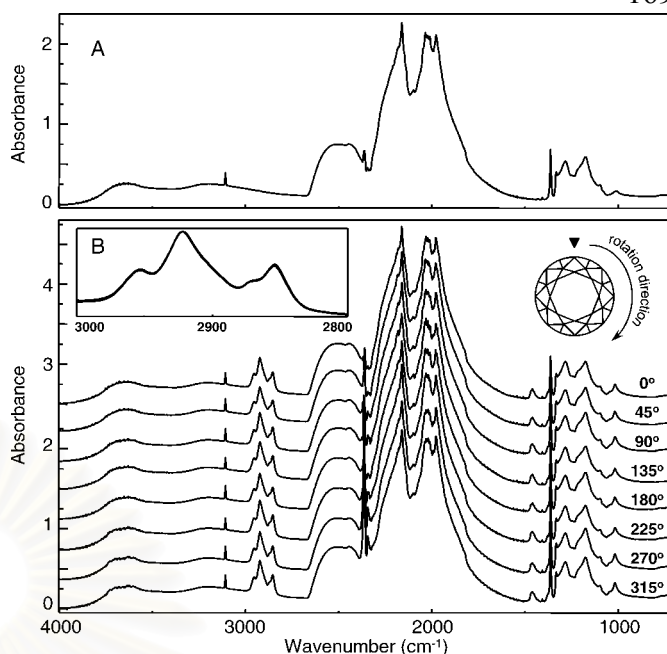


FIG. 4. (A) Transflectance spectra of the employed diamond IRE (0.0910 ct type IaB). (B) ATR spectra of a minute amount of mineral oil on the culet of the diamond IRE with different angles of diamond rotation. The inset shows the superimposition of the ATR spectra of the mineral oil in the CH stretching region.

PLAN, Nicolet) attached to the FT-IR spectrometer was coupled into the diamond while the transreflectance radiation was collected via the built-in  $15\times$  Cassegrainian objective through the table facet. Reflection with normal incidence from a gold mirror was employed as a background for all ATR FT-IR spectra acquired by the microscope.

As shown in Fig. 3, unlike conventional IREs<sup>7–13</sup> and commercially available diamond IREs,<sup>14,15</sup> the sampling area of the novel IRE is the sharp pavilion facet of the cut and polished diamond. The effective number of reflections equals two. Due to the divergent nature of the focusing optics, although the radiation was coupled under normal incidence to the table facet, the angle of incidence at the diamond/sample interface was not well defined but instead covered a range of angles. As a result, the observed spectrum is the collective spectral information of all possible angles.

## RESULTS

Transflectance spectra of the employed diamond IRE (i.e., ATR spectra of air) are shown in Fig. 4A. Since diamond is absorbing in the mid-infrared region, absorptions at the characteristic frequencies of diamond are expected when it is employed as an IRE for ATR measurements. The three fundamental absorption bands and the absorption bands associated with nitrogen and hydrogen impurities in the diamond crystal structure were clearly observed. The employed diamond IRE is classified as a type IaB diamond based on the spectral envelope in the one-phonon region. Since the bands are unique to diamond, they appear in all ATR FT-IR spectra acquired with the diamond IRE with a specular reflection from a gold mirror as a reference. ATR spectra of a minute

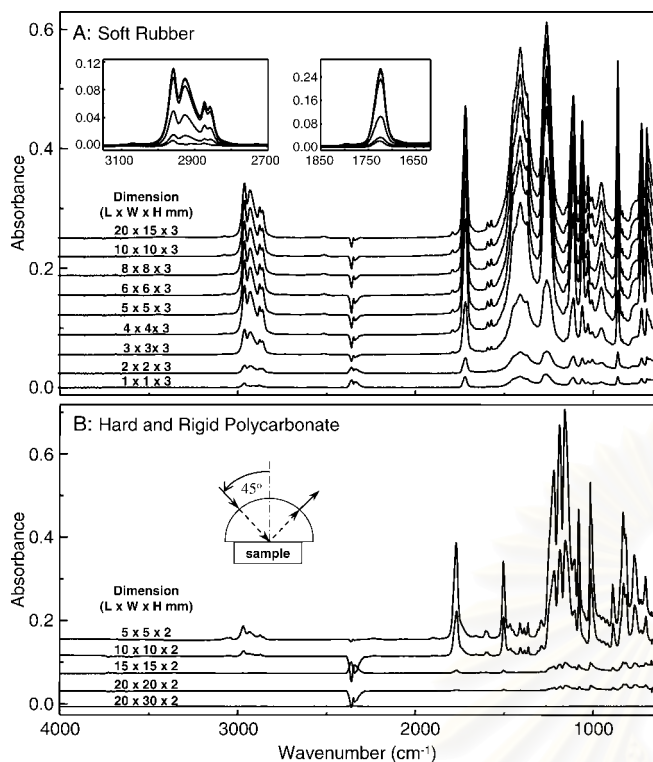


FIG. 5. (A) ATR spectra of soft rubbers of different sizes. The observed spectra do not change when the size is greater than  $5 \times 5$  mm. (B) ATR spectra of mirror-flat polycarbonate specimens of different sizes. The specimens were pressed against the hemispherical ZnSe IRE. The shown spectra were those with unchanged absorption as the pressure was increased.

amount of mineral oil deposited on the culet are shown in Fig. 4B. The mineral oil covers the culet and a very small portion of the pavilion facet near the culet. When the diamond IRE was rotated to different angles with respect to a reference position, the observed spectra were superimposed. Although there are some negligible discrepancies among the observed spectra due to minor variations associated with the diamond alignment, Fig. 4B indicates that it does not have any influence on the observed ATR spectra.

Spectra in Fig. 5A show the influence of sample size on the absorption magnitude. According to the optical design of the employed single-reflection ATR accessory, the illumination area on the surface of the hemispherical IRE is relatively small compared to the flat surface of the IRE. The experimental results indicate that the illumination area is approximately  $25\pi$  mm<sup>2</sup> at the center. When optical contact is achieved (i.e., with a soft solid or liquid), further increments of the sample size larger than the illumination area do not increase the absorption. The influence of sample contact is shown in Fig. 5B. ATR spectra of hard and rigid solid polycarbonate with mirror-flat surfaces indicate that the small specimen ( $5 \times 5 \times 2$  mm) possesses a much greater absorption magnitude compared to those of the large specimens. This is due to the insufficient contact between the large polycarbonate sample and the IRE compared to that of the small one. Good contact for a small sample can be achieved by simply applying pressure on the sample against the IRE.<sup>7-9,14,15</sup> A large specimen tends to have a surface with

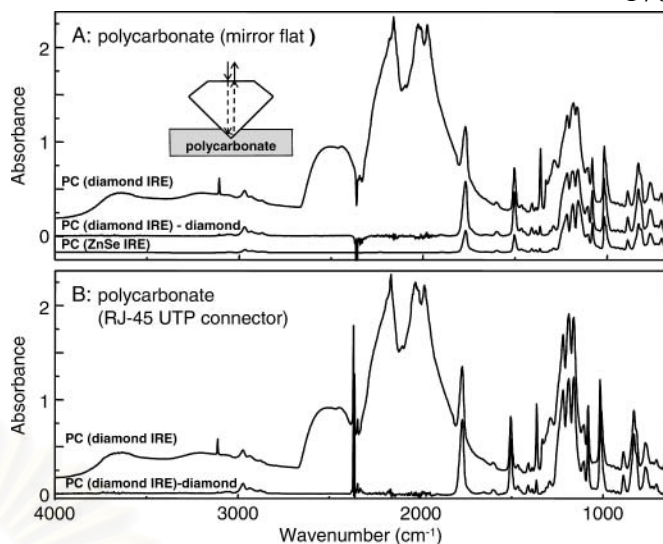


FIG. 6. (A) ATR spectra of a mirror-flat polycarbonate acquired using the novel diamond IRE. The specimen is the same as that in Fig. 5B. (B) ATR spectra of a complex-shaped polycarbonate (an RJ-45 UTP connector for the Ethernet card). When the contributions of the diamond IRE were subtracted, the unique spectral features of the polycarbonate were revealed. An ATR spectrum of polycarbonate acquired using the ZnSe IRE is overlaid for comparison.

local unevenness or a surface with small particles that prevent good contact. As a result, the observed ATR spectrum becomes deteriorated. In the worst case, an ATR spectrum of a hard and rigid solid sample cannot be observed at all.<sup>6</sup>

An ATR spectrum of the same specimen acquired with the diamond IRE, on the other hand, does not suffer from the variation of the sample size since the sampling area is governed by the small contact area of the diamond IRE (see Fig. 6A). The diamond tip (i.e., the culet and part of the pavilion facet) is utilized as the sampling area where the evanescent field interacts with the sample. The contact area between the diamond IRE and sample can be manipulated via the penetration of the diamond tip into the sample. Since the diamond tip is very small, the problems associated with the contact were eliminated while the diamond tip always possesses good contact with the hard and rigid solid sample. Pressure can be applied onto the sample against the diamond IRE to ensure optimal contact during spectral acquisition. ATR spectra of the hard and rigid polycarbonate with complex shapes (RJ-45 UTP connector for Ethernet card) are shown in Fig. 6. Due to the small contact area of the diamond IRE, the observed ATR spectrum was not affected by the surface irregularity or roughness of the specimen. It should be noted that ATR spectra of such specimen cannot be observed by the conventional ATR technique without additional sample preparation. For the current spectral acquisition with the novel diamond IRE, the specimen was simply brought into contact with the IRE and the ATR spectrum was taken. When the absorption of diamond was subtracted from the observed spectra, unique spectral features of the polycarbonates were revealed. However, the contribution of the diamond absorption cannot be completely eliminated due to the differences in the optical configurations of the systems (i.e., diamond/air and diamond/polycarbonate). Although the

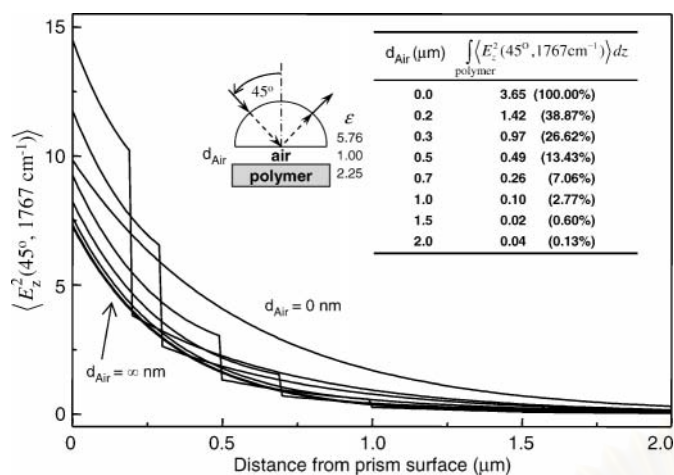


FIG. 7. The MSEvF with different thicknesses of air gaps. The MSEvF integration within the polymer layer (inserted table) decreases significantly as the thickness of the air gap increases. The simulation parameters are shown.

absorption of diamond in the two-phonon region was completely subtracted, absorption of diamond at  $3107\text{ cm}^{-1}$  is still observable. As a result, absorption of diamond in the one-phonon region was still present in the subtracted spectra. Due to strong absorption of the polycarbonate in the region, residual absorption of the diamond in the one-phonon region was obscured.

## DISCUSSION

The ability of the ATR technique to selectively acquire molecular information within the region up to few micrometers from the surface is derived from the unique properties of the evanescent field generated under total internal reflection. According to Eq. 1 and the frequency-dependent nature of the penetration depth, the absorption in an ATR spectrum is strongly dependent on the degree of contact between the IRE and the sample. If good contact is not achieved, integration of the MSEvF within the sample (thus, the absorbance) becomes smaller (see Fig. 7). When good contact is not achieved in the IRE/polymer two-phase system, an air gap exists between the IRE and the polymer. The system becomes a three-phase system (i.e., IRE/air/polymer). The integration of the evanescent field within the polymer is drastically decreased as the thickness of the air gap increases. Although there is a field enhancement within the air gap due to optical effects, the field does not contribute to the absorption of the polymer. Under the conditions defined in Fig. 7, when the thickness of the air gap is greater than  $1.00\ \mu\text{m}$ , the field integration within the polymer becomes insignificantly small compared to that without an air gap. As a result, the absorption of the polymer at the defined frequency cannot be observed. As shown in Fig. 5B, for a hard and rigid solid sample absorption of the small sample with better contact is greater than that of the big sample with poor contact. Since good contact is necessary for the measurement of a good-quality ATR FT-IR spectrum, a small sample or an IRE with a small contact area was employed for contact improvement.<sup>14,15</sup> Since the employed commercial ATR accessory has focusing optics with a small illumination area on the flat surface of the

hemispherical IRE, it is suitable for spectral acquisition of a small, hard and rigid solid sample with a mirror-flat surface. However, for a solid sample with a rough and curved surface or that with a complex shape, good contact with the IRE is not normally achieved while the observed ATR spectrum is deteriorated.

The small diamond IRE eliminates problems associated with sample contact. It can be employed for ATR spectral acquisitions of hard and rigid solid materials that cannot normally be measured by conventional ATR accessories. Since diamond is the hardest known material, it cannot be easily damaged by an excessive force under normal operations. Good contact is always achieved by simply pressing the sample against the diamond IRE. No sample preparation or minimal sample preparation is required when collecting spectra using the novel diamond IRE. Since diamond is an isotropic medium while the coupled radiation from the Cassegrainian objective is non-polarized,<sup>24</sup> rotation of the diamond IRE does not introduce any change in the absorption of diamond. However, a negligible discrepancy between consecutive measurements may be observed since the exact degree of perpendicularity between the coupled radiation and the table facet cannot be re-created. One major drawback of the diamond IRE is its inherent strong absorption in the one-phonon regions. Absorption of the sample in these regions will be masked by the diamond absorptions. However, this problem can be eliminated by employing a synthetic diamond or a type II natural diamond with extremely low nitrogen content.

## CONCLUSION

A novel ATR FT-IR spectral acquisition method using an infrared microscope with a gem-quality faceted diamond as IRE was developed. The small diamond tip eliminates the problems associated with an air gap or insufficient contact between the solid sample and the IRE. The hard and rigid solid sample with a rough surface can be brought into contact with the diamond IRE while pressure can be applied in order to ensure optimal contact during measurement. Since diamond is the hardest known material, ATR FT-IR spectra of hard and rigid solid materials can be measured (especially those with rough surfaces or irregular shape). One of the major drawbacks of the employed type IaB natural diamond IRE is the masking absorption bands in the one-phonon region. However, the problem can be overcome by employing a diamond with low levels of nitrogen impurity or a rare type II natural diamond with extremely low nitrogen impurity.

## ACKNOWLEDGMENTS

The authors gratefully acknowledge support from Chulalongkorn University through University Research Unit and the Ratchadaphisek Somphot Endowment, partial funding from the National Research Council of Thailand (NRCT) through the Nanopolymer Project (contract number GOR-SOR-SOR 52/2547), and an instrumental donation from Seagate Technology Co. Ltd. (Thailand). A fellowship for P.T. from the University Development Committee (UDC) is gratefully acknowledged.

1. N. J. Harrick, *Internal Reflection Spectroscopy* (Harrick Scientific Corporation, Ossining, New York, 1987).
2. V. Koppaka and P. Axelsen, *Langmuir* **17**, 6309 (2001).

3. M. W. Urban, *Attenuated Total Reflection Spectroscopy of Polymers* (American Chemical Society, Washington, D.C., 1996).
4. A. S. Cantor, *J. Control. Release* **61**, 219 (1999).
5. E. Goormaghtigh, V. Raussens, and J.-M. Ruysschaert, *Biochim. Biophys. Acta* **1422**, 105 (1999).
6. S. Ekgasit, *Appl. Spectrosc.* **54**, 756 (2000).
7. T. Buffeteau, B. Desbat, and D. Eyquem, *Vib. Spectrosc.* **11**, 29 (1996).
8. G. Muller and C. Riedel, *Fresenius' J. Anal. Chem.* **365**, 43 (1999).
9. C. M. Balik and W. H. Simendinger, *Polymer* **39**, 4723 (1998).
10. V. Acha, M. Meurens, H. Naveau, and S. N. Agathos, *Biotech. Bioeng.* **68**, 473 (2000).
11. A. J. Sommer and M. Hardgrove, *Vib. Spectrosc.* **24**, 93 (2000).
12. D. J. Lyman, J. Murray-Wijelath, and M. Feughelman, *Appl. Spectrosc.* **55**, 552 (2001).
13. D. J. Lyman and J. Murray-Wijelath, *Appl. Spectrosc.* **59**, 26 (2005).
14. A. M. Young, *Biomaterials* **23**, 3289 (2002).
15. A. M. Young, S. A. Rafeeka, and J. A. Howlett, *Biomaterials* **25**, 823 (2004).
16. S. Ekgasit and A. Padermshoke, *Appl. Spectrosc.* **55**, 1352 (2001).
17. W. N. Hansen, *J. Opt. Soc. Am.* **58**, 380 (1968).
18. W. N. Hansen, "Internal Reflection Spectroscopy," in *Advances in Electrochemistry and Electrochemical Engineering*, R. H. Muller, Ed. (John Wiley and Sons, New York, 1973), vol. 9.
19. F. M. Mirabella, Jr., *J. Polym. Sci. Polym. Phys. Ed.* **21**, 2403 (1983).
20. M. J. Mendelssohn and H. J. Milledge, *Int. Geol. Rev.* **37**, 95 (1995).
21. W. Wang, T. Moses, R. C. Linares, J. E. Shigley, M. Hall, and J. E. Butler, *Gem. Gemology* **39**, 268 (2003).
22. T. C. Hemphill, I. M. Reinitz, M. L. Johnson, and J. E. Shigley, *Gem. Gemology* **34**, 158 (1998).
23. I. M. Reinitz, M. L. Johnson, T. C. Hemphill, A. M. Gilbertson, R. H. Geurts, B. D. Green, and J. E. Shigley, *Gem. Gemology* **37**, 174 (2001).
24. J. E. Katon, *Micron* **27**, 303 (1996).



สถาบันวิทยบริการ  
จุฬาลงกรณ์มหาวิทยาลัย



## CURRICULUM VITAE

**Date of Birth:** October 27, 1978                      **Birth Place:** Nakorn-Radchasisima, Thailand

**Address:** 169/46, Long Had Bangsean Road, Muang, Chonburi 20131, Thailand

### Educations:

Ph.D./ Chemistry	2006	Chulalongkorn University/Thailand
B.Sc. (hons)/ Chemistry	1999	Burapha University/Thailand

### Research Publications:

1. **Thongnopkun, P.;** and Ekgasit, S. FTIR Spectra of Faceted Diamonds and Diamond Simulants. Diamond and Related Material 14 (2005): 1592-1599.
2. Ekgasit, S.; and **Thongnopkun, P.** Transflectance Spectra of Faceted Diamonds Acquired by Infrared Microscopy. Applied Spectroscopy 59 (2005): 1160-1165.
3. Ekgasit, S.; and **Thongnopkun, P.** Novel Attenuated Total Reflection Fourier Transform Infrared Microscopy Using a Gem Quality Diamond as an Internal Reflection Element. Applied Spectroscopy 59 (2005): 1236-1241.

### Scholarships and Awards:

2000 – 2004 : *The University Development Committee (UDC) Ph. D. Scholarship/ Chanthaburi IT Campus of Burapha University*

2005 : *2005 Innovation Award in the subject 'Miniature ATR Infrared Sensor Made of Diamond'/ The National Research Council of Thailand (NRCT)*

2004 : *2004 Innovation Award in the subject 'Accessory for Nondestructive Characterization of Gem and Jewelry Using Infrared Spectroscopy'/ The National Research Council of Thailand (NRCT)*

2001 : *Poster Presentation Award/ Science Society of Thailand at 27<sup>th</sup> Congress on Science and Technology of Thailand (STT)*

### Current Professional:

From May, 2005: College fellow at the Gems College of Burapha University, Chantaburi, Thailand.